DOCTORAL THESES IN FOOD SCIENCES AT THE UNIVERSITY OF TURKU

Multi-omics Study on the Effects of Anthocyanin Extracts from Bilberries and Purple Potatoes on Type 2 Diabetes in Zucker Diabetic Fatty Rats

KANG CHEN

Food Chemistry and Food Development
Department of Life Technologies

DOCTORAL THESES IN FOOD SCIENCES AT THE UNIVERSITY OF TURKU
Food Development (tech)

Multi-omics Study on the Effects of Anthocyanin Extracts from Bilberries and Purple Potatoes on Type 2 Diabetes in Zucker Diabetic Fatty Rats

KANG CHEN

Food Chemistry and Food Development
Department of Life Technologies

TURKU, FINLAND – 2022

Food Chemistry and Food Development
Department of Life Technologies
University of Turku, Finland

Supervised by
Professor Baoru Yang, Ph.D.
Department of Life Technologies
University of Turku, Finland

Professor Kaisa Linderborg, Ph.D.
Department of Life Technologies
University of Turku, Finland

University of Turku
Assistant Professor Maaria Kortesniemi, Ph.D
Department of Life Technologies
University of Turku, Finland

Reviewed by
Professor Shengmin Sang, Ph.D.
Department of Food, Bioprocessing & Nutritional Sciences
North Carolina State University, United States of America

Professor Cristina Andres-Lacueva, Ph.D.
Department of Nutrition and Food Science
University of Barcelona, Spain

Opponent
Professor Francisco A. Tomás-Barberán, Ph.D.
Department of Food Science and Technology
CEBAS-CSIC, Spain

Research director
Professor Baoru Yang, Ph.D.
Department of Life Technologies
University of Turku, Finland

The originality of this dissertation has been checked in accordance with the University of Turku quality assurance system using the Turnitin OriginalityCheck service

ISBN 978-951-29-8773-3 (print)
ISBN 978-951-29-8774-0 (pdf)
ISSN 2323-9395 (print)
ISSN 2323-9409 (pdf)
Painosalama Oy – Turku, Finland 2022

TABLE OF CONTENTS

ABSTRACT

Anthocyanins are a group of flavonoids in purple and red berries, fruits, and tubers. Anthocyanins have been widely reported to have antidiabetic effects, which may arise from the modulation of carbohydrate and lipid metabolism and gut microbiota as well as from antioxidative and inflammatory effects. Anthocyanins can be divided into acylated anthocyanins and nonacylated anthocyanins according to the presence of an acyl group on the sugar residue of the aglycone. Acylation of anthocyanins increases the structural stability of the molecules, which affects their physico-chemical properties, such as a greater capacity to inhibit lipid peroxidation, antioxidant activity, and resistance to digestion compared with their nonacylated counterparts. Previous research has largely focused on the bioactivities of nonacylated anthocyanins from berries and other colored fruits, while the biological effects of acylated anthocyanins have received very little attention in research.

This thesis work investigated the effects of nonacylated anthocyanin extract from bilberries and acylated anthocyanin extract from purple potatoes on the plasma, hepatic, and gut luminal metabolites as well as hepatic transcriptome and gut microbiota in a type 2 diabetes (T2D) model. Zucker diabetic fatty (ZDF) rats were used as an animal model of T2D and fed with anthocyanin extracts for 8 weeks at daily doses of 25 or 50 mg/kg body weight. The lean Zucker rats were used as the healthy control model. Anthocyanin composition in two extracts was measured by high-performance liquid chromatograph and mass spectroscopy. ^{1}H NMR metabolomics, full-length RNA sequencing, and metagenomics were used to study metabolites, transcriptome, and gut microbiota affected by T2D and anthocyanin extracts.

The anthocyanins extracted from bilberries were all nonacylated and consisted of mostly glucosides, galactosides, and arabinosides of delphinidin, petunidin, cyanidin, peonidin, and malvidin. The anthocyanins extracted from purple potatoes were mainly acylated and dominated by petunidin coumaroyl-rutinoside-glucoside, peonidin coumaroyl-rutinoside-glucoside, and petunidin caffeoyl-rutinoside-glucoside. The indicators of feed and water intake, the body weight and ratio of viscera to body weight as well as plasma and hepatic glucose manifested the T2D in ZDF rats. Dysregulated energy metabolism including increased glycolysis influxes and substrates of gluconeogenesis, insulin resistance biomarkers, and lipids were found in T2D of ZDF rats. Defects in gut microbiota also characterized the ZDF rats. Both anthocyanin extracts reduced the levels of fasting plasma and hepatic glucose and branched-chain amino acids (BCAAs), hepatic intermediates of glycolysis and gluconeogenesis as well as regulated plasma lipid profile. However, only the treatment with acylated anthocyanin extract reversed the changes in the intermediates of glycolysis and

gluconeogenesis at systemic level and regulated hepatic lipids. At the gene level, nonacylated anthocyanin extract reversed the expression of *Mgat4a*, *Gstm6*, and *Lpl*, whereas acylated anthocyanin extract reversed the expression of *Mgat4a*, *Jun*, *Fos*, and *Egr1* in the diabetic status. Acylated anthocyanin extract also affected activator protein 1 and interleukin 1 production based on gene set enrichment analysis. For the gut luminal metabolites, both types of anthocyanin extract increased sugars level in cecal content and affected choline metabolism. Acylated anthocyanin extract increased cecal short-chain fatty acids and decreased fecal lactate. Anthocyanin extracts also beneficially modulated gut microbiota composition. Both types of anthocyanin extracts increased the abundance of *Peptostreptococcaceae* sp. and *Marvinbryantia formatexigenes*. Acylated anthocyanin extract decreased the abundances of *Parabacteroides disdasonis*, *Ruminococcus torques*, and *Lanchnospiraceae bacterium 4_1_37FAA*.

This thesis work comprehensively compared the effects of two different types of anthocyanin extracts from different sources on the diabetic state. Different beneficial effects were seen, with the acylated anthocyanin extract from purple potatoes showing more beneficial effects. More importantly, purple potatoes could be considered as a complement or substitute for berries as a source of dietary anthocyanins. Since potatoes are a sustainable staple food, the demand for anthocyanin-rich purple potatoes with a health-promoting effect is likely to increase. Enhanced stability and stronger modulatory effects of acylated anthocyanins may create new opportunities for its use in food applications.

SUOMENKIELINEN ABSTRAKTI

Antosyaanit ovat sinipunaisissa ja punaisissa marjoissa, hedelmissä ja mukuloissa esiintyviä flavonoideja. Antosyaaneilla on havaittu olevan diabetesta ehkäiseviä ominaisuuksia, jotka saattavat liittyä hiilihydraatti- ja rasva-aineenvaihdunnan ja suolistomikrobiston säätelyyn sekä antioksidatiivisiin ja anti-inflammatorisiin ominaisuuksiin. Antosyaanit voidaan luokitella asyloituihin tai asyloimattomiin antosyaaneihin riippuen siitä, onko aglykonin sokeriosaan kiinnittynyt asyyliryhmä. Antosyaanien asylointi stabiloi molekyylin rakennetta, mikä vaikuttaa yhdisteen fysikaalis-kemiallisiin ominaisuuksiin parantaen esimerkiksi kykyä estää rasvojen peroksidaatiota, antioksidatiivisuutta ja vastusta ruuansulatukselle verrattuna asyloimattomiin antosyaaneihin. Aiemmat tutkimukset ovat pääosin keskittyneet marjojen ja hedelmien asyloimattomien antosyaanien bioaktiivisuuteen, kun taas asyloitujen antosyaanien biologiset vaikutukset ovat jääneet vähälle huomiolle.

Tässä väitöskirjatyössä tutkittiin mustikan asyloimattomien ja violetin perunan asyloitujen antosyaanien vaikutuksia plasman, maksan ja suoliston ontelon aineenvaihduntatuotteisiin, maksan transkriptomiin sekä suolisto-mikrobistoon tyypin 2 diabetes (T2D) -eläinmallissa. Mallina käytettiin diabeettisia, lihavia Zucker-rottia (ZDF), joille syötettiin antosyaaniuutetta kahdeksan viikon ajan päivittäisellä annoksella 25 tai 50 mg/painokilo. Terveenä kontrollina käytettiin laihoja Zucker-rottia. Uutteiden antosyaanikoostumukset määritettiin korkean erotuskyvyn nestekromatografian ja massaspektrometrian avulla. T2D:n ja antosyaaniuutteiden vaikutusta aineenvaihduntatuotteisiin, transkriptomiin ja suoliston mikrobiotaan tutkittiin ^{1}H NMR -metabolomiikan, täyspitkän RNA:n sekvensoinnin sekä metagenomiikan avulla.

Kaikki mustikasta eristetyt antosyaanit olivat asyloimattomia ja koostuivat lähinnä delfinidiinin, petunidiinin, syanidiinin, peonidiinin ja malvidiinin glukosideista, galaktosideista ja arabinosideista. Violetista perunasta eristetyt antosyaanit olivat pääosin asyloituja, joista runsaimpia olivat petunidiini-(kumaroyylirutinosidi)-glukosidi, peonidiini-(kumaroyylirutinosidi)-glukosidi, petunidiini-(kafeyylirutinosidi)-glukosidi. ZDF-rottien rehun ja vedenkulutus, paino, painon ja sisäelinten suhde sekä plasman ja maksan glukoosiarvojen suhde ilmensivät diabetestilaa. ZDF-rottien energia-aineenvaihdunta oli häiriintynyt T2D-tilassa, mikä ilmeni lisääntyneenä glykolyysin virtauksena sekä glukoneogeneesin substraattien, insuliiniresistenssin biomarkkereiden ja lipidien määränä. ZDF-rotilla ilmeni myös suoliston mikrobiotan häiriöitä. Molemmat antosyaaniuutteet alensivat paastoplasman ja maksan glukoosin ja haaroittuneiden aminohappojen pitoisuutta ja maksan glykolyyttisiä ja glukoneogeneettisia välituotteita, ja säätelivät plasman lipidiprofiilia. Kuitenkin vain asyloituja antosyaaneja sisältävä uute vähensi glykolyysin ja

glukoneogeneesin välituotteiden muutoksia systeemitasolla ja sääteli maksan lipidejä. Geenitasolla asyloimattomia antosyaaneja sisältävä uute vaikutti geenien *Mgat4a*:n, *Gstm6*:n ja *Lpl*:n ekspressioon diabeettisilla rotilla, kun taas asyloituja antosyaaneja sisältävä uute vaikutti *Mgat4a*:n, *Jun*:n, *Fos*:n ja *Egr1*:n ekspressioon. Geenisarjojen rikastamisanalyysin perusteella asyloituja antosyaaneja sisältävällä uutteella oli vaikutus myös aktivaattoriproteiini 1:n ja interleukiini 1:n tuotantoon. Molemmat uutteet lisäsivät paksusuolen alkuosan sokeripitoisuuksia ja vaikuttivat koliiniaineenvaihduntaan suolessa. Asyloituja antosyaaneja sisältävä uute lisäsi lyhytketjuisten rasvahappojen määrää paksusuolen alkuosassa ja vähensi laktaatin määrää ulosteessa. Antosyaani-uutteilla oli myönteinen vaikutus suoliston mikrobiotan koostumukselle. Molemmat uutteet lisäsivät *Peptostreptococcaceae* sp.:n ja *Marvinbryantia formatexigenesin* abundanssia. Asyloitu antosyaani -uute vähensi *Parabacteroides disdasonisin*, *Ruminococcus torquesin* ja *Lanchnospiraceae bacterium 4_1_37FAA*:n abundanssia.

Tämä väitöskirjatyö vertasi kokonaisvaltaisesti kahden erilaisen antosyaaniuutteen vaikutuksia diabeteksessa. Uutteiden vaikutukset erosivat toisistaan, mutta asyloituja antosyaaneja sisältävällä, violetista perunasta eristetyllä uutteella havaittiin enemmän hyödyllisiä vaikutuksia. Violetteja perunoita voitaisiin käyttää antosyaanien lähteenä ravinnossa marjojen ohella tai sijasta. Koska peruna on kestävä peruselintarvike, terveyttä edistäviä antosyaaneja sisältävien perunoiden kysyntä saattaa lisääntyä. Stabiilit antosyaanimolekyylit ja niiden ravitsemusvaikutukset saattavat myös edistää niiden hyödyntämistä erilaisissa elintarvikesovelluksissa.

LIST OF ABBREVIATIONS

AAPP	Acylated anthocyanins extracted from purple potato
ACT	Anthocyanin acyltransferases
AGEs	Advanced glycation end products
AMPK	Adenosine monophosphate activated protein kinase
AP-1	Activate protein 1
ARA	Arachidonic acid
AST	Aspartate transaminase
BCAAs	branched-chain amino acids
BHMT	Betaine-homocysteine *S*-methyltransferase
BUN	Blood urea nitrogen
BW	Body weight
COSY	^{1}H-^{1}H Correlation Spectroscopy
CPMG	Carr–Purcell–Meiboom–Gill
DEGs	Differentially expressed genes
DETs	Differentially expressed transcripts
DHA	Docosahexaenoic acid
DSS	Sodium trimethylsilylpropanesulfonate
EPA	Eicosapentaenoic acid
ESI	Electrospray ionization
FID	Flame-ionization detector
FT	Fourier transform
GC	Gas chromatography
GLUT	Glucose transporter
GO	Gene Ontology
GPCRs	G-protein coupled receptors
HSQC	^{1}H–^{13}C heteronuclear single-quantum correlation spectroscopy
IFNγ	Interferon-γ
IL	Interleukin
JNKs	JUN N-terminal kinases
JRES	*J*-resolved spectroscopy
KEGG	Kyoto Encyclopedia of Genes and Genomes
LC	Liquid chromatography
LEfSe	Linear discriminant analysis effect size
LPS	Lipopolysaccharide
MS	Mass spectrometry
NAAB	Nonacylated anthocyanins extracted from bilberry
NF-κB	Nuclear factor-κB
NGS	Next-generation sequencing
NMR	Nuclear magnetic resonance

PCA	Principal components analysis
PCR	Polymerase chain reaction
PLS-DA	Principal Component Analysis-Discriminant Analysis
PPAR	Peroxisome-proliferator-activated receptor
PPI	Protein-protein interaction
PUFA	Polyunsaturated fatty acids
Q-TOF	Quadrupole/time-of-flight
ROS	Reactive oxygen species
SCFA	Short-chain fatty acids
T2D	Type 2 diabetes
TCA	Tricarboxylic acid
TG	Triglyceride
TLR	Toll-like receptor
TMA	Trimethylamine
TMAO	Trimethylamine *N*-oxide
TMS	Tetramethylsilane
TP	Total protein
TSP	Trimethylsilylpropanoic acid
UHPLC	Ultra-high performance liquid chromatography
WGCNA	Weighted gene coexpression network analysis
ZDF	Zucker diabetic fatty

LIST OF ORIGINAL PUBLICATIONS

I. Chen, K.; Wei, X.; Zhang, J.; Pariyani, R.; Jokioja, J.; Kortesniemi, M.; Linderborg, K. M.; Heinonen, J.; Sainio, T.; Zhang, Y.; & Yang, B. Effects of anthocyanin extracts from bilberry (*Vaccinium myrtillus* L.) and purple potato (*Solanum tuberosum* L. var. 'Synkeä Sakari') on the plasma metabolomic profile of Zucker diabetic fatty rats. *Journal of Agricultural and Food Chemistry.* **2020**, 68 (35), 9436–9450.

II. Chen, K.; Wei, X.; Pariyani, R.; Kortesniemi, M.; Zhang, Y.; & Yang, B. ^{1}H NMR metabolomics and full-length RNA-Seq reveal effect of acylated and nonacylated anthocyanins on hepatic metabolites and gene expression in Zucker diabetic fatty rats. *Journal of Agricultural and Food Chemistry.***2021**, 69 (15), 4423–4437.

III. Chen, K.; Wei, X.; Kortesniemi, M.; Pariyani, R.; Zhang, Y.; & Yang, B. Effects of acylated and nonacylated anthocyanins extracts on gut metabolites and microbiota in diabetic Zucker rats: A metabolomic and metagenomic study. *Food Research International*, **2022**, 153, 110978.

1. INTRODUCTION

Metabolic diseases including dyslipidemia, arteriosclerosis, diabetes, and hypertension, are largely affected by lifestyle choices such as dietary habits. The prevalence of diabetes is a growing challenge to the world, it is estimated that the total number of cases of diabetes will reach 366 million by 2030 due to population expansion, the aging population, and the increasing prevalence of obesity.[1] T2D is a metabolic disease characterized by chronic hyperglycemia resulting from insulin resistance and/or insulin secretion. Considering the adverse effects of drugs, natural products, such as anthocyanins, from fruits and vegetables have been increasingly considered due to their preventive and therapeutic effects as a means of managing the risk of T2D.[2]

Anthocyanins, a major class of bioactive flavonoids responsible for many of the red-orange to blue-violet colors present in plants, are well known to possess antioxidant and anti-inflammatory abilities, and can also modulate energy homeostasis and gut microbiota.[3] While fruits and berries are common sources of nonacylated anthocyanins, purple-fleshed potatoes are rich in acylated anthocyanins. Acylation alters the physical-chemical properties of anthocyanins and enhances the stability. Acylated anthocyanins have been reported to show more resistance to variations in pH, heat, and light[4] and a higher capacity to inhibit lipid peroxidation and antioxidant activity[5] than the nonacylated counterparts. Moreover, acylated anthocyanins from purple sweet potatoes (*Ipomoea batatas* L.) have shown higher resistance to overall simulated digestion *in vitro* compared to nonacylated anthocyanins from red wine.[6] A large-scale dietary survey study across ten countries in Europe has shown the daily intake of anthocyanins, mainly from fruits and wine, to range from 18.73 to 64.88 mg.[7] A clear geographical gradient of anthocyanin intake has also been observed, increasing from south to north Europe.[7] A dietary reference intake for anthocyanins has not been set in the United States or the European Union. China is the first country to set a recommended daily intake of 50 mg for anthocyanins, but the tolerable upper intake level has not been defined.[8]

Potatoes are a major agricultural crop worldwide in terms of production and consumption. Due to the high yield, low production costs (low demand for water and land management), and low greenhouse gas emissions produced by potato cultivation, the dark-colored potato may represent a sustainable and highly cost-effective source of anthocyanins.[9] Dietary anthocyanins are absorbed into enterocytes as intact glycosides or aglycones hydrolyzed by lactate phlorizin hydrolase. The absorbed glycosides and aglycones undergo metabolism by phase I and phase II enzymes and generate phenolic acids and their conjugates. Up to 65% of dietary anthocyanins are not absorbed in the stomach and upper

intestine,[10] and thus transit to the colon, where they are extensively metabolized by gut microbes.

Previously, the biological effects of anthocyanins have mostly been studied using nonacylated anthocyanins[11–13], there has been little research focusing on acylated anthocyanins. Moreover, the metabolic effect of anthocyanins has not been investigated either in humans or animals. Therefore, this thesis study provides an unprecedented report on the metabolomic effects of anthocyanins on plasma, the liver, and the gut in T2D. It is also the first study to compare the biological effect of nonacylated anthocyanins with acylated anthocyanins on T2D using omics tools.

In this thesis, ZDF rats were used as the T2D animal model to investigate and compare the impact of acylated anthocyanins extracted from purple potatoes (*Solanum tuberosum* L. var. 'Synkeä Sakari') and nonacylated anthocyanins extracted from bilberry (*Vaccinium myrtillus* L.). To benefit from the most advanced high throughput methodologies, state-of-art multi-omics approaches were applied. ^{1}H NMR-based metabolomics was used to investigate the metabolites in plasma, the liver, cecal content, and feces. Full-length RNA seq transcriptomics was used to study the hepatic transcriptome. Next Generation Sequencing-based metagenomics was used to study the gut microbiome.

This literature review discusses the general beneficial effect of anthocyanins on type 2 diabetes, omics technologies, and the preprocessing and analysis of large data. Due to the scarcity of previous studies on the biological effect of acylated anthocyanins, and the lack of comparisons between nonacylated and acylated anthocyanins, special emphasis has been placed on these research questions in this research work.

2. REVIEW OF THE LITERATURE

2.1. Type 2 diabetes and Zucker diabetic fatty rat

2.1.1. Diabetes

Diabetes mellitus is a complex chronic metabolic disease that is characterized by hyperglycemia resulting from a deficiency in insulin secretion and/or insulin resistance. Several of the complications due to chronic hyperglycemia include neuropathy, nephropathy, retinopathy, and increased risk of cardiovascular disease. The prevalence of diabetes is a growing challenge to world health; it has been estimated that the total number of cases of diabetes will reach 366 million in 2030 due to population expansion, the aging population, and the increasing prevalence of obesity.[1] The most common two types of diabetes are type 1 and type 2 diabetes. Type 1 diabetes is generally considered to be an immune-associated destruction of insulin-producing pancreatic β cells resulting in deficiency in insulin secretion. It often occurs in children and young adults. The prevalence of T2D is increasing in parallel with the obesity epidemic, and the pathogenesis is mainly related to insulin resistance.[14] In addition to a genetic predisposition, lifestyle changes also affect T2D[15] and healthy food choices are gradually considered as an important approach for the management of the risk of T2D.[16] Considering the adverse effects of drugs, natural products, such as anthocyanins, from fruits and vegetables have been increasingly considered in regards to their beneficial effects on the management of the risk of T2D.[2]

2.1.2. Zucker diabetic fatty rat

Animal models play a crucial role in revealing the pathogenesis of diabetes as they allow the genetic and environmental factors to affect the disease progression.[17] Furthermore, animal models should be carefully selected when conducting investigations into diabetes depending on what aspects of the disease are to be studied.

Zucker diabetic fatty (ZDF) rats were produced in 1961 through a hybrid of Sherman and Merck rats.[18] A missense mutation in the leptin receptor gene was found in ZDF rats, which leads to impaired leptin signaling and subsequently impairs leptin's ability to suppress appetite and thermogenic effects.[18] Thus, these rats have hyperphagia and become obese by 4 weeks of age.[19] These rats are characterized by hyperinsulinemia, hyperlipidemia, hypertension, and impaired glucose tolerance. The homozygous mutation (*fa/fa*) of the leptin receptor gene leads to type 2 diabetes in male ZDF rats, and feeding on a high-energy rodent diet would accelerate the disease progress.[17]

After weaning, between 3 and 8 weeks of age, ZDF rats develop insulin resistance, glucose intolerance, and hyperinsulinemia due to islet hyperplasia which was able to maintain plasma glucose levels at normal levels in the early stage.[20] ZDF rats become diabetic between 8 and 11 weeks of age with high plasma glucose concentration around 500 mg/dL in the fed state, but fasting glycemia could remain normal at least until 10 weeks of age.[20] Fasting hyperglycemia develops along with a decrease in plasma insulin levels between 10–20 weeks of age due to a significant decline in the β cell mass; the islets are highly disorganized with fibrosis leading to fasting hyperglycemia and decreased rate of islet growth.[21] By the age of 20–25 weeks, plasma insulin level in ZDF rats decreases to the level seen in male lean Zucker rats and fasting plasma glucose levels reach > 540 mg/dL. Development of obesity- and hyperglycemia-related complications are common for both male ZDF rats and humans with type 2 diabetes associated with obesity[17,22], including lower hepatic glycogen breakdown, increased gluconeogenesis, and insulin resistance.[22] This pathogenesis of diabetic ZDF rats resembles the development of human T2D, thus providing a rational disease model.

2.1.3. Energy metabolism homeostasis and inflammation in type 2 diabetes

2.1.3.1. Overview of energy metabolism in type 2 diabetes

Under a healthy fasting status, energy metabolism has been thoroughly studied. In general, peripheral adipose tissue lipolysis provides non-esterified fatty acids (free fatty acid) with the ability to generate the substrates for fatty acid β-oxidation, with the formation of the end product of acetyl-CoA being oxidized to CO_2 through the tricarboxylic acid (TCA) cycle. Meanwhile, a high level of produced ATP and gluconeogenic reducing equivalents convert pyruvate and other anaplerotic substrates into glucose through the gluconeogenesis pathway. However, when the amount of acetyl-CoA generated from β-oxidation surpasses the oxidative capacity of the TCA cycle, typically in diabetes, the surplus acetyl-CoA is transferred to ketone body production. Thus, in the setting of type 2 diabetes, dysregulated carbohydrate and lipid metabolisms contribute to excessive glucose and lipid in the liver and at the systemic level.[23] These findings were also verified in the anti-hyperglycemic effect of metformin, which has been verified to exert its effect *via* inhibition of respiration redox reactions by decreasing the level of mitochondrial glycerol-3-phosphate dehydrogenase[24] and complex I and ATP synthase in mitochondria.[25] Thus, the production of ATP and reducing equivalents are reduced, and the subsequent conversion of pyruvate and other anaplerotic substrates to glucose is also restricted. Under the fed state, food intake complicates the hepatic lipid and carbohydrate metabolism, and the liver

absorbs a variety of nutrients through the portal vein, such as fatty acids, sugars, and amino acids. These nutrients entering the liver, combined with the effect of high abundance of insulin secreted from the β cells stimulated by circulatory glucose, promote hepatic *de novo* lipogenesis and glycogen synthesis, while fatty acid β-oxidation and glucose production are restrained.[26] The defect of insulin activity in diabetes disturbs these energy metabolisms.

These complex energy metabolisms are controlled by kinases systems and their involved pathways, such as PI3K/AKT (phosphoinositide 3 kinase/protein kinase B) and AMPK (AMP-activated protein kinase) pathways, which are primary effectors in response to metabolic stress and important to energy metabolism and considered as therapeutic target in metabolic syndromes, particularly diabetes.[27]

Endogenous and exogenous factors can activate PI3K/AKT, such as insulin, growth factors, cytokines, and environmental stresses, which regulate energy metabolism and cell proliferation, motility, differentiation, and survival.[27,28] The PI3K/AKT pathway is required for insulin-dependent regulation of systemic and cellular glucose and lipid homeostasis such as regulating glycogen synthesis (glycogen synthase kinase 3β, GSK3β), gluconeogenesis (forkhead box protein O1, FOXO1) and glucose uptake (TBC1 domain family member 4, TBC1D4).[27,28]

The AMPK pathway can be activated by a series of physiological factors and adipocytokines, such as glucose deprivation, hypoxia, oxidative stress, and muscle contraction. The common results of these stimuli are a reduction in cellular energy level and an increase in AMP/ATP ratio, which are important for AMPK activation.[27,29] AMPK responses to the energy deprivation and increases AMP/ATP ratio caused by these aforementioned physiological factors and adipocytokines and further activates glucose uptake (AS160, a substrate for the protein kinase AKT that links insulin signaling and GLUT4 trafficking), inhibits glycogen synthesis (muscle glycogen synthase, GYS1) and *de novo* lipogenesis (acetyl-CoA carboxylase α, ACC), and enhance β-oxidation, (malonyl-CoA decarboxylase, MCD).[27] The well-known antidiabetic drug metformin has been shown to mainly target phosphorylation of AMPK to elicit its beneficial effects on diabetes.[24,25]

2.1.3.2. Metabolic changes in type 2 diabetes revealed by metabolomics and transcriptomics

The metabolic state changes along with the development of T2D from prediabetes to overt diabetes. Although fasting plasma glucose, oral glucose tolerance tests, or glycated hemoglobin measurements are powerful diagnostic indicators of T2D, the metabolic changes in T2D are important in order to

recognize the pathogenesis.[30] It is known that the carbohydrate, lipid, and protein metabolisms are altered in prediabetes and T2D (**Table 1**).[31]

Metabolomics could provide a real-time functional portrait of the organism, which monitors changes of small precursors, intermediary molecules, and product molecules associated with energy storage and utilization that might promote the understanding of the disease pathogenesis. Therefore, metabolomics becomes a very powerful tool for detecting differences in the molecular profile basis.[32] A range of metabolomic studies measuring the metabolites from biofluids suggest a metabolic disturbance in T2D, evidenced by changes in the levels of biomolecules, such as carbohydrates, lipids, and amino acids.[31]

Hyperglycemia and glycosuria are the two dominant biomarkers in T2D.[33–39] Dysregulated levels of other metabolites involved in glycolysis and gluconeogenesis have been revealed by metabolomics, e.g., lactate, alanine, and pyruvate.[36,40,41] The downstream metabolites in TCA cycle, e.g., 2-oxoglutarate, citrate, succinate, fumarate, and malate, are also disturbed in T2D.[37,38,42] Abnormal circulating levels of palmitate, oleate, stearate, arachidonate, linolenate, eicosadienoate, arachidonate, eicosapentaenoate, and docosahexaenoate were observed in T2D patients.[35,40,43] Ketone bodies (acetone, acetoacetate, and β-hydroxybutyrate), largely produced when glucose is not available for energy utilization, typical in T2D, were observed to be increased.[38,40,41,44] Circulating amino acids and their derived metabolites have also been comprehensively studied in metabolomic analyses. Increased BCAAs and aromatic amino acids (AAAs) have been suggested as biomarkers in T2D due to their associations with insulin resistance. [33–35,45]

Table 1 Alterations of metabolites in patients with type 2 diabetes

Subjects	*Metabolomics approach*	*Biofluid*	*Altered metabolites in T2D*
30 T2D subjects; 30 Healthy subjects[33]	LC-MS/MS	Plasma	(↑): Valine, leucine, isoleucine, xanthine, glutamate, 2-hydroxybutyrate, 3-methyl- 2-oxovalerate, 3-hydroxyisobutyrate, glucose, pyridoxal, glucose (↓): Isobutyrylglycine, L-DOPA
160 T2D subjects; 160 Healthy subjects[34]	LC-MS/MS.	Serum	(↑): Glucose, isoleucine, leucine, tryptophan, valine, glutamine, and tyrosine
A 6-year follow-up study (n=1680)[45]	^{1}H NMR	Serum	(↑): Isoleucine, leucine, valine, phenylalanine, and tyrosine were associated with HOMA-IR for men; (↑): Leucine, valine, and phenylalanine predicted HOMA-IR for women
82 T2D subjects; 36 Healthy subjects[35]*	GC-MS	Serum	(↑): Butyrate, glucose, valine, maltose, glutamate, urate, palmitate, oleate, stearate, arachidonate (↓): Lactate, lysine, glucuronolactone
26 T2D subjects; 26 Healthy subjects[40]*	GC-MS	Plasma	(↑): Lactate, alanine, 2-hydroxyisobutyrate, 3-hydroxybutyrate, phosphate, leucine, isoleucine, serine, pyroglutamate, palmitate, oleate, stearate, arachidonate, 1-monostearin, 1-monopalmitin (↓): 2-ketoisocaproic acid
105 T2D subjects; 77 Healthy subjects[42]*	UPLC-QTOF-MS	Plasma	(↑): Itaconate, leucine, phosphatidylcholine (18:0/0:0), glucose, sphingosine-1-phosphate (↓): Inosine, urate, 3-hydroxymethylglutarate, succinate, taurine, creatine
44 Obese T2D subjects; 12 Obese subjects without T2D[44]*	GC-TOF-MS	Plasma	(↑): 3-hydroxybutryrate, oleate, gluconate, fructose, palmitoleate, 3,6-anhydrogalactose, glucuronate, glucose, heptadecanoic acid, inulobiose, leucine, 2-hydroxybutyrate, palmitate, 2-deoxyerythritol, 2-ketoisocaproate, uridine, cysteine, stearate, xylose, histidine (↓): Benzylalcohol, benzoate, lysine, arachidonate, ethanolamine, glycine, glycerol-3-phosphate
18 T2D subjects; 19 Healthy subjects[36]*	^{1}H NMR	Serum	(↑): Fumarate, glucose, pyruvate, methylamine, dimethylamine, uridine, trimethylamine N-oxide, mannose (↓): phenylalanine, serine. taurine, threonine, pyroglutamate, glycine

Subjects	*Metabolomics approach*	*Biofluid*	*Altered metabolites in T2D*
26 T2D subjects; 27 Healthy subjects[46]*	UPLC/Q-TOF-MS	Plasma	(↑): Lysine, laurate, myristate, leucine, glucose, phenylalanine, carnitines, lyso-phosphatidylcholines (14:0, 16:1, 18:1, 18:3, 20:5, 22:6), Lyso-phosphatidylethanolamine (18:2, 22:6) (↓): serine, Lyso-phosphatidylethanolamine (18:1)
60 T2D subjects; 25 Healthy subjects[43]*	LC-MS/MS	Plasma	(↑): Myristate, palmitate, palmitoleate, stearate, oleate, linoleate, linolenic acid, γ-linolenate, eicosadienoic acid, arachidonate, eicosapentaenoate, docosahexaenoate
33 T2D subjects; 20 Healthy subjects[41]*	^{1}H NMR	Urine	(↑): Lactate, alanine, creatine, citrate, dimethylamine, glycine, glucose, acetate, betaine, 3-hydroxybutyrate, hippurate, trimethylamine N-oxide, acetone, acetoacetate
11 T2D subjects; 16 Healthy subjects[37]*	^{1}H NMR	Urine	(↑): Alanine, hippurate, phenylalanine, glucose, citrate, phospho(enol)pyruvate, tyrosine (↓): Glutamate, N-methylnicotinamide, glutamine, uridine
30 T2D subjects; 12 Healthy subjects[38]*	^{1}H NMR	Urine	(↑): Citrate, acetate, acetoacetate, butyrate, trimethylamine, dimethylamine, dimethylglycine, betaine, 3-hydroxybutyrate, trimethylamine N-oxide, 2-hydroxybutyrate, alanine, glucose, glutamine, taurine, N-methylnicotinamide, ornithine, N-methyl-2-pyridone-5-carboxamide (↓): Creatine, malate, creatinine, succinate, 2-oxoglutarate, fumarate, leucine, isoleucine, tryptophan, histidine, N-methylnicotinate, allantoin
81 T2D subjects; 42 Healthy subjects[39]*	UPLC-QTOF-HDMS	Urine	(↑): Acylcarnitines, glycine, glucose, 3-indoxylsulfate, (↓): Citric acid, urate, kynurenic acid, lysine glucuronolactone

Note: The references with * were adapted from the review.[31]

(↑) and (↓) indicate the increase and decrease of metabolites in T2D.

Abbreviations: LC-MS/MS, liquid chromatography with tandem mass spectrometry; ^{1}H NMR, proton nuclear magnetic resonance; GC-TOF-MS, gas chromatography-time-of-flight mass spectrometry; UPLC/Q-TOF-MS, ultra-performance liquid chromatography-quadrupole/time-of-flight mass spectrometry; GC-TOF-MS, gas chromatography time-of-flight mass spectrometry; UPLC-QTOF-HDMS, ultra-performance liquid chromatography-quadrupole/time-of-flight mass spectrometry

The changed gene expression pattern in T2D has been widely studied using microarray[47,48] and next-generation sequencing[49], which has supported the changed energy metabolism and immune response in T2D. Clarifying the differentially expressed genes (DEGs) and the underlying functional pathways are important for disease diagnosis, pathological mechanism exploration, and treatment.

Two hundred and fourteen DEGs were revealed by the next-generation sequence in 22-week-old ZDF rats with T2D compared to lean Zucker rats.[50] These DEGs were enriched in glucose metabolism (such as *Gck*, *Igfbp1*, and *Pck1*), lipid metabolism (such as *Pnlip*), and protein metabolism (such as *Cpa1/2*, *Ctrl*, *Ctrb2*, and *Cela2a*). Enriched pathways were also involved in inflammatory responses, for example, p38 MAPK signaling, PPAR (peroxisome-proliferator-activated receptor) α/RXR (retinoid X receptor) α activation, and LPS (lipopolysaccharide) /IL (interleukin)-1-mediated inhibition of RXR function. DEGs involved in liver injury (such as *Irf1*, *Nr0b2*, and *Tnfrsf1b*) and endoplasmic reticulum stress (such as *Xbp1*, *Myh11*, *Atp2a1*, *Ephx2*, and *Cth*) were also found. A hepatic transcriptome study for type 2 diabetes in cynomolgus monkeys showed twelve enriched KEGG pathways responsible for DEGs. The most relevant pathways were PPAR signaling pathway, retinol metabolism, and steroid biosynthesis pathway. Others are ECM-receptor interaction, hypertrophic cardiomyopathy, p53 signaling, and immunity-related pathways including graft-versus-host disease, type 1 diabetes mellitus, allograft rejection, antigen processing and presentation, and autoimmune thyroid disease.[51] A hepatic transcriptome study applied for human showed that hepatic DEGs in patients with type 2 diabetes compared to healthy subjects were enriched in type 2 diabetes-related pathways: MAPK pathway, PI3K/AKT signaling pathway, insulin resistance, hippo signaling pathway and hypoxia-inducible factor-1 signaling pathway.[52]

Another human study showed upregulated KEGG pathways in T2D patients: toll-like receptor signaling pathway and inflammatory mediator regulation of TRP channels.[53] *Db/db* mice[54] showed the outstanding activated gluconeogenesis revealed by microarray. Another RNA-seq hepatic transcriptomic study in *db/db* mice[55] showed upregulated DEGs were enriched in KEGG pathways: drug metabolism, valine, leucine and isoleucine degradation, metabolism of xenobiotics by cytochrome P450, retinol metabolism, and oxidative phosphorylation. Gene ontology analysis based on those DEGs showed upregulated genes were enriched in metabolic process, for example, cellular lipid metabolic process and carboxylic acid metabolic process; downregulated genes were enriched in immune response-related terms, for example, adaptive immune response and lymphocyte-mediated immunity. These transcriptomic studies revealed the altered transcriptomic profile in type 2 diabetes, which are largely

related to metabolic and immunological aspects. Perturbation in this intricate immune-metabolic crosstalk would cause altered metabolic states in type 2 diabetes.

2.1.3.3. Inflammation in type 2 diabetes

Low-grade and chronic inflammation in the liver, skeletal muscle, and adipose tissue have been considered to be contributing factors in the development of insulin resistance and diabetes.[56] Under an acute inflammation (infection or tissue injury), a transient adaptive decrease of insulin sensitivity occurs and diverts the utilization of glucose from major glucose-consumers (for example, skeletal muscle or liver during the fasting state) to leukocytes and other types of cells to serve as a transient adaptive mechanism replenishing the increased energy demand during infection and tissue repair.[57] Such adaptive mechanism (insulin resistance) caused by chronic inflammation can lead to type 2 diabetes.[57] This adaptive response has been termed "*para*-inflammation" which was considered to characterize the immune responses where sustained tissue stress and malfunction were induced by a variety of stimuli, e.g., advanced glycation end products (AGEs)[58,59], reactive oxygen species (ROS), and oxidized lipoproteins.[60] AGEs can accumulate under pro-oxidative conditions and hyperglycemia, such as aging and diabetes. ROS produced by phagocytes can convert lipoproteins to inflammatory signals by oxidizing their lipid and protein components.[57] *Para*-inflammation could trigger maladaptive chronic non-resolving immune activation and inhibit insulin signaling pathways and prompt the development of insulin resistance.[57]

Furthermore, consumption of high-energy food or overfeeding has been linked with *para*-inflammation. When caloric intake exceeds the energy expenditure, overloaded tricarboxylic acid cycle inputs would form an excessive amount of mitochondrial NADH (mtNADH) and ROS.[61] When an excessive amount of mtNADH cannot be dissipated by oxidative phosphorylation, the mitochondrial proton gradient increases and single electrons are transferred to oxygen, resulting in the formation of superoxide anion, nitrogen oxide, peroxynitrite, and other free radicals[61], which might induce inflammation and insulin resistance.[57] High caloric intake-induced oxidative stress has been proposed to activate the nuclear factor κB (NF-κB)[62] and increase its downstream proinflammatory cytokines.[63] Consumption of excessive high-saturated fatty acid diet, particularly in western diets, leads to circulating and adipose tissue-resident immune cell activation *via* TLR-4 (toll-like receptor 4) signaling, leading to subsequent release of TNF-α (tumor necrosis factor-α) and other pro-inflammatory cytokines release.[56] The resultant inflammation involves adipose tissue recruitment of pro-inflammatory M1 macrophages, which partly contribute to insulin resistance.[56] A similar immunological pathway might occur in the fatty liver with hepatic fibrosis since inhibiting hepatic TNF-α expression could improve hepatic insulin resistance.[64]

Pro-inflammatory cytokines and chemokines such as IL-6, IL-1β, MCP-1 (Monocyte chemoattractant protein-1), and TNF-α contribute to the development of T2D and obesity.[65] Neutralization of TNF-α improves insulin sensitivity.[66] Moreover, anti-inflammatory cytokine levels are also changed in T2D. Administration of IL-10 could reverse IL-6-induced insulin resistance *in vivo*[67] and *in vitro*[68]. One pharmacological review pointed out that NF-κB plays the primary role in inflammatory-induced insulin resistance.[69] JUN N-terminal kinases (JNKs) which have a pro-inflammatory role are also important mediators of obese-related insulin resistance.[70]

NF-κB, a nuclear transcription factor, is a critical regulator of immune and inflammatory responses and can be activated by a series of oxidative stress and pro-inflammatory stimuli, such as AGEs, cytokines, free radicals, and bacterial or viral antigens. The downstream outputs include the expression of cytokines (IL-1, IL-2, IL-6, TNF-α, etc.), chemokines (IL-8, MCP1, eotaxin, etc.), acute phase proteins, immunoreceptors, cell adhesion molecules (vascular cell adhesion molecule-l, VCAM-l), growth factors, and inducible enzymes including COX-2 (cyclooxygenase-2) and iNOS (inducible nitric oxide synthase).[69] The activity of NF-κB is mediated by a family of inhibitors of NF-κB (IκB). A deactivated form of NF-κB is combined with IκB proteins in cytoplasm.[69] The canonical signaling pathway that is required for activation of NF-κB is dependent on the activation of IκB kinase (IKK) complex. Pro-inflammatory signals can activate IKK complex to degrade IκB proteins that combined with NF-κB and further release NF-κB p65:p50 heterodimer for nuclear translocation.[69,71] Overexpression of IKKβ, an upstream activator of NF-κB, damaged the insulin signaling in the HEK293 cell line.[72] $Ikk^{+/-}$ *ob/ob* mice with the reduction of IKKβ expression could be protected from the development of insulin resistance.[72] Hepatic overexpression of IκB retained global insulin sensitivity in transgenic mice.[73] JNKs which have a pro-inflammatory role are also important mediators of insulin resistance, the JNK pathway is over-activated in the liver, muscle, and adipose tissue in T2D and obesity[74–76], while blocking JNK pathway protects against insulin resistance.[74]

Lifestyle and gut microbiota also contribute to regulating hepatic insulin resistance. Decreasing body weight of as low as 8% can reduce steatosis and improve hepatic insulin resistance in patients with obesity and T2D.[77,78] A cause-effect relationship was found between the microbiota, fat content, and insulin resistance, transplantation of gut microbiota from *ob/ob* to germ-free mice enhanced the adiposity and insulin resistance.[79] Systemic chronic inflammation plays an important role in the pathogenesis of obesity-related insulin resistance, as displayed by increased inflammatory biomarkers in patients with obesity-related insulin resistance. Mitigating inflammation might be an important strategy to suppress insulin resistance.

2.1.4. Gut microbiota in type 2 diabetes

2.1.4.1. Gut microbiota

The gut microbiota is considered to be a major "organ" in the human body with at least 10^{14} bacteria belonging to over 1,000 prevalent bacterial species and about 3.3 million genes (150 times more genes compared to the human genome), which has an impact on the digestion of complex nutrient, the development of innate and adaptive immunity, and functions in regulating metabolic pathways in health and in disease.[80]

The profile of gut microbiota is in a dynamic way influenced by genetics, lifestyle, drug (especially antibiotics), and diet.[81] Interestingly, initiation of microbiota colonization in the gut starts at birth. The mode of delivery can shape the type of microorganisms that colonize the gut of newborns. Vaginally delivered newborns display a microbiota composition dominated by *Lactobacillus*, *Prevotella,* and *Sneathia*. Resembling the maternal vaginal microorganisms. *Staphylococcus*, *Corynebacterium,* and *Propionibacterium* dominate in neonates delivered by cesarean section.[82] During early infanthood, the gut microbiota profile undergoes a gradual change induced by diet, such as breast milk and the introduction of complementary foods, and possibly by disease. Actinobacteria, particularly genus *Bifidobacterium*, dominate the gut microbiota of breastfed infants. By such change, the microbiota profile shifts towards that of the adult and remains relatively stable in the healthy state of subjects during their later life.[83,84] Moreover, physical exercise can also increase the abundance of beneficial microbial species.[85]

Host-symbiotic microbiota interactions play important roles on host physiology. Gut barrier, consisting of physical (such as gut epithelial cells) and chemical (such as antimicrobial peptides) barrier, is the first frontline against gut luminal exogenous molecules and pathogens. Gut microbiota can affect gut epithelial morphology, mucus production, secretion of immune factors (such as antimicrobial peptides), and gut permeability when interacting with mucosal immune cells and contiguous layer of epithelial cells.[83] Damage to the gut barrier leads to the translocation of luminal molecules into endothelium and even systemic circulation, which, in turn, aggregate the intercellular connections (such as adherens junctions and tight junctions between epithelial cells) and induce an inflammatory response.[86] One of the consequences of such is linked to metabolic endotoxemia, which is associated with regulation of fat storage and development of obesity and type 2 diabetes.[87] In particular, dysregulated gut microbiota composition may destroy gut barrier and induce exposure of LPS to systemic circulation rendering chronic low-grade inflammation (para-inflammation), which is linked to adiposity, insulin resistance, and *de novo* synthesis of triglycerides.[87,88] LPS is a large glycolipid molecule derived from the outer

membrane of gram-negative bacteria, which could induce the innate immune-system response by binding to TLR-4 and its co-receptors.[83] TLR-4 belongs to TLR family, one of the pattern-recognition receptors. When these receptors are activated, the myeloid differentiation primary-response protein 88 (MyD88, adaptor proteins of Toll-like receptors) is recruited and activates pro-inflammatory signaling cascades, for example, the NF-κB pathway.[89] More importantly, such activation has been associated with dysregulation of glucose metabolism, insulin resistance, and type 2 diabetes.[83,90,91] Moreover, deletion of MyD88 protects against adiposity and insulin resistance in mice.[92]

2.1.4.2. SCFA and other gut metabolites related to type 2 diabetes

The gut microbiota can exclusively ferment complex carbohydrates and plant polysaccharides to produce short-chain fatty acids (SCFAs) mainly consisting of acetate, propionate, and butyrate. Bacteroidetes (gram-negative) and Firmicutes (gram-positive) are the most abundant phyla in the intestine, with members of the Bacteroidetes mainly producing acetate and propionate, while Firmicutes mostly produce butyrate in the human gut.[93–95]

A review[56] systematically summarized that SCFAs could mediate immune responses, such as cytokine and chemokine production in intestinal epithelial and mononuclear cells, neutrophil chemotaxis, immune cell differentiation, inflammasome activation, and anti-inflammatory processes; impact the hematopoietic repertoire through their signaling *via* G protein-coupled receptors (GPCRs), such as GPR41, GPR43, and GPR109A; exert beneficial effects on gut barrier, body weight, glucose homeostasis, and insulin sensitivity; regulate leptin production and lipolysis in adipocytes, suppress appetite, and protect against insulin-mediated fat accumulation.

When dietary fibers are absent, depleted SCFAs and compromised epithelial barrier integrity would occur in the gut, thereby leading to systemic endotoxemia, resulting in adipose tissue inflammation and insulin resistance.[96] Adipokine production by adipose tissue is important for inflammation and insulin resistance, SCFAs can directly regulate adipokine production in adipose tissue and thereby play a significant part in inflammation and insulin resistance.[97]

SCFAs act as ligands for GPCRs, and are therefore able to activate anti-inflammatory signaling cascades.[98] In addition, SCFAs have also been proposed to inhibit histone deacetylases (HDACs) and exert anti-inflammatory effects in the intestinal mucosa.[98] For example, butyrate suppresses LPS-induced NF-κB activation through GPR109A in normal and cancer colon cell lines as well as in the colon of a normal mouse.[99] In addition, the acetate/GPR43 pathway stimulates potassium efflux and hyperpolarization in HT-29 and NMC460 colonic cells, leading to NLRP3 inflammasome activation[100] which has been reported to repair the mucosal barrier and protect against DSS-induced colitis.[101]

Metabolomics analysis based on the NMR has shown butyrate content in mice intestine had a positive relationship with the intestinal *Foxp3* mRNA transcription level and the proportion of regulatory T cells.[102] Butyrate intervention could not only increase the number of regulatory T cells in the colon but also affect systemic immunity. Intake of butyrate and propionate produced by fermentation of starch could increase the number of regulatory T cells in the thymus and spleen.[103]

Butyrate is a primary energy source for colonocytes. It is mainly produced by anaerobes, absorbing and metabolizing butyrate by the epithelial cells needs oxygen and therefore promotes hypoxia-inducible factor which is a transcription factor coordinating barrier protection.[104] In addition, butyrate promotes the epithelial barrier function by stimulating the production of tight junctions through the activation of STAT3 and SP1. Butyrate also promotes the antimicrobial peptide production mediated by GPR43.[105–107] Butyrate, propionate, and acetate have shown a protective effect against diet-induced obesity and insulin resistance in mice, while only propionate-fed mice showed reduced fasting glucose.[108,109] Only butyrate and propionate, but not acetate, have been shown to improve oral glucose tolerance, reduce food intake, and induce gut hormones.[108] Butyrate supplementation in the diet has been shown to reduce diet-induced insulin resistance and adiposity in mice possibly through increasing energy expenditure and mitochondria function, manifested by activated AMP kinase, p38, and peroxisome proliferator–activated receptor-γ coactivator-1α.[109] However, acetate-treated type 2 diabetic Otsuka Long-Evans Tokushima fatty rats showed an improved glucose tolerance and a marked reduction in lipid accumulation in the adipose tissue and liver.[110]

Although high-fat diet-induced obesity in mice[111] and T2D patients[112] showed the lack of SCFAs in the gut, contrary results have also been observed. Cecal and/or fecal SCFAs levels are higher in genetic models of obese *ob/ob* mice and ZDF rats, and obese human subjects.[79,113–116] It has been speculated that this increase in SCFAs is the result of the increased amount of substrates for microbial fermentation due to increased food intake over the intervention period,[117] increased microbial fermentation of non-digestible carbohydrates by the gut microbiota in the colon of the obese rats[113], and decreased colonic absorption with obesity.[116]

Apart from SCFA, other metabolites linked to gut microbiota also affect type 2 diabetes.

Bile acids are steroid compounds derived from cholesterol in the liver with the aim of absorbing dietary lipids. Primary bile acids synthesized in hepatocytes are conjugated with taurine and glycine in the liver and then metabolized into secondary bile acids by the gut microbiota. About 95% of bile acids are reabsorbed through enterohepatic circulation. The interactions between gut

microbiota and the bile acid pool can shape the gut microbiota composition and biological function of bile function. Bile acids can regulate hepatic glucose homeostasis, induce insulin secretion, and reduce inflammation.[118] For instance, lithocholic acid, a secondary bile acid, can stimulate secretion of the gut hormone glucagon-like peptide-1 (GLP-1) and further regulate glucose metabolism and improve insulin sensitivity by binding to G protein-coupled bile acid receptor-1 and the nuclear farnesoid X receptor.[119]

Trimethylamine (TMA) can exclusively be produced by the gut microbes from ingested lecithin, carnitine, choline, and betaine, which are abundant in animal products, particularly in red meat. TMA subsequently diffuses into the hepatic vein and hepatocytes, where it is oxidized by hepatic flavin-containing monooxygenase 3 (FMO3) to trimethylamine *N*-oxide (TMAO).[120] In a case-control clinical study that incorporated 2,694 participants, a higher level of plasma TMAO was linked to an increased risk of T2D.[121] In a recent Mendelian randomization study with 149,821 subjects, genetically predicted higher TMAO was not associated with the incidence of T2D, whereas T2D patients have higher TMAO levels.[122] Diet supplementation of TMAO to T2D mice induced by a high-fat diet exacerbated insulin resistance and impaired glucose tolerance by affecting insulin signaling pathway in the liver, glucose metabolism, and inducing pro-inflammatory immune response in adipocyte.[123] Deletion of FMO3 expression in mice lowered levels of TMAO and glucose as well as insulin in plasma, whereas overexpression of FMO3 caused insulin resistance and led to the increment of glucose secretion *in vitro*.[122] In an intervention study of 504 overweight and obese adults, diet restriction-induced reduction of TMAO led to an improvement in insulin sensitivity.[124]

Indole is produced from tryptophan by the bacterial enzyme tryptophanase.[125] Indole has been reported to affect GLP-1 production by enteroendocrine L-cells.[126] Indolepropionic acid, a derivative of tryptophan produced by gut microbiota, was found to be linked to a lower risk of T2D and decreased inflammation as well as increased insulin sensitivity.[127] Indole-3-acetic acid (IAA), a microbial metabolite from tryptophan, protected against high-fat diet-induced hepatotoxicity in mice by alleviating insulin resistance, lipid accumulation, hepatic oxidative stress, and inflammation.[128]

2.1.4.3. Gut microbiota composition and type 2 diabetes

In human and animal studies, there is no general uniformity in gut microbiota profiles found in T2D patients (**Table 2**). This inconsistency is probably due to confounding variables including the study populations, diet, medication use, and different sequencing platforms, etc. Those variables may not be associated with the disease of interest but probably influence the gut microbiota profile to differing extents.[129]

However, several specific taxa of gut microbes have been repeatedly reported to be associated with T2D. These patients showed higher levels of species from *Lactobacillus* spp.[130–133], and lower levels of *Clostridium* spp.[131,133,134] The abundance of *Lactobacillus* spp. had a positive correlation with plasma levels of glycated hemoglobin (HbA1c) and fasting glucose, whereas the abundance of *Clostridium* spp. negatively correlated with plasma levels of fasting glucose, HbA1c, triglycerides, C-peptide, and insulin, but positively correlated with plasma levels of adiponectin and high-density lipoprotein (HDL) cholesterol.[133] Although *Bifidobacterium* is considered to be a probiotic, both negative[135] and positive[130,136] associations have been reported between *Bifidobacterium* and type 2 diabetes. Two metagenomic sequencing studies organized in Chinese and European cohorts[131,137] and one qPCR study[138] simultaneously found that *Faecalibacterium prausnitzii* and *Roseburia intestinalis*, considered to produce butyrate and have anti-inflammatory properties[139], were decreased in T2D patients. Two recent review articles have shown *Akkermansia muciniphila* concentration was consistently reported as inversely correlated with obesity and diabetes.[83,118] Several experimental studies have shown that administration of prebiotic[140] or metformin[141] would increase the abundance of *Akkermansia muciniphila*, which would possibly induce improvements in metabolic function, glucose tolerance, and systemic inflammation.[83]

The trialogue between gut microbiota, immunity, and metabolism has been constantly reported as being intertwined but has not been fully deciphered, which needs further study.

Table 2. Gut microbiota changes in type 2 diabetes

Subjects	***Method(s)***	***Alterations of gut microbiota in T2D***
80 Chinese: 50 T2D patients and 30 healthy individuals[130]	qPCR	(↑): *Lactobacillus*, *L. bugaricus*, *L. rhamnosum* and *L. acidophilus* (↓): *Bifidobacteria* and *B. adolescentis*
70 Japanese: 60 T2D patients and 10 healthy individuals[136]	16S rRNA seq	(↑): Lactobacillales and *Bifidobacterium* (↓): *Clostridium cluster IV* and *XIVa*
516 Finnish: 352 prediabetes, 164 controls[142]	16S rRNA seq	(↑): *Anaerostipes* (↓): *Christencenellacea*, *Ruminococcaceae*, and *Methanobrevibacter*
36 Danish: 18 T2D patients and 18 controls[134]*	qPCR and 16S rRNA seq	(↑): *Betaproteobacteria* (↓): *Clostridia* and Firmicutes Bacteroidetes/Firmicutes ratio has a positive correlation with glucose level.
345 Chinese: 145 T2D patients and 200 control[137]*	16S rRNA seq	(↓): Butyrate-producing bacteria (*Faecalibacterium prausnitzii, Clostridiales* sp. SS3/4, *Roseburia sp*)
145 Europeans: 53 T2D patients, 49 individuals with impaired glucose tolerance, and 43 individuals with normal glucose tolerance[131]*	16S rDNA seq	(↑): Four *Lactobacillus* spp. (↓): Five *Clostridium* spp.
121 Chinese: 44 controls, 64 prediabetes, 13 T2D patients[143]*	16S rDNA seq	(↓): *Bacteroides*, *Verrucomicrobiae*, and butyrate-producing bacteria (e.g., *Faecalibacterium prausnitzii* and *Akkermansia muciniphila*)
100 Japanese: 50 T2D patients, 50 controls[144]*	RT-qPCR	(↑): *Lactobacillus reuteri, Lactobacillus plantarum* (↓): *Clostridium coccoides*, *Atopoium*, and *Prevotella*
44 Russian: 24 prediabetes, 20 T2D patients and 48 controls[145]*	16S rRNA seq	(↑): *Blautia* and *Serratia*
53 Italian: 40 T2D patients and 13 controls[146]*	16S rRNA seq	(↑): *Collinsella, Enterobacteriaceae, Lactobacillus,* and *Streptococcus* (↓): *Bacteroides* and *Prevotella*
102 Danish: 75 T2D patients and 277 controls[147]*	qPCR & 16s rDNA seq	(↓): *Prevotella copri, Bacteroides vulgatus,* and butyrate-producing bacteria including *Faecalibacterium prausnitzii, Akkermansia muciniphila, Firmicutes sp.*, and *Clostridia sp*.
112 Colombian: 28 T2D patients and 84 controls[148]*	16S rRNA seq	(↑): *Clostridiaceae 02d06* (↓): *Enterococcus casseliflavus*

Subjects	***Method(s)***	***Alterations of gut microbiota in T2D***
40 Chinese ethnic minority: 20 Uygurs and 20 Kazaks; 10 for each T2D and control groups)[149]*	16S rRNA seq	(↑): *Veillonellaceae* (↓): *Planococcaceae* and *Coriobacteriaceae* in Kazaks T2D. *Erysipelotrichaceae* in Uygurs T2D
36 Iranian: 18 T2D and 18 controls[132]	RT-qPCR	(↓): *Bifidobacterium*
268 Danish: 134 prediabetes, 134 controls[150]*	16S rRNA seq	(↑): *Dorea, Sutterella*, and *Streptococcus* (↓): Butyrate-producing bacteria (*Clostridium* and *Akkermansia muciniphilia*)
46 Polish: 23 T2D patients and 23 controls[151]*	16S rRNA seq	(↑): Firmicutes/Bacteroidetes ratio and phylum Verrucomicrobia (↓): SCFA-producing bacteria (*Roseburia* and *Faecalibacterium*)
100 Chinese: 65 T2D patients and 35 controls[152]*	16S rRNA seq	(↑): SCFA-producing bacteria (*Lachnospiraceae* and *Ruminococcaceae*), *Proteobacteria*, and Firmicutes/ Bacteroidetes ratio

Note: The studies with * were adapted from the review.[118]
(↑) and (↓) indicate the increase and decrease of metabolites.
Abbreviations: qPCR, quantitative polymerase chain reaction; SCFA, short-chain fatty acid; T2D, type 2 diabetes; 16S rRNA seq, 16S ribosomal RNA sequencing

2.2. Anthocyanins

2.2.1. Introduction of anthocyanins

Anthocyanins (Greek anthos = flower, and kianos = blue) are natural pigments characterized by the blue, red, or purple colors found in many plants. Chemically, anthocyanins are glycosides of polyhydroxy and polymethoxy derivatives of 2-phenylbenzopyrylium or flavylium salts.

To date, more than 600 different anthocyanins have been identified. Diversities of anthocyanins are due to the number of hydroxy groups, the nature and number of sugar moiety attached to the aglycone molecule, the position of the attachment, and the nature and number of aliphatic or aromatic acids acylated to the sugars in the aglycone molecule. The six most common aglycones are: cyanidin, delphinidin, pelargonidin, peonidin, petunidin, and malvidin (**Figure 1A**).

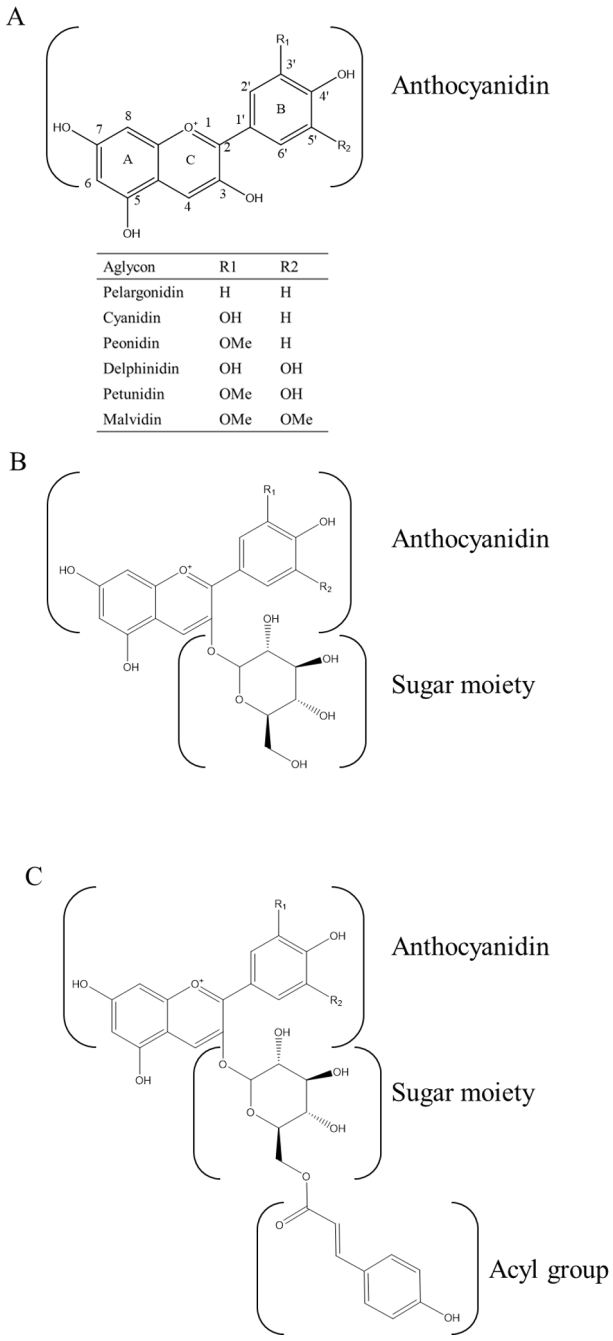

Aglycon	R1	R2
Pelargonidin	H	H
Cyanidin	OH	H
Peonidin	OMe	H
Delphinidin	OH	OH
Petunidin	OMe	OH
Malvidin	OMe	OMe

Figure 1. Structures of common anthocyanins. An example of nonacylated and acylated anthocyanins. Glucose is attached to the C3 position of anthocyanidin (A) to form nonacylated anthocyanin (B). Based on nonacylated anthocyanin, *p*-coumaric acid is acylated with a glucose residue at the C6 position to form acylated anthocyanin (C).

The most common anthocyanidin glycosides are 3-monoglycosides, 3,5-diglycosides 3-triglycosides and 3,7-diglycosides are also found.[153] The most common sugars are glucose, rhamnose, galactose, arabinose, fructose, xylose, as well as rutinose. Structurally different anthocyanins can be found in fruits, vegetables, and tubers, such as grapes, a variety of berries, red cabbage, black carrot, purple corn, red radish, and purple-fleshed potatoes.[154,155] In addition to their use as colorants in the food and cosmetic industry, anthocyanins have been applied in the pharmaceutical industry as anthocyanins exhibit strong antioxidant and antiproliferative activities contributing to the prevention of neuronal disease, cardiovascular disease, inflammation, diabetes, and improvement of vision.[156]

2.2.2. Acylated anthocyanins and nonacylated anthocyanins

Acylation is a common and biochemically significant modification of plant secondary metabolites, which plays a crucial role in altering their polarity and chemical stability.[157] The acylation process of anthocyanins in plants is catalyzed by anthocyanin acyltransferases (ACT), which have a high substrate specificity for both the anthocyanin acceptors and the acyl group donors. In plants, there are mainly two types of ACTs which are classified based on the acyl group donors: the serine carboxypeptidase-like (SCPL) group using acyl-activated sugar as acyl group donor and the BAHD family using acyl-CoA as acyl group donor.[158]

Figure 1B–C shows examples of acylated and nonacylated anthocyanins. The sugar residues attached to the anthocyanidins can be further acylated by enzymes in plants with organic acids which include cinnamic acids such as caffeic acid, *p*-coumaric acid, ferulic acid, sinapic acid, and aliphatic acids such as acetic, malonic, malic, succinic acid. Acyl groups are usually bonded to the C-6 position of the sugar.[159] Multiple acyl groups could be present in the same anthocyanin glycoside molecules, forming poly-acylated anthocyanins.

As reviewed, anthocyanins with acylating groups are more stable during processing and storage than their nonacylated counterparts.[159] Anthocyanin glycosyl acylation typically decreases the polarity of anthocyanins and the stacking of the acyl groups with the pyrylium ring of the flavylium cation reduces the susceptibility of a nucleophile attack by water.[159] This steric hindrance effect of acylated anthocyanins hinders hydrophilic initiation of the interaction between anthocyanins and their membrane carriers (bilitranslocases) in the process of digestion.[160] Carbon-carbon double bonds in the aromatic acyl groups are conjugated systems, which lead to possessing light energy-absorbing and potential electron-donating abilities contributing to the stability of anthocyanins under light irradiation. Free carboxyl groups in some acyl groups could decrease the pH values of the environmental solutions, enhancing the stability of anthocyanins by forming a more stable form (flavylium cations).[161] This physico-chemical change caused by the acylation process leads to acylated

anthocyanins being more resistant to variations in pH, heat, and light[4] and a higher capacity to inhibit lipid peroxidation and higher antioxidant activity[5] than the corresponding nonacylated counterparts.

Bioavailability of anthocyanins is an important issue which should be clarified when addressing their biological effects. A bioavailability study has shown that acylated anthocyanins from purple-fleshed sweet potato have displayed higher resistance to digestion under simulated conditions *in vitro*, when compared to nonacylated anthocyanins from red wine, with a degradation percentage at the intestinal level of about 30% and 45%, respectively.[162] Another bioavailability study has illustrated that acylated anthocyanins showed an 11–14-fold decrease in its recovery (ranged from 0.020 to 0.038 %) in urine compared to their nonacylated counterparts, using purple carrots (*Daucus carota* L.) as the source of anthocyanins.[163] A similar result of lower transport efficiency of acylated anthocyanins compared to nonacylated anthocyanins was also observed in an intestinal caco-2 cell line model.[164] An *in vitro* study showed that 71.8 ± 0.3% of acylated petunidin glycosides from purple potato may reach the colon after simulated digestion.[165] An *in vitro* gastric MKN-28 cell line study showed that the transport efficiency of two acylated anthocyanins extracted and purified from purple sweet potato was lower than nonacylated malvidin 3-*O*-glucoside by 20–30% due to steric hindrance of the more complex structures.[166] Blocking GLUT1 and GLUT3 lowered transport efficiency of both purified acylated and nonacylated anthocyanin, indicating GLUT1 and GLUT3 participated in the anthocyanin absorption.[166] However, a computational study compared the affinity of acylated anthocyanin malvidin 3-*O*-(6-*O*-coumaroyl)-glucoside-5-*O*-glucoside and nonacylated anthocyanin malvidin 3,5-*O*-diglucoside to GLUT1 and GLUT3, with the nonacylated anthocyanin showing higher affinity for GLUT1 and the acylated anthocyanin having higher affinity for GLUT3.[167]

Thus, acylated anthocyanins could be expected to be exposed more to colonic microbiota than nonacylated anthocyanins. The complex anthocyanin-gut microbe interactions in the large intestine shape the gut microbiota profile and short-chain fatty acid production.[168] Those anthocyanin metabolites produced by gut microbiota are further absorbed into the systemic circulation.[169]

2.2.3. Anthocyanins from bilberries and potatoes

The bilberry (*Vaccinium myrtillus* L.) plant is a low-growing shrub and mainly grows in northern Europe and is also found in North America and Asia. Bilberry belongs to the genus *Vaccinium* (**Figure 2A**), which includes, among other species, blueberries (*Vaccinium corymbosum*) and cranberries (*Vaccinium macrocarpon*). In Finland, bilberries grow in moist, coniferous forests and favors moderate shade and moderately humid ground conditions. Bilberries are one of the richest natural source of anthocyanins, which give the blue color to the

berries.[170] The anthocyanins from bilberries consist mostly of glucosides, galactosides, and arabinosides of delphinidin, petunidin, cyanidin, peonidin, and malvidin.[171] The total anthocyanin content of bilberries ranges from 300 to 700 mg/100 g in fresh bilberries depending on growing conditions, and the degree of ripeness of the bilberries.[172]

Potatoes (*Solanum tuberosum* L.), an economically important staple crop, is the fourth largest food crop after wheat, rice, and corn; it prevails across the world and has a successful large-scale production, consumption, affordability, and an easy availability for markets. Potatoes are also a critical crop in terms of food security in the face of population growth and increased demand for food, providing carbohydrates, proteins, minerals (potassium, phosphorous, and magnesium), vitamins (B6, B3, and C), and are rich in antioxidants.[173]

Attention has been drawn to purple-red potatoes because of their antioxidative activities.[174] Anthocyanins are the major components contributing to the color of the potato. Almost all the anthocyanins from purple-red potato anthocyanins are acylated derived from delphinidin, cyanidin, petunidin, pelargonidin, peonidin, and malvidin and acylated with hydroxycinnamic acids, such as coumaric, ferulic, and caffeic acids.[174] As acylated anthocyanins have a better stability compared to nonacylated anthocyanins, purple-red potatoes have great potential to promote public health by increasing the dietary intake of these compounds. The anthocyanin content in dark-colored potatoes ranged from 20 to 150 mg/100 g in the fresh weight in different cultivars.[175] The anthocyanins content of the cultivar 'Synkeä Sakari' used in this study could yield 70 mg/100 g in fresh purple potatoes (**Figure 2B**).[176] As anthocyanins are usually ingested in combination with different food sources, the food matrices could affect the absorption of anthocyanins. Glucose and proteins have been shown to decrease the transport efficiency of anthocyanins by 3–7% in gastric cells and 2–3% in intestinal cells, but starch has not been shown to influence the absorption of anthocyanins[6]. This demonstrates another advantage of the utilization of purple potatoes as a new source of anthocyanins since starches are the major component of the potato.

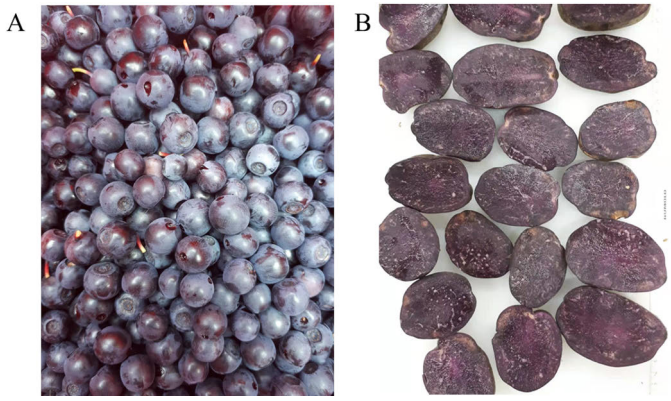

Figure 2. Examples of the phenotypes of bilberries (*Vaccinium myrtillus* L.) (A) and the purple pigmented potatoes (*Solanum tuberosum* L. 'Synkeä Sakari') (B). (Photographs by Maaria Korsteniemi).

2.3. Anthocyanins and type 2 diabetes

The beneficial effects of anthocyanins on type 2 diabetes have been extensively studied *in vitro* and *in vivo*. Anthocyanins are considered to be effective dietary supplements for mitigating type 2 diabetes.[11–13,177–182] **Figure 3** shows the annual number of publications and citations from 2010 to November of 2021 retrieved from the Web of Science index by searching with the keyword "anthocyanins AND diabetes", indicating significantly increased attention to this area.

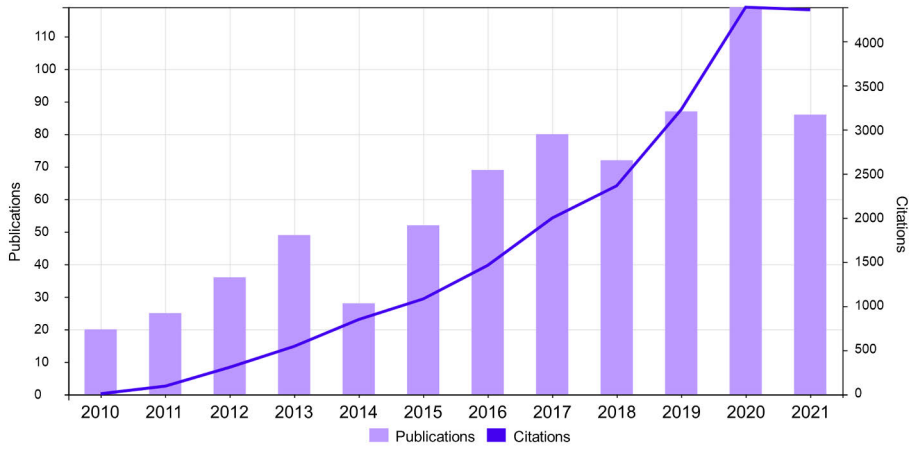

Figure 3. The number of publications and citations per year from a Web of Science searching for articles with the topics "anthocyanins AND diabetes", taken November 2021.

2.3.1. Antidiabetic effect of anthocyanins *in vitro*

One of the antidiabetic mechanisms of anthocyanins is the inhibiting activities of α-glucosidase and pancreatic α-amylase, which shares the same mechanism with some anti-diabetic drugs such as acarbose that aim at mitigating carbohydrate digestion and limiting the absorption of glucose in the digestive system.[183,184]

The inhibition ability of anthocyanins (both acylated and nonacylated anthocyanins) is structure-dependent, as the types of anthocyanidin core and glucosyl group affect the inhibition ability; this has been extensively discussed elsewhere.[185] Recent advances in structure-based design and computational techniques have shown that malvidin 3-*O*-arabinodside and pelargonidin 3-*O*-rutinoside selected from 665 monomeric anthocyanins (nonacylated anthocyanins) were predicted as two of the lowest binding energies with human pancreatic amylase and to interact with amino acid residues of human pancreatic amylase (Asp197 and Glu233) through hydrogen bonds, therefore inhibiting its catalytic mechanism.[186]

Acylated anthocyanins have been reported to have greater inhibitory activity on α-glucosidase and α-amylase (**Table 3**).[187,188] An enzyme inhibition study has shown acylated anthocyanins exhibited stronger inhibitory effects on an immobilized α-glucosidase (e.g., maltase) that mimics the interaction in the small intestine than nonacylated anthocyanins, and that anthocyanin deacylation results in a marked reduction of the inhibitory activity on immobilized maltase.[187] A recent study comparing the inhibitory effect of nonacylated anthocyanin extracts from berries, monoacylated anthocyanin extract from purple sweet potato, and diacylated anthocyanin extract from purple sweet potato against α-amylase and α-glucosidase showed that diacylated anthocyanin possessed the most potent inhibitory ability on these enzymes. Its inhibitory efficacy on α-glucosidase is similar to that of acarbose, which is one of the antidiabetic drugs used to reduce the digestion and absorption of carbohydrates.[188] However, the inhibitory effect of monoacylated anthocyanins showed very little difference from nonacylated anthocyanin extracts, which might be due to a lower concentration of monoacylated anthocyanins. The highest inhibitory activity of diacylated anthocyanins might be due to the higher affinity and certain key enzyme binding sites.[188] This protein-anthocyanin binding might also protect acylated anthocyanins from degradation and increase their antioxidant ability.[189]

In addition, a range of *in vitro* studies conducted on the antidiabetic effect of anthocyanins have been carried out in cell lines including H4IIE rat liver cells, L6 myotubes muscle cells, pancreatic β-cells of rat (INS-1832/13) and mouse (βTC-tet), hepatocytes (HepG2 cells) with induced insulin resistance, 3T3-L1 adipocytes, and Langerhans cells (**Table 3**). Conclusions on the effect of

anthocyanins can be summarized as follows: 1) they decrease glucose production, increase glucose uptake, and increase insulin sensitivity in liver and muscle cell lines,[190] 2) they stimulate insulin release and increase proliferation of β cells in β cell lines[191,192], 3) they suppress the expression of lipogenic and inflammatory factor, decrease leptin secretion, promote lipolytic action, and increase glucose transport in adipocytes cell lines.[193,194]

Table 3 *In vitro* modulatory effects of anthocyanins.

Source of anthocyanins	***Main anthocyanin(s)***	***Model***	***Effects***
Anthocyanins extract from purple sweet potato (*Ipomoea batatas*)[184]	Cya-3-(6"-caf-6"'-hba-sop)-5-glu, peo-3-(6",6"'-dicaf-sop)-5-glu, peo-3-(6"-caf-6"'-p-hba-sop)-5-glu, peo-3-(6"-caf-6"'-fer-sop)-5-glu	Enzyme inhibition study; human liver cell line HepG2 cells	Inhibited α-amylase, α-glucosidase, and xanthine oxidase.
Pure nonacylated anthocyanins[186]	18-20 varieties of nonacylated anthocyanins	Enzyme inhibition study;	Inhibited α-amylase and α-glucosidase. Structure-dependent enzymes inhibition property.
Pure nonacylated anthocyanins and diacylated anthocyanins[187]	Cya-3-(2-(6-fer-gpy)-6-caf-glup)-5-glup; cya- and peo-3-(2-(6-fer-gpy)-6-caf-glup)-5-glup; pg-3-(2-(6-3-gpy-caf)-gpy)-6-caf-glup)-5-glup; pg-3-(2-(6-caf-glu)-6-caf-glup)-5-glup; pg-, cya-, and peo-3-(2-gpy-glup)-5-glup-3-sop-5-glu	Enzyme inhibition study	Diacylated anthocyanin showed the most potent to inhibit α-glucosidase compared to other anthocyanins.
Nonacylated anthocyanin extracts from (*V. corymbosum* L. × *V. angustifolium* Aiton.; *V. ashei* Reade) berries. Monoacylated and diacylated anthocyanin extracts from purple sweet potatoes (*Ipomoea batatas* L. cultivar Eshu No. 8)[188]	Del-, cya-, pet-, peo-, and mal-3-gal, glu, ara; cya-, pet-, and peo-3-hba-sop-5-glu; cya- and peo-3-(6"-caf-sop)-5-glu; cya- and peo-fer-sop-5-glu; cya-3-caf-sop-5-glu; peo-3-(6'-caf-6"-hba-sop)-5-glu; peo-3-(6'-caf-6"-fer-sop)-5-glu	Enzyme inhibition study	Diacylated anthocyanin extracts showed the highest inhibition ability of α-amylase and α-glucosidase than monoacylated anthocyanin extracts and deacylated anthocyanin extract.
Purified anthocyanin: from maqui berry (*Aristotelia chilensis*)[190]	Del-3-sb-5-gluc	H4IIE rat hepatoma cells and L6 myotubes	Decreased glucose production, increase glucose uptake.
Anthocyanin extract from Canadian lowbush blueberry (*Vaccinium angustifolium*)[191]	Not available	βTC-tet cells (Mouse pancreatic islet β cell)	Increased proliferation.

Source of anthocyanins	*Main anthocyanin(s)*	*Model*	*Effects*
Purified anthocyanins from *Cornus* fruits (*C. officinalis and C. mas*)[192]	Cya-3-glu, del-3-glu, cya-3-gal, and pg-3-gal, and anthocyanidins (cyanidin, delphinidin, pelargonidin, malvidin, and petunidin)	Rodent pancreatic β-cells (INS-1832/13)	Enhanced insulin secretion and prevent insulin resistance.
Anthocyanin extract from mulberries (*Morus alba* L.)[196]	Cya-3-glu, cya-3-rut, pg-3-glu, and other phenolic and flavonoid compounds	HepG2 cells	Enhanced the glycogen content and suppressed levels of glucose production by regulating key enzymes.
Standard reference[193]	Cya-3-glu	3T3-L1 adipocytes and human omental adipocytes	Enhanced glucose transport, GLUT4 membrane translocation, and insulin sensitivity.
Anthocyanin extract Purple sweet potato (*Ipomoea batatas* L.)[194]	Not available	3T3-L1 adipocytes	Suppressed leptin secretion. Exerted anti-inflammatory, lipolytic effects on adipocytes and radical scavenging and reducing activity.

Note: Anthocyanidins: cya, cyanidin; del, delphinidin; pg, pelargonidin; peo, peonidin; pet, petunidin. Acyl moieties: caf, caffeoyl; hba, hydroxybenzoyl; fer, feruloyl; mal, malonyl; pyr, pyranosyl; gpy, glucopyranosyl. Sugar moieties: glu, glucoside; gal, galactoside; rut, rutinoside; sop, sophoroside; glup; glucopyranoside; sb, sambubioside.

2.3.2. Antidiabetic effect of anthocyanins *in vivo*

Many diabetic animal models and clinical trials have been applied to the study of the anti-diabetic effect of anthocyanins using either anthocyanin-rich extract or isolated compounds and these studied anthocyanins were mainly from berries in a nonacylated form. The antidiabetic effects of nonacylated anthocyanins have been extensively reviewed.[11–13,177–182] It can be summarized that anthocyanin-rich extracts could improve insulin sensitivity, lipid profile, glucose level, and body weight gain, Their repeatedly reported antidiabetic effects have been focused on energy metabolism and inflammation including 1) inhibiting digestive enzymes; 2) modulating AMP-activated protein kinase (AMPK) activation and AMPK-mediated GLUT4 expression and translocation; 3) suppressing peroxisome proliferator-activated receptor gamma (PPARγ) and phosphoinositide 3 kinase/protein kinase B (PI3K/Akt)-mediated lipid and glucose metabolism; 4) suppressing NF-κB activation and downstream of inflammatory cytokines expression such as IL-1β and IL-6; 5) activating nuclear factor erythroid 2-related factor 2 (Nrf2). Variations in the antidiabetic mechanism of anthocyanins were most likely due to the different sources, extraction methods, differences in composition and structures of anthocyanins studied, and study purposes. In **Table 4**, the recent studies related to antidiabetic effect of anthocyanins, especially acylated anthocyanins are summarized

2.3.2.1. Energy metabolism in type 2 diabetes modulated by anthocyanins

Anthocyanins have been reported to activate AKT and AMPK. When considering the liver and muscles as the major energy expenditure organs, the regulatory effects of the two types of anthocyanins on these two organs are discussed separately.

Similar to nonacylated anthocyanins, feeding acylated anthocyanin extract for 12−32 weeks (200−700 mg/kg body weight/day) also modulated AMPK[197–200] and AKT[201,202] in liver of high-fat diet- or streptozotocin-induced diabetic animals. AMPK-mediated phosphorylation (activation) of acetyl-coenzyme A carboxylase (ACC) contributing to lipid synthesis and PI3K/AKT-mediated suppression of phosphoenolpyruvate carboxykinase (PEPCK) and glucose 6-phosphatase (G6pase) contributing to gluconeogenesis were observed by the intervention of nonacylated anthocyanin extract from berries or acylated anthocyanin extract from purple sweet potatoes. (**Table 4**) Mice fed with a high-fat diet and a daily 200 mg/kg body weight acylated anthocyanin extract from purple sweet potatoes for 4 weeks showed increased phosphorylation of AMPK and ACC in liver compared to mice fed with a high-fat diet alone.[197] Honeyberry nonacylated anthocyanin extract predominant in cyanidin 3-*O*-glucoside showed similar result, that is, an increased phosphorylation of AMPK and ACC in

liver.[203] *Db/db* diabetic mice fed with nonacylated anthocyanin extract from mulberry for 2 weeks showed hepatic activation of AKT and an increased level of PEPCK and G6pase.[28] When an acylated anthocyanin extract from purple sweet potato was given daily to high-fat diet-induced obese mice for 5 weeks, the IRS-1(Insulin receptor substrate 1)/PI3K/Akt pathway was modulated by the extract, which contributed to the hypoglycemic effect.[202] A daily intake of 500 mg/kg body weight acylated anthocyanin extract from purple sweet potato for 4 weeks activated AKT and increased the level of PEPCK and G6pase in the liver of diabetic mice induced by high-fat diet and STZ.[198] Acylated anthocyanins from the fruits of the *Lycium ruthenicum* Murray increased activation of AKT, hepatic gene expression of PEPCK, G6pase, and hepatic and adipose gene expression of GLUT4 in mice with insulin resistance induced by high-fat diet.[204]

The energy regulatory effect of anthocyanin in muscles was relatively less extensively reported compared to the liver. Nonacylated bilberry anthocyanin extract was given to KK-Ay diabetic mice for 5 weeks, AMPK was activated in skeletal muscle, white adipose tissue, and the liver.[200] Intervention of purple corn anthocyanin extract containing both acylated and nonacylated anthocyanins for 8 weeks increased GLUT4 gene expressions in muscle in *db/db* diabetic mice.[199] *Db/db* diabetic mice fed with nonacylated anthocyanin extract from mulberry for 2 weeks activated AMPK and AKT simultaneously and increased levels of GLUT4 in the plasmatic membrane of skeletal muscle[205]; this might have been due to the crosstalk between AMPK and AKT through mTOR and FOXO.[28]

However, AMPK and AKT activation levels and downstream effectors might not always be coherent between nonacylated and acylated anthocyanin. A study compared the AKT phosphorylation ability of acylated and nonacylated anthocyanin in aorta by a single oral dose of acylated anthocyanin extract from purple carrot and equivalent amount of nonacylated anthocyanin (1 mg/kg body weight, cyanidin 3-*O*-glycoside and delphinidin 3-*O*-ruthenoside), acylated anthocyanin extract showed a higher level of AKT phosphorylation compared to other two nonacylated anthocyanins.[206] Potential different antidiabetic targets between acylated and nonacylated anthocyanin are discussed here. Glycerol-sn-3-phosphate acyltransferase (GPAT) is a rate-limiting enzyme in the glycerol 3-phosphate pathway, converting glycerol-3-phosphate and acyl-CoA into phosphatidic acid which is the precursor of triglyceride and glycerophospholipids. Suppression of GPAT1 by nonacylated anthocyanin has been repeatedly reported, for which the potential mechanism might be PPARγ/PKC-mediated.[207–209] However, acylated anthocyanins have not been verified to act through this mechanism, although both types of anthocyanins have shown cholesterol- and TAG-lowering effects in animal models and in humans in recent reviews.[185,210–212] NAD^+ depletion caused by oxidation of excessive substrates (free fatty acid, glucose, and lactate) and other cellular stresses has

been detected and contributed to the dysregulation of energy metabolism and inflammation in type 2 diabetes and obesity.[213,214] Feeding acylated anthocyanin extract from purple sweet potatoes for 20 weeks restored NAD^+ levels in high-fat diet-induced obese mice.[214] Such change has not been reported after intake of nonacylated anthocyanins in obesity and diabetes.

Although anthocyanins have been widely reported to affect key enzymes and genes of metabolic pathways as mentioned above, there has been no study focusing on the effect of anthocyanins on metabolome and transcriptome in diabetes by using omics technologies.

2.3.2.2. Inflammation modulated by anthocyanins in type 2 diabetes

Both types of anthocyanin extracts have been reported to decrease activation of NF-κB, JNK, and their downstream pro-inflammatory cytokines in diabetes (**Table 4**). Supplementation of purple rice anthocyanin extracts (700 mg/kg body weight/day) predominated by cyanidin 3-glucoside to STZ-induced diabetic mice for 4 weeks resulted in decreased levels of TLR-4, phosphorylated IKKβ, and the downstream IL-6 and COX-2 in the heart.[215] Another study showed that supplementation of diets with 8% wild blueberry powder for 8 weeks in obese Zucker rats decreased expression of NF-κB p50, IL-6, and TNF-α in the liver and abdominal adipose tissue and increased adiponectin expression in adipose tissue.[216] Oral administration of nonacylated anthocyanin cyanidin 3-*O*-glucoside (0.2% in diet) for 5 weeks in high-fat diet and *db/db* mice alleviated insulin resistance and pro-inflammatory cytokines (IL-6, TNF-α, and MCP-1), by the modulation of the JNK pathway.[217]

Consuming 700 mg/kg body weight/day acylated anthocyanin extract from purple sweet potatoes for 20 weeks inhibited the activation of IKKβ and JNK1 and improved the IRS-1/PI3k/Akt insulin signaling pathway in liver of high-fat diet-induced obese mice.[202] Feeding acylated anthocyanin extract from purple sweet potatoes for 20 weeks (700 mg/kg body weight/day) to high-fat diet-induced diabetic mice suppressed the NF-κB p65 nuclear translocation and nucleotide oligomerization domain protein1/2 (NOD1/2) signaling as well as the downstream inflammation-related genes (IL-6, IL-1β, MCP-1, TNF-α).[214] The decreased IL-1β might be partly due to the NLR family pyrin domain containing 3 (NLRP3) inflammasome activation by the acylated anthocyanin extract.[214] Acylated anthocyanin extract from black goji berry (*Lycium ruthenicum*) fed to mice with atherosclerosis decreased arterial NF-kB p65 and VCAM-1 expression, plasma TNF-α, and IL-1β, and hepatic CYP7A1 and SREBP-2 expression.[218]

NF-κB can be activated through many membrane receptors in signaling transduction, such as T-cell receptors, TNF receptors, IL-1 receptors, TLR-4, and B-cell receptors, etc.[69] Both types of anthocyanins have been reported to alleviate NF-κB through downregulating TLR-4.[204,215]

Although no study has been conducted to compare acylated and nonacylated anthocyanins in terms of their ability to attenuate the NF-κB pathway, a study comparing the effects of five structurally different anthocyanins on AGEs formation which is able to induce the activation of NF-κB pro-inflammatory signaling, acylated anthocyanins petunidin 3-rutinoside-(coumaroyl)-5-glucoside showed the strongest anti-AGEs effects by reducing the glycation progression, followed by diglycoside of anthocyanidins (cyanidin 3-sophoroside and delphinidin 3-sambubioside) and then monoglycoside of anthocyanidins (pelargonidin 3-glucoside and delphinidin 3-glucoside).[219] This indicates that acylated anthocyanins might have a better role in inhibiting the activation of NF-κB compared to nonacylated anthocyanins.

Acylated anthocyanins from difference food sources may differ in their effects on inflammation pathways. *In vitro*, anthocyanin-rich extracts of purple potatoes and purple carrots suppressed lipopolysaccharide (LPS)-induced phosphorylation of JNK and IkBα in mucosal innate immune cells, purple potato anthocyanins more efficiently inhibited the JNK and IkBα phosphorylation than purple carrots anthocyanins.[165]

Nrf2 is a transcription factor regulating the expression of antioxidant proteins and protecting against oxidative damage triggered by injury and inflammation.[210] Nonacylated anthocyanins have been reviewed to be able to upregulate Nrf2 *in vitro* and in different tissues of animal models[178,210,220], the effect of acylated anthocyanins on Nrf2 has not been studied *in vivo*. An *in vitro* study showed that the anthocyanin fraction of purple sweet potato did not induce Nrf2 transactivation in Huh-7 cells.[184]

Table 4 Modulatory effects of anthocyanins on diabetic or obese animal models.

Source of anthocyanins	***Main anthocyanin(s)***	***Model***	***Effects***
Purple sweet potato (cultivar '*NingZi No. 2*') anthocyanin extract[221]	Peo-3-caf-sop-5-glu, peo-3- (6",6"'-dicaf-sop)-5-glu, peo-3- caf-hba-sop-5-glu, peo-3-(6"-caf-6"'-fer-sop)-5-glu, cya3-(6"-caf-6"'-fersop)-5-glu	HFD-induced obese SD rat; 100-400 mg/kg bodyweight; 6 weeks	Decreased adipocyte number and size of adipose tissue. Decreased glucose, triglyceride, and total cholesterol levels. Reduced the level of ROS and inhibited the receptor of AGE products and thioredoxin interacting protein in the hypothalamus. Preserved the leptin signaling capability, leading to a decrease in hypothalamic AMPK activity.
Acidified ethanol Anthocyanin extract from mulberry (*Morus alba* L.)[201]	Cya-3-glu, cya-3-rut, pg-3-glu	*db/db* mice; 50 and 125mg/kg body weight; 8 weeks	Modulated AKT, GSK3β, and FOXO1 in liver, muscle, and adipose tissues. Decreased triglycerides, LDL, insulin, blood glucose, leptin, β cell protection. Reversed insulin resistance by regulating AMPK/ACC/mTOR pathway.
Anthocyanin powder from two blueberries (*Tifblue and Rubel* cultivars, 1:1)[222]	Del-3-gal, peo-3-glu, mal-3-gal, cya-3-gal, pet-3-gal	Zucker diabetic fatty rats; Diet containing 2% (wt/wt) for 90 days	Reduced triglycerides, fasting insulin. Improved insulin sensitivity. Reduced abdominal fat mass, increased adipose and skeletal muscle PPAR activity, and affected PPAR transcripts involved in fat oxidation and glucose uptake/oxidation (*Fas, Irs1, Pfk, Glut4*)
Anthocyanin extract from mulberry (*Morus alba* L.)[223]	Cya-3 -glu, cya-3-rut, pg-3-glu, pg-3-rut	Zucker diabetic fatty rats; 125 and 250 mg/kg body weight; 5 weeks	Decreased glucose level. Maintained insulin level and β cell histology.
Anthocyanin extract from blueberry (*Vaccinium angustifolium*)[224]	Mal-3-glu, Mal-3-gal, Del-3-gal, Del-3-glu, Mal-3-ara	HFD-induced diabetic C57b1/6J mice; 500 mg/kg body weight for one dose	Hypoglycemic effect.

Source of anthocyanins	***Main anthocyanin(s)***	***Model***	***Effects***
Anthocyanin extract from mulberry (*Morus Australis Poir*)[225]	Cya-3-glu, cyan-3-rut and peg-3-glu	HFD-induced obese C57b1/6J mice; Diet containing 4% (wt/wt); 90 days	Decreased body weight, food intake, cholesterol, triglycerides, glucose, and leptin levels.
Anthocyanin extract from purple rice (*Oryza sativa* L.)[215]	Cya-3-glu	STZ-induced diabetes SD rat; 250 mg/kg body weight; 4 weeks	Decreased blood glucose and gene expression of COX-2 and IL-6 inflammatory marker in heart. Decreased TLR4 protein and p65-NF-κB levels in heart. Activated p-Ikkα/β in heart.
Anthocyanin extract from purple sweet potato (*Ipomoea batatas* L.)[214]	Peo-3-(6-caf-gpy-glup)-5-glu, peo-3-(2-(6-caf-gpy)-6-caf-glup)-5-β-D-glup, peo-3-(2-(6-fer gpy)-6-caf glup)-5-glup, cya-3- (6-cou)-glup	HFD-induced obese C57BL/6 mice; 700 mg/kg/day; 20 weeks	Ameliorated obesity and liver injuries. Blocked hepatic oxidative stress. Restored NAD^+ level in liver. Suppressed the NF-κBp65 nuclear translocation, NOD1/2 signaling, the NLRP3 inflammasome activation and inflammation-related genes (TNF-α, MCP-1, and IL-1) in liver.
Commercial bilberry anthocyanin extract (*Vaccinium myrtillus*)[200]	Not available	KK-A^y diabetic mice; Diet containing 2.7% (wt/wt); 5 weeks	Decreased blood glucose and triglycerides and cholesterol. Improved insulin sensitivity. Inactivated acetyl-CoA carboxylase and activated PPARa, acyl-CoA oxidase, and carnitine palmitoyltransferase-1A in liver. Decreased PEPCK and G6pase in liver. Activated AMPK in white adipose tissue, skeletal muscle, and the liver. Upregulated GLUT4 in white adipose tissue and skeletal muscle
Anthocyanin extrat from bilberry (*Vaccinium myrtillus*)[226]	Del-, cya-, pet-, peo- and mal--derived nonacylated anthocyanins	high-sucrose diet-induced insulin resistant mice; 0.2 mg/mL anthocyanin in	Showed the antioxidant property and changed genes expression in metabolic pathway (*ACC1, Bcl2, Akt, mTOR, GPDH1, HK2, GLUT1*, and *GLUT4*).

Source of anthocyanins	*Main anthocyanin(s)*	*Model*	*Effects*
		drink water;15 weeks	
Purified anthocyanin extracted from purple corn[227]	Cya-3-glu	KK-Ay diabetic mice; Diet containing 0.2% (wt/wt) for 12 weeks	Normalized hyperglycemia, hyperinsulinemia and hyperleptinemia. Decreased gene expression of *Fas, Gpat, Srebp-1* in liver.
Purified anthocyanin[207]	Cya-3-glu	KKAy diabetic mice; Diet containing 100 mg/kg; 12 weeks	Ameliorating hepatic steatosis by decreasing hepatic mtGPAT1 activity. Anthocyanin inhibits high glucose-induced hepatic mtGPAT1 activation and prevents fatty acid synthesis through PKC.
Purified anthocyanin[228]	Cya-3-glu	*db/db* diabetic mice; Diet containing 100 mg/kg; 8 weeks	Increased the GSH synthesis through PKA-CREB-dependent induction of Gclc expression. Attenuated lipid peroxidation, neutrophil infiltration, and hepatic steatosis.
Anthocyanin extract from mulberry (*Morus alba* L.) fruits[229]	Que-3-glu and other phenolic acids	HFD- induced obese Syrian golden hamster; Diet containing 2% (wt/wt); 12 weeks	Reduced serum triacylglycerol, cholesterol, free fatty acid, and the LDL/ HDL ratio. Decreased hepatic lipids and hepatic PPAR-γ, fatty acid synthase, and HMG-CoA reductase.
Anthocyanin extract from purple sweet potato (*Ipomoea batatas* L.)[230]	Peo-3-(6-caf-gpy-glup)-5-glu, peo-3-(2-(6-caf-gpy)-6-caf-glup)-5-β-D-glup, peo-3-(2-(6-fer gpy)-6-caf glup)-5-glup, cya-3- (6-cou)-glup	HFD- induced obese C57BL/6 mice; 500 mg/kg/day; 32 weeks	Alleviated the cognitive impairment. Decreased the expression of Iba1, TNF-α, IL-1β, SOCS3, galectin-3 in hippocampus. Increased insulin signaling molecules including the p-IRS1 (Tyr608), PI3K p110α, and p-AKT (Ser473). Increased Bcl-2, diminished the Bak and the cleaved-caspase3 in hippocampus.
Purple sweet potato anthocyanin extract (*Ipomoea batatas* L.)[197]	Peo-3-(6-caf-gpy-glup)-5-glu, peo-3-(2-(6-caf-gpy)-6-caf-glup)-5-β-D-glup, peo-	HFD- induced obese ICR mice;	Reduced weight gain and hepatic triglyceride accumulation and improved serum lipid parameters.

Source of anthocyanins	*Main anthocyanin(s)*	*Model*	*Effects*
	3-(2-(6-fer gpy)-6-caf glup)-5-glup, cya-3- (6-cou)-glup	200 mg/kg per day;4 weeks	Increased the phosphorylation of AMPK and acetyl-coenzyme A carboxylase (ACC) in the liver.
Purple sweet potato anthocyanin extract (*Ipomoea batatas* L.)[202]	Cyanidin acyl glucosides and peonidin acyl glucosides	HFD- induced obese ICR mice; 700 mg/kg/day; 20 weeks	Improved the fasting blood glucose level, glucose, insulin tolerance and oxidative-stress-mediated endoplasmic reticulum stress. Suppressed ROS production and GSH and antioxidant enzymes activities. Suppressed the JNK1and Ikb kinase β activation and NFkB p65 nuclear translocation. Restored the impairment of the insulin receptor substrate-1/phosphoinositide 3 kinase/protein kinase B (Akt) insulin signaling in the livers.
Purple sweet potato anthocyanin extract (*Ipomoea batatas* L.)[198]	Cya-3-sop-5-glu, peo-3-sop-5-glu, cyanidin-3-hba-sop-5-glu, peo-3-hba-sop-5-glu, cya-3-(6″-fer- sop)-5-glu, peo-3-(6″-fer-sop)-5-glu, cya-3-caff-hba-sop-5-glu, cya-3-(6″-caff-sop)-5-glu, cya-3-(6″-caf-6‴-fer-sop)-5-glu, peo-3-caf-hba-sop-5-glu, peo-3-caf-sop-5-glu, peo-3-(6″-caf-6‴-fer-sop)-5-glu, Peo-3-(6″-hba-6‴-fer-sop)-5-glu	HFD and streptozotocin - induced obese ICR mice 500 mg/kg body weight; 12 weeks	Activated AMPK in liver Increased GLUT4, glucokinase, and insulin receptor α in liver. Upregulated glycolysis key genes (*Pfk* and *Pkm*) Downregulated gluconeogenic genes (*G6pase* and *Pepck*).
Acylated anthocyanin extract from purple carrot and pure cya-3-glu and del-3-rut[206]	Cya-3-(2″-xyl-6-glu-gal), cya-3-(2″-xyl-gal), cya-3-(2″-xylose-6″-sin-glu-gal, cya-3-(2″-xyl-6″-fer-glu-gal, cya-3-(2″-xyl-6″(4-cou)-glu-gal	Wistar rats; Single intragastric doses	Acylated anthocyanin induced the highest level of Akt phosphorylation in aorta than cya-3-glu and del-3-rut
Blue Congo potatoes[231]	Acylated anthocyanins dominant by pet-3-cou-rut-5-glu	Streptozotocin-induced diabetic Wistar rats; 165 mg/kg bodyweight; 2 weeks	Lowered blood glucose, glycated hemoglobin, malondialdehyde levels in plasma. Restored antioxidant enzyme activities Improved glucose tolerance, Inhibited oxidative modified proteins OMP, AGE, and advanced oxidation protein products formation in plasma.

Source of anthocyanins	***Main anthocyanin(s)***	***Model***	***Effects***
Anthocyanin extract from Mulberry (*Morus alba* L.)[205]	Cya-3-glu, cya-3-rut	*Db/db* diabetic mice; diet containing 0.5%, w/w; 6 weeks	Decreased blood levels of glucose and HbA1c Increased insulin sensitivity. Activated pAMPK and p-Akt substrate of 160 kDa (pAS160) and enhanced GLUT4 in skeletal muscles. Increased pAMPK and decreased the levels of G6pase and PEPCK in the liver.
Anthocyanin extract from Honeyberry (*Lonicera caerulea*)[203]	Nonacylated anthocyanin dominant by cya-3-glu	HFD-induced obese ICR mice; diet containing 0.5%-1%, w/w; 6 weeks.	Decreased the expressions of adipogenic genes (SREBP-1c, C/EBPα, PPARγ, FAS) in liver. Increased mRNA and protein levels of CPT-1 and PPARα and increased the phosphorylation of AMPK and ACC in liver.
Anthocyanin extract from purple corn (*Zea mays* L.)[199]	Nonacylated anthocyanins dominant by cya-3-glu and peo-3-glu; acylated anthocyanins dominant by cya-3-(6"-mal-glu) and peo-3-(6"-mal-glu)	*db/db* diabetic mice; 10 or 50 mg/kg body weight; 8 weeks	Increased C-peptide and adiponectin and decreased HbA1c and glucose levels in plasma. Prevented pancreatic β-cell damage and increased insulin content. Increased the phosphorylation of AMPK and decreased PEPCK, G6pase genes in liver, and increased GLUT4 expression in skeletal muscle.
Anthocyanin extract from black goji berry (*Lycium ruthenicum*)[218]	Pet-3-rut-cou-5-glu as the main anthocyanin	HFD and vitamin-D3- induced atherosclerosis rat, 50-200 mg/kg body weight; 8 weeks	Decreased TG, TC, LDL-C, TNF-α, IL-6 levels, and atherogenic index and increased HDL-C concentrations. Upregulated NF-κB, VCAM-1, and CYP7A1, and downregulated SREBP-2.
Anthocyanin extract from black goji berry (*Lycium ruthenicum*)[204]	Del-3-6″-rha-glu-5-glu, pet-3-rut-cou-5-glu, pet-3-rut-caf-5-glu, pet-3-6-cou-rha-pyr)-glup-5-glup	HFD-induced insulin resistance C57BL/6J mice; 50-200 mg/kg body weight; 12 weeks	Decreased weight gain, hepatic lipid, dyslipidemia, inflammation, and oxidative stress. Inactivated TLR4/NF-κB/JNK in the liver tissues and ameliorated oxidative stress and insulin resistance by activating the Nrf2/HO-1/NQO1 and IRS-1/AKT pathways.

Note: Anthocyanidins: cya, cyanidin; del, delphinidin; mv, malvidin; pg, pelargonidin; peo, peonidin; pet, petunidin. Acyl moieties: ace, acetyl; caf, caffeoyl; cou, coumaroyl; hba, hydroxybenzoyl; mal, malonyl; oxa, oxaloyl; sin, sinapoyl; suc, succinyl; pyr, pyranosyl; gpy, glucopyranosyl. Sugar moieties: glu, glucoside; gal, galactoside; rut, rutinoside; sop, sophoroside; xyl, xyloside; glup; glucopyranoside. Other abbreviations: ACC, acetyl-CoA carboxylase; AKT, protein kinase B; AMPK, AMP-activating protein kinase; Bcl-2, B-cell lymphoma 2; CPT, carnitine palmitoyltransferase; CYP7A1, cytochrome P450 family 7 subfamily A member 1; C/EBPα, CCAAT enhancer binding protein α; FAS, fatty acid synthase; FOXO1, forkhead box protein O1; Gclc, glutamate--cysteine ligase catalytic subunit; GSK3, Glycogen synthase kinase-3; GLUT, glucose transporter; G6pase, Glucose 6-phosphatase; HbA1c, hemoglobin A1c; HFD, high-fat diet; HMG-CoA, 3-hydroxy-3-methylglutaryl-CoA; HO-1, Heme oxygenase 1; IL, interleukin; IRS-1, Insulin receptor substrate 1; mtGPAT1, mitochondria glycerol-3-phosphate acyltransferase 1; mTOR, mammalian target of rapamycin; NF-κB, nuclear factor-κB; NLRP3, NOD-, LRR- and pyrin domain-containing protein 3; Nrf2, nuclear factor-erythroid factor 2-related factor 2; NOD, nucleotide-binding oligomerization domain; NQO1, NAD(P)H quinone dehydrogenase 1; SOCS3, suppressor of cytokine signaling 3; SREBP-2, sterol regulatory element-binding protein 2; TNF, tumor necrosis factor; PEPCK, phosphoenolpyruvate carboxykinase; PPARγ, peroxisome proliferator-activated receptor γ; VCAM-1, vascular cell adhesion protein 1.

The potential antidiabetic effects of anthocyanins have been studied in several clinical trials. **Table 5** summarizes studies related to the effect of anthocyanins on plasma glucose, lipids, and insulin resistance in patients who are overweight, have metabolic syndrome, or have T2D. Obese and insulin resistance patients consuming a smoothie containing 22.5 g blueberry powder (1:1 mixture of *Vaccinium ashei* and *V. corymbosum*) twice a day for 6 weeks showed an increased insulin sensitivity in 67% of the patient compared to the control group.[232] An intervention study showed that consumption of a capsule containing 80 mg anthocyanin from bilberries (*V. myrtillus*) and black currents (*Ribes nigrum*) significantly decreased the serum triglycerides by 23.0%, serum LDL (low-density lipoprotein cholesterol) by 7.9%, and increased serum HDL (high-density lipoprotein cholesterol) by 19.4% in T2D patients.[233]

Intake of anthocyanin extract or intact fruit containing anthocyanins showed different results on postprandial insulin and inflammatory response. In addition, long-term anthocyanins intervention studies resulted in controversial outcomes related to the systemic lipid profile and glucose level.[234–238] The substantiation of the antidiabetic effect of anthocyanins in clinical trials is far from complete, this is because of the small number of subjects, diverse dosages, and methods of anthocyanins preparation, as well as the small amount of information about the anthocyanin purities in these studies.

Despite the inconsistency between and within the animal and human studies, the beneficial effect of anthocyanins has been widely observed. However, these studies have failed to recognize the differences in biological function due to the difference in molecular structures between acylated and nonacylated anthocyanins and their effect on the metabolic profile. Moreover, there has been renewed interest in the biological function and the potential for application of acylated anthocyanins.

Table 5. The potential antidiabetic effects of anthocyanins shown in clinical trials

Source of anthocyanins	***Subject***	***Dosage and intervention period***	***Effects***
Commercial bilberry (*Vaccinium myrtillus*) anthocyanins extract capsule[239]	16 overweight volunteers	0.47 g bilberry extract for one dose	Improved oral glucose tolerance but not for plasma insulin level and anti-inflammatory markers.
Freeze-dried highbush blueberries (50/50 blend of *Vaccinium virgatum* and *Vaccinium corymbosum*)[234]	52 men with type 2 diabetes	22 g freeze-dried blueberry twice a day for 8 weeks	Lowered hemoglobin A1c, triglycerides, AST, and ALT. Fasting plasma glucose, serum insulin, total cholesterol, LDL, HDL, C-reactive protein concentrations, blood pressure, and body weight were not changed.
Dried strawberry (*Fragaria*×*ananassa*) and cranberry (*Vaccinium macrocarpon* L.) polyphenol extracts[235]	41 insulin-resistant overweight or obese human subjects	333 mg extracts daily for 6 weeks	Improved insulin sensitivity. No differences were detected for total cholesterol, triglyceride, fasting glucose, markers of inflammation, and oxidative stress.
Freeze-dried mixed blueberry (1:7, *Vaccinium angustifolium Aiton*: *Vaccinium corymbosum* L)[236]	48 participants with metabolic syndrome	50 g freeze-dried blueberries daily for 8 weeks	Decreased systolic and diastolic blood pressures. Serum glucose, total cholesterol, and triglyceride were not affected.
Pomegranate juice (anthocyanins 100.46 mg/L, total phenolics 69 mg/L, total flavonoids 283.02 mg/L)[237]	30 participants with metabolic syndrome	500 ml daily for 7 days	Improved triglyceride and VLDL, fasting blood glucose, insulin, and HOMA-IR of the participants did not show any significant difference.
Bilberry (*Vaccinium myrtillus*)[238]	47 participants with metabolic syndrome	200 g bilberry purée for 8 weeks (total 1.38 g anthocyanins)	Decreased fasting serum triglycerides. Fasting blood glucose, cholesterol, and insulin were not infected.

Source of anthocyanins	***Subject***	***Dosage and intervention period***	***Effects***
Anthocyanin extracts from bilberry (*Vaccinium myrtillus*) and blackcurrant (*Ribes nigrum*)[233]	58 diabetic patients	160 mg anthocyanins extract daily for 24 weeks	Decreased serum LDL, triglycerides, fasting plasma glucose, and insulin resistance. Increased total radical-trapping antioxidant parameter.
Commercial strawberry powder[240]	24 overweight adults	34 g strawberry powder for one dose	Attenuated the postprandial inflammatory response and increased insulin sensitivity.

Abbreviations: AST, aspartate aminotransferase; ALT, alanine aminotransferase; HDL, high-density lipoprotein; HOMA-IR, homeostatic model assessment for insulin resistance); LDL, low-density lipoprotein; VLDL, very-low-density lipoprotein.

2.3.3. Gut microbiota modulated by anthocyanins in type 2 diabetes

The hydrolases in the upper intestine, including β-glucosidase, cannot hydrolyze all glycosidic bonds of anthocyanins and thus many anthocyanins remain in an intact form, such as anthocyanidin-rhamnoside, -rutinoside, and others.[241] Moreover, there are no endogenous esterases in humans to release phenolic acids of acylated anthocyanin. Thus, the esterase activity of colonic microflora is required for the metabolism of acylated anthocyanin.[242] As aforementioned, a large amount of nonabsorbed anthocyanins reaching the colon are metabolized by gut microbiota and acylated anthocyanins may be more exposed to gut microbiota than nonacylated anthocyanins.[165] The complex anthocyanin-gut microbe interactions in the colon also shape the gut microbiota profile and short-chain fatty acid production.

The most abundant metabolites of acylated and nonacylated anthocyanin are phenolic acids and phenolic acid conjugates which have been extensively reviewed elsewhere.[180,185] Although nonacylated anthocyanins have been repeatedly reported to modulate the abundance of *Bifidobacteria* spp., *Lactobacilli* spp., and *Clostridium* spp..[178,180] However, contradictory results have been observed. For example, nonacylated anthocyanins extract from blackcurrant increased the abundance of *Bifidobacterium* spp. in healthy humans[243], while black raspberry decreased the abundance of *Bifidobacterium* in F-344 rats.[244] This might be due to interspecies differences, different metabolic states, and anthocyanin vehicles as well as structures of anthocyanins in these studies. To address these influences, this review examined the gut microbiota regulation effect of anthocyanins on the condition of obesity and diabetes for the first time and the acylated anthocyanins-related gut microbiota studies are also included in **Table 6**.

Feeding high-fat diet-induced obese mice with daily 150 mg/kg body weight black rice nonacylated anthocyanin extract for 14 weeks increased the abundance of *Bacteroides*, *Akkermansia*, *Lactobacillus*, *Ruminococcaceae,* and *Alloprevotella* at genus level; at the species level, the extract decreased the proportions of *Dorea_sp._*5-2 *Blautia coccoides*, *Lactobacillus gasseri*, *Mucispirillum schaedleri*, *Akkermansia muciniphila*, and *Parabacteroides merdae*, while the diversity and richness of the microbiota were not changed.[245] Supplementation of the diet containing 2.35% freeze-dried strawberry to diabetic *db/db* mice for 10 weeks increased gut microbiota diversity and decreased the abundance of Verrucomicrobia at the phylum level.[246] Feeding purified cyanidin 3-glucoside (7.2 mg/kg/day) and Saskatoon berry powder containing cyanidin-3-glucoside (8.0 g/kg/day, equivalent cyanidin 3-glucoside in the berry) to high fat-high sucrose diet-induced insulin-resistant C57 BL/6J mice for 11 weeks resulted in a decrease of *Lachnospiraceae* and *Erysipelotrichaceae* and an

increase of the Bacteroidetes/Firmicutes and family *Muriculaceae*.[247] Increased abundance of *Prevotella* and Bacteroidetes/Firmicutes ratio and strengthened gut barrier integrity were found in *db/db* diabetic mice when fed with 150 mg/kg body weight pelargonidin 3-*O*-glucoside for 8 weeks.[248]

Very few studies have been carried out on the modulatory effect of acylated anthocyanins on gut microbiota in obesity and type 2 diabetes. Incubation of purple sweet potato acylated anthocyanins extract with gut microbiota *in vitro* induced the growth of *Bifidocterium* and *Lactobacillus* spp., inhibited the growth of *Prevotella* and *Clostridium histolyticum*, and increased SCFAs production.[249] Acylated and nonacylated might have different impacts on gut microbiota composition in diabetes. An *in vitro* study compared the effect of purified nonacylated anthocyanin, monoacylated anthocyanin, and diacylated anthocyanin on antioxidant abilities and prebiotic activity, the results showed that diacylated anthocyanin has the best antioxidant ability and inhibition on growth of harmful bacteria (*Staphylococcus aureus* and *Salmonella typhimurium*) followed by monoacylated anthocyanin and then nonacylated anthocyanin.[250] One study compared the effect of the supplementation of acylated anthocyanin-rich Concord grape on the gut microbiota composition at the phylum level in obese mice for 12 weeks with nonacylated anthocyanin-rich berries. Obese mice fed with Concord grape showed the highest level of Actinobacteria, followed by obese mice fed with berries and then obese mice.[251]

Table 6 The gut microbiota regulation effects of anthocyanins on obesity/diabetes and effects of acylated anthocyanins on gut microbiota.

Source of anthocyanins	***Main anthocyanin(s)***	***Methods***	***Effect***
Anthocyanin extract from black rice (*Oryza sativa* L. Japonica)[245]	Cya-3,5-diglu, cya-3-glu, cya-3-rut, peo-3-glu	HFD- induced obese C57BL/6J mice; 150 mg/kg bodyweight; 14 weeks	Decreased body weight gain, triglycerides, total cholesterol, steatosis scores, and insulin resistance index. Improved the gene expression profiles involved in lipid metabolism. Increased the abundances of *Bacteroides*, *Akkermansia*, *Lactobacillus*, *Ruminococcaceae_UCG014,* and *Alloprevotella* at genus level; at the species level, decreased the proportions of *Dorea_sp._5-2 Blautia coccoides*, *Lactobacillus gasseri, Mucispirillum schaedleri, Akkermansia muciniphila* and *Parabacteroides merdae.* The diversity and richness of microbiota were not changed.
Freeze-dried strawberry[246]	Not available	*Db/db* diabetic mice; diet containing 2.35% freeze-dried strawberry; 10 weeks	α-diversity and β-diversity were different at the phylum and genus levels. At the phylum level, decreased the abundance of Verrucomicrobia; at the genus level, increased *Bifidobacterium*. PICRUSt revealed significant differences in 45 predicted metabolic functions.
Purified anthocyanin[247]	Cya-3-glu	High fat-high sucrose diet-induced insulin-resistant C57 BL/6J mice; 7.2 mg/kg body weight; 11 weeks	Decreased *Lachnospiraceae* and *Erysipelotrichaceae* and increased the Bacteroidetes/Firmicutes and family *Muriculaceae*.
Purified anthocyanin[248]	Pg-3-glu	*db/db* diabetic mice; 150 mg/kg body weight; 8weeks	Decreased plasma glucose and promoted glucose uptake. Induced autophagy by modulating Transcriptional factor EB. Increased abundance of *Prevotella*, Bacteroidetes/Firmicutes ratio, and intestinal barrier integrity.

Source of anthocyanins	***Main anthocyanin(s)***	***Methods***	***Effect***
Concord grape freeze-dried powder[251]	Acylated mono-glycosylated delphinidins and petunidin	Polygenic obese C57 BL/6J mice; the dose of grape powder normalized to 400 μg/g total anthocyanin content; 12 weeks	Increased the abundance of Actinobacteria.
Anthocyanin extract from black goji berry (*Lycium ruthenicum*)[218]	Pet-3-rut-cou-5-glu as the main anthocyanin	High-fat diet and vitamin-D3- induced atherosclerosis rat with obesity, 50-200 mg/kg body weight; 8 weeks	Increased the abundance of *Bifidobacterium, Lactobacillus, Roseburia, Akkermansia,* and *Lachnospiraceae_NK4A136_group* and decreased *Prevotellaceae_NK3B31_group.* Improved gut barrier.
Anthocyanins extract from purple sweet potato (*Ipomoea batats* L. Lam)[249]	Cya-3-caf-cou-diglu-5-glu, cya-3-fer-sop-5-glu, cya-3-sin-diglu-5-xyl, pg-3-ace-diglu-5-glu, cya-3-hba-oxa-diglu-5-glu, cya-3-diglu-5-glu, cya-3-difer-sop-5-glu, cya-3-caf-fer-sop-5-glu	In vitro stimulation of gut microbiota	Induced the growth of *Bifidocterium* spp. and *Lactobacillus* spp. and inhibited the growth of *Prevotella* and *Clostridium histolyticum.* Increased SCFAs.
Purified anthocyanins from purple sweet potato (*Ipomoea batatas* L. Lam.)[250]	Peo-3-sop-5-glu; peo-3-fer- sop-5-glu; peo-3-caf-sop-5-glu; peo-3-caf-hba-sop-5-glu; peo-3-caf-fer-sop-5-glu	Antioxidant activities, proliferative effects on probiotics, and their inhibition on harmful bacteria *in vitro* were tested	Diacylated anthocyanin had the best antioxidant ability and inhibition ability to harmful bacteria (*Staphylococcus aureus* and *Salmonella typhimurium*), followed by monoacylated anthocyanin and nonacylated anthocyanin.

Note: Anthocyanidins: cya, cyanidin; del, delphinidin; mv, malvidin; pg, pelargonidin; peo, peonidin; pet, petunidin. Acyl moieties: ace, acetyl; caf, caffeoyl; cou, coumaroyl; hba, hydroxybenzoyl; fer, feruloyl; mal, malonyl; oxa, oxaloyl; sin, sinapoyl; suc, succinyl; pyr, pyranosyl; gpy, glucopyranosyl. Sugar moieties: glu, glucoside; gal, galactoside; rut, rutinoside; sop, sophoroside; xyl, xyloside; glup; glucopyranoside

2.4. “Omics'' technology

As the comprehensive understanding of mammalian systems biology is being enhanced, and emerging challenges in the health context, for example, metabolic disease, new infectious agents, antibiotic resistance, or even the increased prevalence of cancer, high-throughput analytical technologies and techniques have been introduced. These technologies and techniques measure and profile multilevel biomolecular structures and metabolic processes, from the single-cell level to the systemic level.[252]

In general, the scientific research fields linked with the measurement of such biological molecules by a high-throughput technology are called “omics”. Omics approaches are referred to as the “collective characterization and quantification of pools of biological molecules that translate into the structure, function, and dynamics of an organism”[253], such as genomics, transcriptomics, proteomics, metabolomics.

The ending “ome” is used to address the targets of the “omics” study, such as the genome, proteome, transcriptome, or metabolome, respectively. More specifically, the genome includes the information about the gene structure, sequences, function, and evolution. Genomics aims at a characterization and quantification of genes. The transcriptome is the full range of all messenger RNA in a cell, tissue, or organism. Transcriptomics aims to identify and quantify each RNA molecule. The proteome is the set of all the proteins in an organism. Proteomics is the study of those proteins in relation to their biochemical properties and functional roles. The metabolome is the collection of all metabolites in a cell, tissue, or organism, which are the end products of the metabolic processes. Metabolomics aims to perform metabolic profiling or quantify all metabolites involved in the metabolic processes.[254]

2.4.1. NMR metabolomics

Metabolomics aims to measure the small molecules derived from biochemical processes, known as metabolites, which create a “snapshot” of the metabolic state of cells, tissues, or biofluids and directly reflects the underlying biochemical activity and their interactions in a biological system.

In the field of medicine, diagnosing and predicting diseases has been implemented by metabolomics using serum, urine, feces, and tissue extracts. The key step in metabolomics lies in extracting information about the metabolites from complex spectroscopy whether it is derived from nuclear magnetic resonance (NMR) spectroscopy or other approaches, such as mass spectrometry including LC-MS (liquid chromatography-mass spectrometry), GC-MS (gas

chromatography-mass spectrometry), CE-MS (capillary electrophoresis-mass spectrometry), and FT-IR (Fourier transform infrared spectroscopy), etc.

The advantages of using NMR for metabolomics compared to other metabolomic approaches include the fact that:

1. It needs only little or no separation from the samples, keeping the metabolic state in the original stage that the study purpose requires. It is also non-destructive as regards the samples which can also be further used and tested. It needs no chemical derivatization (e.g., silylation required in GC) before testing.

2. It provides non-biased identification and quantification. Usually, standards are added to the samples and set as 0 ppm. The most common standards are Tetramethylsilane (TMS), Sodium trimethylsilylpropanesulfonate (DSS), and Trimethylsilylpropanoic acid (TSP). Standards allow every metabolite to match their identical chemical shift.

3. It does not require identical spectral acquisition conditions. The difference in the sample and solvent preparation, the conditions for the equipment (especially for columns) for LC-MS or GC-MS metabolomics renders a low analytical reproducibility. For NMR metabolomics, the accurate identification of metabolites could be achieved everywhere.

4. It allows the identification of novel compounds, 2D spectra, and other techniques, e.g., LC-NMR, help researchers elucidate unknown compounds.

5. NMR is particularly amenable to compounds that are less tractable to GC-MS or LC-MS analysis (e.g., sugars, amines, volatile ketones, and relatively non-reactive compounds)

6. It yields less solvent waste compared to the MS methods, which means it is more environmentally friendly.

The richness of chemical information that is "NMR visible" makes it a feasible technic for researchers. NMR spectroscopy has been applied in studying metabolic processes since the early 1970s, when scientists applied an isotope-tracer to study ethanol metabolism.[255] NMR spectroscopy is considered to be a high-throughput fingerprinting technology. Commonly, 10 to 100 or more samples are involved in one typical 1D ^{1}H NMR experiment and 25-200 metabolites could be identified depending on the sample resources. However, the sensitivity of NMR analysis to the chemical environment is recognized as a challenge. Changes in pH, ionic strength, temperature, protein content, etc. among samples will cause differences in the chemical shift and line widths. Thus, this approach often requires precisely controlled pH and/or temperature when preparing the samples to avoid possible peak shifting.

2.4.2. Data-processing before interpreting ^{1}H NMR spectra

Proton signals acquired with the ^{1}H NMR instrument are in the time domain, which needs to be transformed into a form of data in the frequency domain. Fourier transform (FT) provides the solution. To tackle significant phase distortions or non-zero baselines caused by water signals or other abundant metabolites, phase correction must be applied. Baseline artifacts can be from various aspects, e.g., the presence of macromolecules, signals from compounds that heavily overlap, and others.[256]

Unstable NMR spectrometer and improper shimming could impose unexpected distortions to the line shape due to the inhomogeneity of the magnetic field. These distortions impede all signals in the same way. Reference deconvolution giving a single peak is used to correct distortions by using a reference signal to compensate the distortions caused by the unstable spectrometer.[257] One of the applications is that when a spectrum with broad linewidth, a reference deconvolution (e.g., shim correction in Chenomx software) could be applied to obtain a perfect line shape and then subjected to further identification and quantification. However, this cannot be applied in spectra with an extremely broad linewidth, e.g., a linewidth greater than 2-3 Hz could lead to a large number of zigzags in the line shape.

As discussed above, a chemical shift of certain metabolites could be changed in the spectra due to differences in the sample pH, temperature, and ionic strengths, etc. Thus, spectral alignment is extremely crucial to spectra binning and further subsequent analysis, which can shift and align peak positions in spectra and ensure that the peaks in the same chemical shift correspond to the same compounds and their peak intensity can be comparable after binning. Different sample types have different vulnerabilities to being affected by environmental factors, such as pH. Serum is most stable and less likely to have signals with a chemical shift drift because serum is a "natural buffer" with a constant pH of around 7.4. In the case of other sample types, for instance, various tissues and feces, mixing a pH buffer solution to the sample (e.g., 90 mmol/L NaH_2PO_4, pH = 7.4) could stabilize the pH and ionic strengths of the sample. If adding extra buffer cannot be achieved or is not practical due to large numbers of samples and diluted samples (e.g., urine), several computational methods have been introduced, as reviewed comprehensively, such as interval correlated shifting (*i*coshift), correlation optimized warping (COW), fuzzy warping, peak alignment by beam search, dynamic time wrapping, and hierarchical cluster-based peak alignment.[258]

2.4.3. Two approaches to interpret metabolomic NMR spectra: chemometrics and quantitative metabolomics

The spectral complexity and the nature of the samples necessitates two different approaches to interpreting NMR metabolomic data. Currently, the most widely used and conventional method to analyze the data is chemometrics.

Chemometrics is a category of chemical informatics that applies statistics and pattern-recognition approaches to analyze spectral or structural information generated from chemicals.[259] It is often applied to metabolomics when it was assumed that comprehensive spectral interpretation was not achievable or that their precise resonance compositions were uncertain. It is a useful tool for making rapid screening when conducting the high-throughput screening.

In this method, the compounds usually are not initially identified and only their spectral patterns and intensities are recorded, statistically compared and used to identify the relevant spectral features that distinguish sample classes. Specifically, to deal with the question of spectral assignment and compound identification, chemometric methods employ a process known as spectral binning to align and automatically "digitize" peaks that may belong to the same compound. The spectrum is subdivided into a number of bins, and the intensities of each bin (peak intensity under the curve) is subjected to further analysis. After binning, digitized bins, in the form of peak intensities, can be subjected to multivariate statistical analysis. Quantitative metabolomics (also called magnetic resonance diagnostics or targeted profiling) is different from the chemometric method. Identification and quantification of compounds occurs in the first place once the NMR spectra are acquired. This process is made by comparing the NMR spectrum to a spectral reference library obtained from pure compounds.[260]

2.4.4. Data-processing after interpreting ^{1}H NMR spectra

The intensity of each bin or the concentration of each metabolite is determined after chemometric and quantitative analysis. The next step is to correct inherent intensity or concentration differences. For instance, urine is not under strict physiological control and the concentration of metabolites is affected greatly by dilution effects.[261] Therefore, it is necessary to conduct proper normalization in order to compensate for the variations in metabolite concentration/intensity. However, there are biological samples that are under physiological control, for example, plasma. For these samples, normalization or scaling might not be needed. In general, there are two normalization categories: physiological normalization and numerical normalization. Physiological normalization aims to find a constant that the calculation of the metabolite concentration can rely on. Such as creatinine in urine samples. This method is commonly applied in the situation that creatinine clearance in the sampling subject is considered normal

and constant. Another method of physiological normalization is testing the electrolyte for the water balance by an osmometer; the metabolite concentration/intensity of the bin can be normalized by osmolality. However, constant creatinine clearance is not always a realistic assumption in the situation of metabolic disease. Therefore, numerical normalization is introduced. The commonly used approaches for urine samples are constant sum (CS), constant sum excluding lactate, glucose, and urea (CS-LGU), and total spectral area (TSA).[262] In the CS method, it is assumed that the total sum of all metabolite concentrations is a constant from all samples when applying numerical methods, which means the total quantity of dissolved metabolites is constant and the metabolites have approximately equal shares of up- and down-regulated features. The disadvantage of this method is that it could cause data distortion and produce incomparable data when researchers compare the spectra with certain extremely high concentration of metabolites (e.g., glucose from diabetes group) to the spectra without them (e.g., healthy control group). A study[263] supported this idea by showing that the CS method failed to acquire authentic metabolite concentrations when adding high concertation of glucose. CS-LGU can be used to tackle this situation. Several advanced numerical normalization methods have also been introduced: Quantile, Loess, Linear, Spline, and Probabilistic quotient normalization.[264] Probabilistic quotient normalization was found to outperform other numerical normalization methods.[258,265]

Scaling transforms the data to be normal distribution and reduces the spread of the data from spectral signal intensities across samples. As reviewed above, metabolite concentrations in urine can vary greatly and range over several orders of magnitude. This could cause a bias[266], which makes a small number of metabolites dominate the result of multivariate statistical analyses. Therefore, it is often necessary to scale metabolite intensities to avoid this kind of bias before making any further analysis. There are many scaling methods: Pareto scaling, Autoscaling, Centering, Mean centering.[267] For NMR binned data, Pareto scaling is thought to be an appropriate scaling method when aimed to explore data by multivariate analysis, the variable is divided by the square root of the standard deviation.[267]

2.4.5. Multivariate analysis

Univariate approaches in omics studies are widely used to explore important features or biomarkers. One disadvantage of univariate methods is that they often ignore the correlations among variables. However, multivariate methods consider all variables and reveal data patterns, trends, and outliers. Thus, multivariate methods are considered more suitable for large “omics” dataset analysis.

Multivariate analysis includes two broad categories: supervised and unsupervised methods.

Principal component analysis (PCA) is an unsupervised data-reduction and clustering method in a data matrix X, which reduces the dimensions of the data and plots the data to a new coordinate system where most of the data variance lies in the first few principal components. The score plot of PCA models shows how samples cluster in the coordinates constituted by principal components indicating which principal component explains the clustering of the samples. The loading plot of PCA models explains how variables correlate and contribute the clustering in the score plot. The parameters R^2 and Q^2 represent goodness-of-fit (explained variation) and predictive ability, respectively.[268] Hierarchical cluster analysis (HCA) is another commonly used unsupervised multivariate analysis. The result of HCA is usually presented with heatmap and in the form of a dendrogram. The distance between clusters, calculated by different algorithms in different situations, indicates the similarity or dissimilarity of clusters.[269]

Partial least squares discriminant analysis (PLS-DA) is a supervised clustering method and includes two data matrixes, X and Y (Y is group label matrix). The group information is used to maximize the separation between different groups. Orthogonal PLS-DA divides X matrix into two parts, one is correlated to Y and the other is not correlated to Y, which improves interpretability. One important issue associated with the supervised method is its propensity to data overfitting.[270] This occurs when the algorithm achieves an outcome with fake significant separation by picking up random noise rather than real peak intensities or metabolite concentrations. Thus, model validation to avoid overfitting is necessary. Common validation methods include cross-validation and permutation test.

2.5. Transcriptomics and metagenomics

2.5.1. Transcriptomics

Transcriptomics is the study of the transcriptome—the whole set of gene expression products that are transcribed from the genome in a tissue type or a particular cell. Genome-wide mapping of gene expression in tissue biopsies has proved valuable for identifying novel diagnostic, prognostic, and therapeutic markers in various diseases.[271] The liver, an important target organ in T2D for therapy, plays a pivotal role in energy metabolism, disease-associated gene expressions can be evaluated by transcriptomics. Transcriptomics is commonly used to detect the expression of genome-wide protein-coding gene (mRNA) and is also a tool for detecting non-protein-coding genes (miRNA, lncRNA, circRNA, etc.). Generally, there are two commonly used biological techniques aimed to

study the transcriptome: DNA microarray and RNA-seq. DNA microarray is a hybridization-based technique and RNA-seq is a sequence-based approach.

In terms of the RNA-seq technique, the first generation of sequencing of RNA-seq is Sanger sequencing which was first commercialized in 1986, however, the low-throughput of this method impeded its application. The next-generation sequencing (NGS) method for large-scale, automated transcriptome analyses was the second-generation sequence to replace Sanger sequencing, which has been the dominant transcriptomics technique during the past decade.[272] NGS generates a large number of short reads, which span up to several hundred nucleotides, which can then be computationally combined into overlapping 'contigs' consisting of millions of nucleotides and valuable information on the abundance of gene expression products. Nevertheless, it is difficult to reconstruct and quantify alternative transcripts using short reads, and it is further complicated by the requirement of an amplification step and statistical assignment of the most probable combination of exons to transcripts; thus, it is still computationally challenging and not very accurate. Uneven read coverage, complex splicing, and potential sequencing bias further complicate the task.[273]

Clearly, the ability to produce longer reads would minimize perturbation of transcript integrity, allowing the sequencing of entire isoforms, which would be ideal for elucidating transcriptome complexity and quantifying isoforms and genes, including alternative splicing, alternative transcriptional start and ending, as well as the underlying biology.[274] Recent advances in nanopore sequencing technology allow sequencing of long RNA sequences up to 100 kilobases (kb), which spans the full-length distribution of spliced genes in humans (for protein-coding genes 1-3 kb is typical with outliers such as Titin at more than 80kb).[275] Nanopore sequencing reads information of nucleotides sequence by threading long DNA strands through a small hole known as a nanopore and detecting electrical current changes caused by DNA's four components without complex splicing and computational biases.[276] Testing of nanopore sequencing was proved even more sensitive and accurate compared to real-time PCR for detecting bacterial biodefense pathogens.[277]

After acquiring a sequence, databases, e.g., NR (NCBI non-redundant protein sequences), Pfam (Protein family). KOG/COG/eggNOG (Clusters of Orthologous Groups of proteins), Swiss-Prot (A manually annotated and reviewed protein sequence database), KEGG (Kyoto Encyclopedia of Genes and Genomes), GO (Gene Ontology), can be used to annotate gene function. In which KEGG and GO are the most popular databases to illustrate the gene function. The KEGG database provides the understanding of high-level functions and utilities of the biological system at the molecular level. KEGG pathway is a collection of manually drawn pathway maps illustrating the current knowledge

of the molecular interaction, reaction, and relation networks for Metabolism, Genetic Information Processing, Environmental Information Processing, Cellular Processes, Organismal Systems, Human Diseases, Drug Development.[278] The GO database is a database resource providing a set of structured, controlled vocabularies for community use in annotating genes, gene products, and sequences. The GO provides a consistent description of the attributes of genes and gene products, covering three key biological domains: molecular function, biological process, and cellular component.[279]

When investigating a biological function, it might be sometimes not be sufficient to pinpoint one or a few genes. Determining a set of genes in a specific biological pathway or genes with similar functions is very important to decipher a biological function at the transcriptional level. Enrichment analysis is usually based on the gene set based on the KEGG pathway or GO or even a customized gene set. Simply by chance, a certain number of genes may appear in the set of interesting genes modified in different physiological or pathological conditions or by dietary interventions. Thus, a statistical tool is needed to evaluate the enrichments. An enrichment ratio should be calculated first (equation 1 and 2) and then the significance (p value) of the enrichment is computed using the hypergeometric test (equation 3).[280] A small p value indicates a high probability that the enrichment is not produced simply by chance.

$$K_{exp} = (n/m)*j \quad (1)$$

$$r = k/K_{exp} \quad (2)$$

$$p = \sum_{i=k}^{n} \frac{\binom{m-j}{n-i}\binom{j}{i}}{\binom{m}{n}} \quad (3)$$

n = number of genes in our interesting gene set
m = number of genes in our reference gene set
k = number of genes of the subset in our interesting gene set
j = number of genes of the subset in our reference gene set
K_{exp} = number of genes that are expected to be in our interesting gene set
r = ratio of enrichment
p = significance of the ratio of enrichment

2.5.2. Whole-genome sequencing for gut microbiota

Metagenome was first introduced in 1988 to investigate the genomes of the total microbiota found in nature.[281] Metagenomics is a new method in microbiological research, which refers to using functional gene screening and/or sequencing analysis as a research method to study whole microbial genomes and result in outcomes of microbial diversity, population structure, evolutionary relationships, functional activity, and the relationship with the environment. Whole metagenome shotgun sequencing is to randomly break DNA into small pieces

for sequencing and reassembly. Random overlapping sequences assist in the reassembly into the native DNA order by sophisticated computational approaches. Species classification can be done by analyzing sequence data from both 16S rDNA sequencing and whole metagenome shotgun sequencing, whereas only whole metagenome shotgun sequencing produces information on functional gene composition. Gene annotation is similar to that in transcriptomics.

3. AIMS OF THE STUDY

The general aim of the study was to use multi-omics to investigate the effect of nonacylated anthocyanins from bilberries (*Vaccinium myrtillus* L.) and acylated anthocyanins from purple potatoes (*Solanum tuberosum* L. var. 'Synkeä Sakari') on type 2 diabetes of Zucker diabetic fatty rats. The objects of the individual studies were to:

I Characterize the anthocyanin composition from bilberries (*Vaccinium myrtillus* L.) and purple potatoes (*Solanum tuberosum* L. var. 'Synkeä Sakari') and observe the effect of both types of anthocyanin extracts on plasma and hepatic metabolomic profile of Zucker diabetic fatty rats.

II Investigate the effects of acylated and nonacylated anthocyanins extracts on hepatic gene expression in Zucker diabetic fatty rats.

III Investigate the effects of acylated and nonacylated anthocyanins extracts on gut metabolite profiles and microbiota in Zucker diabetic fatty rats.

4. MATERIALS AND METHODS

4.1. Extraction, purification, and identification of anthocyanin-rich extracts from bilberries and purple potatoes

Certified organic fresh bilberries (*Vaccinium myrtillus* L.), purchased from Pakkasmarja Oy (Suonenjoki, Finland), were collected from the Kainuu region, Finland. Purple potatoes (*Solanum tuberosum* L.) of the cultivar 'Synkeä Sakari', provided by Clanet Oy (Espoo, Finland), were cultivated and harvested in 2017 in the Lohja area, Finland. The potatoes were washed, sliced and freeze-dried before extraction. Anthocyanins in the bilberries and purple potatoes were extracted with 70% v/v aqueous ethanol containing 2% v/v acetic acid with a solid-liquid ratio of 1:5 (w/v). This extraction procedure was repeated three times, and the resulting extracts were combined and filtered. The solvent was removed with vacuum evaporation. After evaporation, each of the extracts was loaded onto a column packed with equilibrated Amberlite XAD-16 (Sigma–Aldrich, Steinheim, Germany) adsorbent for purification. When the adsorption was saturated, the column was first washed with purified water to elute the sugars and organic acids, after which anthocyanins were eluted with ethanol. The eluent was collected and concentrated by vacuum rotary evaporation to remove the ethanol. Finally, the extracts were lyophilized and stored at −80 °C until analysis.

The composition of anthocyanins, flavonol glycosides and hydroxycinnamic acids derivatives was analyzed by reversed-phase high-performance liquid chromatography (HPLC) with diode array detector (DAD) (Shimadzu, Kyoto, Japan). Kinetex Polar C18 column (2.6 µm, 150 × 4.60 mm, Phenomenex, Torrance, CA) was used for chromatographic separation.

The elution solvents consisted of formic acid, acetonitrile and water 5/3/92 (v/v, A) and 5/55/40 (v/v, B), and elution gradient was as follows: 4–20% B, 0–5 min; 20–22% B, 5–30 min; 22–28% B, 30–38 min; 28–32% B, 38–42 min; 32–35% B, 42–50 min; 35–90% B, 50–55 min; 90–35% B, 55–58 min; 4% B, 58–62 min at flow rate 0.5 mL/min.[282] Three replicate samples of each extract were dissolved with MeOH/HCl 99/1 and filtrated (0.45 µm, PTFE; VWR, Radnor, PA). Absorption maximum at 520 nm was used for detecting anthocyanins, and those at 354 and 320 nm for flavonol glycosides and hydroxycinnamic acid derivatives, respectively. For quantification, anthocyanins were calculated as cyanidin 3-*O*-glucoside equivalents (Extrasynthese, Genay, France). Flavonol glycosides were quantified as quercetin 3-*O*-rutinoside equivalents (Extrasynthese, Genay, France).

Hydroxycinnamic acids were calculated as caffeic acid equivalents (Sigma–Aldrich, St. Louis, MO).

The qualitative analysis was carried out using Bruker Elute UHPLC system coupled with high-resolution Bruker Impact IITM UHR-QqTOF (Ultra-High Resolution Qq-Time-Of-Flight) mass spectrometry in positive auto-MS/MS mode using electrospray ionization in a range of 190–800 nm. The parameters of mass spectrometer were set as follows: the capillary voltage 4.5 kV, the nebulizer gas (N_2) pressure 2.0 bar, the drying gas (N_2) flow 8.0 L/min, the end plate offset 500 V, the drying gas temperature was 200 °C, and mass range 20 to 1,000 *m/z*. Calibration was carried out by injecting 10 mM sodium formate at a flow rate of 180 µL/min from a direct infusion syringe pump to the six-port valve in a high-precision calibration mode. The instrument was controlled, and the data was handled with the Compass DataAnalysis software 4.4 (Bruker Daltonik GmbH, Bremen, Germany). The mass measurement errors (ppm) were calculated as the difference between the measured accurate mass and the calculated theoretical mass of a given molecular formula, shown in parts per million (equation 4).

$$\text{Mass error} = \frac{m_{\text{measured}} - m_{\text{theoretical}}}{m_{\text{theoretical}}} \times 10^6 \qquad (4)$$

4.2. Experimental design of animal study and animal housing

Male ZDF rats were used to evaluate impacts of anthocyanins extracts from bilberries and purple potatoes on type 2 diabetes by multi-omics. Lean Zucker rats (fa/+) were chosen as healthy controls. All experimental protocols were approved by the Institutional Animal Ethics Committee of Peking University (No. LA2016285) and carried out in accordance with national and international guidelines for the care and use of laboratory animals.

Male ZDF and lean Zucker rats of 3-week-old were purchased from Beijing Vital River Laboratory Animal Technology Co., Ltd. (Beijing, China). The rats were maintained in a specific pathogen-free environment at the Animal Housing Unit of Peking University (Beijing, China) under a controlled temperature (23–25 °C) and a 12-h light/12-h dark cycle. After one week of adaptation, the ZDF rats were randomly divided into five groups (n = 8 per group), receiving eight weeks of daily feeding as follows: (1) ZDF rats fed with high-fat diet Purina #5008 and non-acylated anthocyanin extract from bilberry at a daily dosage of 50 mg/kg body weight (high dose NAAB, H-NAAB); (2) the ZDF rats fed with Purina#5008 diet and acylated anthocyanin extract from purple potato at a daily dosage of 50 mg/kg body weight (high dose AAPP, H-AAPP); (3) the ZDF rats fed with Purina #5008 diet and non-acylated anthocyanin extract from bilberries

at a daily dosage of 25 mg/kg body weight (low dose NAAB, L-NAAB); (4) the ZDF rats fed with Purina#5008 diet and acylated anthocyanin extract from purple potatoes at a daily dosage of 25 mg/kg body weight (low dose AAPP, L-AAPP); (5) ZDF rats fed only with Purina #5008 diet as the diabetic model group (M). The lean Zucker rats were divided into two groups (n = 8 per group), one fed with a normal diet (ND) and the other with a high-fat Purina #5008 diet as a control group (Con). (**Figure 4**) The number of animals in each group was determined based previous studies[283,284] and degree of freedom (E)[285]. The dosages of anthocyanin extracts were determined based on previous animal[223] and human[292] studies, which are achievable from human diet. The anthocyanin extracts were given by gavage. The feed supply was replaced once every two days to prevent oxidization of the fats in the diets. Metabolic cages were used to monitor the feed and water intake on the 30th day and the 60th day of the intervention. After 8 weeks of intervention, the rats were euthanized under isoflurane anesthesia after overnight fasting. Plasma samples were collected by centrifuging the blood samples at 3,000 × *g* for 10 min at 4 ℃. The plasma samples were stored at −80 °C until analyses.

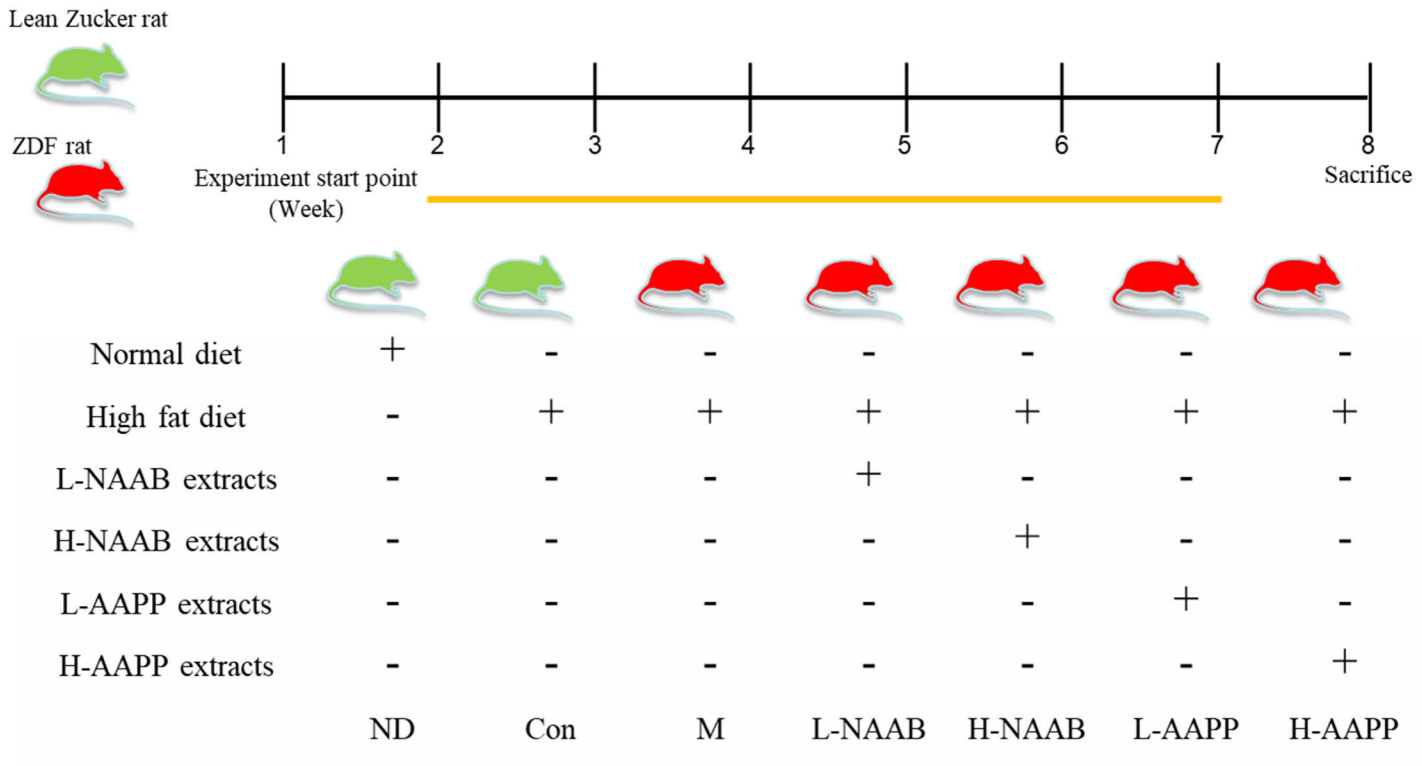

Figure 4. Schematic presentation of the rat feeding study.

4.3. NMR metabolomics for plasma, liver, feces, and cecal content

In **Study I**, an aliquot of 220 µL plasma was mixed with 440 µL ice-cold phosphate buffer (90 mmol/L NaH_2PO_4, pH=7.4) containing 15% D_2O to minimize variations in pH. After vortexing, the samples were centrifuged at 12,000 × *g* for 10 min at 4 ℃ to separate the precipitates. Aliquots of 600 µL of the resulting supernatants were transferred into 5-mm NMR tubes. In **Study II**, the liver was homogenized in liquid nitrogen and around 0.2 g homogenized liver sample was weighed and resuspended in 4 mL/g methanol and 0.85 mL/g Milli Q water. After vortexing, 2 mL/g chloroform was added and then vortexed again. Then, 2 mL/g chloroform and 2 mL/g water were added and vortexed for 1 min. Samples were left on ice for 30 mins and then centrifuged at 2,000 × *g* for 10 min at 4 ℃. The upper layer was the aqueous extract, and the lower layer was the lipid extract. Freeze-drying and nitrogen gas were used to remove the solvents from the aqueous and lipid extracts, respectively. 530 µL ice-cold phosphate buffer (90 mmol/L KH_2PO_4, pH=7.4) and 70 µL Chenomx Internal Standard (Edmonton, Alberta, Canada) containing 5 mM DSS-d_6 and 0.1% w/v NaN_3 were added to aqueous extracts. 600 µL ice-cold chloroform-*d* containing 0.03% TMS were added to lipophilic extracts. The solutions were transferred into 5-mm NMR tubes. In **Study III**, the frozen fecal and cecal content samples were freeze-dried and weighed. 800 µL ice-cold phosphate buffer (90 mmol/L NaH_2PO_4, pH = 7.4) was added into 50 mg freeze-dried samples. The samples were homogenized by vortexing at 3,000 Hz for 2 minutes and centrifuged at 4 ℃ and 3,000 × *g* for 15 minutes. 570 µL of supernatants and 60 µL Chenomx Internal Standard solution containing 5 mM DSS-d_6 and 0.1% w/v NaN_3 (Edmonton, Alberta, Canada) were added into the Eppendorf tube and vortexed. An aliquot of 600 µL of resulted solutions were transferred into 5-mm NMR tubes.

All NMR spectra were acquired at 298 K from a 600 MHz Bruker Avance-III NMR spectrometer (Bruker BioSpin AG, Fällanden, Switzerland) equipped with a Prodigy TCI cryoprobe and a precooled SampleJet sample changer. In **Study I**, the Carr–Purcell–Meiboom–Gill (CPMG) pulse sequence (*cpmgpr*) was used to acquire 1D ^{1}H-NMR spectra of plasma samples. The parameters used for the 1D CPMG pulse sequence were as follows: spectral sweep width, 16.02 ppm; data points, 64 K; flip angle of radiofrequency pulse, 90°; total relaxation delay (RD), 5 secs. T2 filtering was obtained with an echo time of 2 ms repeated 64 times, resulting in a total duration of effective echo time of 256 ms, and the number of scans was 128. The chemical shift of alpha-glucose (δ = 5.23 ppm) was used to align the spectra. The 1D ^{1}H NMR spectra of plasma were binned into 0.01 ppm integral regions using the Chenomx NMR software suite

(Professional edition, version 7.5, Chenomx, Edmonton, AB, Canada), and the water region (δ 4.70−4.95 ppm) was removed.

In **Study II**, a NOESY presaturation pulse (*noesypr1d*) was used to acquire a one-dimensional ^{1}H-NMR spectra of hepatic aqueous and lipid extracts samples. The parameters for the 1D NOESY presaturation pulse sequence were as follows: spectral sweep width, 16.02 ppm; data points, 64 K; total relaxation delay (RD), 5 s; acquisition time was 3.40 s; the number of scans was 128. All the spectra were manually phase- and baseline-corrected with Topspin-3.5 software (Bruker). The chemical shift of DSS-d_6 (δ = 0.00 ppm) or TMS (δ = 0.00 ppm) was used to align the spectra. The 1D ^{1}H NMR spectra of the hepatic lipid extract were binned into 0.01 ppm integrated spectral buckets. The 1D ^{1}H NMR spectra of the hepatic aqueous extract were binned into 0.005 ppm integrated spectral buckets.

In **Study III**, a NOESY presaturation pulse (*noesypr1d*) was used to acquire one-dimensional ^{1}H-NMR spectra of feces and cecal content. One-dimensional ^{1}H-NMR spectra were recorded using the *noesypr1d* pulse program. The parameters were as follows: spectral sweep width, 16.02 ppm; data points, 64 K; total relaxation delay (RD), 5 s; acquisition time, 6.81 s; the number of scans, 128. Water suppression was achieved by setting O1P at 4.701 ppm. The chemical shift of DSS-d_6 (δ = 0.00 ppm) was used to align the spectra. The water peak region at 4.68–4.95 was excluded. The "*i*coshift" procedure was used to align NMR spectra in MATLAB (R2012a, The Mathworks Inc., Natick, MA, USA).[286] The 1D ^{1}H NMR spectra from feces and cecal content were binned with 0.001 ppm bin width.

Metabolites were identified based on the acquired 1D 1H NMR chemical shifts reported in the literature, Chenomx NMR Suite 8.1–9 software (Chenomx Inc., Edmonton, Alberta, Canada), and the metabolite database Human Metabolome Database (HMDB, http://www.hmdb.ca). The identification was further confirmed by 2D ^{1}H–^{13}C heteronuclear single-quantum correlation spectroscopy (HSQC, *hsqcedetgpsisp2.3*), ^{1}H-^{1}H Correlation Spectroscopy (COSY, *cosygpmfqf*) and *J*-resolved spectroscopy (JRES, *jresgpprqf*).

4.4. Hepatic transcriptome analysis and nanopore technology

4.4.1. Liver RNA extraction and cDNA preparation

In **Study II**, total RNA isolation was performed with TRIzol reagent (Takara, Japan) according to the manufacturer's instructions. The purity of the RNA was monitored using a Nano Photometer® spectrophotometer (IMPLEN, CA, USA). One µg of the total RNA was prepared for cDNA libraries using cDNA-PCR Sequencing Kit (SQK-PCS109) protocol provided by Oxford Nanopore

Technologies (ONT, Oxford, UK). Briefly, full-length cDNAs were formed by enrichment of reverse transcriptase and adding defined PCR adapters directly to both ends of the first-strand cDNA, followed by cDNA amplification (PCR for 14 circles with LongAmp Tag, 8 minutes for elongation time). The PCR products were then subjected to ONT adaptor ligation using T4 DNA ligase. Agencourt XP beads were used for DNA purification according to ONT protocol. The resulting cDNA libraries were added to the FLO-MIN109 flow cells and run on a PromethION platform (Biomarker Technology Company, Beijing, China).

4.4.2. Transcriptome data analysis

The MinKNOW software (version 2.0) was used to conduct the base calling of the raw signal data and convert the fast5 files into fastq files. Firstly, these raw data were then filtered to remove short reads (below 500 bp) and the reads with an average read quality score below 7. The rRNA was excluded after mapping to the rRNA database. Next, full-length, non-chimeric (FLNC) transcripts were obtained by searching for primers at both ends of the reads. A Mimimap2 alignment program[287] was used to obtain clusters of FLNC transcripts by mapping to a reference genome (Rnor_5.0). The consensus isoforms were obtained after polishing within each cluster by pinfish (https://github.com/nanoporetech/pinfish). Mapped reads were further collapsed by *cDNA_Cupcake* package (https://github.com/Magdoll/cDNA_Cupcake) with the parameters of min-identity = 90% and min-coverage = 85%. Full-length reads were mapped to the reference genome (Rnor_5.0). Reads with a match quality above 5 were further used for quantification. Expression levels were estimated by counts per million (CPM) (equation 5).

$$\mathrm{CPM} = \frac{\text{number of reads mapped to transcript}}{\text{total reads aligned in sample}} \times 10^6 \qquad (5)$$

.

Package *edgeR* was used for the calculation of differentially expressed transcripts or genes between two groups.[288] The resulting p values were adjusted by the Benjamini and Hochberg's approach. Genes and transcripts with an adjusted p value < 0.05 and fold change ≥ 2 were considered as differentially expressed genes (DEGs) and differentially expressed transcripts (DETs). Two-side hypergeometric test was used as the statistical test method and Benjamini and Hochberg were used as FDR correction method in GO/KEGG enrichment analysis.

4.4.3. Protein-protein interaction (PPI) network construction

A protein-protein interaction (PPI) network can be used to map networks of protein interactions depending on their physical or functional association, which is a platform that can systematically identify disease-related genes.[289] DEGs

were used for PPI network construction based on protein-protein interaction by the Search Tool for the Retrieval of Interacting Genes/Proteins (STRING; https://string-db.org/). The data framework of predicted gene interactions generated from STRING was subjected to Cytoscape (Version:3.2.1; https://cytoscape.org/) to form a visual PPI network map. Cytoscape is a software capable of integrating data into a unified conceptual framework. The value of the degree measures how many neighbors a node directly connects to. In this study, the top 10 genes with the highest degree were considered as hub genes.

4.4.4. Enrichment analysis based on KEGG and GO

As earlier mentioned, KEGG and GO are commonly used bioinformatic libraries that provides comprehensive information on the function of genes. The KEGG pathway enrichment analysis of DEGs was implemented using the *enrichKEGG* function based on R software (Version 3.4.1). KEGG pathways with corrected p values (q values) < than 0.25 and rich factor > 1 were considered significantly enriched. The greater the rich factor, the greater the degree of enrichment. ClueGO visualizes the selected GO terms in a functionally grouped annotation network that reflects the relationships between the terms based on the similarity of their associated genes.[290] In the network, the size of the nodes represents the statistical significance of the terms. The degree of connectivity between terms (edges) is calculated using kappa statistics. Only significantly enriched GO terms with kappa score > 0.03 were shown in the network.

4.4.5. Weighted gene coexpression network analysis

Weighted gene co-expression network analysis (WGCNA) was applied for conducting the scale-free network topology analysis of RNA-seq data, using the WGCNA function based on R software (Version 3.4.1). Genes with similar expression patterns were clustered into a module by calculating the expression correlation between genes. All detected genes were used for analysis. To identify those modules with clinical relevance, Pearson's correlation was used to analyze the correlation between modules and clinical traits.

4.5. Metagenomics for gut microbiota

4.5.1. DNA extraction and sequencing of fecal microbiota

Total bacteria DNA was extracted from colonic content by using a TIANamp Stool DNA kit (TIANGEN Bio-Tech Co., Ltd, Beijing, China) according to the manufacturer's instruction. The concentrations and quality of DNA were examined by agarose gel electrophoresis (Promega, St. Louis, MO, USA) and a

nanodrop instrument (NanoDrop Technologies, Wilmingto, USA). The DNA library was constructed by using NEXTflex Rapid DNA-Seq Kit (Illumina, 96 reactions) including DNA fragmentation and adapter ligation. The DNA library was then sequenced on Illumina Hiseq X10 platform with 2 × 150 bp paired reads (Institute of Microbiology, Chinese Academy of Science, Beijing, China).

4.5.2. DNA sequence assembly and annotation

Raw data processing was similar to the previous study.[291] Briefly, raw data generated from the Illumina Hiseq X10 platform were processed by the MOCAT2 software package. Raw reads were filtered to obtain clean reads by removing low quality and short reads, raw reads mapped to rat genome were also removed to avoid host contamination. Scaftigs (minimum length, 500 bp) were obtained by using SOAPDenovo v1.06[292] based on clean reads. Prediction of the gene from scaftigs in each sample was processed by using open reading frame prediction based on the MetaGeneMark program. Subsequently, CD-HIT was used to cluster genes from each sample based on the parameters (identity > 95%, overlap > 90%) and the gene catalog was obtained. Unigenes were identified by aligning high-quality reads against the gene catalog using SOAPAligner2 (identity cutoff ≥ 95%) and the corresponding relative abundance of each gene in each sample was calculated. Taxonomic assignment and functional annotation were performed by using DIAMOND (https://github.com/bbuchfink/diamond), an open-source algorithm. The taxonomic composition was acquired by mapping unigenes to the NR meta-database (blastp mode, e value ≤ 1e−5). Lowest Common Ancestor (LCA) algorithm was used to ensure the quality of the annotation. KEGG is a gene function database allowing the depiction of microbiome functions. We mapped the amino acid sequences of the gene catalog into the KEGG database by using the DIAMOND program with default parameters (e value ≤1e−5) and obtained corresponding gene function annotation. We summarized the relative abundance of genes in the same functional level as the relative abundance of each functional category.

4.6. Measurement of the gene expression of *G6PC* and *TBC1D1*

Total RNA was extracted from the liver using a TransZol Up kit (Transgen biotech, Beijing, China). The 1.0 μg extracted total RNA was reverse-transcribed to complementary DNA using a TransScript One-step gDNA Removal and cDNA Synthesis SuperMix (TransGen Biotech, Beijing, China) according to the manufacturer's directions. The expression level of *G6PC* and *TBC1D1* genes in rat livers were measured by quantitative real-time-polymerase chain reaction

(PCR). The primer sequences were as follows: *G6PC*: forward primer CGTCACCTGTGAGACTGGAC, reverse primer GCCCAGTATCCCAACCACAA; *TBC1D1*: forward primer TCGATGACACCTTCGCCAAA, reverse primer TGGCCAATCGTGAAGAGCAT.

4.7. Statistical analysis

Before the univariate analysis of binned data from 1D ^{1}H NMR spectra, the data were tested for homogeneity of variances and normality by the Levene test and Kolmogorov–Smirnov test, respectively. A One-way ANOVA was followed by the post hoc Bonferroni test when the data was normally distributed and variances were homogeneous or else the Kruskal–Wallis test and the post hoc Tamhane test were applied in SPSS statistics 22 (IBM, Armonk, USA) or Prism (GraphPad Software, San Diego, USA) in different cases. The statistical significances are expressed as * $p < 0.05$, ** $p < 0.01$, and *** $p < 0.001$ compared to the M group. The SIMCA-P+ 13 software (MKS Instruments AB, Umeå/Malmö, Sweden) was used for the multivariate data analysis. PCA, PLS-DA, and OPLS-DA were created to analyze group classification and biomarker identification. The (O)PLS-DA models were validated by permutation test (R^2Y-intercept < 0.3–0.4 and Q^2Y-intercept < 0.05) and cross-validated analysis of variance (CV-ANOVA) ($P < 0.05$). In **Study III**, the volcano plot was used to show the log2 of the fold change in levels of metabolites between the groups compared with its P value from the Student's T-test, $P < 0.05$ and fold change > 1 were set as the threshold. Linear discriminant analysis (LDA) effect size (LEfSe) was used to discriminate differentially abundant bacterial taxa, bacterial taxa with a LDA absolute value greater than 2 were considered differentially abundant bacterial (LEfSe: http://huttenhower.sph.harvard.edu/galaxy/). Significantly different genes were identified with $P < 0.05$ by Student's T-test and fold change > 2. Correlation network analysis and visualization were conducted in Cytoscape (Version:3.2.1; https://cytoscape.org/) based on Spearman correlation analysis ($r > 0.4$ or $r < -0.4$; $P < 0.05$).

5. RESULTS AND DISCUSSION

5.1. Identification and quantification of nonacylated anthocyanin from bilberries and acylated anthocyanin from purple potatoes

Anthocyanins, flavonol glycosides, and hydroxycinnamic acids from bilberry and purple potato extracts were identified and quantified (**Figure 5** and **Table 7**). The anthocyanins in the bilberry extract (NAAB) were non-acylated. Each gram of the NAAB extract contained 423.89 ± 7.02 mg of anthocyanins, 14.96 ± 0.54 mg of flavonol glycosides, and 19.30 ± 0.39 mg of hydroxycinnamic acids with chlorogenic acid being dominant. Each gram of the AAPP extract contained 248.74 ± 7.14 mg of anthocyanins and 144.07 ± 4.21 mg of hydroxycinnamic acids consisting of mostly chlorogenic acid, while no flavonol glycosides were detected in AAPP. The anthocyanins of NAAB mostly consisted of glucosides, galactosides and arabinosides of delphinidin, petunidin, cyanidin, peonidin, and malvidin. The purple potato extract (AAPP) contained only acylated anthocyanins, with petunidin coumaroyl-rutinoside-glucoside (160.82 ± 4.39 mg/g) as the dominating compound followed by peonidin coumaroyl-rutinoside-glucoside (40.30 ± 2.23 mg/g) and petunidin caffeoyl-rutinoside-glucoside (12.31 ± 0.26 mg/g). The total anthocyanin content in the extracts was taken into account when determining the daily dosage in the feeding of the experimental rats.

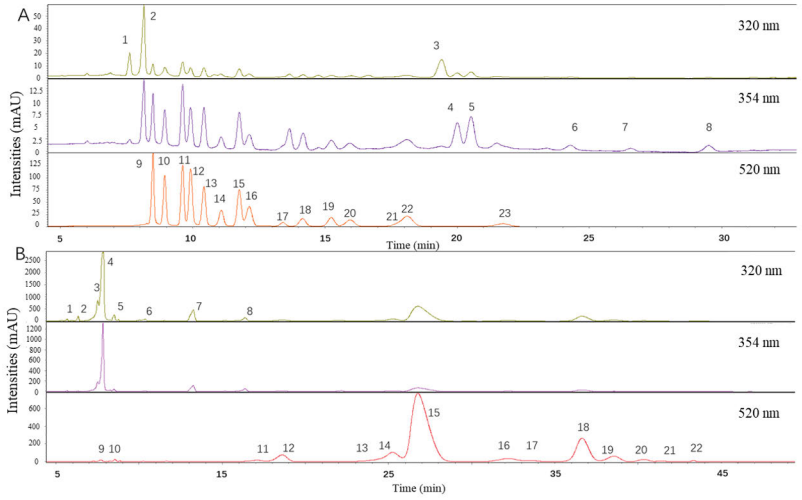

Figure 5. HPLC-DAD chromatograms of the anthocyanin extracts showing anthocyanins (520 nm), flavonol glycosides (354 nm), and hydroxycinnamic acids (320 nm) from bilberries (*V. myrtillus* L.) (A) and purple potato (*S. tuberosum* L. 'Synkeä Sakari') extracts (B). Numbering of the peaks refers to Table 7. Figures reprinted from the original publication **I** with permission from the American Chemical Society.

Table 7. Identification and quantification of anthocyanins, flavonol glycosides and hydroxycinnamic acids in the NAAB and the AAPP based on the HPLC-DAD and UHPLC-ESI(+)-Q-ToF-MS data. The positive ions shown are M^+ for anthocyanins and $[M+H]^+$ for hydroxycinnamic acids and flavonol glycosides. Numbering of the compounds refers to **Figure 5**.

	Tentative identification	***Content (mg/g)***
NAAB extracts		
Hydroxycinnamic acids derivatives (320 nm)		
1	Caffeic acid derivatives	3.03 ± 0.16
2	Chlorogenic acid	10.39 ± 0.36
3	Unknown	5.89 ± 0.17
Total hydroxycinnamic acids		19.30 ± 0.39
Flavonol glycosides (354 nm)		
4	Que-glu, Que-gal	5.31 ± 0.21
5	Que-glucuronide	6.32 ± 0.44
6	Unknown	1.20 ± 0.17
7	Que-ara	0.82 ± 0.07
8	Unknown	1.31 ± 0.06
Total flavonol glycosides		14.96 ± 0.54
Anthocyanins (520 nm)		
9	Del-3-*O*-gal	51.40 ± 2.74
10	Del-3-*O*-glu	41.89 ± 1.57
11	Cya-3-*O*-gal	49.10 ± 1.29
12	Del-3-*O*-ara	53.09 ± 1.87
13	Cya-3-*O*-glu	40.68 ± 1.49
14	Pet-3-*O*-gal	20.72 ± 1.32
15	Cya-3-*O*-ara	37.08 ± 1.02
16	Pet-3-*O*-glu	30.57 ± 0.93
17	Peo-3-*O*-gal	5.57 ± 0.35
18	Pet-3-*O*-ara	12.32 ± 0.39
19	Peo-3-*O*-glu	18.77 ± 0.33
20	Mal-3-*O*-gal	16.23 ± 0.59
21	Peo-3-*O*-ara	3.17 ± 0.08
22	Mal-3-*O*-glu	33.29 ± 0.88
23	Mal-3-*O*-ara	10.01 ± 0.36
Total anthocyanins		423.89 ± 7.02
AAPP extracts		
Hydroxycinnamic acids derivatives (320 nm)		
1	Neochlorogenic acid	1.05 ± 0.05
2	Unknown	3.13 ± 0.13
3	Cryptochlorogenic acid	17.6 ± 0.45
4	Chlorogenic acid	93.01 ± 2.91
5	Caffeic acid	4.17 ± 0.07
6	Unknown	2.75 ± 0.13
7	Unknown	16.23 ± 1.07
8	Chlorogenic acid derivatives	6.13 ± 0.12
Total hydroxycinnamic acids		144.07 ± 4.21

	Tentative identification	*Content (mg/g)*
Anthocyanins (520 nm)		
9	Pet-rut-glu	1.25 ± 0.05
10	Peo-rut-glu	1.30 ± 0.05
11	Pet-cou-rut-glu; Cya-caf- rut-glu	0.92 ± 0.04
12	Pet-caf-rut-glu; Del-cou-rut-glu	12.31 ± 0.26
13	Peo-caf-rut-glu	1.21 ± 0.02
14	Peo-cou-rut-glu	9.06 ± 0.08
15	Pet-cou-rut-glu	160.82 ± 4.39
16	Pet-fer-rut-glu	7.30 ± 0.32
17	Pg-cou-rut-glu	0.96 ± 0.03
18	Peo-cou-rut-glu	40.30 ± 2.23
19	Mal-cou-rut-glu	8.70 ± 0.45
20	Peo-fer-rut-glu	2.81 ± 0.1
21	Mal-fer-rut-glu	0.76 ± 0.02
22	Pet-cou-rut	1.04 ± 0.09
Total anthocyanins		248.74 ± 7.14

Abbreviations: que, quercetin; cya, cyanidin; del, delphinidin; mal, malvidin; pg, pelargonidin; peo, peonidin; pet, petunidin; caf, caffeoyl; cou, caffeoyl; fer, feruloyl; glu, glucoside; ara, arabinoside; rut, rutinoside.; gal: galactoside. Amounts are given as mg per g extracts ± standard deviation, n=3. Tables reprinted from the original publication **I** with permission from the American Chemical Society.

5.2. Effect of anthocyanin extracts on the physiology of the T2D in ZDF rats

Leptin receptor gene defect-induced diabetes in ZDF rats (M group) showed a higher daily intake of water and feed on the 30th day and the 60th day of the intervention compared to the lean Zucker rats (ND and Con groups) (**Figure 6A–B**). In the anthocyanin extracts-treated groups (L-NAAB, H-NAAB, and H-AAPP), the water intake was significantly decreased on the 30th day ($p < 0.05$, $p < 0.05$, and $p < 0.001$) compared to that in the M group. Only L-NAAB group showed decreased water intake on the 60th day ($p < 0.05$). Compared to the M group, the H- AAPP group showed a significant decrease in feed intake on both the 30th day ($p < 0.001$) and 60th day ($p < 0.01$). Overall, a common decrease was observed in weekly feed intake in all treatment groups at the 8th week of the intervention in comparison with the M group, with the reduction being statistically significant in the H-NAAB and H-AAPP groups ($p < 0.05$, $p < 0.05$) (**Figure 6C**). As illustrated in **Figure 6D** and **Table 8**, the M group showed a significant increase in body weight, weight of liver, kidney, epididymal fat, and their percentage of body weight compared to both the ND and Con groups due to excessive weight gain, development of renal edema, and fatty liver, highlighting the defect of the leptin gene. There was no significant effect on body

weight in the anthocyanin-fed groups. However, compared to the M group, the H-AAPP group showed a significant decrease in liver/body weight ratio, kidney weight, and kidney/body weight ratio ($p < 0.05$, $p < 0.05$, $p < 0.05$) and the H-NAAB group showed a lower level of kidney/body weight ratio ($p < 0.05$).

Compared to lean Zucker rats, the ZDF rats were characterized by lower level of aspartate transaminase (AST) and higher fasting level of total protein (TP), blood urea nitrogen (BUN), triglyceride (TG), and glucose. AST and ALT are both indicators of liver injury, however, AST and ALT also present in the liver, heart, muscle, kidney, or blood cells, are involved in amino acid metabolism, and this may have contributed to the circulating level of AST in plasma. The lowered level of AST in the ZDF rats may have resulted from a defect in the *leptin* receptor gene. We did not see higher levels of plasma insulin in the groups of ZDF rats compared to the normal rats in the ND group, indicating possible decline of the function of β-cells in the ZDF rats after age of 10 weeks.[21] Groups fed with the nonacylated anthocyanin extracts (L-NAAB and H-NAAB) showed significantly decreased fasting plasma glucose levels ($p < 0.01$, $p < 0.001$) compared to the rats in the model (M) group fed with the same diet without the anthocyanin extract. The groups fed with the acylated anthocyanin extracts (L-AAPP and H-AAPP) also showed decreased levels of plasma glucose, but the difference did not reach statistical significance.

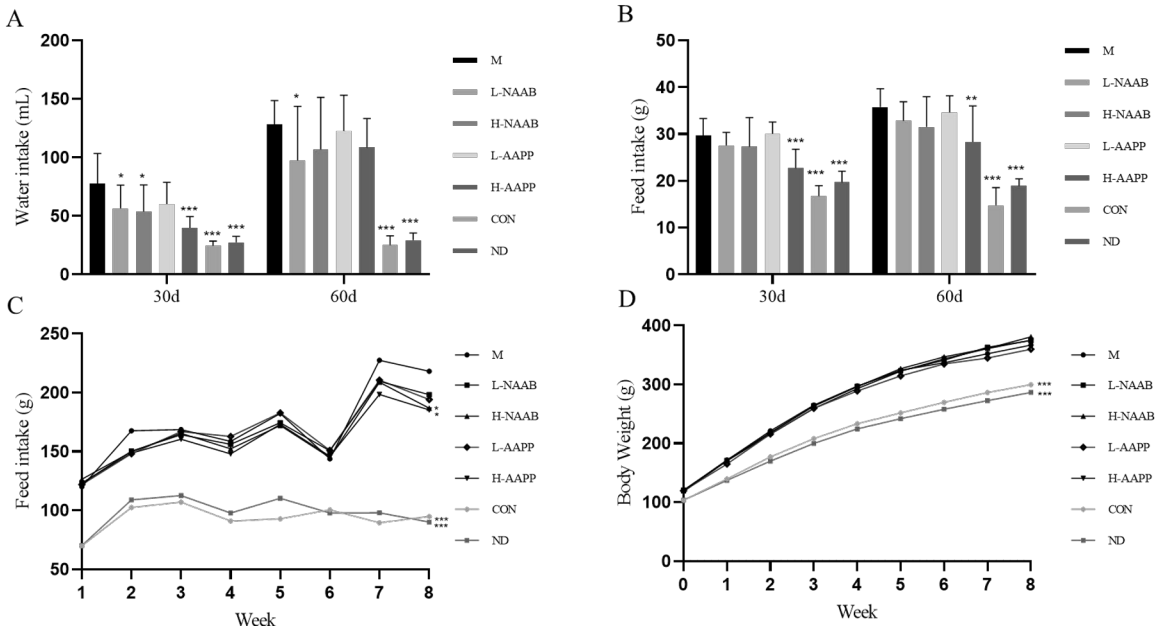

Figure 6. Effect of anthocyanins extracted from bilberries and purple potatoes on water (A) and feed (B) intake on the 30th day and 60th day of intervention, weekly feed intake (C), and weekly body weight (D) in lean Zucker rats and ZDF rats fed with the different experimental diets. Experimental groups: M, ZDF rats given high-fat diet; L-NAAB, ZDF rats fed with high-fat diet supplemented with low-dose nonacylated anthocyanins from bilberries; H-NAAB, ZDF rats fed with high-fat diet supplemented with high-dose nonacylated anthocyanins from bilberries; L-AAPP, ZDF rats fed with high-fat diet supplemented with low-dose acylated anthocyanins from purple potatoes; H-AAPP, ZDF rats fed with high-fat diet supplemented with high-dose acylated anthocyanins from purple potatoes; Con, lean Zucker rats given high-fat diet; and ND, lean Zucker rats given normal diet. *$p < 0.05$, **$p < 0.01$, and ***$p < 0.001$ as compared with the M group. Figures reprinted from the original publication **I** with permission from the American Chemical Society.

Table 8. Changes of fasting plasma parameters in lean Zucker rats and ZDF rats fed on the different experimental diets.

Plasma parameters	*M*	*L-NAAB*	*H-NAAB*	*L-AAPP*	*H-AAPP*	*Con*	*ND*
ALT (U/L)	137.7 ± 22.8	190.1 ± 24.3	196.4 ± 52.7	181.8 ± 33.4	217.2 ± 53.3	164.6 ± 36.9	193.6 ± 54.6
TP (g/L)	63.2 ± 5.3	65.4 ± 6.3	64.2 ± 3.8	60.5 ± 3.7	63.6 ± 6.7	52.8 ± 1.1**	53.2 ± 2.4**
Albumin (g/L)	28.5 ± 1.8	30.2 ± 1.7	30.2 ± 2.1	28.1 ± 1.6	28.1 ±1.6	28.7 ± 1.5	29.1 ± 0.7
AST (U/L)	335.6 ± 136.9	485.4 ± 79.0	462.3 ± 72.2	454.0 ± 99.6	584.6 ± 139.6	869.3 ± 133.4**#	1016.2 ± 229.6**
BUN (mmol/L)	7.3 ± 1.4	7.8 ± 2.3	7.6 ± 1.3	7.2 ± 0.5	7.0 ± 1.4	5.1 ± 0.9**	5.4 ± 0.5**
TG (mmol/L)	8.77 ± 2.75	8.61 ± 4.84	7.55 ± 2.63	6.93± 2.62	6.61 ± 2.22	1.27 ± 0.35**	1.05 ± 0.16**
Insulin (mU/L)	33.67 ± 14.75	29.56 ± 11.47	38.51 ± 13.66	39.91 ± 6.10	42.50 ± 10.23	42.44 ± 24.51	35.44 ± 13.45
Glucose (mmol/L)	23.0 ± 1.9	14.5 ± 3.3***	16.4 ± 4.3**	20.8 ± 7.8	20.4 ± 6.2	10.9 ± 1.3***	8.5 ± 1.0***
Liver (g)	14.67 ± 1.58	14.40 ± 1.72	14.67 ± 0.95	13.78 ± 0.73	14.07 ± 2.30	8.29 ± 0.98**	7.25 ± 0.88**
Liver/BW %	6.61 ± 0.35	6.30 ±0.37	6.28 ± 0.37	6.32 ± 0.37	6.13 ± 0.57*	4.34 ± 0.24**	4.05 ± 0.14**
Epididymal fat (g)	7.57 ± 1.07	7.81 ± 1.48	7.95 ± 0.93	7.94 ± 0.65	7.91 ± 1.20	3.10 ± 0.38**	2.89 ± 0.70**
Epididymal fat/BW %	3.41 ± 0.32	3.39 ± 0.22	3.40 ± 0.21	3.64 ± 0.24	3.44 ± 0.27	1.62 ± 0.12**	1.60 ± 0.28**
Kidney (g)	2.76 ± 0.30	2.54 ± 0.27	2.59 ± 0.20	2.67 ± 0.16	2.47 ± 0.30*	1.89 ± 0.17**	1.72 ± 0.24**
Kidney/BW %	1.24 ± 0.11	1.12 ± 0.18	1.11 ± 0.12*	1.22 ± 0.09	1.09 ± 0.15*	0.99 ± 0.04**	0.96 ± 0.07**

Note: ALT, Alanine Transaminase; TP, Total Protein; AST, Aspartate Transaminase; BUN, Blood Urea Nitrogen; TG, Triacylglycerols; BW, body weight; Data represent the means ± SD; *p<0.05, **p<0.01, ***p<0.001 as compared with M group; #p<0.05 as compared with ND group. Table reprinted from the original publication **I** and **II** with permission from the American Chemical Society.

5.3. ^{1}H NMR metabolomics reveals the effect of anthocyanin extracts on metabolic profile of plasma and liver

Table 9 shows the fold changes and the significance of plasma and liver metabolites in each group compared to the M group. The M group showed higher plasma levels of lipids, branched-chain amino acids (BCAAs: leucine; isoleucine, and valine), lactate, alanine, acetone, pyruvate, citrate, glycerol, unsaturated lipids, glucose, and creatine/creatinine and lower level of glutamine compared to the lean Zucker rats (ND and Con groups). For hepatic metabolites, compared to the lean Zucker rats, the M group showed increased levels of glucose, lactate, alanine, pyruvate, leucine, isoleucine, valine, tyrosine, phenylalanine, glutamine, glutamate, glutamine/glutamate ratio, dimethylamine, dimethylglycine, choline, phosphocholine, taurine, maltose, glycine, glycerol, mannose, triglyceride, total phospholipid, fatty acids residue, polyunsaturated fatty acid, docosahexaenoic acid (DHA), resonance from arachidonic acid and eicosapentaenoic acid (ARA/EPA), oleic acid, sphingomyelin, and monoglyceride.

The higher level of fasting plasma glucose of the diabetic group compared to the lean Zucker rats (Con and ND) examined by ^{1}H NMR was consistent with the level examined by biochemical assays. These two data frameworks of the glucose level were highly positively correlated (r = 0.98, p = 0.00), indicating the accuracy of the plasma metabolites levels identified by ^{1}H NMR. A recent review summarized that excessive substrates of metabolic energy such as carbohydrates and fatty acids exceeding the hepatic capacity to process are the pathogenic driver in the development of nonalcohol fatty liver and insulin resistance.[293] The higher level of fasting plasma and hepatic glucose, the increased body and liver weight, along with elevation of plasma and hepatic lipid profile showed a successful manifestation of type 2 diabetes.

Our previous studies also showed both purple potatoes and anthocyanin extract from purple potatoes of *Solanum tuberosum* L. 'Synkeä Sakari' decreased postprandial levels of plasma glucose and insulin in healthy men.[294,295] In the present study, feeding with anthocyanins, especially with NAAB, reduced the fasting plasma glucose levels compared to the M group. Moreover, both NAAB and AAPP significantly decreased hepatic glucose level. The levels of plasma lipids (resonance signal from fatty acid residue) and unsaturated lipids were decreased in all anthocyanin-treated groups, independent of weight loss. Feeding AAPP slightly improved the hepatic lipid profile by decreasing resonances from fatty acid residues and unsaturated fatty acids. These findings directly reflected the modulatory effect of anthocyanins extracts on glucose and lipid metabolism.

Plasma levels of lactate, citrate, alanine, and pyruvate, as well as hepatic lactate, alanine, and pyruvate, were increased in the M group compared to the

ND and Con groups, indicating an overall high level of glycolysis, which can be interpreted as a compensatory increase in glycolysis in T2D.[296] Several mechanisms are underlying the increased lactate level in T2D. In the aberrant pyruvate metabolism of T2D, pyruvate is converted to lactate instead of being converted to acetyl-CoA due to the inactivation of pyruvate dehydrogenase.[297] Furthermore, chronic hypoxia in skeletal muscle and adipose tissue, commonly found in obesity and disease with the decrease of lactate transporter monocarboxylate transport protein 1, induces the increased lactate level.[298] Moreover, oxidative stress in type 2 diabetes can increase the activities of lactate dehydrogenase and subsequently lead to the increase of the lactate level.[299] Anthocyanins have been shown strong antioxidative activities.[300] In the present study, AAPP significantly decreased plasma lactate and pyruvate levels compared to the M group, all the anthocyanin treatment decreased hepatic levels of glucose, lactate, alanine, and pyruvate, indicating improved glycolysis and lactate metabolism. Another pathway related to antioxidation was also affected: serine can be transformed to glycine and continue to donate the carbon of its side chain to form folate.[301] Acylated anthocyanins extracts from potatoes at both doses (AAPP) decreased the plasma levels of lactate, serine, and glycine, which might have been linked with improvement in the oxidative status in T2D rats. Acylated anthocyanins extract from purple potatoes contained a higher content of chlorogenic acid (93.01 ± 2.91 mg/g) than nonacylated anthocyanins extract from bilberries (10.39 ± 0.36 mg/g), which could also have contributed to the decrease in plasma pyruvate and lactate levels.[302] Glycerol is a crucial intermediate in lipid metabolism in the liver as well as an important substrate for gluconeogenesis.[303] Glycerol was decreased by AAPP in plasma and by all anthocyanins extracts in the liver. Moreover, glycerol, lactate, alanine, and glutamine are the gluconeogenic precursors accounting for over 90% of the overall gluconeogenesis.[304] Another finding was that AAPP effectively downregulated hepatic *G6PC* gene, revealed by both qPCR and full-length RNA-seq. Glucose-6-phosphatase (G6Pase) encoded by *G6PC* gene hydrolyzes glucose 6-phosphate releasing glucose into the circulation.[305] Glycerol as a major gluconeogenic substrate may also induce the expression of G6Pase catalyzing the terminal enzymatic step in gluconeogenesis.[306] In the current study, both the circulating and hepatic level of glycerol and mRNA of *G6PC* gene were decreased in the groups fed with the AAPP (L-AAPP, $P < 0.01$; H-AAPP, $P < 0.0$). Noticeably, chlorogenic acid present in the extract may have had an inhibiting effect on the glucose-6-phosphatase system.[307] TBC1D1 (TBC1 Domain Family Member 1) regulates the translocation of GLUT4 from intracellular vesicles to the surface of cell membranes in response to insulin stimulation, playing an important role in energy homeostasis.[308] TBC1D1-deficiency suppressed hepatic glucose production[309] and TBC1D1 knock-in mice

developed obesity and displayed characteristics of metabolic syndrome due to an increase in the expression of insulin-like growth factor 1 (IGF1) in hepatocytes and activation of the expression of lipogenic genes.[310] In this study, H-AAPP decreased hepatic mRNA levels of *TBC1D1* gene in Zucker diabetic fatty rats (H-AAPP, $P < 0.01$). These results showed improved glycolysis and lactate metabolism and a lower level of gluconeogenesis influenced by anthocyanin extracts.

The increment of circulating branched-chain amino acids (BCAAs), as shown in the M group compared with the lean Zucker rats, is linked with insulin resistance and dysregulation of metabolism of sugars and lipids.[311] Upregulation of hepatic BCAAs quantified by an amino acid analyzer, has also been observed in ZDF rats compared to healthy rats[312], which is consistent with this study. The levels of BCAAs are regulated by the activities of branched chain ketoacid dehydrogenase kinase (BDK) and mitochondrial phosphatase 2C (PP2Cm), known as the Kinase and Phosphatase Pair. In type 2 diabetes and obesity, high activity of PP2Cm leads to hyperphosphorylation of BDK by PP2Cm resulting in suppression of BDK activity and therefore increasing levels of BCAAs. Moreover, a high level of PP2Cm activity can activate ATP-citrate lyase and upregulate the conversion of citrate to acetyl CoA and malonyl CoA, which are the immediate substrates for lipogenesis and inhibit fatty acid oxidation *via* allosteric inhibition of carnitine palmitoyltransferase-1.[313] In this study, the groups fed with the anthocyanin extracts showed an overall decreasing trend in plasma and hepatic BCAAs, possibly indicating improvement in insulin sensitivity and reduction in lipogenesis. Furthermore, the first step to break down the BCAA by branched-chain aminotransferases occurs in the extrahepatic organs[314], therefore, both the hepatic and plasma levels of BCAAs were assumed to have similar changes.

Clinical studies have found that the circulating level of glutamate was positively correlated with insulin resistance[315], and increased glutamine/glutamate ratio predicted a reduced risk for developing diabetes.[315,316] The mechanisms were revealed as follows, increased glutamine and decreased glutamate could be linked with an increased level of GLP-1, improvement in insulin secretion and insulin sensitivity, and enhancement of the vesicle trafficking of GLUT4.[317,318] In the current study, the M group significantly decreased glutamine/glutamate ratio compared to the groups Con and ND, and the treatment with the AAPP significantly increased the glutamine/glutamate ratio, indicating improved insulin secretion and/or insulin sensitivity, however, the hepatic glutamine/glutamate ratio did not show any changes after feeding with anthocyanin extracts.

One of the potential targets of potato anthocyanin extract aimed in T2D is the betaine-homocysteine S-methyltransferase (BHMT) encoded by *Bhmt* which

transfers betaine to dimethylglycine. The hepatic expression of *Bhmt* and dimethylglycine level were increased in the M group compared to the ND and Con groups, the increased hepatic *Bhmt* gene expression was also shown in a previous study in ZDF rats.[319] All anthocyanin extracts decreased the elevated levels of dimethylglycine to a normal state. Decreased expression of *Bhmt* was also observed in all the anthocyanins extracts treatment groups, especially in the AAPP groups showing a statistically significant decrease. However, a metabolomic and genome-wide association study showed the major allele of DMG-dehydrogenase (rs243133) linked with low level of plasma dimethylglycine was associated with an increased risk of incident diabetes.[320] Although the contradictory results present, the changed dimethylglycine mechanism in T2D being less studied needs further investigation.

Table 9. Fold change in the plasma metabolites compared to the M group.

Metabolites	***M/L-NAAB***	***M/H-NAAB***	***M/L-AAPP***	***M/H-AAPP***	***M/CON***	***M/ND***
Plasma metabolites						
3-Hydroxybutyrate	2.07	2.96	2.16	1.05	1.36	1.01
Acetate	1.24	1.33	1.24	0.89	1.20	1.23
Acetoacetate	2.9	4.08	2.13	0.98	1.53	1.51
Acetone	1.65	2.10	1.66	1.17	3.82*	2.88*
Alanine	0.84	0.91	1.01	1.10	1.27	1.08
Choline	0.95	0.99	1.08*	1.28**	1.01	1.19*
Citrate	0.83*	0.99	1.07	0.98	2.12***	1.34***
Creatine/Creatinine	0.85	0.92	0.92	1.03	0.78*	0.91
Formate	1.10	1.14	1.09	1.09	1.32	1.39
Glucose	1.89***	1.47**	1.19	1.19	2.21***	2.98***
Glutamate	0.89	1.00	1.23**	1.66**	1.39*	1.85**
Glutamine	0.95	0.93	0.95	1.03	0.79*	0.78**
Glycerol	0.91	1.17	1.24**	1.32**	1.72***	1.41**
Glycine	0.89	1.20	1.20	1.55	0.69**	0.94
Histidine	0.82	0.90	0.89	0.89	0.45**	0.53**
Isoleucine	1.16	1.32*	1.68***	1.63***	1.95***	1.61***
Lactate	0.86	1.04	1.64**	1.33*	2.26***	1.55**
Leucine	1.21	1.44*	1.84***	1.21	1.85***	1.51**
Lipid	1.17	1.25**	1.37***	1.20*	3.86***	3.91***
Phenylalanine	1.03	1.08	1.18	1.21	1.01	1.15
Pyruvate	1.03	1.08	1.24**	1.32	2.24***	1.86***
Serine	0.98	1.04	1.16**	1.29*	1.03	1.14
Threonine	1.02	1.01	1.11	1.25	1.09	1.11
Tyrosine	0.86	0.96	1.03	1.17	0.90	0.97
Unsaturated fatty acid	1.30*	1.43**	1.50**	1.19	5.32***	6.01***
Valine	1.09	1.11	1.21*	1.37***	1.39***	1.35***

Metabolites	*M/L-NAAB*	*M/H-NAAB*	*M/L-AAPP*	*M/H-AAPP*	*M/CON*	*M/ND*
Hepatic aqueous metabolites						
3-Hydroxybutyrate	0.99	1.52	1.13	0.59*	1.14	0.98
Acetate	1.05	1.41***	1.18	1.00	0.95	0.86
Alanine	1.26**	1.51**	1.45**	1.19	1.56**	1.58***
Aspartate	1.08	1.56*	1.31	1.26	1.00	0.98
Cholate	1.03	1.10	1.20	1.00	1.18	1.57*
Choline	1.17	1.38	1.53*	1.19	0.65***	0.51***
Creatine	1.01	1.44***	1.31*	1.23	1.25*	1.06
Cytidine	1.21**	1.47**	1.50***	1.18	1.11	1.14
Dimethylamine	1.11	1.40*	1.21	1.03	1.61**	2.35***
Dimethylglycine	1.50	1.96**	1.73*	1.61*	1.94**	2.02**
Fumarate	1.56*	2.07*	1.39	1.1	1.28	1.22
Glucose	1.16	1.40***	1.49***	1.39**	2.92***	4.48***
Glutamate	1.05	1.41**	1.44**	1.41*	1.23	1.29**
Glutamine	1.08	1.32	1.42*	1.59**	2.47***	2.96***
Glutamine/Glutamate	1.05	0.94	1.02	1.16	2.07**	2.32***
Glutathione	1.09	1.21	1.48*	1.18	1.24	1.45
Glycerol	1.08	1.54***	1.49***	1.65**	2.42***	2.27***
Glycine	1.07	1.48***	1.41***	1.38***	1.41***	1.28***
Histidine	1.08	1.47***	1.38**	1.23**	1.07	1.15
Isoleucine	0.99	1.46***	1.29**	1.2	1.18*	1.30**
Lactate	1.14*	1.40**	1.40**	1.14*	1.78***	2.28***
Leucine	1.00	1.48***	1.30**	1.23*	1.15	1.25*
Lysine	1.07	1.54***	1.36*	1.30**	1.12	1.02
Malate	1.34	1.69**	1.29	1.18	1.22	1.19
Maltose	1.09	1.54**	1.47*	1.63***	4.18***	4.97***
Mannose	1.24**	1.58***	1.50***	1.38**	1.71***	2.18***
Methionine	1.00	1.41**	1.37**	1.40*	1.26	1.35**
Phenylalanine	0.93	1.44**	1.22	1.20*	1.11	1.27*
Phosphocholine	1.16	1.21	1.15	0.96	1.10	1.35*
Pyruvate	1.43**	1.41**	1.91***	1.18	1.11	1.50***
Succinate	1.08	1.17	1.51	1.23	1.62	2.06*
Taurine	1.26*	1.38	1.49*	1.17	1.89**	1.98***
Tyrosine	1.06	1.60**	1.33**	1.32**	1.27**	1.28**
Uracil	1.10	1.52*	1.33**	1.30*	1.09	1.05
Uridine	1.15	1.14	1.21*	0.94	1.00	1.39*
Valine	1.01	1.50***	1.31**	1.24*	1.13	1.23*
Xanthosine	0.91	0.96	1.16	1.08	0.97	1.13
Hepatic lipid metabolites						
ARA+EPA	1.05	0.95	1.13*	1.18*	1.40***	1.37**
Cholesterol	0.95	0.97	1.02	1.12	1.09	1.15
DHA	1.14	0.99	1.17	1.12	2.64***	2.75***
Diglyceride	1.11	1.14	1.02	1.06	1.11	1.13
Fatty acid residue (FA, -(CH2)n-)	1.03	0.93	1.16	1.12	1.46**	1.46**
Linoleic acid	1.08	1.00	1.2	1.16	1.16	1.19
Monoglyceride	1.07	1.05	1.30**	1.26*	1.55***	1.51***
Oleic acid	0.93	0.92	1.17	0.98	1.51**	1.43*
Omega-3 fatty acid	1.04	0.97	1.13	1.18**	2.04***	2.35***
PC/PE	1.21	1.02	1.33	1.00	1.63**	1.82***

Metabolites	*M/L-NAAB*	*M/H-NAAB*	*M/L-AAPP*	*M/H-AAPP*	*M/CON*	*M/ND*
Phosphatidylcholine (PC)	1.05	100	1.08	1.16	1.48	1.56
Phosphatidylethanolamine (PE)	1.00	1.08	0.96	1.17	1.08	1.02
Phosphatidylserine	1.25	2.21	0.87	1.59	0.43**	0.37***
Plasmalogen	0.97	1.04	0.87	1.05	1.05	0.96
PUFA	1.04	0.94	1.13	1.18*	1.63***	1.59***
Sphingomyelin	1.05	0.93	1.25	1.19	1.39*	1.39*
Total phospholipids	1.04	1.01	1.00	1.14	1.28**	1.33**
Triglyceride	1.04	0.95	0.97	0.98	1.88***	2.28***

FA, Fatty acid; DHA, docosahexaenoic acid; EPA, dcosapentaenoic acid; ARA, arachidonic acid; PUFA, polyunsaturated fatty acids. *p<0.05, **p<0.01, ***p<0.001 as compared with M group. Tables reprinted from the original publication **I** and **II** with permission from the American Chemical Society.

5.4. A Full-length RNA-Seq reveals the effects of anthocyanin extracts on transcriptome in Zucker diabetic fatty rats

The liver plays an important role in glucose and lipid metabolism in T2D. The summary in a recent review indicated that anthocyanins may have beneficial effects on the diabetic liver by increasing AMP-activated protein kinase phosphorylation (AMPK), protein kinase C phosphorylation, glutathione synthesis, insulin sensitivity, peroxisome proliferator-activated receptor α palmitoyltransferase-1 A, glycogen synthesis, glucose transporter 1 and 4, PI3K/AKT signaling and decreasing, lipogenesis, oxidative damage, acetyl-CoA, gluconeogenesis, and mTOR signaling.[212] A transcriptomic study has shown that a nonacylated anthocyanin pelargonidin 3-*O*-glucoside extracted from wild raspberries had a beneficial effect on hepatic transcriptome in *db/db* mice through regulating genes involved in glucose and lipid metabolism.[321] However, the effect of acylated anthocyanin on hepatic transcriptome and metabolic profile of the healthy or type 2 diabetic state has not been reported previously. **Study II** is the first study to compare the effects of nonacylated anthocyanins from berries and nonacylated anthocyanins from potatoes on the hepatic metabolic profile and transcriptome in diabetes.

5.4.1. Overview of statistics for DEGs and DETs

Transcripts were sequenced by full-length RNA-seq. Differentially expressed genes (DEGs) and differentially expressed transcripts (DETs) were defined in six comparisons: ND/M, Con/M, L-NAAB/M, H-NAAB/M, L-AAPP/M, and H-AAPP/M (**Figure 7A–B**). In the ND/ M and Con/M comparisons, a large number of DEGs and DETs proved the distinguished transcriptomic profiles caused by

the difference between healthy control and the diabetic model (ND/M: 691 upregulated and 1,098 downregulated DEGs, 2,469 upregulated and 2,483 downregulated DETs) and by the defect of leptin receptor gene (Con/M: 421 upregulated and 827 downregulated DEGs, 1,341 upregulated and 1,889 downregulated DETs). Among the anthocyanin extract-treated groups, feeding with H-AAPP altered the greatest numbers of genes and transcripts (101 upregulated and 179 downregulated DEGs, 89 upregulated and 780 downregulated DETs) compared to the M group. The heatmaps of the DEGs and DETs showed that the H-AAPP could regulate the transcriptome profile in the M group towards that of the ND and Con groups (**Figure 7C–D**), indicating that among all the anthocyanin extract-treated groups, H-AAPP might exert the most beneficial effect on ZDF rats

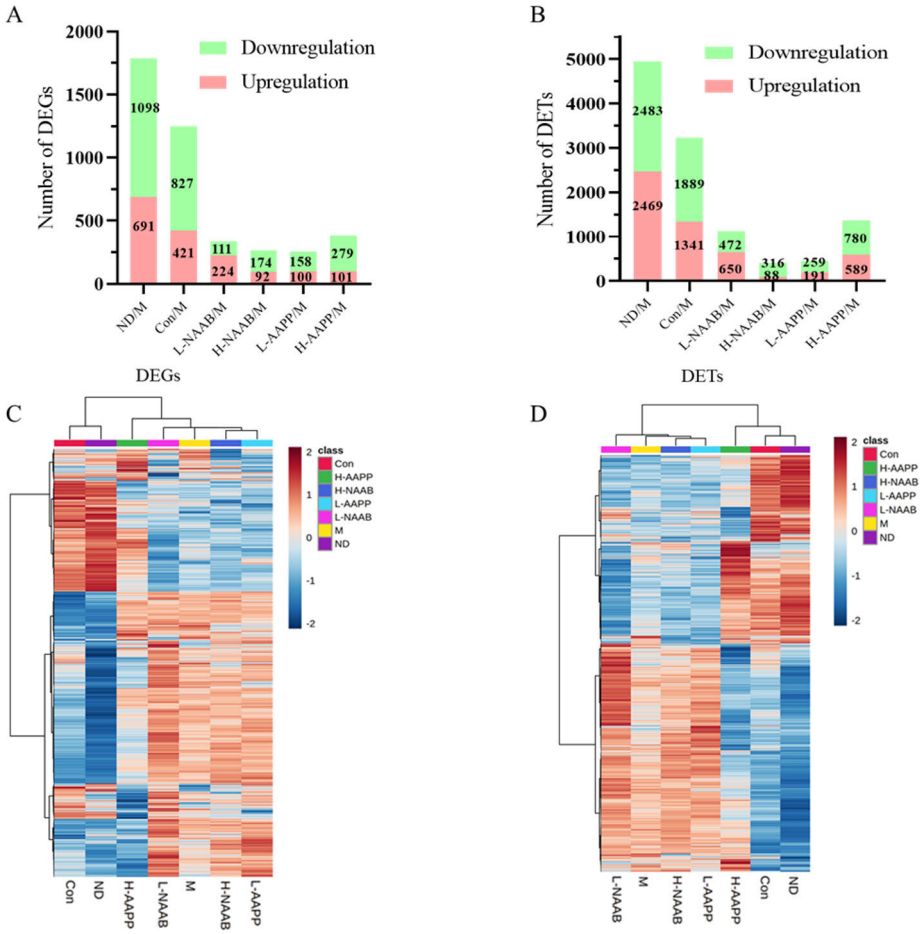

Figure 7. Statistics of DEGs **(A)** and DETs **(B).** Heatmap of DEGs **(C)** and DETs **(D)**. In the heatmaps, red represents the upregulated genes or transcripts, blue represents the downregulated genes or transcripts. Figures reprinted from the original publication **II** with permission from the American Chemical Society.

5.4.2. Genes restored by anthocyanin extracts in ZDF rats

Venn diagrams (**Figure 8**) were used to show which dysregulated genes (we discussed only known genes) were reversed by NAAB and AAPP. NAAB increased the expression of *LOC103692167, Mgat4a, Gstm6, Atxn7l2* and decreased expression of *Lpl* (**Figure 8A and C**). AAPP increased the expression of *Isg20l2* and *Mgat4a* and decreased expression of *Smpd3, Plp1, Clstn3, Pkm, RGD1561662, Pde6c, Egr1,* and *Gdf15* (**Figure 8B and D**).

Gstm6, encoding glutathione S-transferase associated with the glutathione metabolism, metabolism of xenobiotics by cytochrome P450 and drug metabolism, was reported to be downregulated in both insulin-resistant and diabetic mice and involved in the progression of T2D.[322,323] Expression of *Mgat4a* was increased by both types of anthocyanin extracts (NAAB and AAPP), which was decreased in the M group compared to the Con group. A study has shown that genetic inactivation of the *Mgat4a* gene encoding the N-acetylglucosaminyl transferase GnT-4a in mice caused the improper assembling of glucose transporter 2 N-glycan, which led to a failed interaction between the plasma membrane lectin galectin 9 and glucose transporter 2 (GLUT2), causing GLUT2 internalization and therefore suppressing glucose uptake and glucose-stimulated insulin secretion.[324] A fat-enriched diet was also reported to inhibit the expression of the *Mgat4a.*[325] Both NAAB and AAPP reversed the down-regulation of *Mgat4a* in diabetic ZDF rats, indicating the potential role of anthocyanins in restoring the function of glucose transporter 2 in diabetes.

Genetically overexpressed hepatic *Lpl* encoding lipoprotein lipase in mice would cause a two-fold increase in hepatic triglyceride content and insulin resistance partly due to the impaired ability of insulin to suppress endogenous glucose production associated with defects in insulin activation of insulin receptor substrate-2-associated phosphatidylinositol 3-kinase activity.[326] A higher expression level of *Lpl* was observed in the M group compared to the Con group, which was downregulated by both L-NAAB and H-NAAB, suggesting an improved insulin sensitivity.

Egr1 encoding early growth response protein 1 can be transiently activated by glucagon and mediate glucagon-regulated gluconeogenesis.[327] *Smpd3* gene encodes nSMase2 (neutral sphingomyelinase) which is the most studied enzyme in the sphingomyelinase family. Abnormalities in sphingolipid metabolism have been associated with the pathogenesis of obesity/diabetes.[328,329] Evidence has shown that sphingomyelin metabolites (e.g., ceramide and sphingosine) could serve as signaling molecules affecting a series of physiological and pathological process including cell growth, survival, and death.[330,331] Elevated TNF-α and insulin in *ob/ob* mice might cause an increased level of *Smpd3* in adipose tissue.[332] AAPP decreased hepatic expression of *Egr1* and *Smpd3,* indicating the beneficial effects.

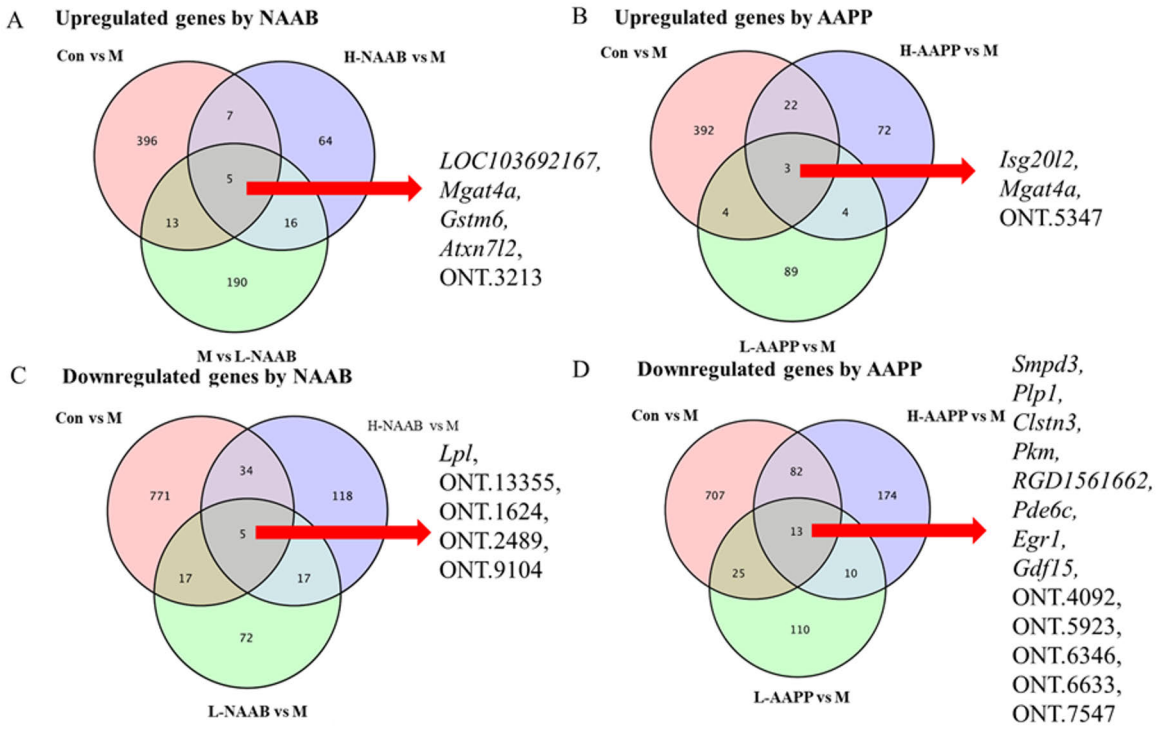

Figure 8. Venn diagrams showing downregulated genes in the M group compared to the Con group were upregulated by NAAB (A) and AAPP (B) and upregulated genes in the M group compared to the Con group were downregulated by NAAB (C) and AAPP (D). Figures reprinted from the original publication **II** with permission from the American Chemical Society

5.4.3. Functionally grouped annotation network based on ClueGO

DEGs in each comparison were subjected to ClueGO to generate functionally grouped annotation networks (in **Publication II**) and their summary overview charts (**Figure 9A–F**). The top 3 functional groups with the most abundant enriched GO terms in the comparisons are highlighted in bold. The label of the functional group in the overview chart is named by the group leading term (the most significant term in the group).

The functionally grouped annotation networks based on the DEGs in ND/M and Con/M comparisons shared massive identical GO terms, such as monocarboxylic acid metabolic process, carboxylic acid biosynthetic process, fatty acid metabolic process, lipid metabolic process, and response to organic substance, etc. Lipid-related metabolism was the major transcriptomic difference between ZDF rats and lean Zucker rats. (**Figure 9A–B**)

However, we did not observe similar GO terms between the networks generated by DEGs between L-NAAB/M and H-NAAB/M comparisons except that L-NAAB regulated the genes in cellular response to fatty acid and H-NAAB regulated the genes in the regulation triglyceride metabolic process. (**Figure 9C–D**) In L-AAPP/M and H-AAPP/M comparisons, the networks showed similar terms interleukin 1 beta production and lipid-related GO terms (L-AAPP, triglyceride catabolic process; H-AAPP, long-chain fatty acid biosynthetic process). These results from the ClueGo analysis indicated both NAAB and AAPP might regulate the lipid metabolism in T2D and AAPP could affect the cytokine interleukin 1 beta production. (**Figure 9E–F**)

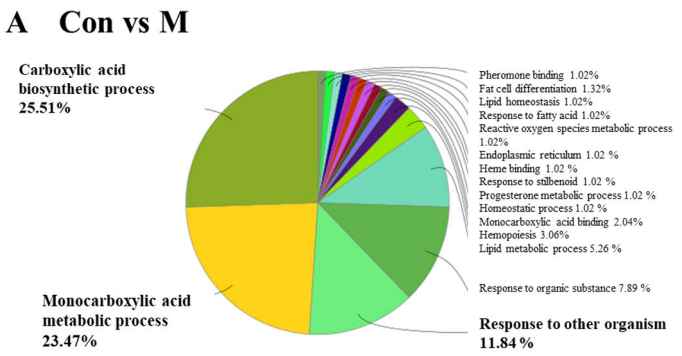

B ND vs M

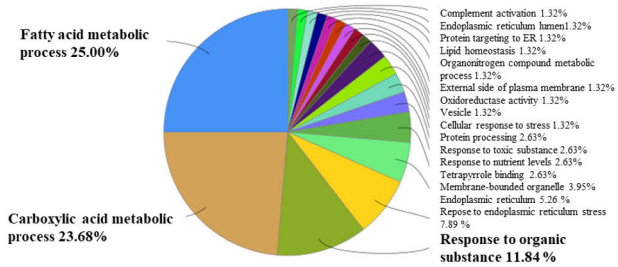

C L-NAAB vs M

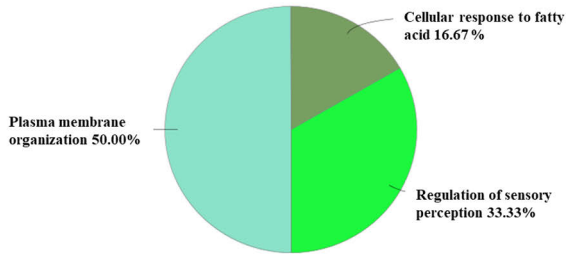

D H-NAAB vs M

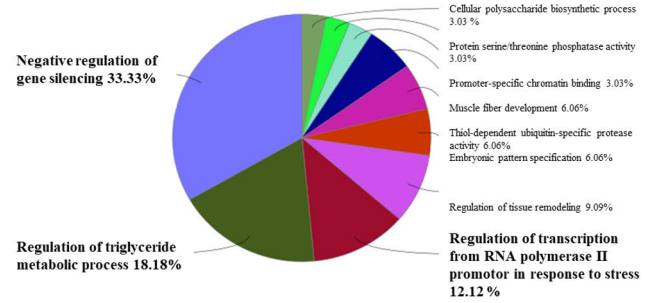

E L-AAPP vs M

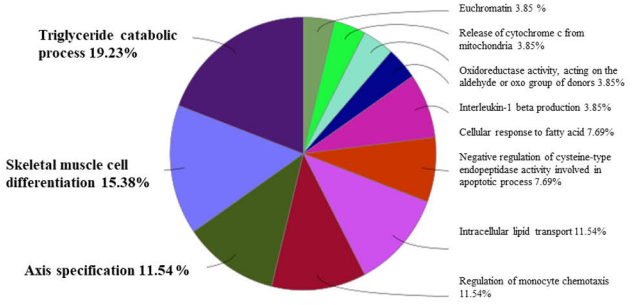

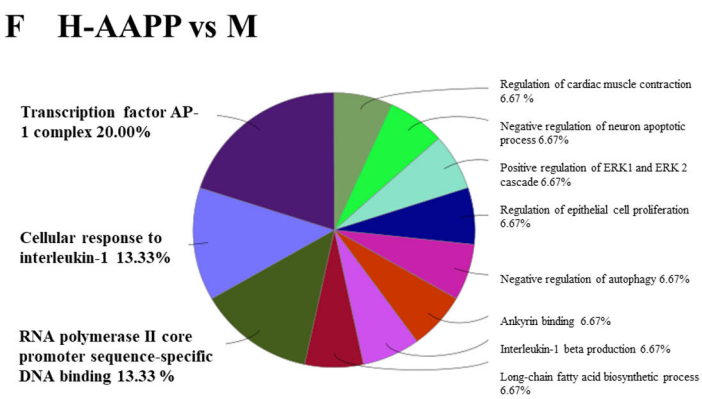

Figure 9. Overview chart generated from a functionally grouped network of enriched GO terms based on DEGs in Con/M **(A)**, ND/M **(B)**, L- NAAB/M **(C)**, H-NAAB/M **(D)**, L-AAPP/M **(E)**, and H-AAPP/M **(F)** comparisons. The top three functional groups with the most abundant GO terms in each comparison are highlighted in bold. Figures reprinted from the original publication **II** with permission from the American Chemical Society.

5.4.4. PPI network analysis and WGCNA analysis

We next applied the PPI network construction based on DEGs in each comparison to show the top 10 genes with the highest degree of connectivity, which showed major contributors in the difference between the groups. The top 10 genes with the highest degree of connectivity with other genes were considered as hub genes which usually play an essential role in gene regulation and biological processes. (**Figure 10A–F**)

In the Con/M comparison, the M group showed upregulated *Fasn*, *Acly*, *Acaca*, and *Srebf1*. Interestingly, sterol regulatory element-binding protein 1(SREBP-1) encoded by *Srebf1* is a transcription factor modulating the expression of *Fasn* (encoding fatty-acid synthase), *Acly* (ATP citrate lyase), *Acaca* (Acetyl-CoA carboxylase 1). These genes encode key enzymes for fatty acid synthesis, suggesting excessive fatty acid synthesis as the major characteristic in ZDF rat.[333] *Src*, as an essential coordinator of hepatic glucose production, could be activated in type 2 diabetes by reactive oxygen species (ROS), TGF-beta, and G-protein coupled receptors (GCPRs).[334] *Gapdh* gene encoding glyceraldehyde 3-phosphate dehydrogenase was reported to be upregulated in the diabetic liver, which is in accordance with this study.[335] Moreover, as previously mentioned, lipid metabolism-associated GO terms account for a large number of enriched GO terms in functionally grouped networks generated by the DEGs between diabetic rats and healthy rats. Thus, ZDF rats might be characterized by excessive fatty acid synthesis and a high level of glucose production.

Fos and *Jun* are two subunits of activator protein 1 (AP-1) which is an important transcriptional regulator mediating gene regulation in response to a variety of physiological and pathological stimuli, including stress signals, growth factors, infections, and cytokines as well as oncogenic stimuli.[336] It has been reported that oxidative stress in the ZDF rats could activate JNK and further positively regulate AP-1[337]; also suppression of JNK has been reported to improve glucose tolerance and insulin resistance in diabetic mice.[338] In this study, the M group had a higher level of *Jun* expression compared to the ND group ($P < 0.05$, data not shown), and both *Jun* and *Fos* expressions were downregulated by the AAPP extracts. The high-dose bilberry anthocyanin extract (H-NAAB) downregulated *Jun* expression. AP-1 might be a target that is regulated by both anthocyanins extract, especially AAPP, possibly alleviating insulin resistance and improving glucose tolerance. Enriched GO terms-based functionally grouped networks also showed H-AAPP regulated transcriptional factor AP-1 complex. Anthocyanin extract from black rice[339] and purple sweet potatoes[340] have been reported to suppress the activity of NF-κB and AP-1 in RAW 264.7 macrophage cell line, both two transcriptional factors are involved in inflammatory response. In addition, one common enriched GO term in the functionally grouped networks was regulated by both AAPP-treated groups: interleukin 1 beta production. Interleukin 1 beta production could be induced by both NF-κB and AP-1 and have been reported to be suppressed by anthocyanin-rich fractions from red raspberries *in vitro*[341], purple sweet potatoes in hypercholesterolemic rabbits[342], and blueberry powder in Wistar rats.[343]

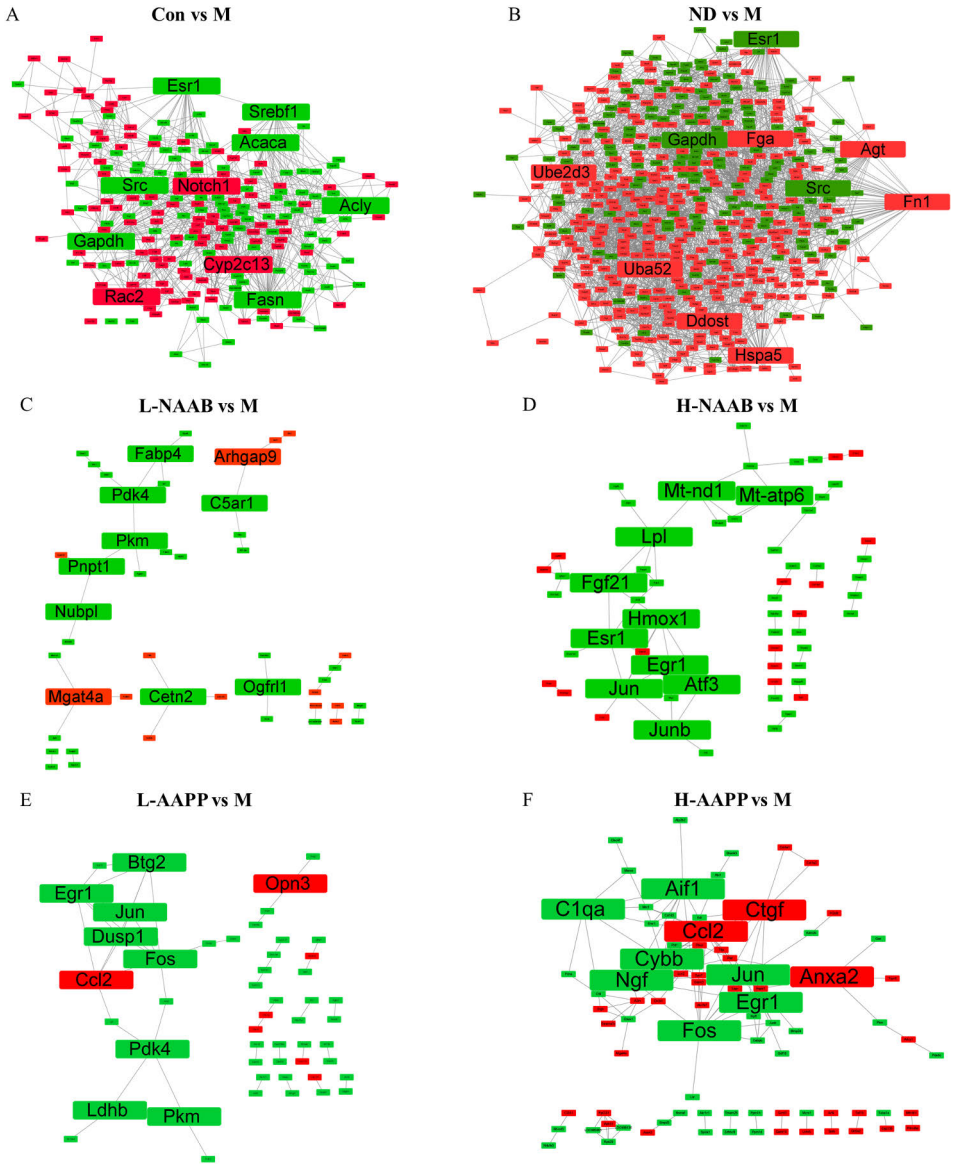

Figure 10. PPI network generated by DEGs in Con/M **(A)**, ND/M **(B)**, L-NAAB/M **(C)**, H-NAAB/M **(D)**, L-AAPP/M **(E)**, and H-AAPP/M **(F)** comparisons. The top 10 genes with the highest degree are highlighted with larger fonts. Genes with red color represent upregulation of genes in the group compared to the M group. Genes with the green color represent the downregulation of genes in the group compared to the M group. Figures reprinted from the original publication **II** with permission from the American Chemical Society.

WGCNA analysis was conducted to detect the comprehensive correlations between DEGs and clinical traits including body weight, AST, ALT, blood urea nitrogen, plasma glucose, and insulin as well as hepatic glucose and liver/body weight ratio. Twelve co-expression modules were identified (**Figure 11A**). MEgrey60 and MEtan modules showed a positive correlation with body weight, liver weight/body weight ratio, plasma glucose, hepatic glucose and negative correlation with AST. MEgreen and MEgreenyellow modules showed a negative correlation with body weight, liver weight/body weight ratio, plasma glucose, hepatic glucose and positive correlation with AST. Next, we wanted to see the functions of genes in MEgrey60 and MEtan modules as well as genes in MEgreen and MEgreenyellow modules and therefore conducted a KEGG pathway enrichment analysis. We found genes in MEgrey60 and MEtan modules were significantly enriched in 20 KEGG pathways (**Figure 11B**), which were mainly involved in lipid metabolism (fatty acid metabolism, biosynthesis of unsaturated fatty acids, regulation of lipolysis in adipocytes), amino acid metabolism (glycine, serine and threonine metabolism, cysteine and methionine metabolism, glutathione metabolism), diabetes (maturity onset diabetes of the young, type II diabetes mellitus, type I diabetes mellitus, insulin signaling pathway), metabolic pathways, pyruvate metabolism, AMPK signaling pathway, PPAR signaling pathway, and Th17 cell differentiation. Genes in MEgreen and MEgreenyellow modules were enriched in 12 KEGG pathways (**Figure 11C**) which were mainly involved in arachidonic acid metabolism, retinol metabolism, metabolic pathways, protein export, protein processing in endoplasmic reticulum, steroid hormone biosynthesis, complement and coagulation cascades, linoleic acid metabolism, and inflammatory mediator regulation of TRP channels. These enriched pathways might play an important role in type 2 diabetes and suggest a relationship to the clinical parameters.

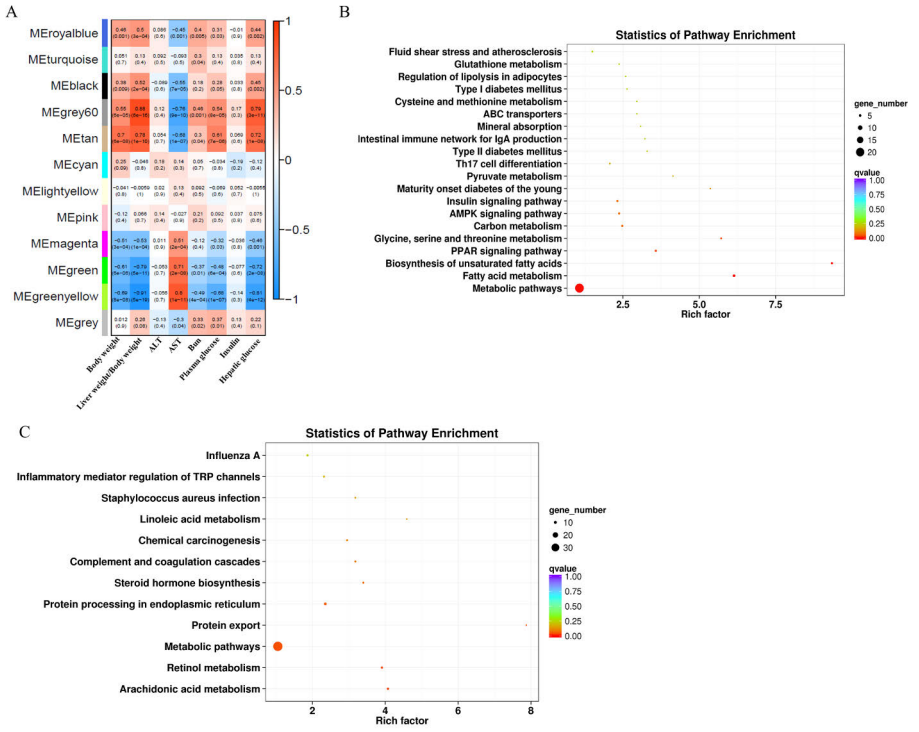

Figure 11. Heatmap of the correlation between clinical traits and module eigengenes (A). Each column corresponds to a clinical trait, and each row corresponds to a module. Each cell contains the correlation coefficients which correspond to the cell color; green represents a negative correlation, and red represents a positive correlation. The p values are stated in the brackets. KEGG pathway enrichment analysis based on the genes in MEgrey60 and MEtan modules (B). KEGG pathway enrichment analysis based on the genes in MEgreen and MEgreenyellow modules (C). Figures reprinted from the original publication **II** with permission from the American Chemical Society.

5.5. Metagenomic reveals the effects of anthocyanin extracts on gut microbiota and metabolites in Zucker diabetic fatty rats

5.5.1. Changes in gut microbiota composition

Distinguished gut microbiota composition was observed between ZDF rats and lean Zucker rats. The number of species was increased in the ZDF rats (**Figure 12A)**, which was in accordance with the result of another ZDF rat study recently published.[283] However, other indicators for microbiota diversity indexes were not seen as being changed. (**Figure 12B–C**) Fecal microbial composition at the

phylum level is shown in **Figure 12D**. PCA revealed a distinguished separation in bacteria abundance between the lean Zucker rats fed with a normal diet (ND), lean Zucker rats fed with a high-fat diet (Con), and ZDF rats (**Figure 12E**). Although the Bacteroidetes/Firmicutes ratio has been suggested as a marker of metabolic disease,[135] the Bacteroidetes/Firmicutes ratio did not show consistent associations with T2D.[135] In this study, ZDF rats did not show an increased Bacteroidetes/Firmicutes ratio. (**Figure 12F)**

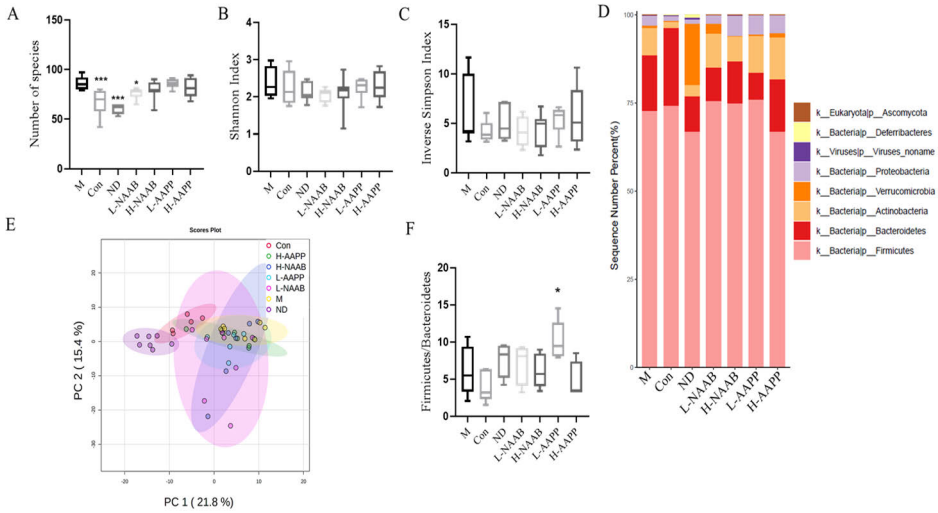

Figure 12. The gut microbiota richness index: number of species **(A)**. The gut microbiota diversity indexes: Shannon index and inverse Simpson index **(B** and **C)**. Gut microbial composition at phylum level **(D)**. Principal component analysis of gut microbiota abundance **(E)**. The ratio of Bacteroidetes to Firmicutes **(F)**. *$p < 0.05$, **$p < 0.01$, and ***$p < 0.001$ as compared with the M group. Figures reprinted from the original publication **III** with permission from the Elsevier.

The abundance of species *Clostridium hathewayi*[137], family *Lachnospiraceae*[137], and genus *Bifidobacterium*[135] have been observed to be increased in the gut of T2D patients. In the current study, the abundance of species *Clostridium hathewayi*, *Lanchnospiraceae bacterium 1_7_47FAA*, and *Bifidobacterium pseudolongum* were observed to be increased in the ZDF rats compared to the lean Zucker rats. **(Figure 13A–B)** Species *Dorea formicigenerans*, showing a positive correlation with inflammatory markers in obesity[344], was also increased in ZDF rats. **(Figure 13A–B)** *Akkermansia muciniphila* has shown to have a negative association with T2D in human[135] and

to affect glucose metabolism, lipid metabolism, and intestinal immunity[345], it was decreased in the M group compared to the ND group. (**Figure 13A–B)**

We found anthocyanin extracts showed a beneficial effect on the gut microbiota composition of ZDF rats. The abundance of genus *Parabacteroides* has been reported to be increased in patients with nonalcoholic steatohepatitis[346] and positively correlated with splenic CD4+ Th17 cells and serum proinflammatory cytokine IL-17 in arthritic mice.[347] The family *Peptostreptococcaceae* has been observed to be significantly lower in T2D patients[348,349] L-NAAB and AAPP decreased species in genus *Parabacteroides* (including species *P. merdea, P. distasonis,* and *P. goldsteinii* decreased by L-NAAB; species *P. distasonis* decreased by L-AAPP; species *P. distasonis* and *P. goldsteinii* decreased by H-AAPP) and increased species in family *Peptostreptococcaceae* (including species *P. noname unclassified*), indicating L-NAAB and AAPP might improve glucose homeostasis and inflammation in diabetes through modulating these microbes. (**Figure 13C, E–F)** Moreover, the species *Ruminococcus torques* known to decrease the barrier integrity of the gut[350] was reported to be positively associated with insulin resistance in obesity.[344] The abundance of *Ruminococcus torques* was decreased by AAPP (**Figure 13E–F)**, suggesting a beneficial effect on the gut barrier and insulin homeostasis. The abundance of genus *Marvinbryantia* has been reported to be decreased in patients with hypertension and positively correlated with intestinal vitamin D which is one of the novel risk factors for hypertension.[351] Increased genus *Marvinbryantia* (including *M. formatexigenes*) in NAAB and L-AAPP might alleviate the potential risk for hypertension in T2D. (**Figure 13C–D, E)** A recent review[180] summarized the effect of various dietary anthocyanins on microbiota in humans and animals. Several studies showed that anthocyanins affected bacterial *Lactobacillus* spp. and *Bifidobacterium* spp. For example, anthocyanin extract from blackcurrants increased the abundances of *Lactobacilli* and *Bifidobacteria* in the human gut; anthocyanin extract from black raspberries increased gut *Anaerovorax* and *Dorea* and decreased *Bifidobacterium* and *Lactococcus* levels in rats. However, these results were not seen in our study. This inconsistency is likely due to the various anthocyanins present (anthocyanin extracts or anthocyanin-rich fruits), hosts (rat, mice, or human), and technics of the sequencing (metagenomics sequencing and 16S rRNA sequencing).[180]

At the pathway level, a defect in the leptin receptor gene in ZDF rats (M group) showed depleted flagellar assembly and bacterial chemotaxis and enriched ABC transporters pathways. (**Figure 14)** These findings were in accordance with the previous study in T2D patients.[152,352] As regards the KEGG pathways affected by anthocyanin extracts (**Figure 14C–F)**, we considered that bilberry anthocyanins and low-dose potato anthocyanin extracts (L-AAPP) decreased sphingolipid metabolism, high-dose bilberry anthocyanins (H-NAAB) and

potato anthocyanins at both doses (AAPP) increased purine metabolism, AAPP increased oxidative phosphorylation, DNA replication, phenylpropanoid biosynthesis, and RNA polymerase and decreased HIF-1 signaling pathway. Purine metabolism was one of the most changed pathways by AAPP and L-NAAB. Tea polyphenols have been reported to modulate gut purine metabolism, which contributes to improvement of high-fat diet-induced gut microbiota dysbiosis.[353] AAPP and L-NAAB might improve gut dysbiosis in diabetes through this pathway. In addition, purine metabolism is closely related to glycine, serine and threonine metabolism[354] which was also significantly enriched in AAPP groups from the metabolomic data. A clinical study showed that obese subjects who lost weight had an upregulated oxidative phosphorylation pathway in gut microbiota compared to those who failed to lose weight.[355] In this study, only the AAPP upregulated the oxidative phosphorylation pathway in the gut microbiota and might have a similar beneficial effect to that of weight loss.

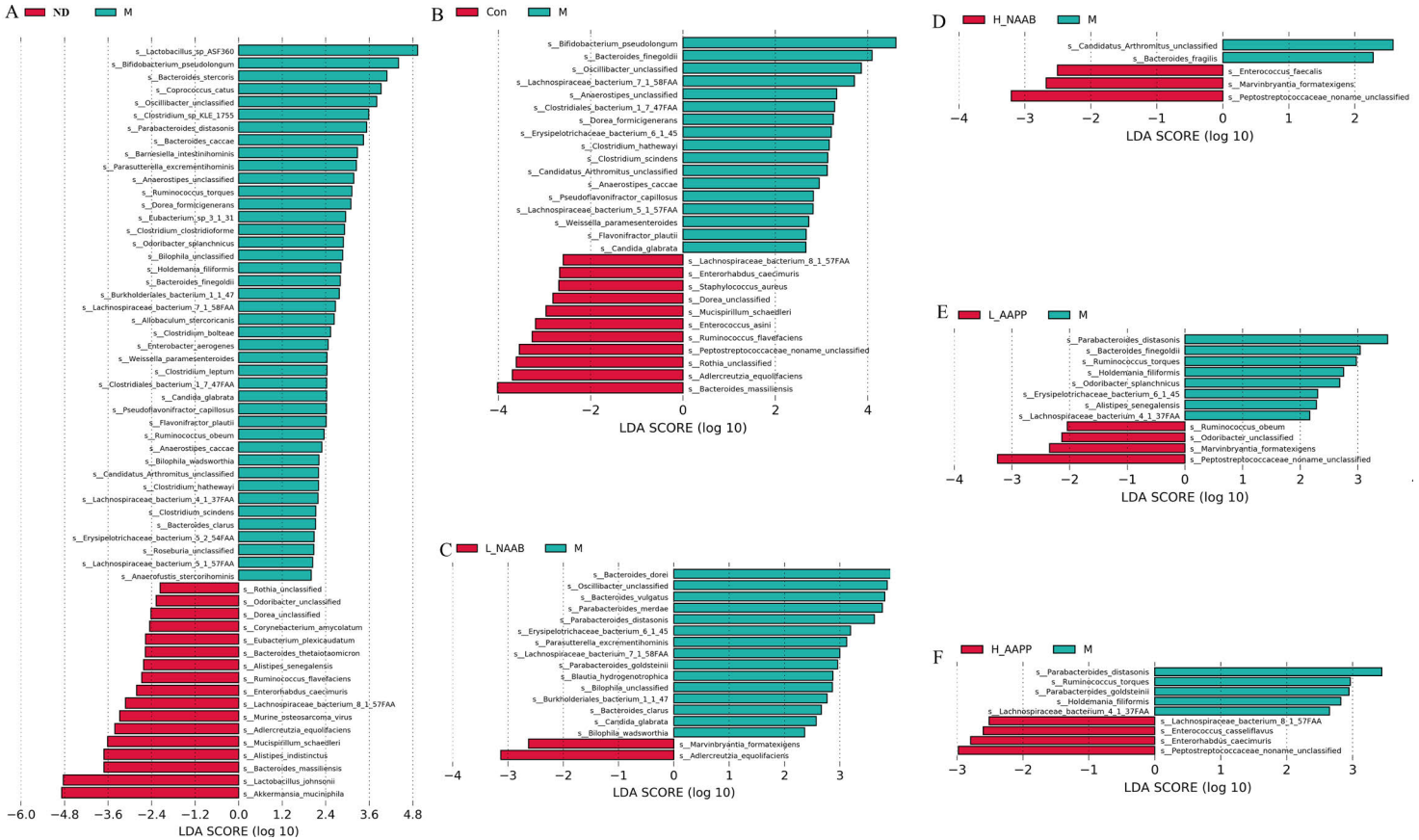

Figure 13. The results of LEfSe (LDA Effect Size) analysis at the species level. The histogram of LDA score showed the differentially abundant species (the absolute value of LDA greater than 2) in comparisons between different groups: M/ND (A), M/Con (B), M/L-NAAB (C), M/H-NAAB (D), M/L-AAPP (E), and M/H-AAPP (F). The length of the bars (LDA Score) represents the influencing degree of the species. The species with positive or negative LDA score have higher or lower abundance in the M group. Figures reprinted from the original publication **III** with permission from the Elsevier.

Figure 14. Extended error bar plots identifying significantly altered KEGG pathways of gut microbiota in M/ND (A), M/Con (B), M/L-NAAB (C), M/H-NAAB (D), M/L-AAPP (E), and M/H-AAPP (F) comparisons. Figures reprinted from the original publication **III** with permission from the Elsevier.

5.5.2. Changes in gut luminal metabolites and pathway analysis

In **Study III**, we compared the effect of nonacylated anthocyanins with their acylated counterparts on intestinal luminal metabolites in type 2 diabetes. **Figure 15–18** shows the volcano plots with fold change of the fecal metabolites at 3 timepoints and cecal metabolites, compared to the M group.

Different intestinal luminal metabolic profiles between ZDF rats and lean Zucker rats were observed. In this study, the defect of *leptin* receptor gene in ZDF rats led to an increased level of SCFAs in feces at week 1 (**Figure 15A–B**), 4 (**Figure 16A–B**), and 8 (**Figure 17A–B**) compared to the lean Zucker rats (no significant change of butyrate at week 1), this might be the result of the increased amount of substrates for microbial fermentation due to increased food intake over the intervention period and increased microbial fermentation of non-digestible carbohydrates by the gut microbiota in the colon of the obese rats,[113] and decreased colonic absorption with obesity.[116] Higher fecal concentrations of SCFAs were also observed in another ZDF rat study.[113] Compared with the lean Zucker rats in the ND and Con groups, the M group showed an increased abundance of Actinobacteria identified as a potential butyrate producer at the phylum level, the family *Clostridiales* producing short-chain fatty acids, genus *Bifidobacterium* (belonging to the phylum Actinobacteria) producing acetate and lactate[356], *Lachnospiraceae bacterium 7_1_58FAA* producing propionate[357], and *Anaerostipes caccae* producing butyrate.[356] A study has investigated 32 SCFA-producing species from the top 56 most abundant species in gut microbiota to study their abilities to produce SCFAs.[358] Among these SCFA-producing species, the abundances of *Bacteroides finegoldii* producing propionate and acetate and *Clostridium scindens* producing acetate were increased in the M group compared to the ND and Con groups. (**Figure 13A–B**)

Inconsistent results have been reported on the effect of anthocyanins on the production of SCFAs by gut microbiota.[248,359] In **Study III**, H-AAPP showed the increased acetate, propionate, and butyrate levels in cecal content, whereas the fecal propionate was decreased by L-NAAB and H-AAPP at week 8. (**Figure 18F; Figure 17C and F)** Succinate, pyruvate, malate, and fumarate, as byproducts of anaerobic fermentation, participate in the production of propionate.[360] Cecal succinate and malate were also increased by H-AAPP, which might partly contribute to the increased propionate level in the H-AAPP group. (**Figure 18F)** Moreover, several gut bacteria producing propionate were found to be decreased in the L-NAAB, L-AAPP, and H-AAPP groups, e.g. *Lachnospiraceae bacterium 4_1_37FAA*[357] and *Parabacteroides distasonis* which has been reported as one of the major propionate-producers among the dominant species in gut flora.[358] (**Figure 13C, E, and F)** A reduced abundance of these microbes has likely contributed to the decrease in the fecal propionate

in L-NAAB, L-AAPP (non-significant decrease), and H-AAPP groups at week 8. (**Figure 17C, E, and F)** In addition, a study has shown that microbiota-produced succinate in cecum, a substrate of intestinal gluconeogenesis, could improve glycemic control and hepatic glucose production.[349] Therefore, increased cecal succinate in the H-AAPP group might decrease hepatic glucose production in diabetic rat through activating intestinal gluconeogenesis. Fecal lactate was higher in the M group compared to the ND and Con groups at week 8, and only the groups fed AAPP showed a decreased level of lactate compared with the M group at week 8. (**Figure 17A, B, E, and F**) Changes in the gut microbiota composition and metabolism lead to disruption of lactate production and utilization. A previous study reported the highest abundance of lactate-producing bacteria in T2D human subjects, followed by obese and lean participants.[361] Increasing abundances of lactate-producing bacteria (e.g., *Bacteroides finegoldii, Bifidobacterium pseudolongum*)[358] and/or decreased lactate consumption in gut microbiota metabolism is likely to contribute to the increase of lactate in the M group. (**Figure 13A–B**) AAPP reversed lactate level at week 8 by decreasing lactate-producing bacteria, *Parabacteroides distasonis* and *Ruminococcus torques*[358] and/or the increased lactate utilization. (**Figure 13E–F**) However, AAPP increased lactate level at week 1 (**Figure 15F**), indicating different impacts of AAPP on fecal lactate at different stages of diabetes.

Anthocyanins are well-known for their ability of hypoglycaemic effect largely due to the inhibitory effects of anthocyanins on carbohydrate digesting enzymes: α-glucosidase and pancreatic α-amylase in the upper intestine.[362] In **Study III**, we found all anthocyanins treatment groups showed an overall increasing trend of cecal sugars including ribose, arabinose, galactose, xylose, and glucose (**Figure 18C–F)**, which might benefit the glycaemic response and insulin stimulation.

Unabsorbed choline can be metabolized into trimethylamine (TMA) by gut anaerobic bacteria. TMA can be further catabolized into dimethylamine (DMA) and methylamine (MA), and can also be transported into the liver through the portal vein and oxidized to trimethylamine oxide which is considered to be a proatherogenic metabolite.[363] The increase in the fecal TMA at week 4 and 8 and cecal TMA in were found in the ZDF rats (**Figure 16B; Figure 17A–B; Figure 18A–B)**, indicating a potential risk of atherogenesis. Anthocyanin extracts also affected the choline metabolism in the gut. For example, both types of anthocyanin extracts increased fecal choline at week 1 (**Figure 15C–F)**; AAPP reversed the decreased fecal choline level at week 8 in the M group (**Figure 17E–F)**; cecal TMA was decreased by NAAB (**Figure 18C–D)**, whereas cecal DMA was decreased in all anthocyanin-treated groups (non-significant decrease in H-NAAB group) (**Figure 18C–F)**. However, dynamic changes of choline

metabolism in the gut induced by anthocyanin extracts and underlying metabolism remain a research question for the future.

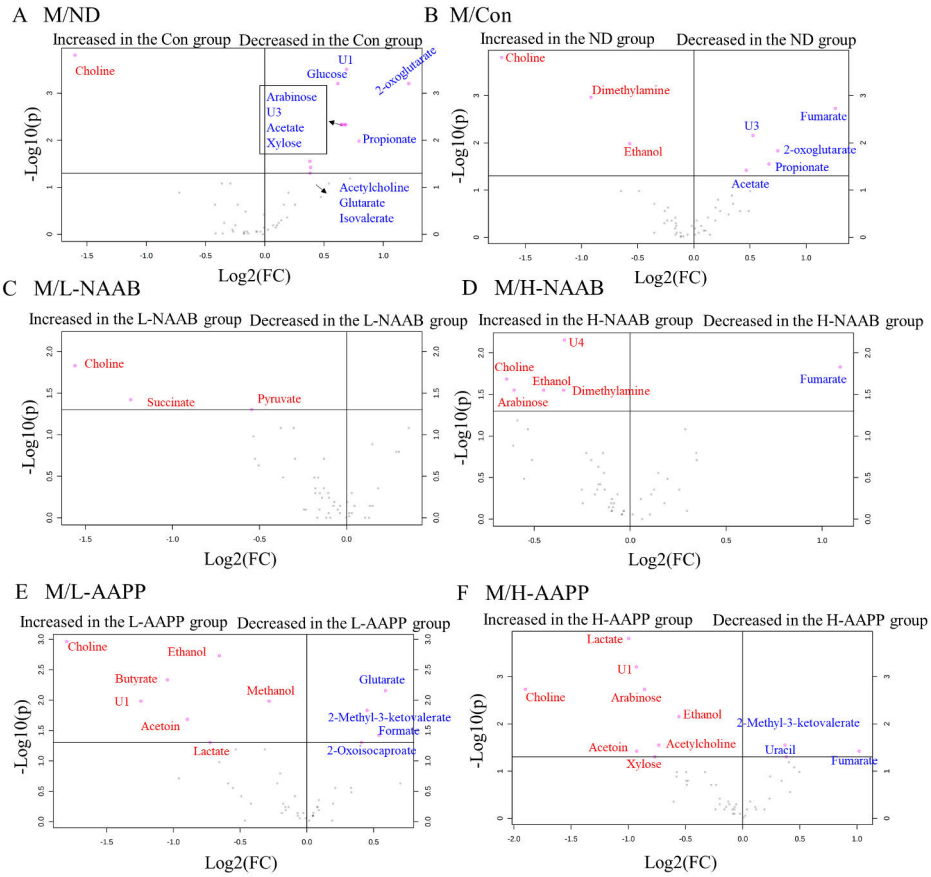

Figure 15. Volcano plots showing the significantly different metabolites from feces at week 1 in M/ND (A), M/Con (B), M/L-NAAB (C), M/H-NAAB (D), M/L-AAPP (E), and M/H-AAPP (F) comparisons. Significance versus log2 fold change is plotted on the y and x axes, respectively. U1, U3, and U4 represent for unknown metabolites 1, 3, and 4. Figures reprinted from the original publication **III** with permission from the Elsevier.

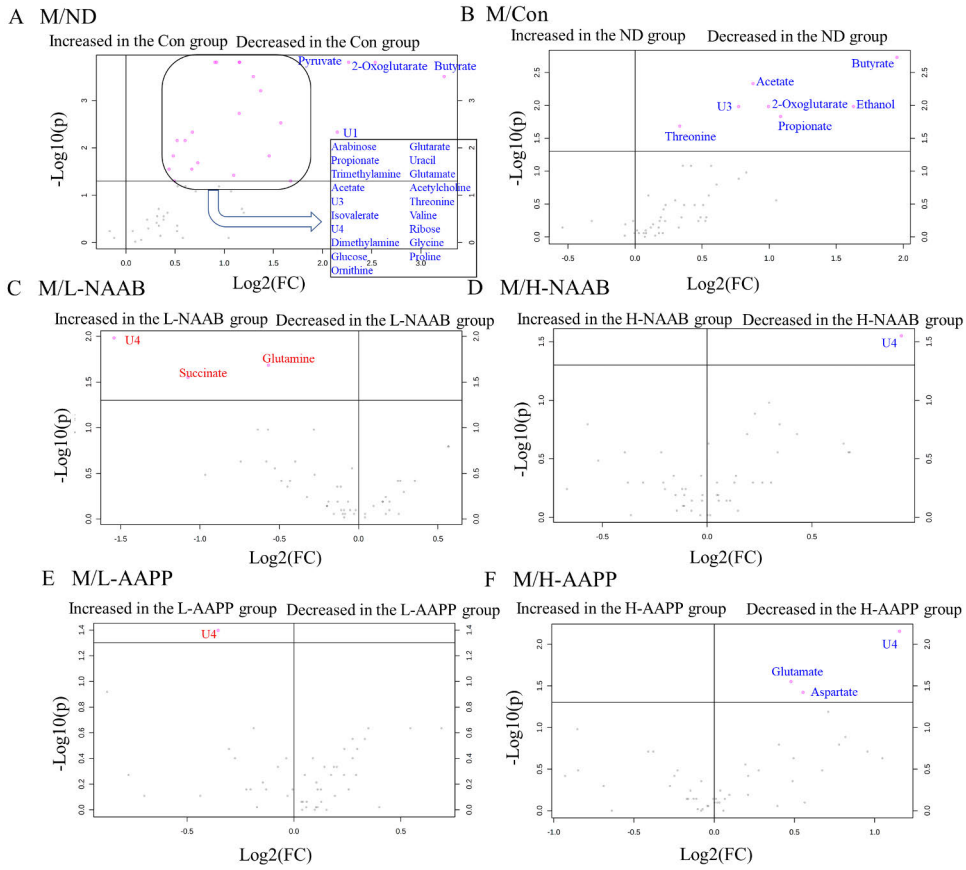

Figure 16. Volcano plots showing the significantly different metabolites from feces at week 4 in M/ND (A), M/Con (B), M/L-NAAB (C), M/H-NAAB (D), M/L-AAPP (E), and M/H-AAPP (F) comparisons. Significance versus log2 fold change is plotted on the y and x axes, respectively. U1, U3, and U4 represent for unknown metabolites 1, 3, and 4. Figures reprinted from the original publication **III** with permission from the Elsevier.

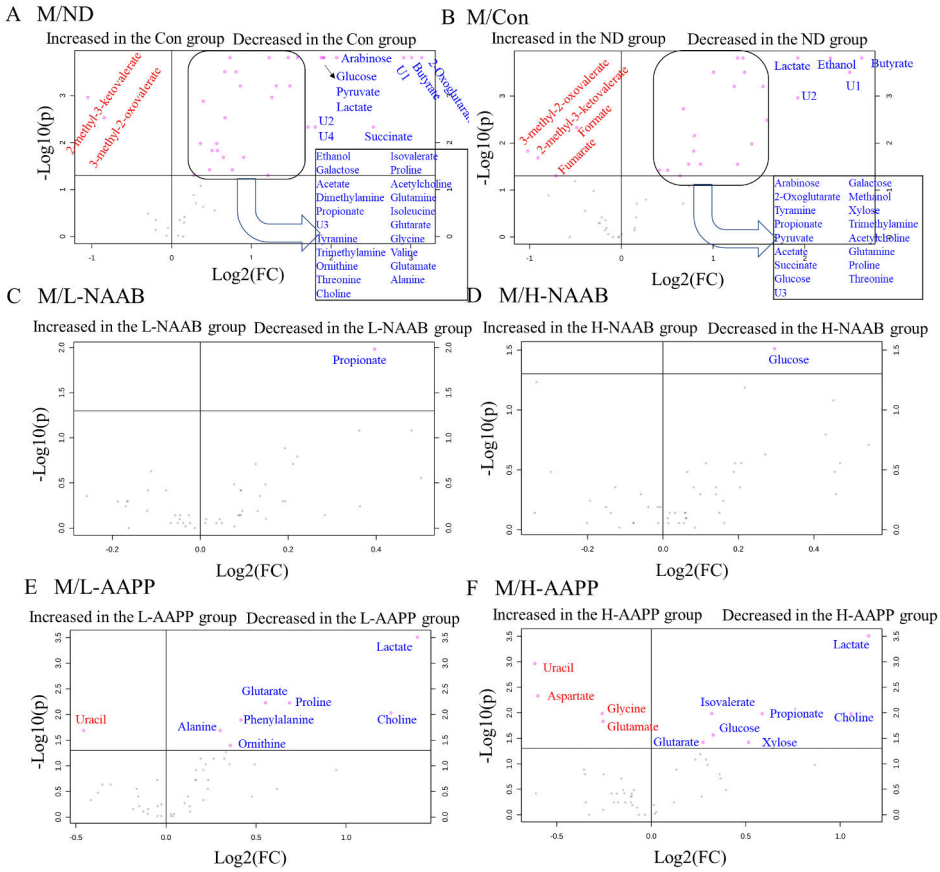

Figure 17. Volcano plots showing the significantly different metabolites from feces at week 8 in M/ND (A), M/Con (B), M/L-NAAB (C), M/H-NAAB (D), M/L-AAPP (E), and M/H-AAPP (F) comparisons. Significance versus log2 fold change is plotted on the y and x axes, respectively. U1, U2, U3, and U4 represent for unknown metabolites 1, 2, 3, and 4. Figures reprinted from the original publication **III** with permission from the Elsevier.

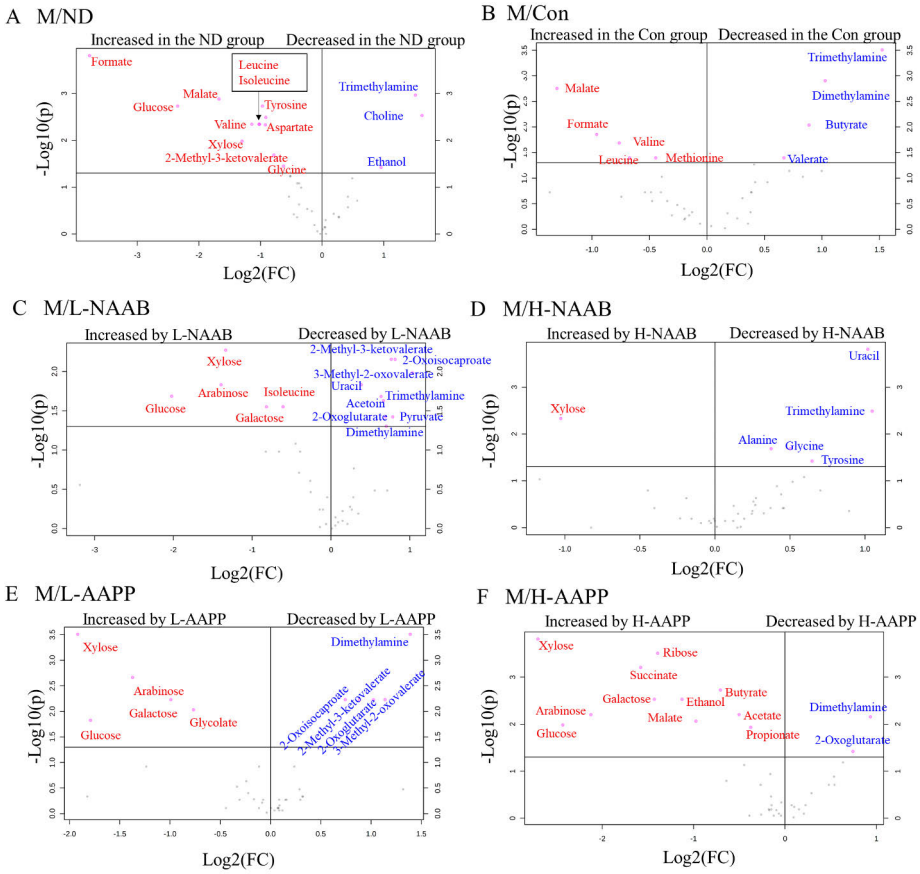

Figure 18. Volcano plots showing the significantly different metabolites from cecal content at week 8 in M/ND (A), M/Con (B), M/L-NAAB (C), M/H-NAAB (D), M/L-AAPP (E), and M/H-AAPP (F) comparisons. Significance versus log2 fold change is plotted on the y and x axes, respectively. Figures reprinted from the original publication **III** with permission from the Elsevier.

In the metabolic pathway analysis based on fecal metabolites (**Figure 19–21**), pyruvate metabolism was altered at all three time points in the M group compared to the ND and Con groups, which was modulated by AAPP at week 1 and 8 (**Figure 19A–B; Figure 21A–B**). As diabetes progressed, glycine, serine and threonine metabolism emerged as the altered pathway in the M group compared to ND group at week 8 (**Figure 21A**), which was modulated by AAPP (**Figure 21E–F**). A recent review showed the deficiency of glycine in T2D and a supplement of glycine can improve the insulin response and glucose production.[364] AAPP might reduce plasma and hepatic glucose shown in sections 5.3 through modulating glycine, serine and threonine metabolism in the gut.[364] Glutamine and glutamate metabolism and alanine, aspartate and glutamate

metabolism were altered in the feces of diabetes patients[152], which was in agreement with the current study (**Figure 20A; Figure 21A**). Only H-AAPP modulated glutamine and glutamate metabolism at week 4 and 8 (**Figure 20F; Figure 21F**). In the metabolic pathway analysis based on cecal metabolites (**Figure 22**), although citrate cycle was not significantly changed between the M group and ND/Con groups, both doses of AAPP modulated this pathway (**Figure 22E–F**). H-AAPP altered more pathways related to glycolysis/gluconeogenesis and other amino acid-related pathways than other anthocyanin-treated groups (**Figure 22F**). A Chinese twin clinical study showed that the citrate cycle has been reported to be altered in the feces of obese patients[365], indicating the potential beneficial effect of AAPP on obesity.

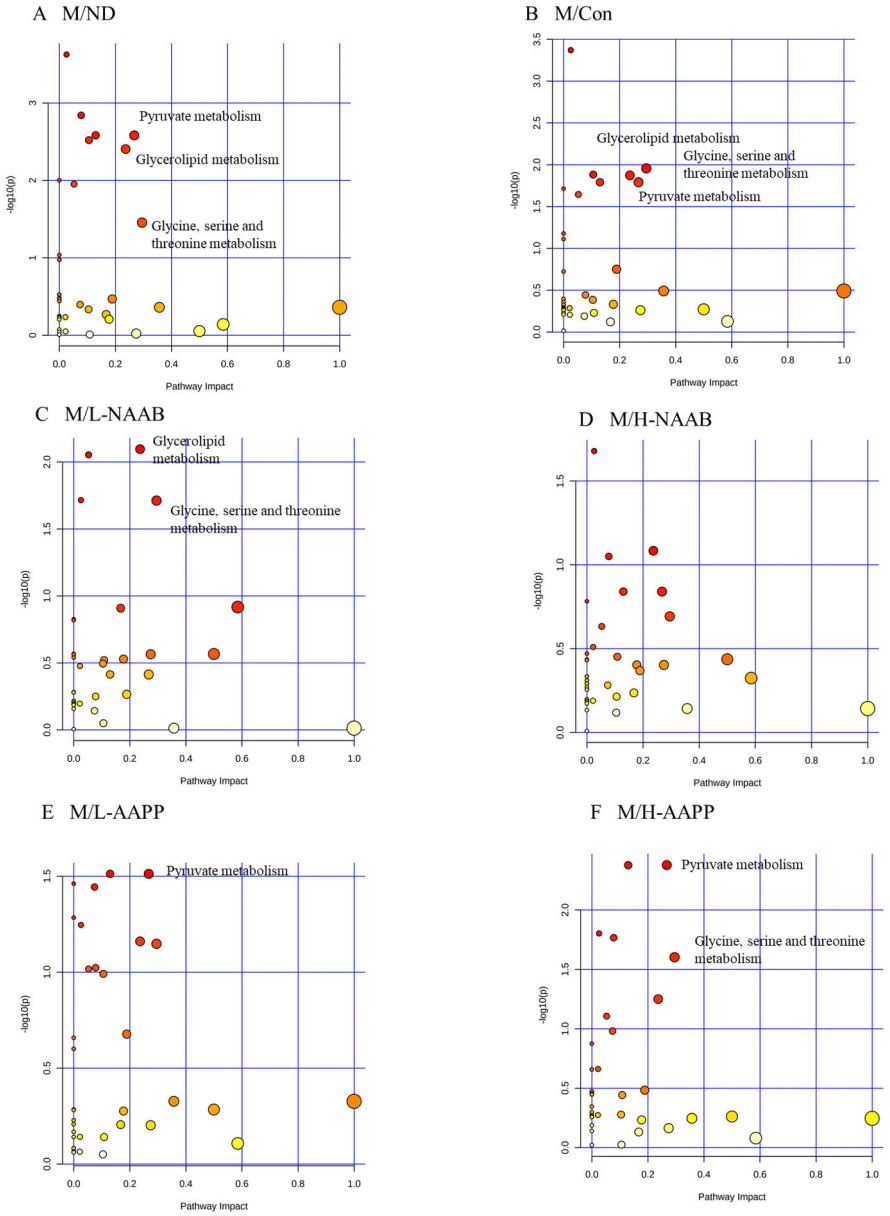

Figure 19. Metabolic pathway analysis generated with the MetaboAnalyst software package based on fecal metabolites at week 1, showing altered pathways in M/ND (A), M/Con (B), M/L-NAAB (C), M/H-NAAB (D), M/L-AAPP (E), and M/H-AAPP (F) comparisons. The p-values in the Y-axis are generated from the pathway enrichment analysis, and the X-axis presents the pathway impact values from pathway topology analysis. The node color indicates the p-value from the pathway enrichment analysis (more reddish color indicates more significant changes in the pathway), whereas the node size reflects the pathway impact score. Figures reprinted from the original publication **III** with permission from the Elsevier.

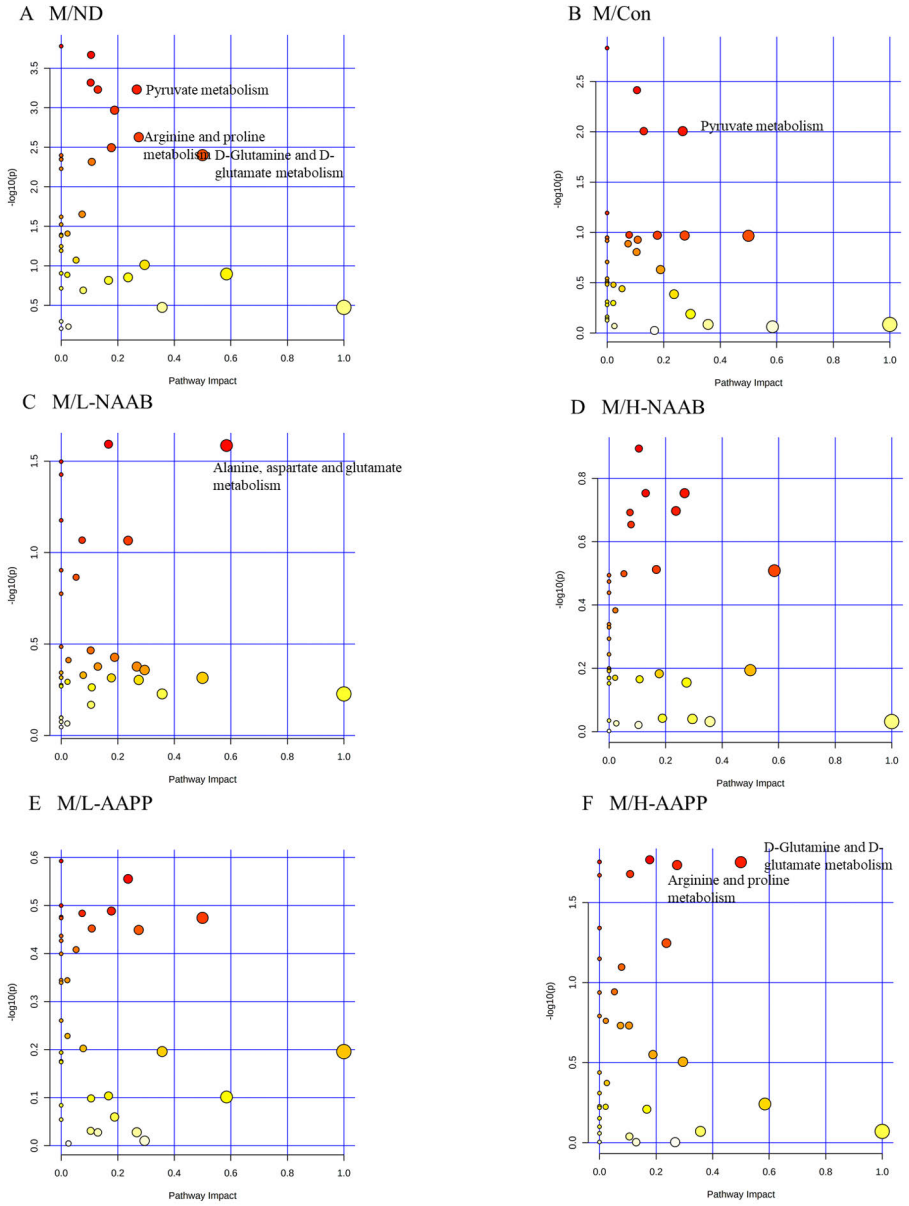

Figure 20. Metabolic pathway analysis generated with the MetaboAnalyst software package based on fecal metabolites at week 4, showing altered pathways in M/ND (A), M/Con (B), M/L-NAAB (C), M/H-NAAB (D), M/L-AAPP (E), and M/H-AAPP (F) comparisons. The p-values in the Y-axis are generated from the pathway enrichment analysis, and the X-axis presents the pathway impact values from pathway topology analysis. The node color indicates the p-value from the pathway enrichment analysis (more reddish color indicates more significant changes in the pathway), whereas the node size reflects the pathway impact score. Figures reprinted from the original publication **III** with permission from the Elsevier.

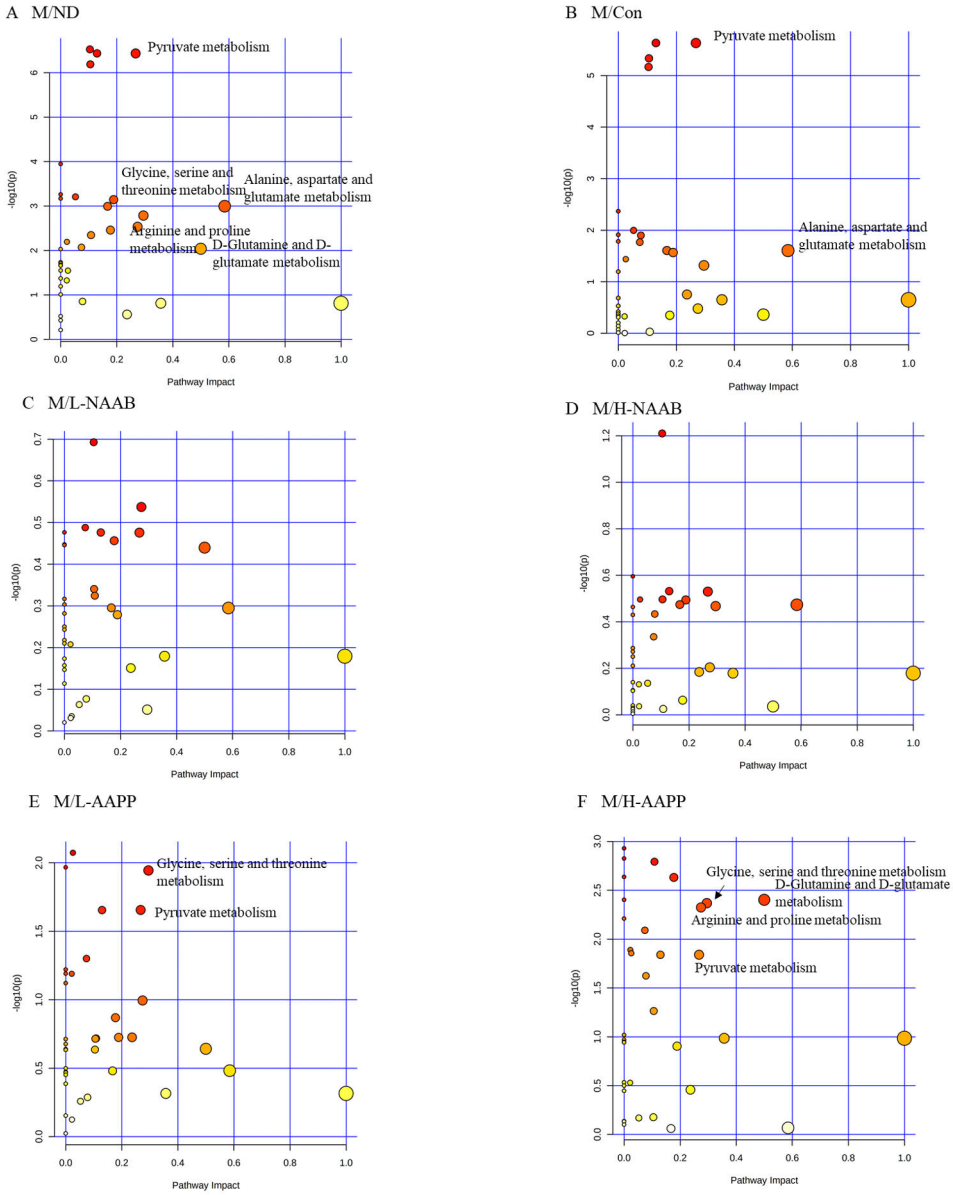

Figure 21. Metabolic pathway analysis generated with the MetaboAnalyst software package based on fecal metabolites at week 8, showing altered pathways in M/ND (A), M/Con (B), M/L-NAAB (C), M/H-NAAB (D), M/L-AAPP (E), and M/H-AAPP (F) comparisons. The p-values in the Y-axis are generated from the pathway enrichment analysis, and the X-axis presents the pathway impact values from pathway topology analysis. The node color indicates the p-value from the pathway enrichment analysis (more reddish color indicates more significant changes in the pathway), whereas the node size reflects the pathway impact score. Figures reprinted from the original publication **III** with permission from the Elsevier.

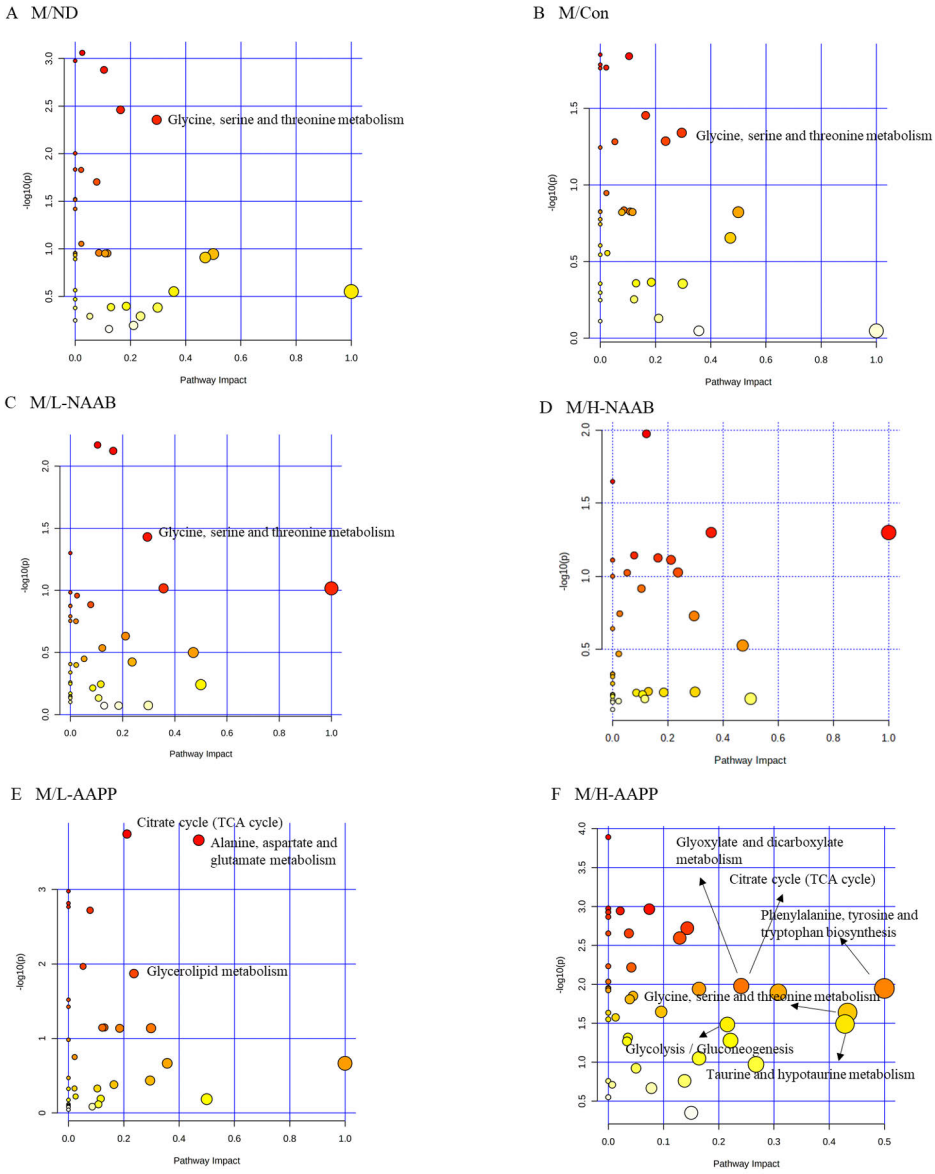

Figure 22. Metabolic pathway analysis generated with the MetaboAnalyst software package based on cecal metabolites, showing altered pathways in M/ND (A), M/Con (B), M/L-NAAB (C), M/H-NAAB (D), M/L-AAPP (E), and M/H-AAPP (F) comparisons. The p-values in the Y-axis are generated from the pathway enrichment analysis, and the X-axis presents the pathway impact values from pathway topology analysis. The node color indicates the p-value from the pathway enrichment analysis (more reddish color indicates more significant changes in the pathway), whereas the node size reflects the pathway impact score. Figures reprinted from the original publication **III** with permission from the Elsevier.

6. SUMMARY AND CONCLUSION

This thesis is the first research work to compare the biological function of acylated anthocyanins from purple potatoes and nonacylated anthocyanins from bilberries in type 2 diabetes of ZDF rats by using multi-omics. The bilberry anthocyanins consisted of mostly glucosides, galactosides, and arabinosides of delphinidin, petunidin, cyanidin, peonidin, and malvidin. The anthocyanins from the purple potatoes contained mainly acylated anthocyanins, with petunidin coumaroyl-rutinoside-glucoside as the dominating compound, followed by peonidin coumaroyl-rutinoside-glucoside and petunidin caffeoyl-rutinoside-glucoside. The anthocyanins in bilberries were exclusively nonacylated, whereas almost all the anthocyanins in the purple potatoes were acylated.

Multi-omics strategies including metabolomics, transcriptomics, and metagenomics were used to investigate the metabolites, transcripts, and microbiota affected by these two types of anthocyanins in diabetic rats. Distinguished metabolic and transcriptomic profiles as well as gut microbiota, were found in the diabetes of ZDF rats compared to the lean Zucker rats. Feed and water intake, body weight, viscera weigh and their ratio to body weight, as well as plasma and hepatic glucose showed a successful establishment of an animal model of T2D. Excessive glycolysis in T2D was manifested by increased plasma and hepatic intermediates of glycolysis including lactate, pyruvate, alanine. Increased levels were found for circulating BCAAs and glutamine/glutamate ratio, which are considered as biomarkers of insulin resistance. Increase in gluconeogenesis-related substrates (glycerol, lactate, alanine, etc.) and genes expression (*G6pc* and *Egr1*) were also observed. Transcriptomic analysis showed that T2D in ZDF rats was mainly characterized by active lipid synthesis, followed by dysregulated glucose metabolism and inflammatory response. ZDF rats showed higher levels of fecal SCFAs and lactate as well as altered choline metabolism in gut. Several gut microbiotas with health-compromising effects or known to be increased in T2D were found more abundant in ZDF rats, such as *Clostridium hathewayi*, *Lanchnospiraceae bacterium 1_7_47FAA*, *Bifidobacterium pseudolongum,* and *Dorea formicigenerans*. *Akkermansia muciniphila,* as a health-promoting bacterium, which has been constantly reported to be decreased in T2D, was decreased in ZDF rats.

Acylated anthocyanins extract and nonacylated anthocyanins extract exhibited some common beneficial effects in modulating metabolites, gene expression, and gut microbes. Each type of anthocyanin extracts also had their own exclusive effect. Generally, the acylated anthocyanin extract showed a more modulatory effect than the nonacylated. A reduced fasting plasma glucose level

was seen in all anthocyanin-fed groups, with a stronger impact shown in the groups fed with a nonacylated anthocyanins extract. Both anthocyanin extracts restored the hepatic levels of multiple metabolites (glucose, lactate, alanine, glycerol, and pyruvate) involved in glycolysis and gluconeogenesis as well as the content of BCAAs and the lipid profile. However, only the acylated anthocyanins extract showed a reversing effect on glycolysis and gluconeogenesis on a systemic level. In addition, acylated anthocyanins extract increased the plasma glutamine/glutamate ratio and decreased the plasma levels of serine, and glycine. At the gene level, nonacylated anthocyanins' extract regulated the expression of *Mgat4a*, *Gstm6*, and *Lpl*, whereas acylated anthocyanins modified the expression of *Mgat4a*, *Jun*, *Fos*, and *Egr1*. Of all the anthocyanin treatment groups, the group treated with a high-dose of potato anthocyanins (H-AAPP) showed a transcriptomic closer toward the lean Zucker rats. Metagenomics showed that anthocyanin extracts also beneficially modulated the gut microbiota composition. Both types of anthocyanins increased the abundance of *Peptostreptococcaceae noname unclassified* and *Marvinbryantia formatexigenes*. AAPP decreased the abundances of *Parabacteroides disdasonis*, *Ruminococcus torques*, and *Lanchnospiraceae bacterium 4_1_37FAA*.

Omics data showed the ZDF rats were characterized mainly with dysregulated lipid and carbohydrate metabolism. The treatments of nonacylated and acylated anthocyanin extracts regulated metabolites and genes related to the lipid and glucose metabolism, with acylated anthocyanin extracts showing more modulatory effects such as inflammatory response and gut microbiota.

Overall, this study detected extensive changes in the metabolites, genes, and gut microbes in T2D and a considerable effect of anthocyanin extracts from bilberries and purple potatoes on T2D. These results bring a new perspective for further research on bioavailability and the biological effects of acylated anthocyanins from purple potatoes. Acylated anthocyanins present in dark-colored plants and tubers, such as in the purple potato, and can be easily incorporated into the daily diet. Moreover, the stability of acylated anthocyanins allows them to be added to foods which require processing. Compared to berries, dark-colored potatoes represent a more affordable source of anthocyanins, of which both the global agricultural production and consumption can be realized on a larger scale and in a wider area, which would benefit the patients with metabolic disorders including T2D.

However, there are limitations of this study. Besides acylation being the one factor that affects the bioavailability and biological activities of acylated anthocyanins and non-acylated anthocyanins, the varieties of anthocyanin metabolites determined by the type of aglycone of anthocyanins and acyl group

as well as other phytochemicals in the extracts, such as flavonol glycosides and hydroxycinnamic acids, might play an important role.

7. ACKNOWLEDGEMENTS

This study was carried out at the Food Chemistry and Food Development Unit, at the Department of Life Technologies and the Instrument Center, in the Department of Chemistry, at the University of Turku, as well as at the Department of Toxicology, School of Public Health, Peking University. Anthocyanins were extracted at the Lappeenranta university of technology. Animal housing and interventions were carried out at the Peking university health science center. I am very thankful to the Doctoral Program in Molecular Life Sciences (DPMLS) of the University of Turku Graduate School (UTUGS) for giving me the chance to pursue my doctoral study. I wish to warmly thank the China Scholarship Council, the Finnish Food Research Foundation, DPMLS/UTUGS, and Finland-China Network In Food and Health programme (2021-2024) initiated by the Ministry of Education and Culture of Finland for supporting this doctoral study and providing the opportunity to travel. I am deeply grateful to my supervisors Professor Baoru Yang, Assistant Professor Maaria Kortesniemi, Professor Kaisa M. Linderborg, and to PhD Raghunath Pariyani for all their guidance and help. Professor Baoru Yang is warmly thanked for her trust and support. I wish to thank Jari Heinonen for providing the opportunity in Lappeenranta to finish the anthocyanin extraction. I am grateful to Maaria Kortesniemi and Raghunath Pariyani. They have helped me a lot in the fields of metabolomics. I also want to express my gratitude to Johanna Jokioja, Shuxun Liu, and Ye Tian for guiding me in the use of the LC-MS instruments. I am grateful to my coworkers Professor Yumei Zhang and Professor Xuetao Wei at the Peking university health science center for providing animal housing and the diet intervention. Many thanks to Shuxun Liu, Wenjia He, Yuqing Zhang, Anna Puganen, Salla Hakkola, Liz Gutierrez Quequezana, Jukka-Pekka Suomela, Oskar Laaksonen and other present and former colleagues for the friendship and support during my stay in Turku. The technical and administrative personnel of the Department of Life Technologies is warmly thanked: Anu Hirvensalo, Mirva Jalo, Heli Kuusela, Leena Neuvonen, Tapio Ronkainen and Jani Sointusalo. My warm thanks to my wife Xiangrong Fang for her love, you bring out the best in us. My son, Yihe Chen, thank you for bringing us a lot of joy and happiness. Special thanks go to my parents Ying Kang and Bo Chen, they encourage me when I feel stressed and trust me for every goal I commit to. I am happy to have good friends Jinghui Yang, Chang Liu, Weihua Zhang in Turku, we had a lot of fun together.

Kang Chen

Turku, February 2022

8. REFERENCES

(1) Sarah Wild, G. R. Global Prevalence of Diabetes：Estimates for the Year 2000 and Projections for 2030. *World Health* **2004**, *27*, 1047–1053.

(2) Colberg, S. R.; Sigal, R. J.; Fernhall, B.; Regensteiner, J. G.; Blissmer, B. J.; Rubin, R. R.; Chasan-Taber, L.; Albright, A. L.; Braun, B. Exercise and Type 2 Diabetes: The American College of Sports Medicine and the American Diabetes Association: Joint Position Statement. *Diabetes Care* **2010**, *33* (12).

(3) Belwal, T.; Nabavi, S. F.; Nabavi, S. M.; Habtemariam, S. Dietary Anthocyanins and Insulin Resistance: When Food Becomes a Medicine. *Nutrients* **2017**, *9*, 1111.

(4) Xu, J.; Su, X.; Lim, S.; Griffin, J.; Carey, E.; Katz, B.; Tomich, J.; Smith, J. S.; Wang, W. Characterisation and Stability of Anthocyanins in Purple-Fleshed Sweet Potato P40. *Food Chemistry* **2015**, *186*, 90–96.

(5) Moriya, C.; Hosoya, T.; Agawa, S.; Sugiyama, Y.; Shin-ya, K.; Terahara, N.; Kumazawa, S. New Acylated Anthocyanins from Purple Yam and Their Antioxidant Activity. *Bioscience, Biotechnology, and Biochemistry* **2015**, *79*, 1484–1492.

(6) Oliveira, H.; Perez-Gregório, R.; de Freitas, V.; Mateus, N.; Fernandes, I. Comparison of the in Vitro Gastrointestinal Bioavailability of Acylated and Non-Acylated Anthocyanins: Purple-Fleshed Sweet Potato vs Red Wine. *Food Chemistry* **2019**, *276* (September 2018), 410–418.

(7) Zamora-Ros, R.; Knaze, V.; Luján-Barroso, L.; Slimani, N. Estimation of the Intake of Anthocyanidins and Their Food Sources in the European Prospective Investigation into Cancer and Nutrition (EPIC) Study. *British Journal of Nutrition* **2011**, *106* (7), 1090–1099.

(8) Wallace, T. C.; Giusti, M. M. Anthocyanins. *Advances in Nutrition* **2015**, *6* (5), 620–622.

(9) Tim, H.; Chatterton, J.; Daccache, A.; Williams, A. The Impact of Changing Food Choices on the Blue Water Scarcity Footprint and Greenhouse Gas Emissions of the British Diet: The Example of Potato, Pasta and Rice. *Journal of Cleaner Production* **2016**, 4558–4568.

(10) He, J.; Monica, G. Anthocyanins: Natural Colorants with Health-Promoting Properties. *Annual Review of Food Science and Technology* **2010**, *1* (1), 163–187.

(11) Morais, C.; de Rosso, V. V.; Estadella, D.; Pisani, L. Anthocyanins as Inflammatory Modulators and the Role of the Gut Microbiota. *Journal of Nutritional Biochemistry* **2016**, *33*, 1–7.

(12) Gowd, V.; Jia, Z.; Chen, W. Anthocyanins as Promising Molecules and Dietary Bioactive Components against Diabetes e A Review of Recent Advances. *Trends in Food Science & Technology* **2017**, *68*, 1–13.

(13) Dorota, R.; Regulska-ilow, B. The Significance of Anthocyanins in the Prevention and Treatment of Type 2 Diabetes. **2018**.

(14) Uusitupa, M.; Khan, T. A.; Viguiliouk, E.; Kahleova, H.; Rivellese, A. A.; Hermansen, K.; Pfeiffer, A.; Thanopoulou, A.; Salas-Salvadó, J.; Schwab, U.; Sievenpiper, J. L. Prevention of Type 2 Diabetes by Lifestyle Changes: A Systematic Review and Meta-Analysis. *Nutrients 2019, Vol. 11, Page 2611* **2019**, *11* (11), 2611.

(15) Logan, P. Liver and Diabetes. A Vicious Circle. *Bone* **2014**, *23* (1), 1–7.

(16) Wang, S.; Zhu, F. Antidiabetic Dietary Materials and Animal Models. *Food Research International* **2016**, *85*, 315–331.

(17) Al-Awar, A.; Kupai, K.; Veszelka, M.; Szucs, G.; Attieh, Z.; Murlasits, Z.; Török, S.; Pósa, A.; Varga, C. Experimental Diabetes Mellitus in Different Animal Models. *Journal of Diabetes Research* **2016**, *9051426*.

(18) Terrettaz, J.; Jeanrenaud, B. In Vivo Hepatic and Peripheral Insulin Resistance in Genetically Obese (Fa/Fa)

Rats. *Endocrinology* **1983**, *112* (4), 1346–1351.

(19) Phillips, M. S.; Liu, Q.; Hammond, H. A.; Dugan, V.; Hey, P. J.; Caskey, C. T.; Hess, J. F. Leptin Receptor Missense Mutation in the Fatty Zucker Rat. *Nature Genetics* **1996**, *13* (1), 18–19.

(20) Tokuyama, Y.; Sturis, J.; DePaoli, A. M.; Takeda, J.; Stoffel, M.; Tang, J.; Sun, X.; Polonsky, K. S.; Bell, G. I. Evolution of β-Cell Dysfunction in the Male Zucker Diabetic Fatty Rat. *Diabetes* **1995**, *44* (12), 1447–1457.

(21) Artiñano, A. D. A.; Miguel, C. M. Experimental Rat Models to Study the Metabolic Syndrome. *British Journal of Nutrition* **2009**, *102* (9), 1246–1253.

(22) Shiota, M.; Printz, R. L. *Diabetes in Zucker Diabetic Fatty Rat*; . https://doi.org/10.1007/978-1-62703-068-7; 2012; Vol. 933.

(23) Jones, J. G. Hepatic Glucose and Lipid Metabolism. *Diabetologia* **2016**, *59* (6), 1098–1103.

(24) Madiraju, A. K.; Erion, D. M.; Rahimi, Y.; Zhang, X. M.; Braddock, D. T.; Albright, R. A.; Prigaro, B. J.; Wood, J. L.; Bhanot, S.; MacDonald, M. J.; Jurczak, M. J.; Camporez, J. P.; Lee, H. Y.; Cline, G. W.; Samuel, V. T.; Kibbey, R. G.; Shulman, G. I. Metformin Suppresses Gluconeogenesis by Inhibiting Mitochondrial Glycerophosphate Dehydrogenase. *Nature* **2014**, *510* (7506), 542–546.

(25) Bridges, H. R.; Jones, A. J. Y.; Pollak, M. N.; Hirst, J. Effects of Metformin and Other Biguanides on Oxidative Phosphorylation in Mitochondria. *Biochemical Journal* **2014**, *462* (3), 475–487.

(26) Randle, P. J. Regulatory Interactions between Lipids and Carbohydrates: The Glucose Fatty Acid Cycle after 35 Years. *Diabetes/Metabolism Reviews* **1998**, *14* (4), 263–283.

(27) Schultze, S. M.; Hemmings, B. A.; Niessen, M.; Tschopp, O. PI3K/AKT, MAPK and AMPK Signalling: Protein Kinases in Glucose Homeostasis. *Expert Reviews in Molecular Medicine* **2012**, *14* (January 2012), 1–21.

(28) Zhao, Y.; Hu, X.; Liu, Y.; Dong, S.; Wen, Z.; He, W.; Zhang, S.; Huang, Q.; Shi, M. ROS Signaling under Metabolic Stress: Cross-Talk between AMPK and AKT Pathway. *Molecular Cancer 2017 16:1* **2017**, *16* (1), 1–12.

(29) Day, E. A.; Ford, R. J.; Steinberg, G. R. AMPK as a Therapeutic Target for Treating Metabolic Diseases. *Trends in Endocrinology and Metabolism* **2017**, *28* (8), 545–560.

(30) Park, J. E.; Lim, H. R.; Kim, J. W.; Shin, K. H. Metabolite Changes in Risk of Type 2 Diabetes Mellitus in Cohort Studies: A Systematic Review and Meta-Analysis. *Diabetes Research and Clinical Practice* **2018**, *140*, 216–227.

(31) Urpi-Sarda, M.; Almanza-Aguilera, E.; Tulipani, S.; Tinahones, F. J.; Salas-Salvadó, J.; Andres-Lacueva, C. Metabolomics for Biomarkers of Type 2 Diabetes Mellitus: Advances and Nutritional Intervention Trends. *Current Cardiovascular Risk Reports* **2015**, *9*, 12.

(32) Klein, M. S.; Shearer, J. Metabolomics and Type 2 Diabetes: Translating Basic Research into Clinical Application. *The Handbook of Metabonomics and Metabolomic* **2007**, *2016*, 1–36.

(33) Concepcion, J.; Concepcion, J.; Chen, K.; Saito, R.; Gangoiti, J.; Mendez, E.; Nikita, M. E.; Barshop, B. A.; Barshop, B. A.; Natarajan, L.; Sharma, K.; Kim, J. J.; Kim, J. J. Identification of Pathognomonic Purine Synthesis Biomarkers by Metabolomic Profiling of Adolescents with Obesity and Type 2 Diabetes. *PLoS ONE* **2020**, *15* (6 June), 1–17.

(34) Lu, Y.; Wang, Y.; Liang, X.; Zou, L.; Ong, C. N.; Yuan, J. M.; Koh, W. P.; Pan, A. Serum Amino Acids in Association with Prevalent and Incident Type 2 Diabetes in a Chinese Population. *Metabolites* **2019**, *9* (1), 1–10.

(35) Bao, Y.; Zhao, T.; Wang, X.; Qiu, Y.; Su, M.; Jia, W. Metabonomic Variations in the Drug-Treated Type 2 Diabetes Mellitus Patients and Healthy Volunteers. **2009**, 1623–1630.

(36) Jung, J.; Jang, Z.; Hwang, G.-S. Metabolomics Approach for

Discovering Disease Biomarkers and Understanding Metabolic Pathway. *Journal of Analytical Science and Technology* **2011**, *2* (Supplement A), A189–A193.

(37) Van Doorn, M.; Vogels, J.; Tas, A.; Van Hoogdalem, E. J.; Burggraaf, J.; Cohen, A.; Van Der Greef, J. Evaluation of Metabolite Profiles as Biomarkers for the Pharmacological Effects of Thiazolidinediones in Type 2 Diabetes Mellitus Patients and Healthy Volunteers. *British Journal of Clinical Pharmacology* **2007**, *63* (5), 562–574.

(38) Salek, R. M.; Maguire, M. L.; Bentley, E.; Rubtsov, D. V.; Hough, T.; Cheeseman, M.; Nunez, D.; Sweatman, B. C.; Haselden, J. N.; Cox, R. D.; Connor, S. C.; Griffin, J. L. A Metabolomic Comparison of Urinary Changes in Type 2 Diabetes in Mouse, Rat, and Human. *Physiological Genomics* **2007**, *29* (2), 99–108.

(39) Zhang, A. H.; Sun, H.; Yan, G. L.; Yuan, Y.; Han, Y.; Wang, X. J. Metabolomics Study of Type 2 Diabetes Using Ultra-Performance LC-ESI/Quadrupole-TOF High-Definition MS Coupled with Pattern Recognition Methods. *Journal of Physiology and Biochemistry* **2014**, *70* (1), 117–128.

(40) Zeng, M.; Che, Z.; Liang, Y.; Wang, B.; Chen, X.; Li, H.; Deng, J.; Zhou, Z. GC-MS Based Plasma Metabolic Profiling of Type 2 Diabetes Mellitus. *Chromatographia* **2009**, *69* (9–10), 941–948.

(41) Messana, I.; Forni, F.; Ferrari, F.; Rossi, C.; Giardina, B.; Zuppi, C. Proton Nuclear Magnetic Resonance Spectral Profiles of Urine in Type II Diabetic Patients. *Clinical Chemistry* **1998**, *44* (7), 1529–1534.

(42) Kaur, P.; Rizk, N.; Ibrahim, S.; Luo, Y.; Younes, N.; Perry, B.; Dennis, K.; Zirie, M.; Luta, G.; Cheema, A. K. Quantitative Metabolomic and Lipidomic Profiling Reveals Aberrant Amino Acid Metabolism in Type 2 Diabetes. *Molecular BioSystems* **2013**, *9* (2), 307–317.

(43) Xu, W.; Zhang, L.; Huang, Y.; Yang, Q.; Xiao, H.; Zhang, D. Discrimination of Type 2 Diabetes Mellitus Corresponding to Different Traditional Chinese Medicine Syndromes Based on Plasma Fatty Acid Profiles and Chemometric Methods. *Journal of Ethnopharmacology* **2012**, *143* (2), 463–468.

(44) Fiehn, O.; Timothy Garvey, W.; Newman, J. W.; Lok, K. H.; Hoppel, C. L.; Adams, S. H. Plasma Metabolomic Profiles Reflective of Glucose Homeostasis in Non-Diabetic and Type 2 Diabetic Obese African-American Women. *PLoS ONE* **2010**, *5* (12), 1–10.

(45) Urtz, P. W. €; Soininen, P.; Kangas, A. J.; Rönnemaa, T.; Lehtimäki, T.; Kähönen, M.; Viikari, J. S.; Raitakari, O. T.; Ala-Korpela, M. Branched-Chain and Aromatic Amino Acids Are Predictors of Insulin Resistance in Young Adults. *DIABETES CARE* **2013**, *36*, 648–655.

(46) Ha, C. Y.; Kim, J. Y.; Paik, J. K.; Kim, O. Y.; Paik, Y. H.; Lee, E. J.; Lee, J. H. The Association of Specific Metabolites of Lipid Metabolism with Markers of Oxidative Stress, Inflammation and Arterial Stiffness in Men with Newly Diagnosed Type 2 Diabetes. *Clinical Endocrinology* **2012**, *76* (5), 674–682.

(47) Stentz, F. B.; Kitabchi, A. E. Transcriptome and Proteome Expressions Involved in Insulin Resistance in Muscle and Activated T-Lymphocytes of Patients with Type 2 Diabetes. *Genomics, Proteomics and Bioinformatics* **2007**, *5* (3–4), 216–235.

(48) Cui, Y.; Chen, W.; Chi, J.; Wang, L. Comparison of Transcriptome between Type 2 Diabetes Mellitus and Impaired Fasting Glucose. *Medical Science Monitor* **2016**, *22*, 4699–4706.

(49) Jenkinson, C. P.; Göring, H. H. H.; Arya, R.; Blangero, J.; Duggirala, R.; DeFronzo, R. A. Transcriptomics in Type 2 Diabetes: Bridging the Gap between Genotype and Phenotype. *Genomics Data* **2016**, *8*, 25–36.

(50) Xia, C.; Zhang, X.; Cao, T.; Wang, J.; Li, C.; Yue, L.; Niu, K.; Shen, Y.; Ma, G.; Chen, F. Hepatic Transcriptome Analysis Revealing the Molecular Pathogenesis of Type 2 Diabetes Mellitus in Zucker Diabetic Fatty Rats.

Frontiers in Endocrinology **2020**, *11*, Article 565858.

(51) Li, X.; Lin, Z.; Zhan, X.; Gao, J.; Sun, L.; Cao, Y.; Qiu, H. RNA-Seq Analysis of the Transcriptome of the Liver of Cynomolgus Monkeys with Type 2 Diabetes. *Gene* **2018**, *651*, 118–125.

(52) Li, L.; Pan, Z.; Yang, X. Key Genes and Co-Expression Network Analysis in the Livers of Type 2 Diabetes Patients. *Journal of Diabetes Investigation* **2019**, *10* (4), 951–962.

(53) Chen, Z.; Yuan, W.; Liu, T.; Huang, D.; Xiang, L. Bioinformatics Analysis of Hepatic Gene Expression Profiles in Type 2 Diabetes Mellitus. *Experimental and Therapeutic Medicine* **2019**, 4303–4312.

(54) Connor, S. C.; Hansen, M. K.; Corner, A.; Smith, R. F.; Ryan, T. E. Integration of Metabolomics and Transcriptomics Data to Aid Biomarker Discovery in Type 2 Diabetes. *Molecular BioSystems* **2010**, *6* (5), 909–921.

(55) Zhang, F.; Xu, X.; Zhang, Y.; Zhou, B.; He, Z.; Zhai, Q. Gene Expression Profile Analysis of Type 2 Diabetic Mouse Liver. *PLoS ONE* **2013**, *8* (3).

(56) Zmora, N.; Bashiardes, S.; Levy, M.; Elinav, E. The Role of the Immune System in Metabolic Health and Disease. *Cell Metabolism* **2017**, *25* (3), 506–521.

(57) Medzhitov, R. Origin and Physiological Roles of Inflammation. *Nature* **2008**, *454* (7203), 428–435.

(58) Brownlee, M.; Anthony, C.; Helen, V. Advanced Glycosylation End Products in Tissue and the Biochemical Basis of Diabetic Complications. *The New England Journal of Medicine* **1988**, No. 318, 1315–1321.

(59) Yan, S. F.; Barile, G. R.; D'Agati, V.; Yan, S. Du; Ramasamy, R.; Schmidt, A. M. The Biology of RAGE and Its Ligands: Uncovering Mechanisms at the Heart of Diabetes and Its Compilcations. *Current Diabetes Reports* **2007**, *7* (2), 146–153.

(60) Navab, M.; Anantharamaiah, G. M.; Reddy, S. T.; Van Lenten, B. J.; Ansell, B. J.; Fogelman, A. M. Mechanisms of Disease: Proatherogenic HDL - An Evolving Field. *Nature Clinical Practice Endocrinology and Metabolism* **2006**, *2* (9), 504–511.

(61) Ceriello, A.; Motz, E. Is Oxidative Stress the Pathogenic Mechanism Underlying Insulin Resistance, Diabetes, and Cardiovascular Disease? The Common Soil Hypothesis Revisited. *Arteriosclerosis, Thrombosis, and Vascular Biology* **2004**, *24* (5), 816–823.

(62) Patel, C.; Ghanim, H.; Ravishankar, S.; Sia, C. L.; Viswanathan, P.; Mohanty, P.; Dandona, P. Prolonged Reactive Oxygen Species Generation and Nuclear Factor-KB Activation after a High-Fat, High-Carbohydrate Meal in the Obese. *The Journal of Clinical Endocrinology & Metabolism* **2007**, *92* (11), 4476–4479.

(63) Gregersen, S.; Samocha-Bonet, D.; Heilbronn, L. K.; Campbell, L. V. Inflammatory and Oxidative Stress Responses to High-Carbohydrate and High-Fat Meals in Healthy Humans. *Journal of Nutrition and Metabolism* **2012**, *2012*.

(64) Li, Z.; Yang, S.; Lin, H.; Huang, J.; Watkins, P. A.; Moser, A. B.; DeSimone, C.; Song, X.; Diehl, A. M. Probiotics and Antibodies to TNF Inhibit Inflammatory Activity and Improve Nonalcoholic Fatty Liver Disease. *Hepatology* **2003**, *37* (2), 343–350.

(65) Philipp, S. Adipose Tissue: From Lipid Storage Compartment to Endocrine Organ. *Diabetes* **2006**, *55* (6), 1537–1545.

(66) KT, U.; SM, W.; MW, M.; GS, H. Protection from Obesity-Induced Insulin Resistance in Mice Lacking TNF-Alpha Function. *Nature* **1997**, *389* (6651), 610–614.

(67) Kim, H. J.; Higashimori, T.; Park, S. Y.; Choi, H.; Dong, J.; Kim, Y. J.; Noh, H. L.; Cho, Y. R.; Cline, G.; Kim, Y. B.; Kim, J. K. Differential Effects of Interleukin-6 and -10 on Skeletal Muscle and Liver Insulin Action In Vivo. *Diabetes* **2004**, *53* (4), 1060–1067.

(68) Schottelius, A. J. G.; Mayo, M. W.; Balfour Sartor, R.; Baldwin, A. S. Interleukin-10 Signaling Blocks Inhibitor of KB Kinase Activity and

Nuclear Factor KB DNA Binding. *Journal of Biological Chemistry* **1999**, *274* (45), 31868–31874.

(69) Patel, S.; Santani, D. Role of NF-KB in the Pathogenesis of Diabetes and Its Associated Complications. *Pharmacological Reports* **2009**, *61* (4), 595–603.

(70) Hirosumi, J.; Tuncman, G.; Chang, L.; Görgün, C. Z.; Uysal, K. T.; Maeda, K.; Karin, M.; Hotamisligil, G. S. A Central Role for JNK in Obesity and Insulin Resistance. *Nature 2002 420:6913* **2002**, *420* (6913), 333–336.

(71) Giridharan, S.; Srinivasan, M. Mechanisms of NF-KB P65 and Strategies for Therapeutic Manipulation. *Journal of Inflammation Research* **2018**, *11*, 407.

(72) Yuan, M.; Konstantopoulos, N.; Lee, J.; Hansen, L.; Li, Z.-W.; Karin, M.; Shoelson, S. E. Reversal of Obesity- and Diet-Induced Insulin Resistance with Salicylates or Targeted Disruption of Ikkβ. *Science* **2001**, *293* (5535), 1673–1677.

(73) Arkan, M. C.; Hevener, A. L.; Greten, F. R.; Maeda, S.; Li, Z.-W.; Long, J. M.; Wynshaw-Boris, A.; Poli, G.; Olefsky, J.; Karin, M. IKK-β Links Inflammation to Obesity-Induced Insulin Resistance. *NATURE MEDICINE* **2005**, *11* (2).

(74) Hirosumi, J.; Tuncman, G.; Chang, L.; Görgün, C. Z.; Uysal, K. T.; Maeda, K.; Karin, M.; Hotamisligil, G. S. A Central, Role for JNK in Obesity and Insulin Resistance. *Nature* **2002**, *420* (6913), 333–336.

(75) Boden, G. Role of Fatty Acids in the Pathogenesis of Insulin Resistance and NIDDM. *Diabetes* **1997**, *46* (1), 3–10.

(76) Sethi, J. K.; Hotamisligil, G. S. The Role of TNFα in Adipocyte Metabolism. *Seminars in Cell and Developmental Biology* **1999**, *10* (1), 19–29.

(77) Tiikkainen, M.; Bergholm, R.; Vehkavaara, S.; Rissanen, A. Effects of Identical Weight Loss on Body Composition and Features of Insulin Resistance in Obese Women with High and Low Liver Fat Content. *Diabetes* **2003**, *52* (3), 701–707.

(78) Petersen, K.; Dufour, S.; Befroy, D.; Lehrke, M. Reversal of Nonalcoholic Hepatic Steatosis, Hepatic Insulin Resistance, and Hyperglycemia by Moderate Weight Reduction in Patients with Type 2 Diabetes. *Diabetes* **2005**, *54* (3), 603–608.

(79) Turnbaugh, P. J.; Ley, R. E.; Mahowald, M. A.; Magrini, V.; Mardis, E. R.; Gordon, J. I. An Obesity-Associated Gut Microbiome with Increased Capacity for Energy Harvest. *Nature* **2006**, *444* (7122), 1027–1031.

(80) Zhu, B.; Wang, X.; Li, L. Human Gut Microbiome: The Second Genome of Human Body. *Protein and Cell* **2010**, *1* (8), 718–725.

(81) Conlon, M. A.; Bird, A. R. The Impact of Diet and Lifestyle on Gut Microbiota and Human Health. *Nutrients* **2015**, *7* (1), 17–44.

(82) Dominguez-Bello, M. G.; Costello, E. K.; Contreras, M.; Magris, M.; Hidalgo, G.; Fierer, N.; Knight, R. Delivery Mode Shapes the Acquisition and Structure of the Initial Microbiota across Multiple Body Habitats in Newborns. *Proceedings of the National Academy of Sciences of the United States of America* **2010**, *107* (26), 11971–11975.

(83) Blandino, G.; Inturri, R.; Lazzara, F.; Di Rosa, M.; Malaguarnera, L. Impact of Gut Microbiota on Diabetes Mellitus. *Diabetes and Metabolism* **2016**, *42* (5), 303–315.

(84) Cronin, O.; Barton, W.; Skuse, P.; Penney, N. C.; Garcia-Perez, I.; Murphy, E. F.; Woods, T.; Nugent, H.; Fanning, A.; Melgar, S.; Falvey, E. C.; Holmes, E.; Cotter, P. D.; O'Sullivan, O.; Molloy, M. G.; Shanahan, F. A Prospective Metagenomic and Metabolomic Analysis of the Impact of Exercise and/or Whey Protein Supplementation on the Gut Microbiome of Sedentary Adults. *mSystems* **2018**, *3* (3), 1–17.

(85) Mika, A.; Van Treuren, W.; González, A.; Herrera, J. J.; Knight, R.; Fleshner, M. Exercise Is More Effective at Altering Gut Microbial Composition and Producing Stable Changes in Lean Mass in Juvenile versus Adult Male F344 Rats. *PLoS ONE* **2015**, *10* (5), 1–20.

(86) Gassler, N.; Rohr, C.; Schneider, A.; Kartenbeck, J.; Bach, A.; Obermüller, N.; Otto, H. F.; Autschbach, F. Inflammatory Bowel Disease Is Associated with Changes of Enterocytic Junctions. *American Journal of Physiology - Gastrointestinal and Liver Physiology* **2001**, *281* (1 44-1), 216–228.

(87) Moya-Pérez, A.; Neef, A.; Sanz, Y. Bifidobacterium Pseudocatenulatum CECT 7765 Reduces Obesity-Associated Inflammation by Restoring the Lymphocyte-Macrophage Balance and Gut Microbiota Structure in High-Fat Diet-Fed Mice. *PLoS ONE* **2015**, *10* (7), 1–28.

(88) Cani, P. D.; Neyrinck, A. M.; Fava, F.; Knauf, C.; Burcelin, R. G.; Tuohy, K. M.; Gibson, G. R.; Delzenne, N. M. Selective Increases of Bifidobacteria in Gut Microflora Improve High-Fat-Diet-Induced Diabetes in Mice through a Mechanism Associated with Endotoxaemia. *Diabetologia* **2007**, *50* (11), 2374–2383.

(89) Cerf-Bensussan, N.; Gaboriau-Routhiau, V. The Immune System and the Gut Microbiota: Friends or Foes? *Nature Reviews Immunology* **2010**, *10* (10), 735–744.

(90) Feng, H.; Su, R.; Song, Y.; Wang, C.; Lin, L.; Ma, J.; Yang, H. Positive Correlation between Enhanced Expression of TLR4/MyD88/NF-KB with Insulin Resistance in Placentae of Gestational Diabetes Mellitus. *PLoS ONE* **2016**, *11* (6), 1–15.

(91) Han, L. P.; Li, C. J.; Sun, B.; Xie, Y.; Guan, Y.; Ma, Z. J.; Chen, L. M. Protective Effects of Celastrol on Diabetic Liver Injury via TLR4/MyD88/NF- B Signaling Pathway in Type 2 Diabetic Rats. *Journal of Diabetes Research* **2016**, *2016*.

(92) Mahmassani, Z. S.; Reidy, P. T.; McKenzie, A. I.; Petrocelli, J. J.; Matthews, O.; de Hart, N. M.; Ferrara, P. J.; O'Connell, R. M.; Funai, K.; Drummond, M. J. Absence of MyD88 from Skeletal Muscle Protects Female Mice from Inactivity-Induced Adiposity and Insulin Resistance. *Obesity* **2020**, *28* (4), 772–782.

(93) Louis, P.; Flint, H. J. Formation of Propionate and Butyrate by the Human Colonic Microbiota. *Environmental Microbiology* **2017**, *19* (1), 29–41.

(94) Louis, P.; Flint, H. J. Diversity, Metabolism and Microbial Ecology of Butyrate-Producing Bacteria from the Human Large Intestine. *FEMS Microbiology Letters* **2009**, *294* (1), 1–8.

(95) Van Den Abbeele, P.; Belzer, C.; Goossens, M.; Kleerebezem, M.; De Vos, W. M.; Thas, O.; De Weirdt, R.; Kerckhof, F. M.; Van De Wiele, T. Butyrate-Producing Clostridium Cluster XIVa Species Specifically Colonize Mucins in an in Vitro Gut Model. *ISME Journal* **2013**, *7* (5), 949–961.

(96) McKenzie, C. I.; Mackay, C. R.; Macia, L. GPR43 – A Prototypic Metabolite Sensor Linking Metabolic and Inflammatory Diseases. *Trends in Endocrinology & Metabolism* **2015**, *26* (10), 511–512.

(97) Graham, Lord; Giuseppe, M.; Jane, H.; Richard, B.; Stephen, B. Leptin Modulates the T-Cell Immune Response and Reverses Starvation-Induced Immunosuppression. *Nature* **1998**, *394* (6696), 897–901.

(98) Venegas, D. P.; De La Fuente, M. K.; Landskron, G.; González, M. J.; Quera, R.; Dijkstra, G.; Harmsen, H. J. M.; Faber, K. N.; Hermoso, M. A. Short Chain Fatty Acids (SCFAs)Mediated Gut Epithelial and Immune Regulation and Its Relevance for Inflammatory Bowel Diseases. *Frontiers in Immunology* **2019**, *10* (MAR).

(99) Thangaraju, M.; Cresci, G. A.; Liu, K.; Ananth, S.; Gnanaprakasam, J. P.; Browning, D. D.; Mellinger, J. D.; Smith, S. B.; Digby, G. J.; Lambert, N. A.; Prasad, P. D.; Ganapathy, V. GPFM 09A Is a G-Protein-Coupled Receptor for the Bacterial Fermentation Product Butyrate and Functions as a Tumor Suppressor in Colon. *Cancer Research* **2009**, *69* (7), 2826–2832.

(100) Macia, L.; Tan, J.; Vieira, A. T.; Leach, K.; Stanley, D.; Luong, S.; Maruya, M.; Ian McKenzie, C.; Hijikata, A.; Wong, C.; Binge, L.; Thorburn, A. N.; Chevalier, N.; Ang, C.; Marino, E.; Robert, R.; Offermanns, S.; Teixeira, M.

M.; Moore, R. J.; Flavell, R. A.; Fagarasan, S.; Mackay, C. R. Metabolite-Sensing Receptors GPR43 and GPR109A Facilitate Dietary Fibre-Induced Gut Homeostasis through Regulation of the Inflammasome. *Nature Communications* **2015**, *6*, Article number: 6734.

(101) Zaki, H.; Boyd, K. L.; Kastan, M. B.; Lamkanfi, M.; Kanneganti, D. The NLRP3 Inflammasome Protects against Loss of Epithelial Integrity and Mortality during Experimental Colitis. **2010**, *32* (3), 379–391.

(102) Furusawa, Y.; Obata, Y.; Fukuda, S.; Endo, T. A.; Nakato, G.; Takahashi, D.; Nakanishi, Y.; Uetake, C.; Kato, K.; Kato, T.; Takahashi, M.; Fukuda, N. N.; Murakami, S.; Miyauchi, E.; Hino, S.; Atarashi, K.; Onawa, S.; Fujimura, Y.; Lockett, T.; Clarke, J. M.; Topping, D. L.; Tomita, M.; Hori, S.; Ohara, O.; Morita, T.; Koseki, H.; Kikuchi, J.; Honda, K.; Hase, K.; Ohno, H. Commensal Microbe-Derived Butyrate Induces the Differentiation of Colonic Regulatory T Cells. *Nature* **2013**, *504* (7480), 446–450.

(103) Arpaia, N.; Campbell, C.; Fan, X.; Dikiy, S.; Van Der Veeken, J.; Deroos, P.; Liu, H.; Cross, J. R.; Pfeffer, K.; Coffer, P. J.; Rudensky, A. Y. Metabolites Produced by Commensal Bacteria Promote Peripheral Regulatory T-Cell Generation. *Nature* **2013**, *504* (7480), 451–455.

(104) Rivera-Chávez, F.; Zhang, L. F.; Faber, F.; Lopez, C. A.; Byndloss, M. X.; Olsan, E. E.; Xu, G.; Velazquez, E. M.; Lebrilla, C. B.; Winter, S. E.; Bäumler, A. J. Depletion of Butyrate-Producing Clostridia from the Gut Microbiota Drives an Aerobic Luminal Expansion of Salmonella. *Cell Host and Microbe* **2016**, *19* (4), 443–454.

(105) Wang, H. B.; Wang, P. Y.; Wang, X.; Wan, Y. L.; Liu, Y. C. Butyrate Enhances Intestinal Epithelial Barrier Function via Up-Regulation of Tight Junction Protein Claudin-1 Transcription. *Digestive Diseases and Sciences* **2012**, *57* (12), 3126–3135.

(106) Zhao, Y.; Chen, F.; Wu, W.; Sun, M.; Bilotta, A. J.; Yao, S.; Xiao, Y.; Huang, X.; Eaves-Pyles, T. D.; Golovko, G.; Fofanov, Y.; D'Souza, W.; Zhao, Q.; Liu, Z.; Cong, Y. GPR43 Mediates Microbiota Metabolite SCFA Regulation of Antimicrobial Peptide Expression in Intestinal Epithelial Cells via Activation of MTOR and STAT3. *Mucosal Immunology* **2018**, *11* (3), 752–762.

(107) Zheng, L.; Kelly, C. J.; Battista, K. D.; Schaefer, R.; Lanis, J. M.; Alexeev, E. E.; Wang, R. X.; Onyiah, J. C.; Kominsky, D. J.; Colgan, S. P. Microbial-Derived Butyrate Promotes Epithelial Barrier Function through IL-10 Receptor–Dependent Repression of Claudin-2. *The Journal of Immunology* **2017**, *199* (8), 2976–2984.

(108) Lin, H. V.; Frassetto, A.; Kowalik, E. J.; Nawrocki, A. R.; Lu, M. M.; Kosinski, J. R.; Hubert, J. A.; Szeto, D.; Yao, X.; Forrest, G.; Marsh, D. J. Butyrate and Propionate Protect against Diet-Induced Obesity and Regulate Gut Hormones via Free Fatty Acid Receptor 3-Independent Mechanisms. *PLoS ONE* **2012**, *7* (4), 1–9.

(109) Gao, Z.; Yin, J.; Zhang, J.; Ward, R. E.; Martin, R. J.; Lefevre, M.; Cefalu, W. T.; Ye, J. Butyrate Improves Insulin Sensitivity and Increases Energy Expenditure in Mice. *Diabetes* **2009**, *58* (7), 1509–1517.

(110) Yamashita, H.; Fujisawa, K.; Ito, E.; Idei, S.; Kawaguchi, N.; Kimoto, M.; Hiemori, M.; Tsuji, H. Improvement of Obesity and Glucose Tolerance by Acetate in Type 2 Diabetic Otsuka Long-Evans Tokushima Fatty (OLETF) Rats. *Bioscience, Biotechnology and Biochemistry* **2007**, *71* (5), 1236–1243.

(111) Dalby, M. J.; Ross, A. W.; Walker, A. W.; Morgan, P. J. Dietary Uncoupling of Gut Microbiota and Energy Harvesting from Obesity and Glucose Tolerance in Mice. *Cell Reports* **2017**, *21* (6), 1521–1533.

(112) Adachi, K.; Sugiyama, T.; Yamaguchi, Y.; Tamura, Y.; Izawa, S.; Hijikata, Y.; Ebi, M.; Funaki, Y.; Ogasawara, N.; Goto, C.; Sasaki, M.; Kasugai, K. Gut Microbiota Disorders Cause Type 2 Diabetes Mellitus and Homeostatic Disturbances in Gut-Related Metabolism in Japanese Subjects. *Journal of Clinical Biochemistry and Nutrition* **2019**, *64* (3), 231.

(113) Phetcharaburanin, J.; Lees, H.; Marchesi, J. R.; Nicholson, J. K.; Holmes, E.; Seyfried, F.; Li, J. V. Systemic Characterization of an Obese Phenotype in the Zucker Rat Model Defining Metabolic Axes of Energy Metabolism and Host-Microbial Interactions. *Journal of Proteome Research* **2016**, *15* (6), 1897–1906.

(114) Schwiertz, A.; Taras, D.; Schäfer, K.; Beijer, S.; Bos, N. A.; Donus, C.; Hardt, P. D. Microbiota and SCFA in Lean and Overweight Healthy Subjects. *Obesity* **2010**, *18* (1), 190–195.

(115) Murphy, E. F.; Cotter, P. D.; Healy, S.; Marques, T. M.; O'Sullivan, O.; Fouhy, F.; Clarke, S. F.; O'Toole, P. W.; Quigley, E. M.; Stanton, C.; Ross, P. R.; O'Doherty, R. M.; Shanahan, F. Composition and Energy Harvesting Capacity of the Gut Microbiota: Relationship to Diet, Obesity and Time in Mouse Models. *Gut* **2010**, *59* (12), 1635–1642.

(116) Fernandes, J.; Su, W.; Rahat-Rozenbloom, S.; Wolever, T. M. S.; Comelli, E. M. Adiposity, Gut Microbiota and Faecal Short Chain Fatty Acids Are Linked in Adult Humans. *Nutrition and Diabetes* **2014**, *4* (JUNE).

(117) Chen; Wei, X.; Zhang, J.; Pariyani, R.; Jokioja, J.; Kortesniemi, M.; Linderborg, K. M.; Heinonen, J.; Sainio, T.; Zhang, Y.; Yang, B. Effects of Anthocyanin Extracts from Bilberry (Vaccinium Myrtillus L.) and Purple Potato (Solanum Tuberosum L. Var. ' Synkea¨ Sakari ') on the Plasma Metabolomic Profile of Zucker Diabetic Fatty Rats. *Journal of Agricultural and Food Chemistry* **2020**, *68*, 9436–9450.

(118) Tiantian, Z.; Goodarzi, M. O. Metabolites Linking the Gut Microbiome with Risk for Type 2 Diabetes. *Physiology & behavior* **2020**, *9* (2), 83–93.

(119) Pathak, P.; Xie, C. G. N. Intestine Farnesoid X Receptor Agonist and the Gut Microbiota Activate G-Protein Bile Acid Receptor-1 Signaling to Improve Metabolism. *Hepatology* **2018**, *68* (4), 1574–1588.

(120) Bennett, B. J.; Vallim, T. Q. D. A.; Wang, Z.; Shih, D. M.; Meng, Y.; Gregory, J.; Allayee, H.; Lee, R.; Graham, M.; Crooke, R.; Edwards, P. A.; Hazen, S. L.; Lusis, A. J.; Manuscript, A. Trimethylamine-N-Oxide, a Metabolite Associated with Atherosclerosis, Exhibits Complex Genetic and Dietary Regulation. *Cell Metabolism* **2013**, *17* (1), 49–60.

(121) Shan, Z.; Sun, T.; Huang, H.; Chen, S.; Chen, L.; Luo, C.; Yang, W.; Yang, X.; Yao, P.; Cheng, J.; Hu, F. B.; Liu, L. Association between Microbiota-Dependent Metabolite Trimethylamine-N-Oxide and Type 2 Diabetes. *American Journal of Clinical Nutrition* **2017**, *106* (3), 888–894.

(122) Jia, J.; Dou, P.; Gao, M.; Kong, X.; Li, C.; Liu, Z.; Huang, T. Assessment of Causal Direction between Gut Microbiota- Dependent Metabolites and Cardiometabolic Health: A Bidirectional Mendelian Randomization Analysis. *Diabetes* **2019**, *68* (9), 1747–1755.

(123) Gao, X.; Liu, X.; Xu, J.; Xue, C.; Xue, Y.; Wang, Y. Dietary Trimethylamine N-Oxide Exacerbates Impaired Glucose Tolerance in Mice Fed a High Fat Diet. *Journal of Bioscience and Bioengineering* **2014**, *118* (4), 476–481.

(124) Steven M. Singer#, Marc Y. Fink, V. V. A. Gut Microbiota Metabolites, Amino Acid Metabolites, and Improvements in Insulin Sensitivity and Glucose Metabolism: The POUNDS Lost Trial. *Gut* **2019**, *176* (3), 263–270.

(125) Li, G.; Young, K. D. Indole Production by the Tryptophanase TnaA in Escherichia Coli Is Determined by the Amount of Exogenous Tryptophan. *Microbiology* **2013**, *159* (2), 402–410.

(126) Chimerel, C.; Emery, E.; Summers, D. K.; Keyser, U.; Gribble, F. M.; Reimann, F. Bacterial Metabolite Indole Modulates Incretin Secretion from Intestinal Enteroendocrine L Cells. *Cell Reports* **2014**, *9* (4), 1202–1208.

(127) De Mello, V. D.; Paananen, J.; Lindström, J.; Lankinen, M. A.; Shi, L.; Kuusisto, J.; Pihlajamäki, J.; Auriola, S.; Lehtonen, M.; Rolandsson, O.; Bergdahl, I. A.; Nordin, E.; Ilanne-Parikka, P.; Keinänen-Kiukaanniemi, S.; Landberg, R.; Eriksson, J. G.; Tuomilehto, J.; Hanhineva, K.;

Uusitupa, M. Indolepropionic Acid and Novel Lipid Metabolites Are Associated with a Lower Risk of Type 2 Diabetes in the Finnish Diabetes Prevention Study. *Scientific Reports* **2017**, *7*, 46337.

(128) Ji, Y.; Gao, Y.; Chen, H.; Yin, Y.; Zhang, W. Indole-3-Acetic Acid Alleviates Nonalcoholic Fatty Liver Disease in Mice via Attenuation of Hepatic Lipogenesis, and Oxidative and Inflammatory Stress. *Nutrients* **2019**, *11* (9).

(129) Falony, G.; Joossens, M.; Vieira-Silva, S.; Wang, J.; Darzi, Y.; Faust, K.; Kurilshikov, A.; Bonder, M. J.; Valles-Colomer, M.; Vandeputte, D.; Tito, R. Y.; Chaffron, S.; Rymenans, L.; Verspecht, C.; Sutter, L. De; Lima-Mendez, G.; D'hoe, K.; Jonckheere, K.; Homola, D.; Garcia, R.; Tigchelaar, E. F.; Eeckhaudt, L.; Fu, J.; Henckaerts, L.; Zhernakova, A.; Wijmenga, C.; Raes, J. Population-Level Analysis of Gut Microbiome Variation. *Science* **2016**, *352* (6285), 560–564.

(130) Lê, K. A.; Li, Y.; Xu, X.; Yang, W.; Liu, T.; Zhao, X.; Tang, Y. G.; Cai, D.; Go, V. L. W.; Pandol, S.; Hui, H. Alterations in Fecal Lactobacillus and Bifidobacterium Species in Type 2 Diabetic Patients in Southern China Population. *Frontiers in Physiology* **2013**, *3*, Article 496.

(131) Karlsson, F. H.; Tremaroli, V.; Nookaew, I.; Bergström, G.; Behre, C. J.; Fagerberg, B.; Nielsen, J.; Bäckhed, F. Gut Metagenome in European Women with Normal, Impaired and Diabetic Glucose Control. *Nature* **2013**, *498* (7452), 99–103.

(132) Sedighi, M.; Razavi, S.; Navab-Moghadam, F.; Khamseh, M. E.; Alaei-Shahmiri, F.; Mehrtash, A.; Amirmozafari, N. Comparison of Gut Microbiota in Adult Patients with Type 2 Diabetes and Healthy Individuals. *Microbial Pathogenesis* **2017**, *111*, 362–369.

(133) Derrien, M.; Vaughan, E. E.; Plugge, C. M.; Vos, W. M. de. Akkermansia Muciniphila Gen. Nov., Sp. Nov., a Human Intestinal Mucin-Degrading Bacterium. *International Journal of Systematic and Evolutionary Microbiology* **2004**, *54* (5), 1469–1476.

(134) Larsen, N.; Vogensen, F. K.; Van Den Berg, F. W. J.; Nielsen, D. S.; Andreasen, A. S.; Pedersen, B. K.; Al-Soud, W. A.; Sørensen, S. J.; Hansen, L. H.; Jakobsen, M. Gut Microbiota in Human Adults with Type 2 Diabetes Differs from Non-Diabetic Adults. *PLoS ONE* **2010**, *5* (2).

(135) Gurung, M.; Li, Z.; You, H.; Rodrigues, R.; Jump, D. B.; Morgun, A.; Shulzhenko, N. Role of Gut Microbiota in Type 2 Diabetes Pathophysiology. *EBioMedicine* **2020**, *51*, e102590.

(136) Sasaki, M.; Ogasawara, N.; Funaki, Y.; Mizuno, M.; Iida, A.; Goto, C.; Koikeda, S.; Kasugai, K.; Joh, T. Transglucosidase Improves the Gut Microbiota Profile of Type 2 Diabetes Mellitus Patients: A Randomized Double-Blind, Placebo-Controlled Study. *BMC Gastroenterology* **2013**, *13* (1), 1–7.

(137) Wang, J.; Qin, J.; Li, Y.; Cai, Z.; Li, S.; Zhu, J.; Zhang, F.; Liang, S.; Zhang, W.; Guan, Y.; Shen, D.; Peng, Y.; Zhang, D.; Jie, Z.; Wu, W.; Qin, Y.; Xue, W.; Li, J.; Han, L.; Lu, D.; Wu, P.; Dai, Y.; Sun, X.; Li, Z.; Tang, A.; Zhong, S.; Li, X.; Chen, W.; Xu, R.; Wang, M.; Feng, Q.; Gong, M.; Yu, J.; Zhang, Y.; Zhang, M.; Hansen, T.; Sanchez, G.; Raes, J.; Falony, G.; Okuda, S.; Almeida, M.; Lechatelier, E.; Renault, P.; Pons, N.; Batto, J. M.; Zhang, Z.; Chen, H.; Yang, R.; Zheng, W.; Li, S.; Yang, H.; Ehrlich, S. D.; Nielsen, R.; Pedersen, O.; Kristiansen, K.; Wang, J. A Metagenome-Wide Association Study of Gut Microbiota in Type 2 Diabetes. *Nature* **2012**, *490* (7418), 55–60.

(138) Furet, J. P.; Kong, L. C.; Tap, J.; Poitou, C.; Basdevant, A.; Bouillot, J. L.; Mariat, D.; Corthier, G.; Doré, J.; Henegar, C.; Rizkalla, S.; Clément, K. Differential Adaptation of Human Gut Microbiota to Bariatric Surgery-Induced Weight Loss: Links with Metabolic and Low-Grade Inflammation Markers. *Diabetes* **2010**, *59* (12), 3049–3057.

(139) Vrieze, A.; Van Nood, E.; Holleman, F.; Salojärvi, J.; Kootte, R. S.; Bartelsman, J. F. W. M.; Dallinga-Thie, G. M.; Ackermans, M. T.; Serlie, M. J.; Oozeer, R.; Derrien, M.; Druesne, A.; Van Hylckama Vlieg, J. E. T.; Bloks, V. W.;

Groen, A. K.; Heilig, H. G. H. J.; Zoetendal, E. G.; Stroes, E. S.; De Vos, W. M.; Hoekstra, J. B. L.; Nieuwdorp, M. Transfer of Intestinal Microbiota from Lean Donors Increases Insulin Sensitivity in Individuals with Metabolic Syndrome. *Gastroenterology* **2012**, *143* (4), 913-916.e7.

(140) Everard, A.; Lazarevic, V.; Derrien, M.; Girard, M.; Muccioli, G. M.; Neyrinck, A. M.; Possemiers, S.; Van Holle, A.; François, P.; De Vos, W. M.; Delzenne, N. M.; Schrenzel, J.; Cani, P. D. Responses of Gut Microbiota and Glucose and Lipid Metabolism to Prebiotics in Genetic Obese and Diet-Induced Leptin-Resistant Mice. *Diabetes* **2011**, *60* (11), 2775–2786.

(141) Shin, N. R.; Lee, J. C.; Lee, H. Y.; Kim, M. S.; Whon, T. W.; Lee, M. S.; Bae, J. W. An Increase in the Akkermansia Spp. Population Induced by Metformin Treatment Improves Glucose Homeostasis in Diet-Induced Obese Mice. *Gut* **2014**, *63* (5), 727–735.

(142) Org, E.; Blum, Y.; Kasela, S.; Mehrabian, M.; Kuusisto, J.; Kangas, A. J.; Soininen, P.; Wang, Z.; Ala-Korpela, M.; Hazen, S. L.; Laakso, M.; Lusis, A. J. Relationships between Gut Microbiota, Plasma Metabolites, and Metabolic Syndrome Traits in the METSIM Cohort. *Genome Biology* **2017**, *18* (1), 1–14.

(143) Zhang, X.; Shen, D.; Fang, Z.; Jie, Z.; Qiu, X.; Zhang, C.; Chen, Y.; Ji, L. Human Gut Microbiota Changes Reveal the Progression of Glucose Intolerance. *PLoS ONE* **2013**, *8* (8).

(144) Sato, J.; Kanazawa, A.; Ikeda, F.; Yoshihara, T.; Goto, H.; Abe, H.; Komiya, K.; Kawaguchi, M.; Shimizu, T.; Ogihara, T.; Tamura, Y.; Sakurai, Y.; Yamamoto, R.; Mita, T.; Fujitani, Y.; Fukuda, H.; Nomoto, K.; Takahashi, T.; Asahara, T.; Hirose, T.; Nagata, S.; Yamashiro, Y.; Watada, H. Gut Dysbiosis and Detection of "Live Gut Bacteria" in Blood of Japanese Patients with Type 2 Diabetes. *Diabetes Care* **2014**, *37* (8), 2343–2350.

(145) Egshatyan, L.; Kashtanova, D.; Popenko, A.; Tkacheva, O.; Tyakht, A.; Alexeev, D.; Karamnova, N.; Kostryukova, E.; Babenko, V.; Vakhitova, M.; Boytsov, S. Gut Microbiota and Diet in Patients with Different Glucose Tolerance. *Endocrine Connections* **2016**, *5* (1), 1–9.

(146) Candela, M.; Biagi, E.; Soverini, M.; Consolandi, C.; Quercia, S.; Severgnini, M.; Peano, C.; Turroni, S.; Rampelli, S.; Pozzilli, P.; Pianesi, M.; Fallucca, F.; Brigidi, P. Modulation of Gut Microbiota Dysbioses in Type 2 Diabetic Patients by Macrobiotic Ma-Pi 2 Diet. *British Journal of Nutrition* **2016**, *116* (1), 80–93.

(147) Pedersen, H. K.; Gudmundsdottir, V.; Nielsen, H. B.; Hyotylainen, T.; Nielsen, T.; Jensen, B. A. H.; Forslund, K.; Hildebrand, F.; Prifti, E.; Falony, G.; Le Chatelier, E.; Levenez, F.; Doré, J.; Mattila, I.; Plichta, D. R.; Pöhö, P.; Hellgren, L. I.; Arumugam, M.; Sunagawa, S.; Vieira-Silva, S.; Jørgensen, T.; Holm, J. B.; Trošt, K.; Kristiansen, K.; Brix, S.; Raes, J.; Wang, J.; Hansen, T.; Bork, P.; Brunak, S.; Oresic, M.; Ehrlich, S. D.; Pedersen, O. Human Gut Microbes Impact Host Serum Metabolome and Insulin Sensitivity. *Nature* **2016**, *535* (7612), 376–381.

(148) De La Cuesta-Zuluaga, J.; Mueller, N. T.; Corrales-Agudelo, V.; Velásquez-Mejía, E. P.; Carmona, J. A.; Abad, J. M.; Escobar, J. S. Metformin Is Associated with Higher Relative Abundance of Mucin-Degrading Akkermansia Muciniphila and Several Short-Chain Fatty Acid-Producing Microbiota in the Gut. *Diabetes Care* **2017**, *40* (1), 54–62.

(149) Wang, Y.; Luo, X.; Mao, X.; Tao, Y.; Ran, X.; Zhao, H.; Xiong, J.; Li, L. Gut Microbiome Analysis of Type 2 Diabetic Patients from the Chinese Minority Ethnic Groups the Uygurs and Kazaks. *PLoS ONE* **2017**, *12* (3), 1–15.

(150) Allin, K. H.; Tremaroli, V.; Caesar, R.; Jensen, B. A. H.; Damgaard, M. T. F.; Bahl, M. I.; Licht, T. R.; Hansen, T. H.; Nielsen, T.; Dantoft, T. M.; Linneberg, A.; Jørgensen, T.; Vestergaard, H.; Kristiansen, K.; Franks, P. W.; Hansen, T.; Bäckhed, F.; Pedersen, O. Aberrant Intestinal Microbiota in Individuals with Prediabetes. *Diabetologia* **2018**, *61* (4), 810–820.

(151) Dominika, S.; Agnieszka, S.-O.; Przemysław, K.; Magdalena, S. Characteristics of Gut Microbiota in Adult Patients with Type 1 and Type 2 Diabetes Based on Next-generation Sequencing of the 16S RRNA Gene Fragment. *Polish archives of internal medicine* **2018**, *128* (6), 336–343.

(152) Zhao, L.; Lou, H.; Peng, Y.; Chen, S.; Zhang, Y.; Li, X. Comprehensive Relationships between Gut Microbiome and Faecal Metabolome in Individuals with Type 2 Diabetes and Its Complications. *Endocrine* **2019**, *66* (3), 526–537.

(153) Clifford, M. N. Anthocyanins - Nature, Occurrence and Dietary Burden. *Journal of the Science of Food and Agriculture* **2000**, *80* (7), 1063–1072.

(154) Vidana Gamage, G. C.; Lim, Y. Y.; Choo, W. S. Sources and Relative Stabilities of Acylated and Nonacylated Anthocyanins in Beverage Systems. *Journal of Food Science and Technology* **2021**.

(155) Giusti, M. M.; Wrolstad, R. E. Acylated Anthocyanins from Edible Sources and Their Applications in Food Systems. **2003**, *14*, 217–225.

(156) Yousuf, B.; Gul, K.; Wani, A. A.; Singh, P. Health Benefits of Anthocyanins and Their Encapsulation for Potential Use in Food Systems: A Review. *Critical Reviews in Food Science and Nutrition* **2016**, *56* (13), 2223–2230.

(157) D'Auria, J. C. Acyltransferases in Plants: A Good Time to Be BAHD. *Current Opinion in Plant Biology* **2006**, *9* (3), 331–340.

(158) He, F.; Mu, L.; Yan, G. L.; Liang, N. N.; Pan, Q. H.; Wang, J.; Reeves, M. J.; Duan, C. Q. Biosynthesis of Anthocyanins and Their Regulation in Colored Grapes. *Molecules* **2010**, *15* (12), 9057–9091.

(159) Bakowska-Barczak, A. Acylated Anthocyanins as Stable, Natural Food Colorants–a Review. *Polish Journal of Food and Nutrition Sciences* **2005**, *14* (2), 107–115.

(160) Passamonti, S.; Vrhovsek, U.; Mattivi, F. The Interaction of Anthocyanins with Bilitranslocase. *Biochemical and Biophysical Research Communications* **2002**, *296* (3), 631–636.

(161) Zhao, C. L.; Yu, Y. Q.; Chen, Z. J.; Wen, G. S.; Wei, F. G.; Zheng, Q.; Wang, C. De; Xiao, X. L. Stability-Increasing Effects of Anthocyanin Glycosyl Acylation. *Food Chemistry* **2017**, *214*, 119–128.

(162) Oliveira, H.; Perez-gregório, R.; Freitas, V. De; Mateus, N.; Fernandes, I. Comparison of the in Vitro Gastrointestinal Bioavailability of Acylated and Non-Acylated Anthocyanins : Purple- Fl Eshed Sweet Potato vs Red Wine. *Food Chemistry* **2019**, *276* (15), 410–418.

(163) Kurilich, A. C.; Clevidence, B. A.; Britz, S. J.; Simon, P. W.; Novotny, J. A. Plasma and Urine Responses Are Lower for Acylated vs Nonacylated Anthocyanins from Raw and Cooked Purple Carrots. *Journal of Agricultural and Food Chemistry* **2005**, *53*, 6537–6542.

(164) Olejnik, A.; Kowalska, K.; Kidoń, M.; Czapski, J.; Rychlik, J.; Olkowicz, M.; Dembczyński, R. Purple Carrot Anthocyanins Suppress Lipopolysaccharide-Induced Inflammation in the Co-Culture of Intestinal Caco-2 and Macrophage RAW264.7 Cells. *Food and Function* **2016**, *7* (1), 557–564.

(165) Zhang, H.; Hassan, Y. I.; Renaud, J.; Liu, R.; Yang, C.; Sun, Y.; Tsao, R. Bioaccessibility, Bioavailability, and Anti-Inflammatory Effects of Anthocyanins from Purple Root Vegetables Using Mono- and Co-Culture Cell Models. *Molecular Nutrition and Food Research* **2017**, *61* (10), 1–15.

(166) Oliveira, H.; Roma-Rodrigues, C.; Santos, A.; Veigas, B.; Brás, N.; Faria, A.; Calhau, C.; de Freitas, V.; Baptista, P. V.; Mateus, N.; Fernandes, A. R.; Fernandes, I. GLUT1 and GLUT3 Involvement in Anthocyanin Gastric Transport- Nanobased Targeted Approach. *Scientific Reports* **2019**, *9* (1), 1–14.

(167) Han, F.; Oliveira, H.; Brás, N. F.; Fernandes, I.; Cruz, L.; De Freitas, V.; Mateus, N. In Vitro Gastrointestinal

Absorption of Red Wine Anthocyanins – Impact of Structural Complexity and Phase II Metabolization. *Food Chemistry* **2020**, *317* (January), 126398.

(168) Faria, A.; Fernandes, I.; Norberto, S.; Mateus, N.; Calhau, C. Interplay between Anthocyanins and Gut Microbiota. *Journal of Agricultural and Food Chemistry* **2014**, *62*, 6898–6902.

(169) Kay, C. D. Aspects of Anthocyanin Absorption, Metabolism and Pharmacokinetics in Humans. *Nutrition Research Reviews* **2006**, *19*, 137–146.

(170) Chu, W.; Cheung, S. C. M.; Lau, R. A. W.; Benzie, I. F. F. Bilberry (Vaccinium Myrtillus L.). In *Herbal Medicine: Biomolecular and Clinical Aspects: Second Edition*; Benzie IFF, W.-G. S., Ed.; CRC Press/Taylor & Francis, 2011; pp 55–71.

(171) Chen, K.; Wei, X.; Zhang, J.; Pariyani, R.; Jokioja, J.; Kortesniemi, M.; Linderborg, K.; Heinonen, J.; Sainio, T.; Zhang, Y.; Yang, B. Effects of Anthocyanin Extracts from Bilberry (Vaccinium Myrtillus L.) and Purple Potato (Solanum Tuberosum L. Var. 'Synkeä Sakari') on the Plasma Metabolomic Profile of Zucker Diabetic Fatty Rats. *Journal of Agricultural and Food Chemistry 68* (35), 9436–9450.

(172) Burdulis, D.; Šarkinas, A.; Jasutiene, I.; Stackevičiene, E.; Nikolajevas, L.; Janulis, V. Comparative Study of Anthocyanin Composition, Antimicrobial and Antioxidant Activity in Bilberry (Vaccinium Myrtillus L.) and Blueberry (Vaccinium Corymbosum L.) Fruits. *Acta Poloniae Pharmaceutica - Drug Research* **2009**, *66* (4), 399–408.

(173) Christelle M. Andre, *,†,‡; Marc Ghislain, §; Pierre Bertin, #; Mouhssin Oufir, ‡; María del Rosario Herrera, §; Lucien Hoffmann, ‡; Jean-François Hausman, ‡; Yvan Larondelle, † and; Evers‡, D. Andean Potato Cultivars (Solanum Tuberosum L.) as a Source of Antioxidant and Mineral Micronutrients. *Journal of Agricultural and Food Chemistry* **2006**, *55* (2), 366–378.

(174) Gutiérrez-Quequezana, L.; Vuorinen, A. L.; Kallio, H.; Yang, B. Improved Analysis of Anthocyanins and Vitamin C in Blue-Purple Potato Cultivars. *Food Chemistry* **2018**, *242* (March 2017), 217–224.

(175) Wegener, C. B.; Jansen, G. Soft-Rot Resistance of Coloured Potato Cultivars (Solanum Tuberosum L.): The Role of Anthocyanins. *Potato Research* **2007**, *50* (1), 31–44.

(176) Heinonen, J.; Farahmandazad, H.; Vuorinen, A.; Kallio, H.; Yang, B. R.; Sainio, T. Extraction and Purification of Anthocyanins from Purple-Fleshed Potato. *Food And Bioproducts Processing* **2016**, *99*, 136–146.

(177) Hidalgo, M.; Oruna-Concha, M. J.; Kolida, S.; Walton, G. E.; Kallithraka, S.; Spencer, J. P. E.; Gibson, G. R.; De Pascual-Teresa, S. Metabolism of Anthocyanins by Human Gut Microflora and Their Influence on Gut Bacterial Growth. *Journal of Agricultural and Food Chemistry* **2012**, *60* (15), 3882–3890.

(178) Jayarathne, S.; Stull, A. J.; Park, O. H.; Kim, J. H.; Thompson, L.; Moustaid-Moussa, N. Protective Effects of Anthocyanins in Obesity-Associated Inflammation and Changes in Gut Microbiome. *Molecular Nutrition and Food Research* **2019**, *63* (20), 1–18.

(179) Faria, A.; Fernandes, I.; Norberto, S.; Mateus, N.; Calhau, C. Interplay between Anthocyanins and Gut Microbiota. *Journal of Agricultural and Food Chemistry* **2014**, *62* (29), 6898–6902.

(180) Tian. Metabolism of Anthocyanins and Consequent Effects on the Gut Microbiota. *Critical Reviews in Food Science and Nutrition* **2019**, *59* (6), 982–991.

(181) Blesso, C. N. Dietary Anthocyanins and Human Health. *Nutrients* **2019**, *11* (9), 10–13.

(182) Jiang, X.; Li, X.; Zhu, C.; Sun, J.; Tian, L.; Chen, W.; Bai, W. The Target Cells of Anthocyanins in Metabolic Syndrome. *Critical Reviews in Food Science and Nutrition* **2019**, *59* (6), 921–946.

(183) Matsui, T.; Ueda, T.; Oki, T.; Sugita, K.; Terahara, N.; Matsumoto, K. α-Glucosidase Inhibitory Action of

Natural Acylated Anthocyanins. 2. α-Glucosidase Inhibition by Isolated Acylated Anthocyanins. *Journal of Agricultural and Food Chemistry* **2001**, *49* (4), 1952–1956.

(184) Esatbeyoglu, T.; Rodríguez-Werner, M.; Schlösser, A.; Winterhalter, P.; Rimbach, G. Fractionation, Enzyme Inhibitory and Cellular Antioxidant Activity of Bioactives from Purple Sweet Potato (Ipomoea Batatas). *Food Chemistry* **2017**, *221*, 447–456.

(185) Jokioja, J.; Yang, B.; Linderborg, M. K. Acylated Anthocyanins : A Review on Their Bioavailability and Effects on Postprandial Carbohydrate Metabolism and Inflammation. **2021**, No. August.

(186) Xie, L.; Mo, J.; Ni, J.; Xu, Y.; Su, H.; Xie, J.; Chen, W. Structure-Based Design of Human Pancreatic Amylase Inhibitors from the Natural Anthocyanin Database for Type 2 Diabetes. *Food and Function* **2020**, *11* (4), 2910–2923.

(187) Matsui, T.; Ueda, T.; Oki, T.; Sugita, K.; Terahara, N.; Matsumoto, K. R-Glucosidase Inhibitory Action of Natural Acylated Anthocyanins. 2. r-Glucosidase Inhibition by Isolated Acylated Anthocyanins. **2001**.

(188) Yang, Y.; Zhang, J. liang; Shen, L. hong; Feng, L. jie; Zhou, Q. Inhibition Mechanism of Diacylated Anthocyanins from Purple Sweet Potato (Ipomoea Batatas L.) against α-Amylase and α-Glucosidase. *Food Chemistry* **2021**, *359* (1), 129934.

(189) Gong, S.; Yang, C.; Zhang, J.; Yu, Y.; Gu, X.; Li, W.; Wang, Z. Study on the Interaction Mechanism of Purple Potato Anthocyanins with Casein and Whey Protein. *Food Hydrocolloids* **2021**, *111* (June 2020), 106223.

(190) Rojo, L. E.; Ribnicky, D.; Logendra, S.; Poulev, A.; Rojas-Silva, P.; Kuhn, P.; Dorn, R.; Grace, M. H.; Lila, M. A.; Raskin, I. In Vitro and in Vivo Anti-Diabetic Effects of Anthocyanins from Maqui Berry (Aristotelia Chilensis). *Food Chemistry* **2012**, *131* (2), 387–396.

(191) Martineau, L. C.; Couture, A.; Spoor, D.; Benhaddou-Andaloussi, A.; Harris, C.; Meddah, B.; Leduc, C.; Burt, A.; Vuong, T.; Mai Le, P.; Prentki, M.; Bennett, S. A.; Arnason, J. T.; Haddad, P. S. Anti-Diabetic Properties of the Canadian Lowbush Blueberry Vaccinium Angustifolium Ait. *Phytomedicine* **2006**, *13* (9–10), 612–623.

(192) Jayaprakasam, B.; Vareed, S. K.; Olson, L. K.; Nair, M. G. Insulin Secretion by Bioactive Anthocyanins and Anthocyanidins Present in Fruits. *Journal of Agricultural and Food Chemistry* **2005**, *53* (1), 28–31.

(193) Scazzocchio, B.; Varì, R.; Filesi, C.; D'Archivio, M.; Santangelo, C.; Giovannini, C.; Iacovelli, A.; Silecchia, G.; Volti, G. L.; Galvano, F.; Masella, R. Cyanidin-3-O-β-Glucoside and Protocatechuic Acid Exert Insulin-like Effects by Upregulating PPARγ Activity in Human Omental Adipocytes. *Diabetes* **2011**, *60* (9), 2234–2244.

(194) Ju, J. H.; Yoon, H. S.; Park, H. J.; Kim, M. Y.; Shin, H. K.; Park, K. Y.; Yang, J. O.; Sohn, M. S.; Do, M. S. Anti-Obesity and Antioxidative Effects of Purple Sweet Potato Extract in 3T3-L1 Adipocytes in Vitro. *Journal of Medicinal Food* **2011**, *14* (10), 1097–1106.

(195) Xu, Y.; Xie, L.; Xie, J.; Liu, Y.; Chen, W. Pelargonidin-3-O-Rutinoside as a Novel α-Glucosidase Inhibitor for Improving Postprandial Hyperglycemia. *Chemical Communications* **2019**, *55* (1), 39–42.

(196) Yan, F.; Zhang, J.; Zhang, L.; Zheng, X. Mulberry Anthocyanin Extract Regulates Glucose Metabolism by Promotion of Glycogen Synthesis and Reduction of Gluconeogenesis in Human HepG2 Cells. *Food Function* **2016**, *7* (1), 425–433.

(197) Hwang, Y. P.; Choi, J. H.; Han, E. H.; Kim, H. G.; Wee, J. H.; Jung, K. O.; Jung, K. H.; Kwon, K. il; Jeong, T. C.; Chung, Y. C.; Jeong, H. G. Purple Sweet Potato Anthocyanins Attenuate Hepatic Lipid Accumulation through Activating Adenosine Monophosphate-Activated Protein Kinase in Human HepG2 Cells and Obese Mice. *Nutrition Research* **2011**, *31* (12), 896–906.

(198) Jiang, T.; Shuai, X.; Li, J.; Yang, N.; Deng, L.; Li, S.; He, Y.; Guo, H.; Li, Y.; He, J. Protein-Bound Anthocyanin

Compounds of Purple Sweet Potato Ameliorate Hyperglycemia by Regulating Hepatic Glucose Metabolism in High-Fat Diet/Streptozotocin-Induced Diabetic Mice. *Journal of Agricultural and Food Chemistry* **2020**, *68* (6), 1596–1608.

(199) Huang, B.; Wang, Z.; Park, J. H.; Ryu, O. H.; Choi, M. K.; Lee, J. Y.; Kang, Y. H.; Lim, S. S. Anti-Diabetic Effect of Purple Corn Extract on C57BL/KsJ Db/Db Mice. *Nutrition Research and Practice* **2015**, *9* (1), 22–29.

(200) Takikawa, M.; Inoue, S.; Horio, F.; Tsuda, T. Dietary Anthocyanin-Rich Bilberry Extract Ameliorates Hyperglycemia and Insulin Sensitivity via Activation of AMP-Acin Diabetic Mice. *J Nutr* **2010**, *140* (3), 527–533.

(201) Yan, F.; Zheng, X. Anthocyanin-Rich Mulberry Fruit Improves Insulin Resistance and Protects Hepatocytes against Oxidative Stress during Hyperglycemia by Regulating AMPK/ACC/MTOR Pathway. *Journal of Functional Foods* **2017**, *30*, 270–281.

(202) Zhang, Z. F.; Lu, J.; Zheng, Y. L.; Wu, D. M.; Hu, B.; Shan, Q.; Cheng, W.; Li, M. Q.; Sun, Y. Y. Purple Sweet Potato Color Attenuates Hepatic Insulin Resistance via Blocking Oxidative Stress and Endoplasmic Reticulum Stress in High-Fat-Diet-Treated Mice. *The Journal of Nutritional Biochemistry* **2013**, *24* (6), 1008–1018.

(203) Park, M.; Yoo, J. H.; Lee, Y. S.; Lee, H. J. Lonicera Caerulea Extract Attenuates Non-Alcoholic Fatty Liver Disease in Free Fatty Acid-Induced HepG2 Hepatocytes and in High Fat Diet-Fed Mice. *Nutrients* **2019**, *11* (3).

(204) Tian, B.; Zhao, J.; Xie, X.; Chen, T.; Yin, Y.; Zhai, R.; Wang, X.; An, W.; Li, J. Anthocyanins from the Fruits of: Lycium Ruthenicum Murray Improve High-Fat Diet-Induced Insulin Resistance by Ameliorating Inflammation and Oxidative Stress in Mice. *Food and Function* **2021**, *12* (9), 3855–3871.

(205) Choi, K. H.; Lee, H. A.; Park, M. H.; Han, J.-S. Mulberry (*Morus Alba L.*) Fruit Extract Containing Anthocyanins Improves Glycemic Control and Insulin Sensitivity via Activation of AMP-Activated Protein Kinase in Diabetic C57BL/Ksj-Db/Db Mice. *Journal of Medicinal Food* **2016**, *19* (8), 737–745.

(206) Tsutsumi, A.; Horikoshi, Y.; Fushimi, T.; Saito, A.; Koizumi, R.; Fujii, Y.; Hu, Q. Q.; Hirota, Y.; Aizawa, K.; Osakabe, N. Acylated Anthocyanins Derived from Purple Carrot (: Daucus Carota L.) Induce Elevation of Blood Flow in Rat Cremaster Arteriole. *Food and Function* **2019**, *10* (3), 1726–1735.

(207) Honghui, G.; Dan, L.; Wenhua, L.; Xiang, F.; Min, X. Anthocyanin Inhibits High Glucose-Induced Hepatic MtGPAT1 Activation and Prevents Fatty Acid Synthesis through PKCζ. *Journal of lipid research* **2011**, *52* (5), 908–922.

(208) Tsuda, T.; Horio, F.; Uchida, K.; Aoki, H.; Osawa, T. Dietary Cyanidin 3-O-β-D-Glucoside-Rich Purple Corn Color Prevents Obesity and Ameliorates Hyperglycemia in Mice. *The Journal of Nutrition* **2003**, *133* (7), 2125–2130.

(209) Chang, J. J.; Hsu, M. J.; Huang, H. P.; Chung, D. J.; Chang, Y. C.; Wang, C. J. Mulberry Anthocyanins Inhibit Oleic Acid Induced Lipid Accumulation by Reduction of Lipogenesis and Promotion of Hepatic Lipid Clearance. *Journal of Agricultural and Food Chemistry* **2013**, *61* (25), 6069–6076.

(210) Yang, Y.; Zhang, J. liang; Zhou, Q. Targets and Mechanisms of Dietary Anthocyanins to Combat Hyperglycemia and Hyperuricemia: A Comprehensive Review. *Critical Reviews in Food Science and Nutrition* **2020**, *0* (0), 1–25.

(211) Les, F.; Cásedas, G.; Gómez, C.; Moliner, C.; Valero, M. S.; López, V. The Role of Anthocyanins as Antidiabetic Agents: From Molecular Mechanisms to in Vivo and Human Studies. *Journal of Physiology and Biochemistry* **2021**, *77* (1), 109–131.

(212) Gowd, V.; Jia, Z.; Chen, W. Anthocyanins as Promising Molecules and Dietary Bioactive Components against Diabetes – A Review of Recent Advances. *Trends in Food Science and Technology* **2017**, *68*, 1–13.

(213) Fan, L.; Cacicedo, J. M.; Ido, Y. Impaired Nicotinamide Adenine

Dinucleotide (NAD+) Metabolism in Diabetes and Diabetic Tissues: Implications for Nicotinamide-Related Compound Treatment. *Journal of Diabetes Investigation* **2020**, *11* (6), 1403–1419.

(214) Wang, X.; Zhang, Z. F.; Zheng, G. H.; Wang, A. M.; Sun, C. H.; Qin, S. P.; Zhuang, J.; Lu, J.; Ma, D. F.; Zheng, Y. L. The Inhibitory Effects of Purple Sweet Potato Color on Hepatic Inflammation Is Associated with Restoration of Nad+ Levels and Attenuation of Nlrp3 Inflammasome Activation in High-Fat-Diet-Treated Mice. *Molecules* **2017**, *22* (8).

(215) Chen, Y. F.; Shibu, M. A.; Fan, M. J.; Chen, M. C.; Viswanadha, V. P.; Lin, Y. L.; Lai, C. H.; Lin, K. H.; Ho, T. J.; Kuo, W. W.; Huang, C. Y. Purple Rice Anthocyanin Extract Protects Cardiac Function in STZ-Induced Diabetes Rat Hearts by Inhibiting Cardiac Hypertrophy and Fibrosis. *Journal of Nutritional Biochemistry* **2016**, *31*, 98–105.

(216) Vendrame, S.; Daugherty, A.; Kristo, A. S.; Riso, P.; Klimis-Zacas, D. Wild Blueberry (Vaccinium Angustifolium) Consumption Improves Inflammatory Status in the Obese Zucker Rat Model of the Metabolic Syndrome. *Journal of Nutritional Biochemistry* **2013**, *24* (8), 1508–1512.

(217) Guo, H. H.; Xia, M.; Zou, T. B.; Ling, W. H.; Zhong, R. M.; Zhang, W. G. Cyanidin 3-Glucoside Attenuates Obesity-Associated Insulin Resistance and Hepatic Steatosis in High-Fat Diet-Fed and Db/Db Mice via the Transcription Factor FoxO1. *Journal of Nutritional Biochemistry* **2012**, *23* (4), 349–360.

(218) Luo, Y.; Fang, J. L.; Yuan, K.; Jin, S. H.; Guo, Y. Ameliorative Effect of Purified Anthocyanin from Lycium Ruthenicum on Atherosclerosis in Rats through Synergistic Modulation of the Gut Microbiota and NF-KB/SREBP-2 Pathways. *Journal of Functional Foods* **2019**, *59* (December 2018), 223–233.

(219) Ruifeng Wang; Ibrahim Khalifa; Xia Du; Kaikai Li; Yujuan Xu; Chunmei Li. Effects of Anthocyanins on β-Lactoglobulin Glycoxidation: A Study of Mechanisms and Structure–Activity Relationship. *Food & Function* **2021**.

(220) Krga, I.; Milenkovic, D. Anthocyanins : From Sources and Bioavailability to Cardiovascular- Health Bene Fi Ts and Molecular Mechanisms of Action. *Journal of Agricultural and Food Chemistry* **2019**, *67*, 1771–1783.

(221) Zhang, Y.; Niu, F. X.; Sun, J.; Xu, F.; Yue, R. X. Purple Sweet Potato (Ipomoea Batatas L.) Color Alleviates High-Fat-Diet-Induced Obesity in SD Rat by Mediating Leptin's Effect and Attenuating Oxidative Stress. *Food Science and Biotechnology* **2015**, *24* (4), 1523–1532.

(222) Seymour, E. M.; Tanone, I. I.; Urcuyo-Llanes, D. E.; Lewis, S. K.; Kirakosyan, A.; Kondoleon, M. G.; Kaufman, P. B.; Bolling, S. F. Blueberry Intake Alters Skeletal Muscle and Adipose Tissue Peroxisome Proliferator-Activated Receptor Activity and Reduces Insulin Resistance in Obese Rats. *Journal of Medicinal Food* **2011**, *14* (12), 1511–1518.

(223) Sarikaphuti, A.; Nararatwanchai, T.; Hashiguchi, T.; Ito, T.; Thaworanunta, S.; Kikuchi, K.; Oyama, Y.; Maruyama, I.; Tancharoen, S. Preventive Effects of Morus Alba L. Anthocyanins on Diabetes in Zucker Diabetic Fatty Rats. *Experimental and Therapeutic Medicine* **2013**, *6* (3), 689–695.

(224) Grace, M. H.; Ribnicky, D. M.; Kuhn, P.; Poulev, A.; Logendra, S.; Yousef, G. G.; Raskin, I.; Lila, M. A. Hypoglycemic Activity of a Novel Anthocyanin-Rich Formulation from Lowbush Blueberry, Vaccinium Angustifolium Aiton. *Phytomedicine* **2009**, *16* (5), 406–415.

(225) Wu, T.; Qi, X.; Liu, Y.; Guo, J.; Zhu, R.; Chen, W.; Zheng, X.; Yu, T. Dietary Supplementation with Purified Mulberry (Morus Australis Poir) Anthocyanins Suppresses Body Weight Gain in High-Fat Diet Fed C57BL/6 Mice. *Food Chem* **2013**, *141* (1), 482–487.

(226) Singh, S.; Netticadan, T.; Dan Ramdath, D. Expression of Cardiac Insulin Signalling Genes and Proteins in Rats Fed a High-Sucrose Diet: Effect of

Bilberry Anthocyanin Extract. *Genes and Nutrition* **2016**, *11* (1).

(227) Tsuda, T.; Horio, F.; Uchida, K.; Aoki, H.; Osawa, T. Dietary Cyanidin 3-O-β-D-Glucoside-Rich Purple Corn Color Prevents Obesity and Ameliorates Hyperglycemia in Mice. *The Journal of Nutrition* **2003**, *133* (7), 2125–2130.

(228) Zhu, W.; Jia, Q.; Wang, Y.; Zhang, Y.; Xia, M. The Anthocyanin Cyanidin-3-O-β-Glucoside, a Flavonoid, Increases Hepatic Glutathione Synthesis and Protects Hepatocytes against Reactive Oxygen Species during Hyperglycemia: Involvement of a CAMP-PKA-Dependent Signaling Pathway. *Free Radical Biology and Medicine* **2012**, *52* (2), 314–327.

(229) Peng, C. H.; Liu, L. K.; Chuang, C. M.; Chyau, C. C.; Huang, C. N.; Wang, C. J. Mulberry Water Extracts Possess an Anti-Obesity Effect and Ability to Inhibit Hepatic Lipogenesis and Promote Lipolysis. *Journal of Agricultural and Food Chemistry* **2011**, *59* (6), 2663–2671.

(230) Qin, S.; Sun, D.; Mu, J.; Ma, D.; Tang, R.; Zheng, Y. Purple Sweet Potato Color Improves Hippocampal Insulin Resistance via Down-Regulating SOCS3 and Galectin-3 in High-Fat Diet Mice. *Behavioural Brain Research* **2019**, *359*, 370–377.

(231) Strugała, P.; Dzydzan, O.; Brodyak, I.; Kucharska, A. Z.; Kuropka, P.; Liuta, M.; Kaleta-Kuratewicz, K.; Przewodowska, A.; Michałowska, D.; Gabrielska, J.; Sybirna, N. Antidiabetic and Antioxidative Potential of the Blue Congo Variety of Purple Potato Extract in Streptozotocin-Induced Diabetic Rats. *Molecules* **2019**, *24* (17).

(232) Stull, A. J.; Cash, K. C.; Johnson, W. D.; Champagne, C. M.; Cefalu, W. T. Bioactives in Blueberries Improve Insulin Sensitivity in Obese, Insulin-Resistant Men and Women. *The Journal of Nutrition* **2010**, *140* (10), 1764–1768.

(233) Li, D.; Zhang, Y.; Liu, Y.; Sun, R.; Xia, M. Purified Anthocyanin Supplementation Reduces Dyslipidemia, Enhances Antioxidant Capacity, and Prevents Insulin Resistance in Diabetic Patients. *The Journal of Nutrition* **2015**, *145* (4), 742–748.

(234) Stote, K. S.; Wilson, M. M.; Hallenbeck, D.; Thomas, K.; Rourke, J. M.; Sweeney, M. I.; Gottschall-Pass, K. T.; Gosmanov, A. R. Effect of Blueberry Consumption on Cardiometabolic Health Parameters in Men with Type 2 Diabetes: An 8-Week, Double-Blind, Randomized, Placebo-Controlled Trial. *Current Developments in Nutrition* **2020**, No. 3, 1–10.

(235) Paquette, M.; Medina Larqué, A. S.; Weisnagel, S. J.; Desjardins, Y.; Marois, J.; Pilon, G.; Dudonné, S.; Marette, A.; Jacques, H. Strawberry and Cranberry Polyphenols Improve Insulin Sensitivity in Insulin-Resistant, Non-Diabetic Adults: A Parallel, Double-Blind, Controlled and Randomised Clinical Trial. *British Journal of Nutrition* **2017**, *117* (4), 519–531.

(236) Geografis, K. Blueberries Decrease Cardiovascular Risk FactorsinObese Menand Womenwith Metabolic Syndrome. **2011**, 1–33.

(237) Moazzen, H.; Alizadeh, M. Effects of Pomegranate Juice on Cardiovascular Risk Factors in Patients with Metabolic Syndrome: A Double-Blinded, Randomized Crossover Controlled Trial. *Plant Foods for Human Nutrition* **2017**, *72* (2), 126–133.

(238) de Mello, V. D. F.; Lankinen, M. A.; Lindström, J.; Puupponen-Pimiä, R.; Laaksonen, D. E.; Pihlajamäki, J.; Lehtonen, M.; Uusitupa, M.; Tuomilehto, J.; Kolehmainen, M.; Törrönen, R.; Hanhineva, K. Fasting Serum Hippuric Acid Is Elevated after Bilberry (Vaccinium Myrtillus) Consumption and Associates with Improvement of Fasting Glucose Levels and Insulin Secretion in Persons at High Risk of Developing Type 2 Diabetes. *Molecular Nutrition and Food Research* **2017**, *61* (9), 1–26.

(239) Alnajjar, M.; Kumar Barik, S.; Bestwick, C.; Campbell, F.; Cruickshank, M.; Farquharson, F.; Holtrop, G.; Horgan, G.; Louis, P.; Moar, K. M.; Russell, W. R.; Scobbie, L.; Hoggard, N. Anthocyanin-Enriched Bilberry Extract Attenuates Glycaemic Response in Overweight Volunteers

without Changes in Insulin. *Journal of Functional Foods* **2020**, *64* (September 2019), 103597.

(240) Edirisinghe, I.; Banaszewski, K.; Cappozzo, J.; Sandhya, K.; Ellis, C. L.; Tadapaneni, R.; Kappagoda, C. T.; Burton-Freeman, B. M. Strawberry Anthocyanin and Its Association with Postprandial Inflammation and Insulin. *British Journal of Nutrition* **2011**, *106* (6), 913–922.

(241) Scalbert, A.; Morand, C.; Manach, C.; Rémésy, C. Absorption and Metabolism of Polyphenols in the Gut and Impact on Health. *Biomedicine & Pharmacotherapy* **2002**, *56* (6), 276–282.

(242) Plumb, G. W.; Garcia-Conesa, M. T.; Kroon, P. A.; Rhodes, M.; Ridley, S.; Williamson, G. Metabolism of Chlorogenic Acid by Human Plasma, Liver, Intestine and Gut Microflora. *Journal of the Science of Food and Agriculture* **1999**, *79* (3), 390–392.

(243) Molan, A. L.; Liu, Z.; Plimmer, G. Evaluation of the Effect of Blackcurrant Products on Gut Microbiota and on Markers of Risk for Colon Cancer in Humans. *Phytotherapy Research* **2014**, *28* (3), 416–422.

(244) Pan, P.; Lam, V.; Salzman, N.; Huang, Y. W.; Yu, J.; Zhang, J.; Wang, L. S. Black Raspberries and Their Anthocyanin and Fiber Fractions Alter the Composition and Diversity of Gut Microbiota in F-344 Rats. *Nutrition and Cancer* **2017**, *69* (6), 943–951.

(245) Song, H.; Shen, X.; Zhou, Y.; Zheng, X. Black Rice Anthocyanins Alleviate Hyperlipidemia, Liver Steatosis and Insulin Resistance by Regulating Lipid Metabolism and Gut Microbiota in Obese Mice. *Food & Function* **2021**, *12* (20), 10160–10170.

(246) Petersen, C.; Wankhade, U. D.; Bharat, D.; Wong, K.; Mueller, J. E.; Chintapalli, S. V.; Piccolo, B. D.; Jalili, T.; Jia, Z.; Symons, J. D.; Shankar, K.; Anandh Babu, P. V. Dietary Supplementation with Strawberry Induces Marked Changes in the Composition and Functional Potential of the Gut Microbiome in Diabetic Mice. *Journal of Nutritional Biochemistry* **2019**, *66*, 63–69.

(247) Huang, F.; Zhao, R.; Xia, M.; Shen, G. X. Impact of Cyanidin-3-Glucoside on Gut Microbiota and Relationship with Metabolism and Inflammation in High Fat-High Sucrose Diet-Induced Insulin Resistant Mice. *Microorganisms* **2020**, *8* (8), 1–15.

(248) Su, H.; Xie, L.; Xu, Y.; Ke, H.; Bao, T.; Li, Y.; Chen, W. Pelargonidin-3- O-Glucoside Derived from Wild Raspberry Exerts Antihyperglycemic Effect by Inducing Autophagy and Modulating Gut Microbiota. *Journal of Agricultural and Food Chemistry* **2020**, *68* (46), 13025–13037.

(249) Zhang, X.; Yang, Y.; Wu, Z.; Weng, P. The Modulatory Effect of Anthocyanins from Purple Sweet Potato on Human Intestinal Microbiota in Vitro. *J Agric Food Chem* **2016**, *64* (12), 2582–2590.

(250) Sun, H.; Zhang, P.; Zhu, Y.; Lou, Q.; He, S. Antioxidant and Prebiotic Activity of Five Peonidin-Based Anthocyanins Extracted from Purple Sweet Potato (Ipomoea Batatas (L.) Lam.). *Scientific Reports* **2018**, *8* (1), 1–12.

(251) Overall, J.; Bonney, S. A.; Wilson, M.; Beermann, A.; Grace, M. H.; Esposito, D.; Lila, M. A.; Komarnytsky, S. Metabolic Effects of Berries with Structurally Diverse Anthocyanins. *International Journal of Molecular Sciences* **2017**, *18* (2).

(252) Nicholson, J. K.; Holmes, E.; Lindon, J. C. *Metabonomics and Metabolomics Techniques and Their Applications in Mammalian Systems*; . https://doi.org/10.1016/B978-044452841-4/50002-3; Elsevier BV., 2007.

(253) Simó, C., Cifuentes, A., & García-Cañas, V. *Uncovering Informative Content in Metabolomics Data : From Pre-Processing of 1H NMR Spectra to Biomarkers Discovery in Multifactorial Designs*; 2014.

(254) Vailati-Riboni, M.; Palombo, V.; Loor, J. J. What Are Omics Sciences? *Periparturient Diseases of Dairy Cows: A Systems Biology Approach* **2017**, 1–7.

(255) Wilson, D. M.; Burlingame, A. L.; Cronholm, T.; Sjövall, J. Deuterium and Carbon-13 Tracer Studies of Ethanol Metabolism in the Rat by 2H, 1H-Decoupled 13C Nuclear Magnetic Resonance. *Biochemical and Biophysical Research Communications* **1974**, *56* (3), 828–835.

(256) Euceda, L. R.; Giskeødegård, G. F.; Bathen, T. F. Preprocessing of NMR Metabolomics Data. *http://dx.doi.org/10.3109/00365513.2014.1003593* **2015**, *75* (3), 193–203.

(257) Metz, K. R.; Lam, M. M.; Webb, A. G. Reference Deconvolution: A Simple and Effective Method for Resolution Enhancement in Nuclear Magnetic Resonance Spectroscopy. *Concepts in Magnetic Resonance* **2000**, *12* (1), 21–42.

(258) Emwas, A. H.; Saccenti, E.; Gao, X.; McKay, R. T.; dos Santos, V. A. P. M.; Roy, R.; Wishart, D. S. Recommended Strategies for Spectral Processing and Post-Processing of 1D1H-NMR Data of Biofluids with a Particular Focus on Urine. *Metabolomics* **2018**, *14* (3), 1–23.

(259) Trygg, J.; Holmes, E.; Lundstedt, T. Chemometrics in Metabonomics. *Journal of Proteome Research* **2007**, *6* (2), 469–479.

(260) Weljie, A. M.; Newton, J.; Mercier, P.; Carlson, E.; Slupsky, C. M. Targeted Pofiling: Quantitative Analysis Of1H NMR Metabolomics Data. *Analytical Chemistry* **2006**, *78* (13), 4430–4442.

(261) Bjerrum, J. T. veiten. *Metabonomics: Methods and Protocols: Preface*; 2015; Vol. 1277.

(262) Lusczek, E. R.; Lexcen, D. R.; Witowski, N. E.; Mulier, K. E.; Beilman, G. Urinary Metabolic Network Analysis in Trauma, Hemorrhagic Shock, and Resuscitation. *Metabolomics* **2013**, *9* (1), 223–235.

(263) Hochrein, J.; Zacharias, H. U.; Taruttis, F.; Samol, C.; Engelmann, J. C.; Spang, R.; Oefner, P. J.; Gronwald, W. Data Normalization of 1H NMR Metabolite Fingerprinting Data Sets in the Presence of Unbalanced Metabolite Regulation. *Journal of Proteome Research* **2015**, *14* (8), 3217–3228.

(264) Kohl, S. M.; Klein, M. S.; Hochrein, J.; Oefner, P. J.; Spang, R.; Gronwald, W. State-of-the Art Data Normalization Methods Improve NMR-Based Metabolomic Analysis. *Metabolomics* **2012**, *8*, 146–160.

(265) Dieterle, F.; Ross, A.; Senn, H. Probabilistic Quotient Normalization as Robust Method to Account for Dilution of Complex Biological Mixtures . Application in 1 H NMR Metabonomics. *Analytical Chemistry* **2006**, *78*, 4281–4290.

(266) Posma, J. M. *Metabolic Profiling: Methods and Protocols*; . https://doi.org/10.1016/B978-0-12-809633-8.20254-9; 2018; Vol. 1–3.

(267) van den Berg, R. A.; Hoefsloot, H. C. J.; Westerhuis, J. A.; Smilde, A. K.; van der Werf, M. J. Centering, Scaling, and Transformations: Improving the Biological Information Content of Metabolomics Data. *BMC Genomics* **2006**, *7*, 1–15.

(268) Dudzik, D.; Zorawski, M.; Skotnicki, M.; Zarzycki, W.; García, A.; Angulo, S.; Lorenzo, M. P.; Barbas, C.; Ramos, M. P. GC–MS Based Gestational Diabetes Mellitus Longitudinal Study: Identification of 2-and 3-Hydroxybutyrate as Potential Prognostic Biomarkers. *Journal of Pharmaceutical and Biomedical Analysis* **2017**, *144*.

(269) Eriksson, I. Multi- and Megavariate Data Analysis Principles and Spplications. *Journal of Chemometrics* **2002**, *16* (5), 261–262.

(270) Westerhuis, J. A.; Hoefsloot, H. C. J.; Smit, S.; Vis, D. J.; Smilde, A. K.; Velzen, E. J. J.; Duijnhoven, J. P. M.; Dorsten, F. A. Assessment of PLSDA Cross Validation. *Metabolomics* **2008**, *4* (1), 81–89.

(271) Casamassimi, A.; Federico, A.; Rienzo, M.; Esposito, S.; Ciccodicola, A. Transcriptome Profiling in Human Diseases: New Advances and Perspectives. *International Journal of Molecular Sciences* **2017**, *18*, 1652.

(272) Lowe, R.; Shirley, N.; Bleackley, M.; Dolan, S.; Shafee, T. Transcriptomics Technologies. *PLoS Computational Biology* **2017**, *13* (5), 1–23.

(273) Oikonomopoulos, S.; Wang, Y. C.; Djambazian, H.; Badescu, D.; Ragoussis, J. Benchmarking of the Oxford Nanopore MinION Sequencing for Quantitative and Qualitative Assessment of CDNA Populations. *Scientific Reports* **2016**, *6*, 31602.

(274) Li, R.; Ren, X.; Ding, Q.; Bi, Y.; Xie, D.; Zhao, Z. Direct Full-Length RNA Sequencing Reveals Unexpected Transcriptome Complexity during Caenorhabditis Elegans Development. *Genome Research* **2020**, *30* (2), 287–298.

(275) Dong, X.; Tian, L.; Gouil, Q.; Kariyawasam, H.; Su, S.; De Paoli-Iseppi, R.; David, Y.; Prawer, J.; Clark, M. B.; Breslin, K.; Iminitoff, M.; Blewitt, M. E.; Law, C. W.; Ritchie, M. E. The Long and the Short of It: Unlocking Nanopore Long-Read RNA Sequencing Data with Short-Read Tools. *bioRxiv* **2020**, *6*, 1–13.

(276) Müller, C. A.; Boemo, M. A.; Spingardi, P.; Kessler, B. M.; Kriaucionis, S.; Simpson, J. T.; Nieduszynski, C. A. Capturing the Dynamics of Genome Replication on Individual Ultra-Long Nanopore Sequence Reads. *Nature Methods* **2019**, *16* (5), 429–436.

(277) Player, R.; Verratti, K.; Staab, A.; Bradburne, C.; Grady, S.; Goodwin, B.; Sozhamannan, S. Comparison of the Performance of an Amplicon Sequencing Assay Based on Oxford Nanopore Technology to Real-Time PCR Assays for Detecting Bacterial Biodefense Pathogens. *BMC Genomics* **2020**, *21* (1), 1–21.

(278) Goto, M. K. S. KEGG: Kyoto Encyclopedia of Genes and Genomes. *Nucleic Acids Research* **2000**, *28* (1), 27–30.

(279) Harris, M. A.; Deegan, J. I.; Ireland, A.; Lomax, J.; Ashburner, M.; Tweedie, S.; Carbon, S.; Lewis, S.; Mungall, C.; Day-Richter, J.; Eilbeck, K.; Blake, J. A.; Bult, C.; Diehl, A. D.; Dolan, M.; Drabkin, H.; Eppig, J. T.; Hill, D. P.; Ni, L.; Ringwald, M.; Balakrishnan, R.; Binkley, G.; Cherry, J. M.; Christie, K. R.; Costanzo, M. C.; Dong, Q.; Engel, S. R.; Fisk, D. G.; Hirschman, J. E.; Hitz, B. C.; Hong, E. L.; Krieger, C. J.; Miyasato, S. R.; Nash, R. S.; Park, J.; Skrzypek, M. S.; Weng, S.; Wong, E. D.; Zhu, K. K.; Botstein, D.; Dolinski, K.; Livstone, M. S.; Oughtred, R.; Berardini, T.; Li, D.; Rhee, S. Y.; Apweiler, R.; Barrell, D.; Camon, E.; Dimmer, E.; Huntley, R.; Mulder, N.; Khodiyar, V. K.; Lovering, R. C.; Povey, S.; Chisholm, R.; Fey, P.; Gaudet, P.; Kibbe, W.; Kishore, R.; Schwarz, E. M.; Sternberg, P.; Van Auken, K.; Giglio, M. G.; Hannick, L.; Wortman, J.; Aslett, M.; Berriman, M.; Wood, V.; Jacob, H.; Lauledерkind, S.; Petri, V.; Shimoyama, M.; Smith, J.; Twigger, S.; Jaiswal, P.; Seigfried, T.; Howe, D.; Westerfield, M.; Collmer, C.; Torto-Alalibo, T.; Feltrin, E.; Valle, G.; Bromberg, S.; Burgess, S.; McCarthy, F. The Gene Ontology Project in 2008. *Nucleic Acids Research* **2008**, *36* (SUPPL. 1), 440–444.

(280) Zhang, B.; Kirov, S.; Snoddy, J. WebGestalt: An Integrated System for Exploring Gene Sets in Various Biological Contexts. *Nucleic Acids Research* **2005**, *33* (SUPPL. 2), 741–748.

(281) Handelsman, J.; Rondon, M. R.; Brady, S. F.; Clardy, J.; Goodman, R. M. Molecular Biological Access to the Chemistry of Unknown Soil Microbes: A New Frontier for Natural Products. *Chemistry and Biology* **1998**, *5* (10).

(282) Jokioja, J.; Linderborg, K. M.; Kortesniemi, M.; Nuora, A.; Heinonen, J.; Sainio, T.; Viitanen, M.; Kallio, H.; Yang, B. Anthocyanin-Rich Extract from Purple Potatoes Decreases Postprandial Glycemic Response and Affects Inflammation Markers in Healthy Men. *Food Chemistry* **2019**, *310*, 1–13.

(283) Álvarez-Cilleros, D.; Ramos, S.; López-Oliva, M. E.; Escrivá, F.; Álvarez, C.; Fernández-Millán, E.; Martín, M. Á. Cocoa Diet Modulates Gut Microbiota Composition and Improves Intestinal Health in Zucker Diabetic Rats. *Food Research International* **2020**, *132*, e109058.

(284) Improved Metabolic Status and Insulin Sensitivity in Obese Fatty (Fa/Fa) Zucker Rats and Zucker Diabetic Fatty (ZDF) Rats Treated with the Thiazolidinedione, MCC-555. *British*

Journal of Pharmacology **1998**, *125* (8), 1708–1714.

(285) AB, A. Sample Size Calculation for Animal Studies Using Degree of Freedom (E); an Easy and Statistically Defined Approach for Metabolomics and Genetic Research. *Current Trends in Biomedical Engineering & Biosciences* **2017**, *10* (2).

(286) Savorani, F.; Tomasi, G.; Engelsen, S. B. Icoshift: A Versatile Tool for the Rapid Alignment of 1D NMR Spectra. *Journal of Magnetic Resonance* **2010**, *202* (2), 190–202.

(287) Li, H. Minimap2: Pairwise Alignment for Nucleotide Sequences. *Bioinformatics* **2018**, *34*, 3094–3100.

(288) Robinson, M. D.; McCarthy, D. J.; Smyth, G. K. EdgeR: A Bioconductor Package for Differential Expression Analysis of Digital Gene Expression Data. *Bioinformatics* **2009**, *26* (1), 139–140.

(289) Safari-Alighiarloo, N.; Taghizadeh, M.; Rezaei-Tavirani, M.; Goliaei, B.; Peyvandi, A. A. Protein-Protein Interaction Networks (PPI) and Complex Diseases. *Gastroenterology and Hepatology from Bed to Bench* **2014**, *7* (1), 17–31.

(290) Bindea, G.; Mlecnik, B.; Hackl, H.; Charoentong, P.; Tosolini, M.; Kirilovsky, A.; Fridman, W. H.; Pagès, F.; Trajanoski, Z.; Galon, J. ClueGO: A Cytoscape Plug-in to Decipher Functionally Grouped Gene Ontology and Pathway Annotation Networks. *Bioinformatics* **2009**, *25*, 1091–1093.

(291) Cao, J.; Hu, Y.; Liu, F.; Wang, Y.; Bi, Y.; Lv, N.; Li, J.; Zhu, B.; Gao, G. F. Metagenomic Analysis Reveals the Microbiome and Resistome in Migratory Birds. *Microbiome* **2020**, *8* (1), 1–18.

(292) Luo, R.; Liu, B.; Xie, Y.; Li, Z.; Huang, W.; Yuan, J.; He, G.; Chen, Y.; Pan, Q.; Liu, Y.; Tang, J.; Wu, G.; Zhang, H.; Shi, Y.; Liu, Y.; Yu, C.; Wang, B.; Lu, Y.; Han, C.; Cheung, D. W.; Yiu, S.; Peng, S.; Xiaoqian, Z.; Liu, G.; Liao, X.; Li, Y.; Yang, H.; Wang, J.; Lam, T.; Wang, J. SOAPdenovo2 : An Empirically Improved Memory-Efficient Short-Read de Novo Assembler. *GigaScience* **2012**, *1* (18), 1–6.

(293) Friedman, S. L.; Neuschwander-Tetri, B. A.; Rinella, M.; Sanyal, A. J. Mechanisms of NAFLD Development and Therapeutic Strategies. *Nature Medicine* **2018**, *24* (7), 908–922.

(294) Jokioja, J. Anthocyanin-Rich Extract from Purple Potatoes Decreases Postprandial Glycemic Response and Affects Inflammation Markers in Healthy Men. *Food Chemistry* **2019**, *310*, 1–13.

(295) Linderborg, K. M.; Salo, J. E.; Kalpio, M.; Vuorinen, A. L.; Kortesniemi, M.; Griinari, M.; Viitanen, M.; Yang, B. Comparison of the Postprandial Effects of Purple- Fleshed and Yellow-Fleshed Potatoes in Healthy Males with Chemical Characterization of the Potato Meals. **2016**, *67* (5), 581–591.

(296) Guo, X.; Li, H.; Xu, H.; Woo, S.; Dong, H.; Lu, F.; Lange, A. J.; Wu, C. Glycolysis in the Control of Blood Glucose Homeostasis. *Acta Pharmaceutica Sinica B* **2012**, *2* (4), 358–367.

(297) Shulman, G. I. Unraveling the Cellular Mechanism of Insulin Resistance in Humans: New Insights from Magnetic Resonance Spectroscopy. *Physiology* **2004**, *19* (4), 183–190.

(298) Crawford, S. O.; Hoogeveen, R. C.; Brancati, F. L.; Astor, B. C.; Ballantyne, C. M.; Schmidt, M. I.; Young, J. H. Association of Blood Lactate with Type 2 Diabetes: The Atherosclerosis Risk in Communities Carotid MRI Study. *International Journal of Epidemiology* **2010**, *39*, 1647–1655.

(299) Lü, L.; Li, J.; Yew, D. T.; Rudd, J. A.; Mak, Y. T. Oxidative Stress on the Astrocytes in Culture Derived from a Senescence Accelerated Mouse Strain. *Neurochemistry International* **2008**, *52* (1–2), 282–289.

(300) Yang, H.; Pang, W.; Lu, H.; Cheng, D.; Yan, X.; Cheng, Y.; Jiang, Y. Comparison of Metabolic Profiling of Cyanidin-3-O-Galactoside and Extracts from Blueberry in Aged Mice. *Journal of Agricultural and Food Chemistry* **2011**, *59* (5), 2069–2076.

(301) Rawat, A.; Misra, G.; Saxena, M.; Tripathi, S.; Dubey, D.; Saxena, S.; Aggarwal, A.; Gupta, V.; Khan, M. Y.

1H NMR Based Serum Metabolic Profiling Reveals Differentiating Biomarkers in Patients with Diabetes and Diabetes-Related Complication. *Diabetes & Metabolic Syndrome: Clinical Research & Reviews* **2019**, *13* (1), 290–298.

(302) Ruan, Z.; Yang, Y.; Zhou, Y.; Wen, Y.; Ding, S.; Liu, G.; Wu, X.; Liao, P.; Deng, Z.; Assaad, H.; Wu, G.; Yin, Y. Metabolomic Analysis of Amino Acid and Energy Metabolism in Rats Supplemented with Chlorogenic Acid. *Amino Acids* **2014**, *46*, 2219–2229.

(303) Mahendran, Y.; Cederberg, H.; Vangipurapu, J.; Kangas, A. J.; Soininen, P.; Kuusisto, J.; Uusitupa, M.; Ala-Korpela, M.; Laakso, M. Glycerol and Fatty Acids in Serum Predict the Development of Hyperglycemia and Type 2 Diabetes in Finnish Men. *Diabetes Care* **2013**, *36* (11), 3732–3738.

(304) Hatting, M.; Tavares, C. D. J.; Sharabi, K.; Rines, A. K.; Puigserver, P. Insulin Regulation of Gluconeogenesis. *Annals of the New York Academy of Sciences* **2018**, *1411* (1), 21–35.

(305) Jawad, A. H.; Ibrahim, A. E.; Alsayed, R.; Hallab, Z. S.; Al-qaisi, Z. Study the Impact of Glucose-6-Phosphatase Activity in Type 2 Diabetic Patients and Non Diabetic Counterparts. *Preprints* **2016**, *137* (10), 1–6.

(306) Kalemba, K. M.; Wang, Y.; Xu, H.; Chiles, E.; McMillin, S. M.; Kwon, H.; Su, X.; Wondisford, F. E. Glycerol Induces G6pc in Primary Mouse Hepatocytes and Is the Preferred Substrate for Gluconeogenesis Both in Vitro and in Vivo. *Journal of Biological Chemistry* **2019**, *294* (48), 18017–18028.

(307) Hemmerle, H.; Burger, H. J.; Below, P.; Schubert, G.; Rippel, R.; Schindler, P. W.; Paulus, E.; Herling, A. W. Chlorogenic Acid and Synthetic Chlorogenic Acid Derivatives: Novel Inhibitors of Hepatic Glucose-6-Phosphate Translocase. *Journal of Medicinal Chemistry* **1997**, *40* (2), 137–145.

(308) Sakamoto, K.; Holman, G. D. Emerging Role for AS160/TBC1D4 and TBC1D1 in the Regulation of GLUT4 Traffic. *American Journal of Physiology - Endocrinology and Metabolism* **2008**, *295* (1), 29–37.

(309) Szekeres, F.; Chadt, A.; Tom, R. Z.; Deshmukh, A. S.; Chibalin, A. V.; Björnholm, M.; Al-Hasani, H.; Zierath, J. R. The Rab-GTPase-Activating Protein TBC1D1 Regulates Skeletal Muscle Glucose Metabolism. *American Journal of Physiology - Endocrinology and Metabolism* **2012**, *303* (4), 524–533.

(310) Chen, L.; Chen, Q.; Xie, B.; Quan, C.; Sheng, Y.; Zhu, S.; Rong, P.; Zhou, S.; Sakamoto, K.; MacKintosh, C.; Wang, H. Y.; Chen, S. Disruption of the AMPK-TBC1D1 Nexus Increases Lipogenic Gene Expression and Causes Obesity in Mice via Promoting IGF1 Secretion. *Proceedings of the National Academy of Sciences of the United States of America* **2016**, *113* (26), 7219–7224.

(311) Lian, K.; Du, C.; Liu, Y.; Zhu, D.; Yan, W.; Zhang, H.; Hong, Z.; Liu, P.; Zhang, L.; Pei, H.; Zhang, J.; Gao, C.; Xin, C.; Cheng, H.; Xiong, L.; Tao, L. Impaired Adiponectin Signaling Contributes to Disturbed Catabolism of Branched-Chain Amino Acids in Diabetic Mice. *Diabetes* **2015**, *64* (2), 49–59.

(312) Wijekoon, E.; Skinner, C.; Brosnan, M.; Brosnan, J. Amino Acid Metabolism in the Zucker Diabetic Fatty Rat: Effects of Insulin Resistance and of Type 2 Diabetes. *Can J Physiol Pharmacol* **2004**, *82* (7), 506–514.

(313) Denis McGarry, J. Dysregulation of Fatty Acid Metabolism in the Etiology of Type 2 Diabetes. *Diabetes* **2002**, *51* (1), 7–18.

(314) Lake, A. D.; Novak, P.; Shipkova, P.; Aranibar, N.; Robertson, D. G.; Reily, M. D.; Lehman-Mckeeman, L. D.; Vaillancourt, R. R.; Cherrington, N. J. Branched Chain Amino Acid Metabolism Profiles in Progressive Human Nonalcoholic Fatty Liver Disease. *Amino Acids* **2015**, *47* (3), 603–615.

(315) Roberts, L. D.; Koulman, A.; Griffi, J. L. Towards Metabolic Biomarkers of Insulin Resistance and Type 2 Diabetes: Progress from the Metabolome.

diabetes-endocrinology **2014**, *2* (1), 65–75.

(316) Chen, S.; Akter, S.; Kuwahara, K.; Matsushita, Y.; Nakagawa, T.; Konishi, M.; Honda, T.; Yamamoto, S.; Hayashi, T.; Noda, M.; Mizoue, T. Serum Amino Acid Profiles and Risk of Type 2 Diabetes among Japanese Adults in the Hitachi Health Study. *Scientific Reports* **2019**, *9* (1), 1–9.

(317) Comar, J. F.; Oliveira, D. S. De; Bracht, L.; Kemmelmeier, F. S.; Peralta, R. M.; Bracht, A. The Metabolic Responses to L-Glutamine of Livers from Rats with Diabetes Types 1 and 2. *PLoS ONE* **2016**, *11* (8), 1–16.

(318) Greenfield, J. R.; Sadaf Farooqi, I.; Keogh, J. M.; Henning, E.; Habib, A. M.; Blackwood, A.; Reimann, F.; Holst, J. J.; Gribble, F. M. Oral Glutamine Increases Circulating GLP-1, Glucagon and Insulin Levels in Lean, Obese and Type 2 Diabetic Subjects. *The American Journal Of Clinical Nutrition* **2015**, *89* (1), 106–113.

(319) Kwak, H. C.; Kim, Y. M.; Oh, S. J.; Kim, S. K. Sulfur Amino Acid Metabolism in Zucker Diabetic Fatty Rats. *Biochemical Pharmacology* **2015**, *96* (3), 256–266.

(320) Magnusson, M.; Wang, T. J.; Clish, C.; Engström, G.; Nilsson, P.; Gerszten, R. E.; Melander, O. Dimethylglycine Deficiency and the Development of Diabetes. *Diabetes* **2015**, *64* (8), 3010–3016.

(321) Su, H.; Bao, T.; Xie, L.; Xu, Y.; Chen, W. Transcriptome Profiling Reveals the Antihyperglycemic Mechanism of Pelargonidin-3-O-Glucoside Extracted from Wild Raspberry. *Journal of Functional Foods* **2020**, *64*, 103657.

(322) Pass, G. J.; Becker, W.; Kluge, R.; Linnartz, K.; Plum, L.; Giesen, K.; Joost, H. G. Effect of Hyperinsulinemia and Type 2 Diabetes-like Hyperglycemia on Expression of Hepatic Cytochrome P450 and Glutathione S-Transferase Isoforms in a New Zealand Obese-Derived Mouse Backcross Population. *Journal of Pharmacology and Experimental Therapeutics* **2002**, *302* (2), 442–450.

(323) Meng, Y.; Guan, Y.; Zhang, W.; Wu, Y. E.; Jia, H.; Zhang, Y.; Zhang, X.; Du, H.; Wang, X. RNA-Seq Analysis of the Hypothalamic Transcriptome Reveals the Networks Regulating Physiopathological Progress in the Diabetic GK Rat. *Scientific Reports* **2016**, *6*, 34138.

(324) Ohtsubo, K.; Takamatsu, S.; Minowa, M. T.; Yoshida, A.; Takeuchi, M.; Marth, J. D. Dietary and Genetic Control of Glucose Transporter 2 Glycosylation Promotes Insulin Secretion in Suppressing Diabetes. *Cell* **2005**, *123*, 1307–1321.

(325) Rudman, N.; Gornik, O.; Lauc, G. Altered N-Glycosylation Profiles as Potential Biomarkers and Drug Targets in Diabetes. *FEBS Letters* **2019**, *593*, 1598–1615.

(326) Kim, J. K.; Fillmore, J. J.; Chen, Y.; Yu, C.; Moore, I. K.; Pypaert, M.; Lutz, E. P.; Kako, Y.; Velez-Carrasco, W.; Goldberg, I. J.; Breslow, J. L.; Shulman, G. I. Tissue-Specific Overexpression of Lipoprotein Lipase Causes Tissue-Specific Insulin Resistance. *Proceedings of the National Academy of Sciences of the United States of America* **2001**, *98*, 7522–7527.

(327) Shen, N.; Jiang, S.; Lu, J. M.; Yu, X.; Lai, S. S.; Zhang, J. Z.; Zhang, J. L.; Tao, W. W.; Wang, X. X.; Xu, N.; Xue, B.; Li, C. J. The Constitutive Activation of Egr-1/C/Ebpa Mediates the Development of Type 2 Diabetes Mellitus by Enhancing Hepatic Gluconeogenesis. *American Journal of Pathology* **2015**, *185* (2), 513–523.

(328) Summers, S. A.; Nelson, D. H. A Role for Sphingolipids in Producing the Common Features of Type 2 Diabetes, Metabolic Syndrome X, and Cushing's Syndrome. *Diabetes* **2005**, *54* (3), 591–602.

(329) Shimabukuro, M.; Zhou, Y.-T.; Levi, M.; Unger, R. H. Fatty Acid-Induced β Cell Apoptosis: A Link between Obesity and Diabetes. *Proceedings of the National Academy of Sciences* **1998**, *95* (5), 2498–2502.

(330) Hannun, Y. A.; Obeid, L. M. The Ceramide-Centric Universe of Lipid-Mediated Cell Regulation: Stress

Encounters of the Lipid Kind. *Journal of Biological Chemistry* **2002**, *277* (29), 25847–25850.

(331) Futerman, A. H.; Hannun, Y. A. The Complex Life of Simple Sphingolipids. *EMBO reports* **2004**, *5* (8), 777–782.

(332) Samad, F.; Hester, K. D.; Yang, G.; Hannun, Y. A.; Bielawski, J. Altered Adipose and Plasma Sphingolipid Metabolism in Obesity: A Potential Mechanism for Cardiovascular and Metabolic Risk. *Diabetes* **2006**, *55* (9), 2579–2587.

(333) Xiao, X.; Song, B. SREBP : A Novel Therapeutic Target The Activation Process of SREBPs The Effects of Insulin on SREBPs. *Acta Biochim Biophys Sin* **2013**, *45* (1), 2–10.

(334) Taniguchi, K.; Xia, L.; Goldberg, H. J.; Lee, K. W. K.; Shah, A.; Stavar, L.; Masson, E. A. Y.; Momen, A.; Shikatani, E. A.; John, R.; Husain, M.; Fantus, I. G. Inhibition of Src Kinase Blocks High Glucose-Induced EGFR Transactivation and Collagen Synthesis in Mesangial Cells and Prevents Diabetic Nephropathy in Mice. *Diabetes* **2013**, *62*, 3874–3886.

(335) Beisswenger, P. Glyceraldehyde-3-Phosphate Dehydrogenase Activity as an Independent Modifier of Methylglyoxal Levels in Diabetes. *Biochimica et Biophysica Acta (BBA) - Molecular Basis of Disease* **2002**, *1637* (1), 98–106.

(336) Hess, J.; Angel, P.; Schorpp-Kistner, M. AP-1 Subunits: Quarrel and Harmony among Siblings. *Journal of Cell Science* **2004**, *117*, 5965–5973.

(337) Ndisang, J. F.; Lane, N.; Jadhav, A. The Heme Oxygenase System Abates Hyperglycemia in Zucker Diabetic Fatty Rats by Potentiating Insulin-Sensitizing Pathways. *Endocrinology* **2009**, *150*, 2098–2108.

(338) Kaneto, H.; Nakatani, Y.; Kawamori, D.; Miyatsuka, T.; Matsuoka, T. A.; Matsuhisa, M.; Yamasaki, Y. Role of Oxidative Stress, Endoplasmic Reticulum Stress, and c-Jun N-Terminal Kinase in Pancreatic β-Cell Dysfunction and Insulin Resistance. *International Journal of Biochemistry and Cell Biology* **2005**, *37*, 1595–1608.

(339) Limtrakul, P.; Yodkeeree, S.; Pitchakarn, P.; Punfa, W. Suppression of Inflammatory Responses by Black Rice Extract in RAW 264.7 Macrophage Cells via Downregulation of NF-KB and AP-1 Signaling Pathways. *Asian Pacific Journal of Cancer Prevention* **2015**, *16* (10), 4277–4283.

(340) Jiang, T.; Zhou, J.; Liu, W.; Tao, W.; He, J.; Jin, W.; Guo, H.; Yang, N.; Li, Y. The Anti-Inflammatory Potential of Protein-Bound Anthocyanin Compounds from Purple Sweet Potato in LPS-Induced RAW264.7 Macrophages. *Food Research International* **2020**, *137*, 109647.

(341) Li, L.; Wang, L.; Wu, Z.; Yao, L.; Wu, Y.; Huang, L.; Liu, K.; Zhou, X.; Gou, D. Anthocyanin-Rich Fractions from Red Raspberries Attenuate Inflammation in Both RAW264.7 Macrophages and a Mouse Model of Colitis. *Scientific Reports 2014 4:1* **2014**, *4* (1), 1–11.

(342) Jawi, I. M.; Indrayani, A. W.; Sutirta-Yasa, I. W. P. Aqueous Extract of Balinese Purple Sweet Potato (Ipomoea Batatas l.) Prevents Oxidative Stress and Decreases Blood Interleukin-1 in Hypercholesterolemic Rabbits. *Bali Medical Journal* **2015**, *4* (1), 37–40.

(343) Lee, S.; Keirsey, K. I.; Kirkland, R.; Grunewald, Z. I.; Fischer, J. G.; de La Serre, C. B. Blueberry Supplementation Influences the Gut Microbiota, Inflammation, and Insulin Resistance in High-Fat-Diet-Fed Rats. *Journal of Nutrition* **2018**, *148* (2), 209–219.

(344) Brahe, L. K.; Le Chatelier, E.; Prifti, E.; Pons, N.; Kennedy, S.; Hansen, T.; Pedersen, O.; Astrup, A.; Ehrlich, S. D.; Larsen, L. H. Specific Gut Microbiota Features and Metabolic Markers in Postmenopausal Women with Obesity. *Nutrition and Diabetes* **2015**, *5*, e159.

(345) Naito, Y.; Uchiyama, K.; Takagi, T. A Nexttgeneration Beneficial Microbe: Akkermansia Muciniphila. *J. Clin. Biochem. Nutr* **2018**, *63* (1), 33–35.

(346) Wong, V. W. S.; Tse, C. H.; Lam, T. T. Y.; Wong, G. L. H.; Chim, A. M. L.; Chu, W. C. W.; Yeung, D. K. W.; Law, P. T. W.; Kwan, H. S.; Yu, J.; Sung, J. J. Y.; Chan, H. L. Y. Molecular Characterization of the Fecal Microbiota

in Patients with Nonalcoholic Steatohepatitis - A Longitudinal Study. *PLoS ONE* **2013**, *8* (4), 1–11.

(347) Liu, X.; Zeng, B.; Zhang, J.; Li, W.; Mou, F.; Wang, H.; Zou, Q.; Zhong, B.; Wu, L.; Wei, H.; Fang, Y. Role of the Gut Microbiome in Modulating Arthritis Progression in Mice. *Scientific Reports* **2016**, *6* (4), 1–11.

(348) Forslund, K.; Hildebrand, F.; Nielsen, T.; Falony, G.; Le Chatelier, E.; Sunagawa, S.; Prifti, E.; Vieira-Silva, S.; Gudmundsdottir, V.; Krogh Pedersen, H.; Arumugam, M.; Kristiansen, K.; Yvonne Voigt, A.; Vestergaard, H.; Hercog, R.; Igor Costea, P.; Roat Kultima, J.; Li, J.; Jørgensen, T.; Levenez, F.; Dore, J.; Bjørn Nielsen, H.; Brunak, S.; Raes, J.; Hansen, T.; Wang, J.; Dusko Ehrlich, S.; Bork, P.; Pedersen, O. Disentangling Type 2 Diabetes and Metformin Treatment Signatures in the Human Gut Microbiota. *Nature* **2015**, *528* (7581), 262–266.

(349) De Vadder, F.; Kovatcheva-Datchary, P.; Zitoun, C.; Duchampt, A.; Bäckhed, F.; Mithieux, G. Microbiota-Produced Succinate Improves Glucose Homeostasis via Intestinal Gluconeogenesis. *Cell Metabolism* **2016**, *24* (1), 151–157.

(350) Deaver, J. A.; Eum, S. Y.; Toborek, M. Circadian Disruption Changes Gut Microbiome Taxa and Functional Gene Composition. *Frontiers in Microbiology* **2018**, *9* (4), 1–9.

(351) Zuo, K.; Li, J.; Xu, Q.; Hu, C.; Gao, Y.; Chen, M.; Hu, R.; Liu, Y.; Chi, H.; Yin, Q.; Cao, Y.; Wang, P.; Qin, Y.; Liu, X.; Zhong, J.; Cai, J.; Li, K.; Yang, X. Dysbiotic Gut Microbes May Contribute to Hypertension by Limiting Vitamin D Production. *Clinical Cardiology* **2019**, *42* (8), 710–719.

(352) Qin, J.; Li, Y.; Cai, Z.; Li, S.; Zhu, J.; Zhang, F.; Liang, S.; Zhang, W.; Guan, Y.; Shen, D.; Peng, Y.; Zhang, D.; Jie, Z.; Wu, W.; Qin, Y.; Xue, W.; Li, J.; Han, L.; Lu, D.; Wu, P.; Dai, Y.; Sun, X.; Li, Z.; Tang, A.; Zhong, S.; Li, X.; Chen, W.; Xu, R.; Wang, M.; Feng, Q.; Gong, M.; Yu, J.; Zhang, Y.; Zhang, M.; Hansen, T.; Sanchez, G.; Raes, J.; Falony, G.; Okuda, S.; Almeida, M.; LeChatelier, E.; Renault, P.; Pons, N.; Batto, J.-M.; Zhang, Z.; Chen, H.; Yang, R.; Zheng, W.; Li, S.; Yang, H.; Wang, J.; Ehrlich, S. D.; Nielsen, R.; Pedersen, O.; Kristiansen, K.; Wang, J. A Metagenome-Wide Association Study of Gut Microbiota in Type 2 Diabetes. *Nature* **2012**, *490* (7418), 55–60.

(353) Zhang, X.; Chen, Y.; Zhu, J.; Zhang, M.; Ho, C.-T.; Huang, Q.; Cao, J. Metagenomics Analysis of Gut Microbiota in a High Fat Diet–Induced Obesity Mouse Model Fed with (−)-Epigallocatechin 3-O-(3-O-Methyl) Gallate (EGCG3″Me). *Molecular Nutrition & Food Research* **2018**, *62* (13), 1800274.

(354) Teresa, F.; Ronald, B.; Ye, Y.; Huan, S.; Yelena, C.; Pan, D.; Yan, Z.; Parag, S. De Novo Synthesis of Serine and Glycine Fuels Purine Nucleotide Biosynthesis in Human Lung Cancer Tissues. *The Journal of biological chemistry* **2019**, *294* (36), 13464–13477.

(355) Louis, S.; Tappu, R.-M.; Damms-Machado, A.; Huson, D. H.; Bischoff, S. C. Characterization of the Gut Microbial Community of Obese Patients Following a Weight-Loss Intervention Using Whole Metagenome Shotgun Sequencing. **2016**.

(356) Rivière, A.; Selak, M.; Lantin, D.; Leroy, F.; De Vuyst, L. Bifidobacteria and Butyrate-Producing Colon Bacteria: Importance and Strategies for Their Stimulation in the Human Gut. *Frontiers in Microbiology* **2016**, *7* (979), 1–21.

(357) Reichardt, N.; Duncan, S. H.; Young, P.; Belenguer, A.; McWilliam Leitch, C.; Scott, K. P.; Flint, H. J.; Louis, P. Phylogenetic Distribution of Three Pathways for Propionate Production within the Human Gut Microbiota. *ISME Journal* **2014**, *8* (6), 1323–1335.

(358) Gotoh, A.; Nara, M.; Sugiyama, Y.; Sakanaka, M.; Yachi, H.; Kitakata, A.; Nakagawa, A.; Minami, H.; Okuda, S.; Katoh, T.; Katayama, T.; Kurihara, S. Use of Gifu Anaerobic Medium for Culturing 32 Dominant Species of Human Gut Microbes and Its Evaluation Based on Short-Chain Fatty Acids Fermentation Profiles. *Bioscience, Biotechnology and Biochemistry* **2017**, *81* (10), 2009–2017.

(359) Morissette, A.; Kropp, C.; Songpadith, J. P.; Moreira, R. J.; Costa, J.; Mariné-Casadó, R.; Pilon, G.; Varin, T. V.; Dudonné, S.; Boutekrabt, L.; St-Pierre, P.; Levy, E.; Roy, D.; Desjardins, Y.; Raymond, F.; Houd, V. P.; Marette, A. Blueberry Proanthocyanidins and Anthocyanins Improve Metabolic Health through a Gut Microbiota-Dependent Mechanism in Diet-Induced Obese Mice. *American Journal of Physiology - Endocrinology and Metabolism* **2020**, *318* (6), E965–E980.

(360) Connors, J.; Dawe, N.; Van Limbergen, J. The Role of Succinate in the Regulation of Intestinal Inflammation. *Nutrients* **2019**, *11* (1), 1–12.

(361) Remely, M.; Aumueller, E.; Jahn, D.; Hippe, B.; Brath, H.; Haslberger, A. G. Microbiota and Epigenetic Regulation of Inflammatory Mediators in Type 2 Diabetes and Obesity. *Beneficial Microbes* **2014**, *5* (1), 33–43.

(362) Ali Asgar, M. Anti-Diabetic Potential of Phenolic Compounds: A Review. *International Journal of Food Properties* **2013**, *16* (1), 91–103.

(363) Chen, M.; Lu, B.; Li, Y.; Wang, Y.; Zheng, H.; Zhong, D.; Liao, Z.; Wang, M.; Ma, F.; Liao, Q.; Xie, Z. Metabolomics Insights into the Modulatory Effects of Long-Term Compound Polysaccharide Intake in High-Fat Diet-Induced Obese Rats. *Nutrition and Metabolism* **2018**, *15* (1), 1–15.

(364) Alves, A.; Bassot, A.; Bulteau, A.-L.; Pirola, L.; Morio, B. Glycine Metabolism and Its Alterations in Obesity and Metabolic Diseases. *Nutrients* **2019**, *11* (6).

(365) Yu, K.; Yu, C. G.; Yin, X. Q.; Wang, Z. W.; Wang, X. B.; Wang, L. L.; Guo, S.; An, Y. X.; Zhao, D. Metabolites of Gut Microbiome Are Associated with Glucose Metabolism in Non-Diabetic Obese Adults: A Chinese Monozygotic Twin Study. *Diabetology and Metabolic Syndrome* **2021**, *13* (1), 1–8.

.

APPENDIX: ORIGINAL PUBLICATIONS

I. Reprinted from *Journal of Agricultural and Food Chemistry,* 2020, 68, 9436–9450, with permission from American Chemical Society.

II. Reprinted from *Journal of Agricultural and Food Chemistry,* 2021, 6, 4423–4437, with permission from American Chemical Society.

III. Reprinted from *Food Research International*, 2022, 153,110978, with permission from Elsevier.

DOCTORAL THESES IN FOOD SCIENCES AT THE UNIVERSITY OF TURKU

1. **REINO R. LINKO (1967)** Fatty acids and other components of Baltic herring flesh lipids. (Organic chemistry).
2. **HEIKKI KALLIO (1975)** Identification of volatile aroma compounds in arctic bramble, *Rubus arcticus* L. and their development during ripening of the berry, with special reference to *Rubus stellatus* SM.
3. **JUKKA KAITARANTA (1981)** Fish roe lipids and lipid hydrolysis in processed roe of certain *Salmonidae* fish as studied by novel chromatographic techniques.
4. **TIMO HIRVI (1983)** Aromas of some strawberry and blueberry species and varieties studied by gas liquid chromatographic and selected ion monitoring techniques.
5. **RAINER HUOPALAHTI (1985)** Composition and content of aroma compounds in the dill herb, *Anethum graveolens* L., affected by different factors.
6. **MARKKU HONKAVAARA (1989)** Effect of porcine stress on the development of PSE meat, its characteristics and influence on the economics of meat products manufacture.
7. **PÄIVI LAAKSO (1992)** Triacylglycerols – approaching the molecular composition of natural mixtures.
8. **MERJA LEINO (1993)** Application of the headspace gas chromatography complemented with sensory evaluation to analysis of various foods.
9. **KAISLI KERROLA (1994)** Essential oils from herbs and spices: isolation by carbon dioxide extraction and characterization by gas chromatography and sensory evaluation.
10. **ANJA LAPVETELÄINEN (1994)** Barley and oat protein products from wet processes: food use potential.
11. **RAIJA TAHVONEN (1995)** Contents of lead and cadmium in foods in Finland.
12. **MAIJA SAXELIN (1995)** Development of dietary probiotics: estimation of optimal *Lactobacillus* GG concentrations.
13. **PIRJO-LIISA PENTTILÄ (1995)** Estimation of food additive and pesticide intakes by means of a stepwise method.
14. **SIRKKA PLAAMI (1996)** Contents of dietary fiber and inositol phosphates in some foods consumed in Finland.
15. **SUSANNA EEROLA (1997)** Biologically active amines: analytics, occurrence and formation in dry sausages.
16. **PEKKA MANNINEN (1997)** Utilization of supercritical carbon dioxide in the analysis of triacylglycerols and isolation of berry oils.
17. **TUULA VESA (1997)** Symptoms of lactose intolerance: influence of milk composition, gastric emptying, and irritable bowel syndrome.
18. **EILA JÄRVENPÄÄ (1998)** Strategies for supercritical fluid extraction of analytes in trace amounts from food matrices.
19. **ELINA TUOMOLA (1999)** *In vitro* adhesion of probiotic lactic acid bacteria.
20. **ANU JOHANSSON (1999)** Availability of seed oils from Finnish berries with special reference to compositional, geographical and nutritional aspects.
21. **ANNE PIHLANTO-LEPPÄLÄ (1999)** Isolation and characteristics of milk-derived bioactive peptides.
22. **MIKA TUOMOLA (2000)** New methods for the measurement of androstenone and skatole – compounds associated with boar taint problem. (Biotechnology).
23. **LEEA PELTO (2000)** Milk hypersensitivity in adults: studies on diagnosis, prevalence and nutritional management.
24. **ANNE NYKÄNEN (2001)** Use of nisin and lactic acid/lactate to improve the microbial and sensory quality of rainbow trout products.
25. **BAORU YANG (2001)** Lipophilic components of sea buckthorn (*Hippophaë rhamnoides*) seeds and berries and physiological effects of sea buckthorn oils.
26. **MINNA KAHALA (2001)** Lactobacillar S-layers: Use of *Lactobacillus brevis* S-layer signals for heterologous protein production.
27. **OLLI SJÖVALL (2002)** Chromatographic and mass spectrometric analysis of non-volatile oxidation products of triacylglycerols with emphasis on core aldehydes.
28. **JUHA-PEKKA KURVINEN (2002)** Automatic data processing as an aid to mass spectrometry of dietary triacylglycerols and tissue glycerophospholipids.
29. **MARI HAKALA (2002)** Factors affecting the internal quality of strawberry (*Fragaria x ananassa* Duch.) fruit.
30. **PIRKKA KIRJAVAINEN (2003)** The intestinal microbiota – a target for treatment in infant atopic eczema?
31. **TARJA ARO (2003)** Chemical composition of Baltic herring: effects of processing and storage on fatty acids, mineral elements and volatile compounds.
32. **SAMI NIKOSKELAINEN (2003)** Innate immunity of rainbow trout: effects of opsonins, temperature and probiotics on phagocytic and complement activity as well as on disease resistance.
33. **KAISA YLI-JOKIPII (2004)** Effect of triacylglycerol fatty acid positional distribution on postprandial lipid metabolism.

34. **MARIKA JESTOI (2005)** Emerging *Fusarium*-mycotoxins in Finland.
35. **KATJA TIITINEN (2006)** Factors contributing to sea buckthorn (*Hippophaë rhamnoides* L.) flavour.
36. **SATU VESTERLUND (2006)** Methods to determine the safety and influence of probiotics on the adherence and viability of pathogens.
37. **FANDI FAWAZ ALI IBRAHIM (2006)** Lactic acid bacteria: an approach for heavy metal detoxification.
38. **JUKKA-PEKKA SUOMELA (2006)** Effects of dietary fat oxidation products and flavonols on lipoprotein oxidation.
39. **SAMPO LAHTINEN (2007)** New insights into the viability of probiotic bacteria.
40. **SASKA TUOMASJUKKA (2007)** Strategies for reducing postprandial triacylglycerolemia.
41. **HARRI MÄKIVUOKKO (2007)** Simulating the human colon microbiota: studies on polydextrose, lactose and cocoa mass.
42. **RENATA ADAMI (2007)** Micronization of pharmaceuticals and food ingredients using supercritical fluid techniques.
43. **TEEMU HALTTUNEN (2008)** Removal of cadmium, lead and arsenic from water by lactic acid bacteria.
44. **SUSANNA ROKKA (2008)** Bovine colostral antibodies and selected lactobacilli as means to control gastrointestinal infections.
45. **ANU LÄHTEENMÄKI-UUTELA (2009)** Foodstuffs and medicines as legal categories in the EU and China. Functional foods as a borderline case. (Law).
46. **TARJA SUOMALAINEN (2009)** Characterizing *Propionibacterium freudenreichii* ssp. *shermanii* JS and *Lactobacillus rhamnosus* LC705 as a new probiotic combination: basic properties of JS and pilot *in vivo* assessment of the combination.
47. **HEIDI LESKINEN (2010)** Positional distribution of fatty acids in plant triacylglycerols: contributing factors and chromatographic/mass spectrometric analysis.
48. **TERHI POHJANHEIMO (2010)** Sensory and non-sensory factors behind the liking and choice of healthy food products.
49. **RIIKKA JÄRVINEN (2010)** Cuticular and suberin polymers of edible plants – analysis by gas chromatographic-mass spectrometric and solid state spectroscopic methods.
50. **HENNA-MARIA LEHTONEN (2010)** Berry polyphenol absorption and the effect of northern berries on metabolism, ectopic fat accumulation, and associated diseases.
51. **PASI KANKAANPÄÄ (2010)** Interactions between polyunsaturated fatty acids and probiotics.
52. **PETRA LARMO (2011)** The health effects of sea buckthorn berries and oil.
53. **HENNA RÖYTIÖ (2011)** Identifying and characterizing new ingredients *in vitro* for prebiotic and synbiotic use.
54. **RITVA REPO-CARRASCO-VALENCIA (2011)** Andean indigenous food crops: nutritional value and bioactive compounds.
55. **OSKAR LAAKSONEN (2011)** Astringent food compounds and their interactions with taste properties.
56. **ŁUKASZ MARCIN GRZEŚKOWIAK (2012)** Gut microbiota in early infancy: effect of environment, diet and probiotics.
57. **PENGZHAN LIU (2012)** Composition of hawthorn (*Crataegus* spp.) fruits and leaves and emblic leafflower (*Phyllanthus emblica*) fruits.
58. **HEIKKI ARO (2012)** Fractionation of hen egg and oat lipids with supercritical fluids. Chemical and functional properties of fractions.
59. **SOILI ALANNE (2012)** An infant with food allergy and eczema in the family – the mental and economic burden of caring.
60. **MARKO TARVAINEN (2013)** Analysis of lipid oxidation during digestion by liquid chromatography-mass spectrometric and nuclear magnetic resonance spectroscopic techniques.
61. **JIE ZHENG (2013)** Sugars, acids and phenolic compounds in currants and sea buckthorn in relation to the effects of environmental factors.
62. **SARI MÄKINEN (2014)** Production, isolation and characterization of bioactive peptides with antihypertensive properties from potato and rapeseed proteins.
63. **MIKA KAIMAINEN (2014)** Stability of natural colorants of plant origin.
64. **LOTTA NYLUND (2015)** Early life intestinal microbiota in health and in atopic eczema.
65. **JAAKKO HIIDENHOVI (2015)** Isolation and characterization of ovomucin – a bioactive agent of egg white.
66. **HANNA-LEENA HIETARANTA-LUOMA (2016)** Promoting healthy lifestyles with personalized, *APOE* genotype based health information: The effects on psychological-, health behavioral and clinical factors.
67. **VELI HIETANIEMI (2016)** The *Fusarium* mycotoxins in Finnish cereal grains: How to control and manage the risk.
68. **MAARIA KORTESNIEMI (2016)** NMR metabolomics of foods – Investigating the influence of origin on sea buckthorn berries, *Brassica* oilseeds and honey.
69. **JUHANI AAKKO (2016)** New insights into human gut microbiota development in early infancy: influence of diet, environment and mother's microbiota.

70. **WEI YANG (2017)** Effects of genetic and environmental factors on proanthocyanidins in sea buckthorn (*Hippophaë rhamnoides*) and flavonol glycosides in leaves of currants (*Ribes* spp.).
71. **LEENAMAIJA MÄKILÄ (2017)** Effect of processing technologies on phenolic compounds in berry products.
72. **JUHA-MATTI PIHLAVA (2017)** Selected bioactive compounds in cereals and cereal products – their role and analysis by chromatographic methods.
73. **TOMMI KUMPULAINEN (2018)** The complexity of freshness and locality in a food consumption context
74. **XUEYING MA (2018)** Non-volatile bioactive and sensory compounds in berries and leaves of sea buckthorn (*Hippophaë rhamnoides*)
75. **ANU NUORA (2018)** Postprandial lipid metabolism resulting from heated beef, homogenized milk and interesterified palm oil.
76. **HEIKKI AISALA (2019)** Sensory properties and underlying chemistry of Finnish edible wild mushrooms.
77. **YE TIAN (2019)** Phenolic compounds from Finnish berry species to enhance food safety.
78. **MAIJA PAAKKI (2020)** The importance of natural colors in food for the visual attractiveness of everyday lunch.
79. **SHUXUN LIU (2020**) Fermentation with non-*Saccharomyces* yeasts as a novel biotechnology for berry wine production.
80. **MARIKA KALPIO (2020)** Strategies for analyzing the regio- and stereospecific structures of individual triacylglycerols in natural fats and oils.
81. **JOHANNA JOKIOJA (2020)** Postprandial effects and metabolism of acylated anthocyanins originating from purple potatoes.
82. **NIINA KELANNE (2021)** Novel bioprocessing for increasing consumption of Nordic berries.
83. **NIKO MARKKINEN (2021)** Bioprocessing of berry materials with malolactic fermentation.
84. **GABRIELE BELTRAME (2021)** Polysaccharides from Finnish fungal resources.
85. **SALLA LAITO (2022)** Bioactive compounds in oats and gut health
86. **KANG CHEN (2022)** Multi-omics study on the effects of anthocyanin extracts from bilberries and purple potatoes on type 2 diabetes in Zucker diabetic fatty rats

TURUN
YLIOPISTO
UNIVERSITY
OF TURKU